

AD-A253 918



2

PL-TR-92-2052

CLOUD CURVE ALGORITHM TEST PROGRAM

Robert N. Trapnell, Jr.

Computer Data Systems, Inc.
210 W 6th Street Suite 1200
Fort Worth, Texas 76102

28 February 1992

Final Report
10 Jul 89 to 28 Feb 92



Approved for public release; distribution unlimited



PHILLIPS LABORATORY
AIR FORCE SYSTEMS COMMAND
HANSCOM AIR FORCE BASE, MASSACHUSETTS 01731-5000

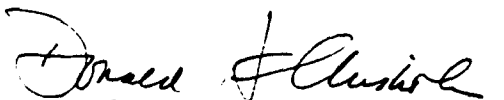
92 5 26 077

92-13862



This technical report has been reviewed and is approved for publication.


JOHN L. SCHATTEL, Captain, USAF
Contract Manager


DONALD A. CHISHOLM
Chief, Atmospheric Prediction Branch
Atmospheric Sciences Division


ROBERT A. McCLATCHEY
Director, Atmospheric Sciences Division

This document has been reviewed by the ESD Public Affairs Office (PA) and is releasable to the National Technical Information Service (NTIS).

Qualified requestors may obtain additional copies from the Defense Technical Information Center. All others should apply to the National Technical Information Service.

If your address has changed, or if you wish to be removed from the mailing list, or if the addressee is no longer employed by your organization, please notify PL/TSI, Hanscom AFB, MA 01731-5000. This will assist us in maintaining a current mailing list.

Do not return copies of this report unless contractual obligations or notices on a specific document requires that it be returned.

REPORT DOCUMENTATION PAGE			Form Approved OMB No. 0704-0188	
<small>Public reporting burden for this collection of information is estimated to average 1 hour per response, including the time for reviewing instructions, searching existing data sources, gathering and maintaining the data needed, and completing and reviewing the collection of information. Send comments regarding this burden estimate or any other aspect of this collection of information, including suggestions for reducing this burden, to Washington Headquarters Services, Directorate for Information Operations and Reports, 1215 Jefferson Davis Highway, Suite 1204, Arlington, VA 22202-4302, and to the Office of Management and Budget, Paperwork Reduction Project (0704-0188), Washington, DC 20503.</small>				
1. AGENCY USE ONLY (Leave blank)	2. REPORT DATE 28 February 92	3. REPORT TYPE AND DATES COVERED FINAL REPORT (10 July 89-28 Feb 92)		
4. TITLE AND SUBTITLE Cloud Curve Algorithm Test Program		5. FUNDING NUMBERS C-WKCS79500(GSA) PE: 63707F PR: 4026 TA: 01 WU: KE Project Order GLH1-6004		
6. AUTHOR(S) Robert N. Trapnell, Jr				
7. PERFORMING ORGANIZATION NAME(S) AND ADDRESS(ES) CDSI, Inc 210 West 6th St., Suite 1200 Fort Worth TX 76102		8. PERFORMING ORGANIZATION REPORT NUMBER None		
9. SPONSORING / MONITORING AGENCY NAME(S) AND ADDRESS(ES) Phillips Laboratory Hanscom AFB MA 01731-5000 Contract Monitor: Captain John Schattel/GPAP		10. SPONSORING / MONITORING AGENCY REPORT NUMBER PL-TR-92-2052		
11. SUPPLEMENTARY NOTES None				
12a. DISTRIBUTION / AVAILABILITY STATEMENT Approved for public release; distribution unlimited		12b. DISTRIBUTION CODE		
13. ABSTRACT (Maximum 200 words) This project had three main objectives: (1) to test variations in the cloud curve algorithm (CCA) methodology to determine the superior algorithm configuration for use with the Air Force Weather Central, Global Spectral Model (AFGWC GSM), (2) to perform inter-model comparisons between CCA (using the AFGWC GSM) and AFGWC's current cloud forecast models (5LAYER in the extratropics and TRONEW in the tropics), persistence and diurnal persistence (used in TRONEW), and (3) to perform inter-model comparisons between CCA (using the AFGWC GSM) and the Geleyn scheme used until May 1985 by the European Centre for Medium-range Weather Forecasts (ECMWF) and using the AFGWC GSM. The basic-CCA approach is to generate relative humidity (RH)-to-cloud conversion curves by relating cumulative frequencies of NWP model forecasted RH to cumulative frequencies of analyzed cloud amount. Once the curves are computed, they can be used to convert an RH forecast to a cloud forecast. The cloud forecast skill of CCA (using the AFGWC GSM) compared to 5LAYER (extratropics) and TRONEW (tropics) varied by season, geographical region and forecast interval.				
14. SUBJECT TERMS cloud diagnosis, global cloud forecasting, numerical weather prediction, cloud-moisture algorithms		15. NUMBER OF PAGES 170		
		16. PRICE CODE		
17. SECURITY CLASSIFICATION OF REPORT Unclassified	18. SECURITY CLASSIFICATION OF THIS PAGE Unclassified	19. SECURITY CLASSIFICATION OF ABSTRACT Unclassified	20. LIMITATION OF ABSTRACT SAR	

PREFACE

The author wishes to gratefully acknowledge the assistance of the following people who so ably assisted in the conduct of this project.

Dr. Kenneth Mitchell, National Meteorological Center, who provided many hours of assistance throughout the entire project both in the context of his affiliation with AFGWC as an IMA reservist and on his own time.

Ms. Beth Matney, Computer Data Systems, Inc., who provided assistance in the software design, coding, testing and implementation phases.

Mr. Don Chisholm, Mr. Doug Hahn and Capt John Schattel of the Phillips Laboratory who provided guidance and assistance throughout the project.

Sgt Lincoln Kroeger, MSgt Paul Jensen, and Mr. Joe Luteran, AFGWC computer operations technical staff, who assisted in the implementation of the algorithm and in the solving of problems associated with real-time production software.

Maj Dan Pophin, Maj James Shaefer, and Mr. Ray Kiess, AFGWC cloud forecast models section, who provided insights into the SLAYER, TRONEW and RTNEPH models and who assisted in the production of shaded hemispheric displays of relative humidity and clouds.

Maj James Davenport, Maj Alan Stein, Maj Peter Rice, Capt James Cramer and Maj Carol Weaver, Hq AFGWC staff, who served as the formal points of contact with AFGWC.

Mr. Bruce Thomas, Aerospace Corporation, who assisted in creating shaded hemispheric displays of relative humidity and clouds prior to AFGWC developing its own in-house capability.



Accession For	
NTIS GRA&I	<input checked="checked" type="checkbox"/>
DTIC TAB	<input type="checkbox"/>
Unannounced	<input type="checkbox"/>
Justification	
By _____	
Distribution/	
Availability Codes	
Dist	Avail and/or Special
A-1	

This page intentionally left blank

TABLE OF CONTENTS

	<u>PAGE</u>
EXECUTIVE SUMMARY	vii
1. INTRODUCTION	1
1.1 Summary of Previous Experimentation	3
1.2 Description of the Current Experiment	7
2. SUMMARY OF RESULTS	23
2.1 Cloud Curve Algorithm	23
2.1 Relative Humidity to Cloud Curves	26
2.2 Basic Algorithm Skill Scores	29
2.3 Effect of the Relative Humidity Trend Technique	30
2.4 Shaded Hemispheric Displays of Relative Humidity and Clouds	32
3. CONCLUSIONS AND RECOMMENDATIONS	36
REFERENCES	37
LIST OF ACRONYMS	39
Appendix A. Plots of Relative Humidity to Cloud Curves	67
Appendix B. Plots of Verification Statistics for Northern Hemisphere Mid-latitude Ocean - 17 Jan 91 to 13 Feb 91	79
Appendix C. Plots of Verification Statistics for Northern Hemisphere Mid-latitude Land - 17 Jan 91 to 13 Feb 91	91
Appendix D. Plots of 20/20 Scores for the Period 01 Aug 91 to 28 Aug 91	103
Appendix E. Plots of 20/20 Scores for the Period 24 Oct 91 to 20 Nov 91	115
Appendix F. Plots of Verification Statistics for European Land for the Period 24 Oct 91 to 20 Nov 91	125
Appendix G. Plots of 20/20 Scores for the Period 16 Jan 91 to 12 Feb 92	137
Appendix H. Plots of 20/20 Scores Showing the Effects of the Relative Humidity Trending Technique	145
Appendix I. Shaded Hemispheric Displays of Relative Humidity and Clouds	

LIST OF FIGURES FOR EXECUTIVE SUMMARY

<u>Figure</u>		<u>Page</u>
I	20/20 Scores for Cloud Forecasts Computed by the 5LAYER Model (to 48 hours only), by Using Persistence and by Using Cloud Curve Algorithm European Land Curves For 6 to 60 and 72 Hour Total Cloud Forecasts Verified Over European Land During the Period from 01 August 1991 to 28 August 1991.	ix
II	20/20 Scores for Cloud Forecasts Computed by the 5LAYER Model (to 48 hours only), by Using Persistence and by Using Cloud Curve Algorithm Northern Hemisphere Mid-Latitude Ocean Curves For 6 to 60 and 72 Hour Total Cloud Forecasts Verified Over Northern Hemisphere Mid-Latitude Ocean During the Period from 01 August 1991 to 28 August 1991.	xi
III	BIAS Scores for Cloud Forecasts Computed by the 5LAYER Model (to 48 hours only), by Using Persistence and by Using Cloud Curve Algorithm European Land Curves For 6 to 60 and 72 Hour Total Cloud Forecasts Verified Over European Land During the Period from 01 August 1991 to 28 August 1991.	xii
IV	Reliability Scores for Cloud Forecasts Computed by the 5LAYER Model (to 48 hours only), by Using Persistence and by Using Cloud Curve Algorithm European Land Curves For 6 to 60 and 72 Hour Total Cloud Forecasts Verified Over European Land During the Period from 01 August 1991 to 28 August 1991.	xiii
V	Sharpness Scores for Cloud Forecasts Computed by the 5LAYER Model (to 48 hours only), by Using Persistence and by Using Cloud Curve Algorithm European Land Curves For 6 to 60 and 72 Hour Total Cloud Forecasts Verified Over European Land During the Period from 01 August 1991 to 28 August 1991.	xiv

EXECUTIVE SUMMARY

This report documents the advanced development of an objective diagnostic cloud forecast scheme known as the cloud curve algorithm (CCA). The CCA was originally developed as part of a pilot project to develop a diagnostic cloud forecast scheme for use with the Air Force Global Weather Central (AFGWC) Global Spectral Model (GSM). Although this study used the AFGWC GSM, the CCA is an objective method which can be used with any numerical weather prediction (NWP) model. In addition, when used in conjunction with a real-time cloud analysis model such as AFGWC's real-time nephanalysis (RTNEPH), the CCA can incorporate a real-time update feature.

This project had three main objectives:

- (1) To test variations in the CCA methodology to determine the superior algorithm configuration in the AFGWC GSM
- (2) To perform inter-model skill comparisons between CCA (using the AFGWC GSM) and AFGWC's current cloud forecast models (5LAYER in the extratropics and TRONEW in the tropics), persistence and diurnal persistence (which TRONEW uses)
- (3) To perform inter-model skill comparisons between CCA (using the AFGWC GSM) and the Geleyn scheme used until May 1985 in the European Center for Medium Range Weather Forecasting (ECMWF) GSM to diagnose cloud for the radiation scheme (using the AFGWC GSM)

The basic CCA approach is to generate relative humidity (RH)-to-cloud conversion curves by relating cumulative frequencies of NWP model forecast RH to cumulative frequencies of analyzed cloud amount. Once the curve is computed, it can be used to convert an RH forecast to a cloud forecast. The following variations in the methodology showed the most skill:

- (1) In compacting GSM RH values on 6 pressure levels to three layers (low,middle,high), the 1000 mb values are ignored because of a moist bias, especially over the low-latitude oceans.
- (2) In computing a total cloud amount from input low, middle and high cloud amounts, a tuned overlap works best in the extratropics while a random overlap works best in the tropics.
- (3) Increasing regional stratification of curves yielded the most skill. In the final phase, curves were computed for: European Land, East Asia Land, North American Land, North Africa/Middle East Land, Northern Hemisphere Mid-Latitude Ocean, Northern Hemisphere Tropical Land and Northern Hemisphere Tropical Ocean.
- (4) CCA showed little sensitivity to the length of the frequency of occurrence accumulation period. In the final phase, an accumulation period of two weeks was used to ensure an adequate sample over small regions.
- (5) The incorporation of a diurnal correction similar to that used by 5LAYER yielded increased skill in the summer over land.

- (6) The incorporation of a binary (up or down) vertical velocity stratification did not yield increased skill. Future tests should use a three category stratification: strong up, strong down, and weak.
- (7) Once a week real-time update of the curves reflected the seasonal changes in RH and cloud amount distributions which sometimes resulted in large variations in the amount of cloud associated with a given input RH value.
- (8) An RH trend approach which tried to capture the RH information contained in the RTNEPH cloud analysis yielded in general more skill over ocean areas, but showed an unexpectedly high moist bias.

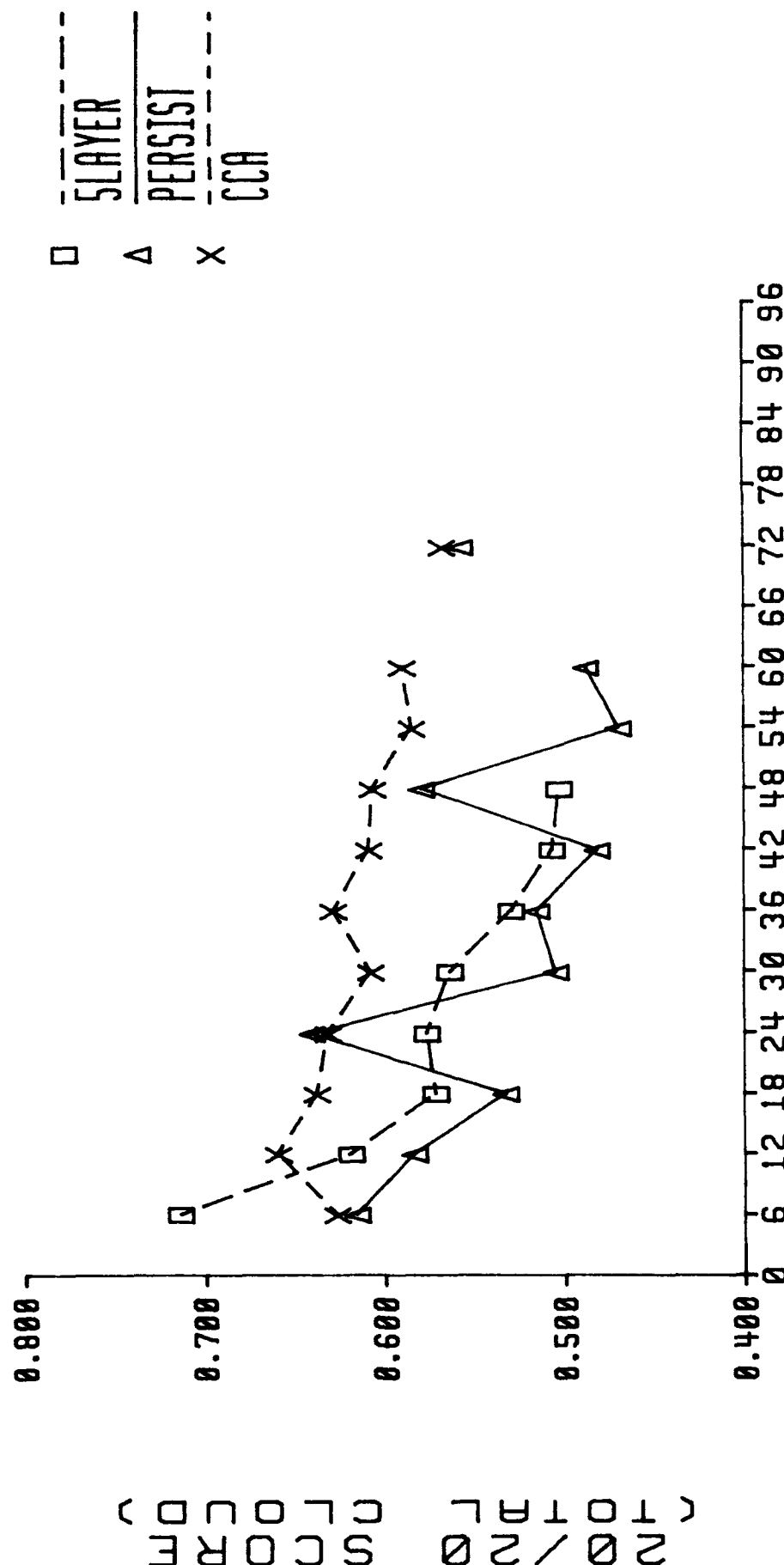
The cloud forecast skill of CCA (using the AFGWC GSM) compared to 5LAYER varied by season and region of the world. The table below shows the forecast length at which CCA outperformed 5LAYER (extratropics) or TRONEW (tropics) based on the 20/20 score for total cloud (- indicates CCA did worse than either 5LAYER or TRONEW at all forecast lengths):

<u>Region</u>	<u>1 Aug 91</u> <u>to</u> <u>28 Aug 91</u>	<u>24 Oct 91</u> <u>to</u> <u>20 Nov 91</u>	<u>16 Jan 92</u> <u>to</u> <u>12 Feb 92</u>
European Land	12 hours	12 hours	36 hours
East Asia Land	12 hours	-	-
North America Land	18 hours	-	-
North Africa/ Middle East Land	-	-	-
Northern Hemisphere			
Mid-Latitude Land	12 hours	-	-
Mid-Latitude Ocean	-	42 hours	36 hours
Tropical Land	-	-	-
Tropical Ocean	-	-	-

Note that CCA did well over Northern Hemisphere Mid-Latitude Land in the summer, but performance dropped off in the autumn and winter. Over Northern Hemisphere Mid-Latitude Ocean the performance was poor in the summer but increased slightly in the autumn and winter. Performance in the tropics was uniformly poor. This is similar to AFGWC's experience which leads them to use diurnal persistence in the tropics rather than 5LAYER.

The 20/20 scores for European Land total cloud in August are shown in Figure I. The 20/20 score is the percentage of forecast grid points verifying within 20% of the observed cloud amount. CCA outperformed 5LAYER by 5.5% at 24 hours and 10.5% at 48 hours. The superior skill of the CCA over European Land appears to be due to the fact that Europe has the most dense upper air and surface observation network. This results in a high quality analysis for both GSM RH and RTNEPH cloud amount. This improves the RH forecasts and the cumulative frequency distribution curves for both RH and cloud amount. The forecasts labeled PERSIST use the RTNEPH cloud analysis. A persistence cloud forecast makes the assumption that the cloud amounts and locations will not change over the

EUROPEAN LAND 01 AUG 91 TO 28 AUG 91



FORECAST LENGTH (HOURS)
Figure I

entire forecast period. The 24 hour peaks in persistence are due to the diurnal cloud cycle. The peaks are reduced in amplitude over the ocean and over land during winter.

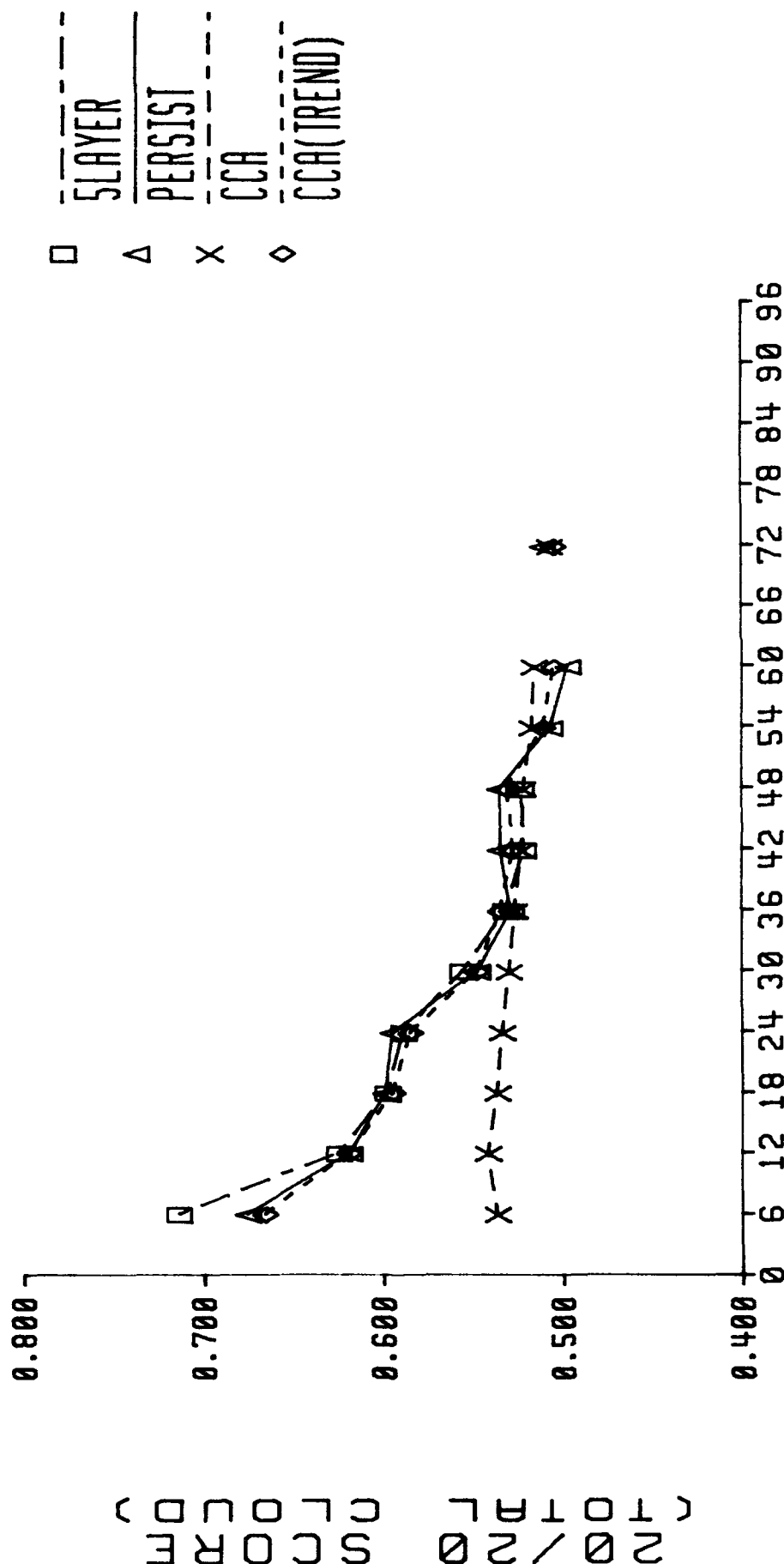
The 20/20 scores for northern hemisphere mid-latitude ocean total cloud in August are shown in Figure II. CCA can do no better than achieve parity with 5LAYER at 42 hours. This poor performance appears to be due to the fact that the GSM has very few RH observations over water. The initial RH analysis is thus the 6 hour GSM forecast from the previous forecast cycle. The primary source of information used to update the analysis is upper air observations over land. The CCA trend approach used RTNEPH analyses to derive initial RH information. The CCA trend approach achieved parity with 5LAYER at 12 hours, which supports the thought that the lack of RH information over oceans in the initial GSM analysis adversely affects the CCA. However, the trend method has a moist bias. That is, the mean forecast cloud amount for the region over the verification period is greater than the mean observed cloud amount.

On the other hand, the bias results for the basic CCA approach are very good. Results for European Land total cloud in August are shown in Figure III. CCA maintained a bias of less than 1% for all but one forecast length, which for all practical purposes is negligible. The 5LAYER shows an increasingly dry bias with increasing forecast lengths. A major hallmark of the CCA is its ability to minimize layer cloud biases, even overcoming biases in the given NWP model's RH forecast. Some layer bias results from the fact that the observed layer cloud amount is stored in 10% increments and that the verifications are performed in 10% increments. Some unavoidable error in the total cloud bias exists because of the vagaries of vertically stacking layered cloud to infer total cloud. That is, for any three given layer fractional cloud amounts, the total cloud depends on the relative position of the cloud in the grid volume. This relative positioning can vary from situation to situation and can therefore only be approximated.

Similarly good results can be shown for European Land summer total cloud reliability (Figure IV) and sharpness (Figure V). Reliability is the sum of the weighted mean average errors for all forecast categories (0%, 10%, 20%, ..., 100%) subtracted from 100. Where the 20/20 score is a measure of how many forecasts verify within a specified category, reliability is a measure of the difference between forecast and observed cloud amount. The CCA reliability scores are consistent with the 20/20 scores showing a crossover after 18 hours and less than a 5% drop over the 72 hour forecast period.

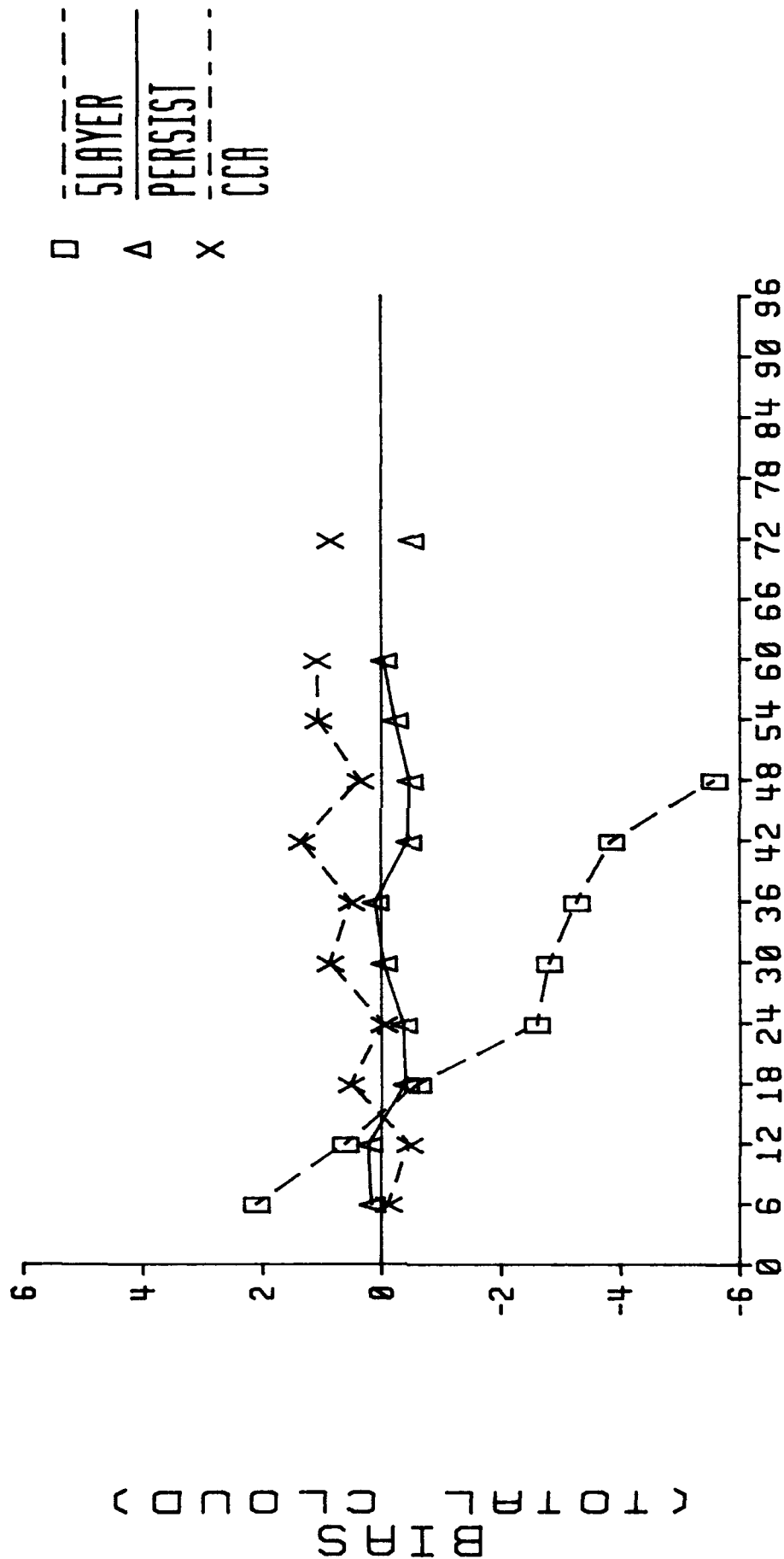
Sharpness, on the other hand, is a measure of the 'binary-ness' of the forecasts, that is, the percent of forecasts in the 0%-20% and 80%-100% ranges. Each grid spacing has its inherent range of sharpness values. The typical sharpness values for a given situation are usually indicated by the sharpness values for persistence forecasts. The CCA sharpness scores (Figure V) are close to the persistence sharpness values. This demonstrates that CCA skill is not due to smoothing, i.e., the forcing of forecast amounts between 20% and 80% simply to achieve high skill scores.

01 AUG 91 TO 28 AUG 91



FORECAST LENGTH (HOURS)
Figure II

EUROPEAN LAND
01 AUG 91 TO 28 AUG 91



FORECAST LENGTH (HOURS)
Figure III

EUROPEAN LAND 01 AUG 91 TO 28 AUG 91

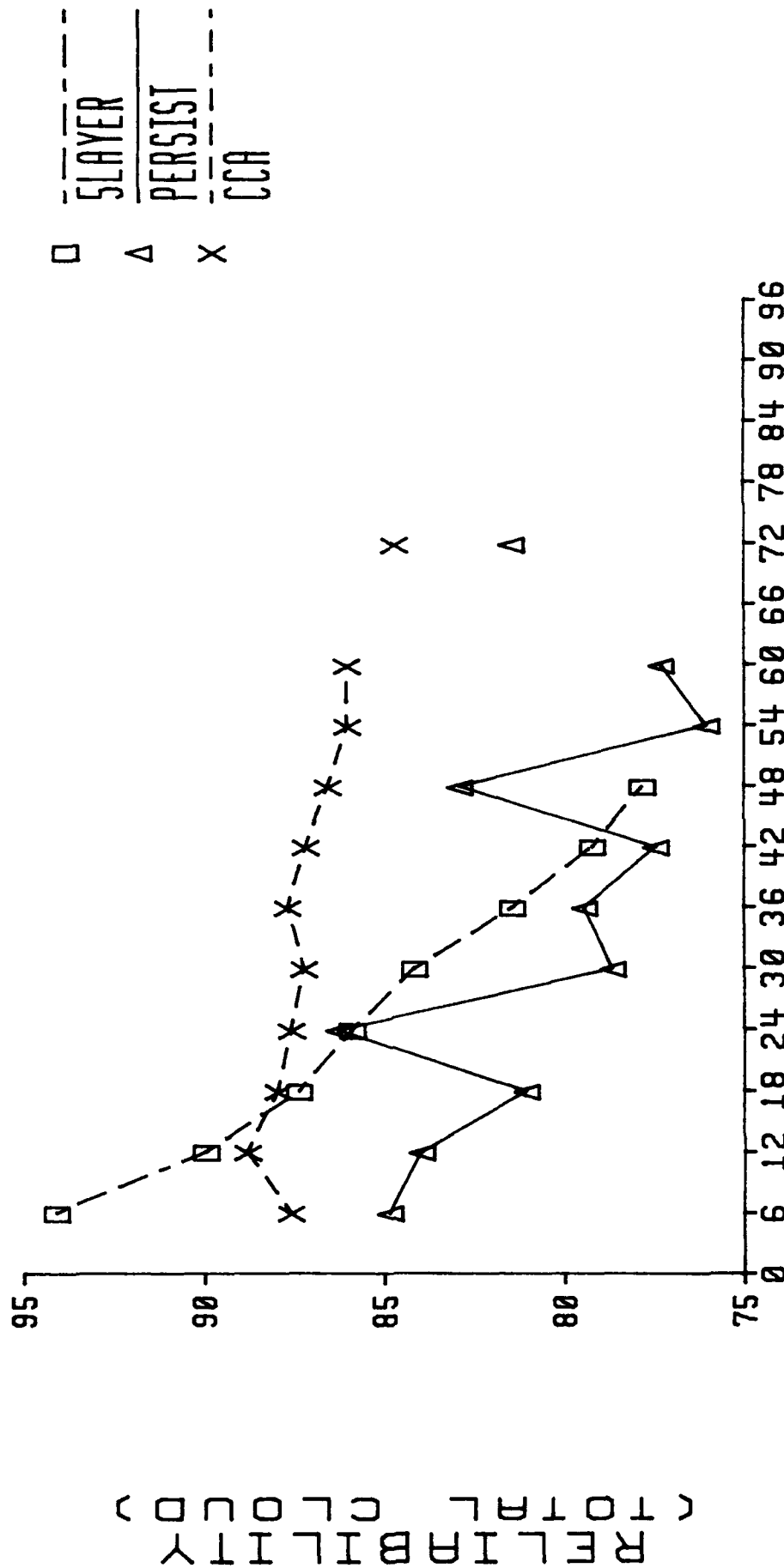
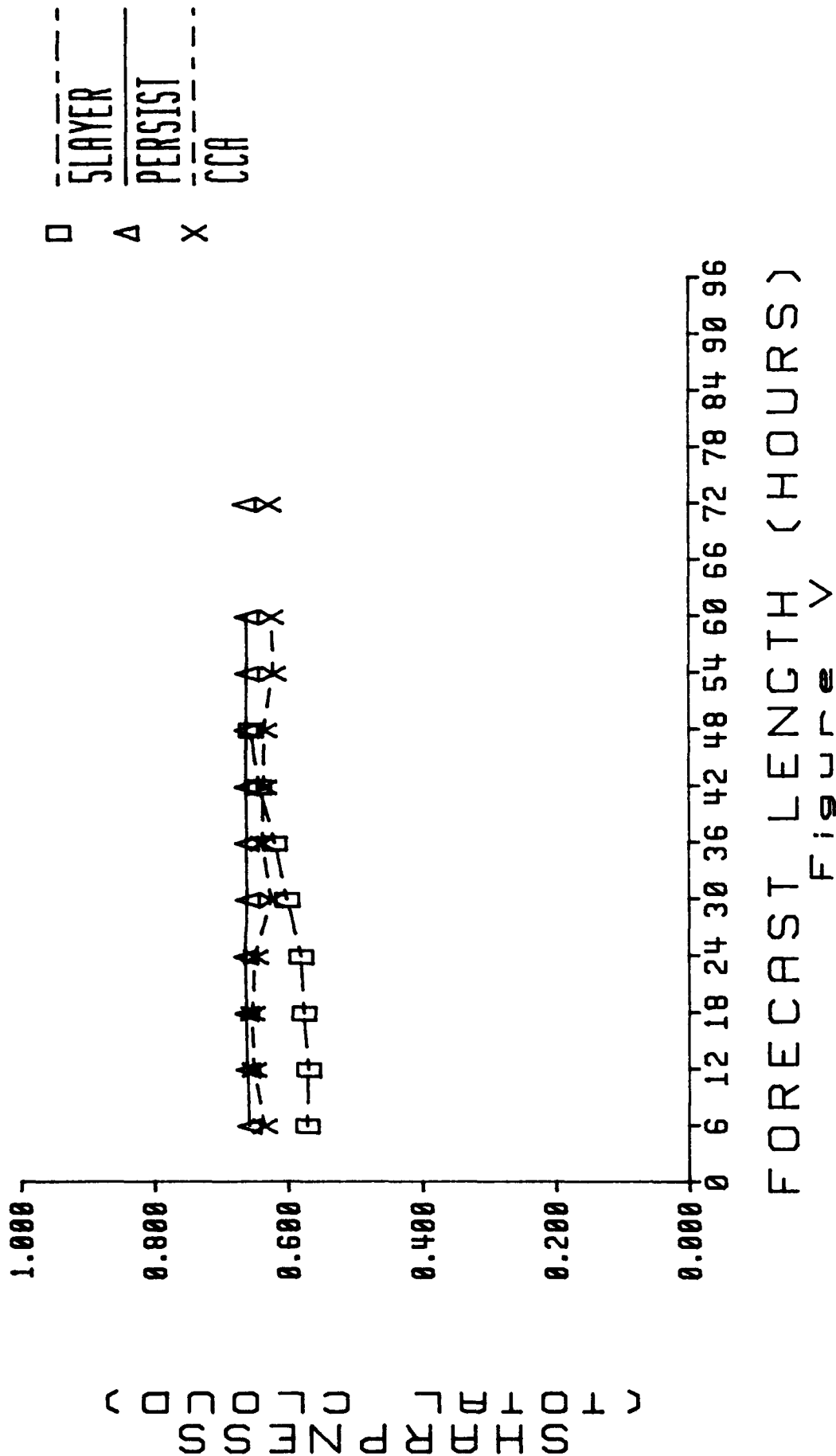


Figure IV
FORECAST LENGTH (HOURS)

EUROPEAN LAND 01 AUG 91 TO 28 AUG 91



The CCA scheme is not the only diagnostic RH-to-cloud scheme available. There are several such schemes detailed in the NWP literature. The forerunner study of Mitchell and Hahn (1989), in which the CCA scheme was first developed, evaluated the use of three diagnostic schemes (borrowed from other NWP models) with the AFGWC GSM. All three yielded large cloud forecast biases and poor skill scores.

NWP models vary widely in the systematic character of their humidity forecast because of the large range of spatial grid resolutions and the vast array of approaches to modeling precipitation, convection, surface evaporation, and planetary boundary layer (PBL). Because of this, an RH-to-cloud scheme borrowed from one model will rarely perform well in another model without substantial, costly trial and error tuning and modification.

The CCA, on the other hand, is an objective methodology. It overcomes the pitfalls of borrowed schemes in that it recognizes and compensates for the humidity forecast biases of a given NWP model. In doing so it yields unbiased cloud forecasts whose sharpness matches that of the verifying cloud analysis.

One of the borrowed schemes used in the Mitchell and Hahn study was the Geleyn scheme (referred to in this report as the ECMWF scheme). It was retained as a baseline scheme in the present study because it was the most skillful of the three borrowed schemes when used with the AFGWC GSM. In the inter-model comparison between the CCA and Geleyn schemes, the CCA scheme was consistently more skillful than the Geleyn (ECMWF) scheme, which gave large negative cloud biases.

On the other hand, in the inter-model comparison between CCA and 5LAYER, we have seen that CCA (using the AFGWC GSM) did not consistently surpass 5LAYER. This head-to-head comparison between CCA and 5LAYER was heavily slanted toward 5LAYER. The 5LAYER uses a detailed RTNEPH cloud analysis on a 25 nm grid which is smoothed to a 100 nm grid. The cloud analysis is converted to a moisture analysis, advected along a forecast trajectory (using GSM winds) and converted back to a cloud forecast. The 5LAYER therefore has detailed moisture information linked to cloud cover over the entire extratropics.

In contrast to the 5LAYER, the AFGWC GSM (regardless of the choice of cloud forecast scheme) suffers from the following major disadvantages:

- (1) No RTNEPH cloud analysis information (or any other cloud information) is used to derive the GSM initial moisture analysis
- (2) The GSM spatial resolution is poor
- (3) The GSM has many pre- and post-processing interpolation steps

The GSM has an RH analysis on the equivalent of a 200 nm grid spacing with input RH information from RAOBs primarily over land. This coarse spatial resolution is maintained throughout the forecast cycle. In addition, errors are introduced in the conversion from spectral space to grid space and in the conversion from sigma layers to pressure levels in GSM pre- and post-processing interpolation steps. These highly smoothed

GSM RH analyses and forecasts are interpolated to the same 100 nm grid used by 5LAYER for the computation of RH-to-cloud curves and the conversion of RH forecasts to cloud forecasts for verification against the 100 nm grid RTNEPH. Given the circumstances, it is surprising that the CCA shows as much skill as it does when used with the AFGWC GSM.

A fairer comparison between CCA in the AFGWC GSM and 5LAYER would require:

- (1) Executing the GSM at much higher spatial resolution
- (2) Outputting the GSM RH forecast directly on GSM sigma-layer surfaces
- (3) Utilizing the RTNEPH directly in deriving the GSM initial moisture analysis

Further more, a more advanced GSM with state-of-the-art parameterized physical processes should be used ,e.g., the Phillips Laboratory Advanced Physics Global Spectral Model. The above recommended efforts were significantly beyond the resources available for this study.

Another NWP model being used at AFGWC is the Relocatable Window Model (RWM) and is a more suitable candidate for comparing CCA to 5LAYER. It was not used in this study because it was not sufficiently ready. It is a higher resolution model used to provide forecasts over smaller forecast areas called windows. These forecast areas are chosen based on the needs of military operations and are usually over land. The RWM is an excellent candidate for the use of CCA. It is a grid point model which gets its initial RH analysis guess from the GSM. However, the RH analysis update is performed on the small RWM grid spacing on the RWM sigma layers. This avoids the pre- and post-processing errors found in the GSM and may give CCA the detailed RH information it needs. CCA should therefore perform much better in the RWM than in the GSM especially if the RTNEPH cloud analysis could be used as a data source for the RWM initial moisture analysis. Presently, the cloud forecast scheme being used by the RWM is borrowed from the Swedish Limited Area Model (SLAM). The scheme is a linear one similar to that of Smagorinski'. Based on the performance of the Geleyn scheme in the GSM, CCA should perform much better than the SLAM scheme in the RWM.

One forecast scheme which was not considered was the Model Output Statistics (MOS). The MOS approach requires that a model be run for at least two years in order to derive the proper MOS equations for forecasting the predictand in a particular region. Once the equations are derived, major changes to the physics of the NWP cannot be changed without forcing the derivation of a new set of MOS equations. The CCA curves, on the other hand, can adjust to the changed model physics within the length of the frequency of occurrence accumulation period.

LIST OF FIGURES FOR FINAL REPORT
(FIGURES CONTAINED IN EACH APPENDIX ARE LISTED IN THE APPENDIX)

<u>Figure</u>		<u>Page</u>
1	5LAYER Condensation Pressure Spread (CPS) to Cloud Curves for 850 mb, 700,mb, 500mb, and 300mb (Valid for all Extratropical Areas and all Forecast Lengths)	4
2	Category (top) and Cumulative (bottom) Frequency of Occurrence (at one percent intervals) of RTNEPH Analyzed Cloud Amounts (Part a) and GSM 24 Hour Forecast RH Amounts (Part b) at 70 kPa over the NH Octagon (Extratropics), Valid at 00Z, 18 January 1985. At bottom, the one-to-one mapping of the RTNEPH observed cloud frequency onto the GSM forecast RH frequency yields a CCA RH-to-Cloud Curve.	8
3	Depiction of the Boundaries of the Northern Hemisphere Mid-Latitude Land Subregions: North America Land, European Land, North Africa/Middle East Land and East Asia Land.	15
4	Monthly Reliability statistics for Scenario 4 (latitude band + land/ocean curves) for Southern Hemisphere Polar for Phase I, Month 8 (17 Jan 91 to 13 Feb 91)	22

This page intentionally left blank

1. INTRODUCTION

The users of forecasts of fractional cloud cover for a given location usually fall into two categories. The first and most general use is in numerical weather prediction models which use fractional cloud cover as part of the parameterized diabatic physics of the model. The success of the cloud cover forecast is determined by the correctness of the radiation budget.²

The second category of users are those to whom the forecast values of fractional cloud cover are important in and of themselves. It is to this second category of users that this development is oriented. The Air Force Global Weather Central (AFGWC) is charged with providing forecasts of fractional cloud amounts to Army, Air Force and Department of Defense customers. The criterion of success for these customers is the correctness of the cloud amount forecast for a specific location at a specific time.³

The primary cloud forecast model at AFGWC is the 5LAYER model. The 5LAYER model forecasts cloud amounts on a 100 nm grid which covers essentially the northern and southern hemisphere extratropical regions. The moisture input to the 5LAYER is the RTNEPH (real-time nephanalysis) real time cloud analysis model.⁴ The RTNEPH blends high resolution satellite data and conventional data to generate a global cloud analysis on a 25 nm grid. The 5LAYER takes the RTNEPH input, smooths the cloud analysis to a 100 nm grid, converts the cloud analysis to a moisture analysis, advects the moisture along a forecast trajectory (computed from GSM wind velocity forecasts), and finally converts the moisture forecast to a cloud forecast.

This quasi-Lagrangian advection scheme was devised because prior to 1985 the AFGWC forecast model was a dry hemispheric primitive equation (PE) model. The only input to the 5LAYER cloud forecast from the PE model was the winds used to compute the trajectories.

The cloud forecast model used in the tropics is called TRONEW. TRONEW uses the concept of diurnal persistence, i.e., the assumption that the cloud cover that is occurring now will repeat itself every 24 hours. This tropical approach is more skillful thus far for cloud forecasting than the use of dynamic models except in the vicinity of moving tropical disturbances.

In 1985, AFGWC installed its Advanced Weather Analysis and Prediction System (AWAPS).⁵ AWAPS includes a high resolution analysis system, a global spectral model (GSM) and a relocatable window model (RWM). The GSM is essentially the model used by the National Meteorological Center (NMC) in the early 1980's.⁶ The NMC GSM was delivered to AFGWC in 1984. Of importance to the cloud forecasting operations at AFGWC is the fact that both the GSM and RWM are moist models. This means that, in theory at least, cloud forecasts can be generated directly from the operational numerical weather prediction model without recourse to an independent cloud forecast model.

Given the desirability of producing global cloud forecasts out to 96 hours using the GSM, there are two questions which must be addressed:

- (1) What cloud forecast scheme gives the most skillful forecasts in the GSM?
- (2) How skillful is the cloud forecast scheme determined in (1) above compared to the 5LAYER or TRONEW?

Cloud forecast schemes fall into two general categories: prognostic and diagnostic. Prognostic schemes predict cloud water/ice content explicitly. However, such schemes are not as clean as the name implies. In addition to being developmentally immature and computationally expensive, prognostic schemes rely on empirical relations between forecast variables and cloud amount forecasts in a manner similar to diagnostic schemes.

Diagnostic schemes, on the other hand, rely solely on the diagnosis of cloud amounts from numerical weather prediction model output fields. Type 1 diagnostic schemes rely solely on forecasts of relative humidity (or some comparable moisture variable) to empirically or statistically derive cloud amount forecasts.

The more complex type 2 diagnostic schemes empirically infer cloud cover from many model output fields. These include not only relative humidity, but also (typically) convective precipitation rate, PBL static stability, PBL inversion height, vertical velocity, wind shear, etc. These schemes therefore require models with complex parameterized physics. A well-known type 2 diagnostic scheme is that used by the ECMWF since May 1985 known as the Slingo⁷ scheme.

Since the AFGWC GSM does not have complex parameterized physics, it follows that any scheme considered for use with the AFGWC GSM must be a Type 1. The typical form of a Type 1 diagnostic scheme is:

$$CL_k = F_k [RH_k, RHC_k, RHm_k] \quad (1)$$

where F often takes the form

$$\left[\frac{RH_k - RHC_k}{RHm_k - RHC_k} \right]^{P_k}, 0 \leq RHC_k \leq RH_k \leq RHm_k \leq 1 \quad (2)$$

where,

- k = level index
- F = functional form of the equation
- P_k = exponent of non-linearity (parameter)
- CL_k = Cloud Amount forecast
- RH_k = Relative Humidity forecast
- RHC_k = Critical Relative Humidity (parameter)
- RHm_k = Maximum Cloud Relative Humidity (parameter)

In equation (2) above, the critical relative humidity is the average relative humidity for a grid volume at which non-zero fractional cloud cover is initially inferred. The concept of inferring non-zero cloud for grid volume mean $RH < 1$ comes from the fact that there is local variance about the mean which yields subgrid regions of saturation and, hence,

clouds. The maximum cloud relative humidity is the average relative humidity for a grid volume at which an overcast (100% cloud) cloud cover is inferred. The equation has six degrees of freedom. In addition to RH_k , RHC_k , RHm_k , and P_k , there is the possibility that P_k can vary in the range from RHC_k to RHm_k and that the functional form of the equation can vary from one forecast length to the next. In all, the specification of these parameters presents a formidable challenge.

The usual approach to specifying the equation above is to archive a set of meteorological data. This data is used to initialize the numerical model to make cloud predictions which are compared to observed cloud. The model is run numerous times until all six degrees of freedom have been subjectively tuned to give the most skillful cloud forecast and/or the best radiation budget. The RH-to-cloud transformation curves thus derived are then incorporated into the model for routine use. They should be retuned (but often are not) whenever a major change is made to the model, e.g., resolution, physics, etc.

In attempting to develop a cloud forecast capability for the AFGWC GSM the question then became: Should AFGWC borrow an existing cloud forecast scheme or would it be necessary to develop a scheme specifically for the AFGWC GSM? If the latter were true, what approach should be taken to develop the tailored scheme? The results of investigations are discussed below.

1.1 Summary of Previous Experimentation. The initial investigation into the possibility of using a borrowed scheme was performed by Mitchell and Warburton⁶. The purpose of this investigation was to determine if the cloud forecast scheme used by AFGWC's 5LAYER model could be incorporated into the AFGWC GSM. This investigation was conducted at the National Meteorological Center (NMC) using the then current NMC GSM (which is the one NMC gave to AFGWC in 1984). Verifying cloud analyses were taken from the 3DNEPH real-time cloud analysis model which was replaced by the RTNEPH in August 1983.

The moisture variable used by the 5LAYER is condensation pressure spread (CPS). CPS is the pressure difference in mb between the pressure of a given parcel of air and the pressure at which the parcel would become saturated if lifted dry adiabatically. Moisture is transformed to cloud and vice versa using a set of empirical CPS-to-cloud curves. There are curves for each of the five levels: gradient, 850 mb, 700 mb, 500 mb and 300 mb. The curves were derived in the early 1960's using a coincident sample of surface cloud reports and RAOBs⁶.

A graph of the CPS curves is shown in Figure 1. The curves follow the general form of equation (1) with the exception that CPS is the moisture variable as opposed to relative humidity. For a given input CPS value, a cloud amount forecast can be determined. Non-zero cloud amounts are found for CPS values in the range between the critical CPS and maximum cloud CPS. The exponent of non-linearity P does vary in the range between the critical CPS and maximum cloud CPS. The curves do not vary from one forecast length to another, from one region to another or from one season to another.

AFCWC SLAYER CPS CURVES

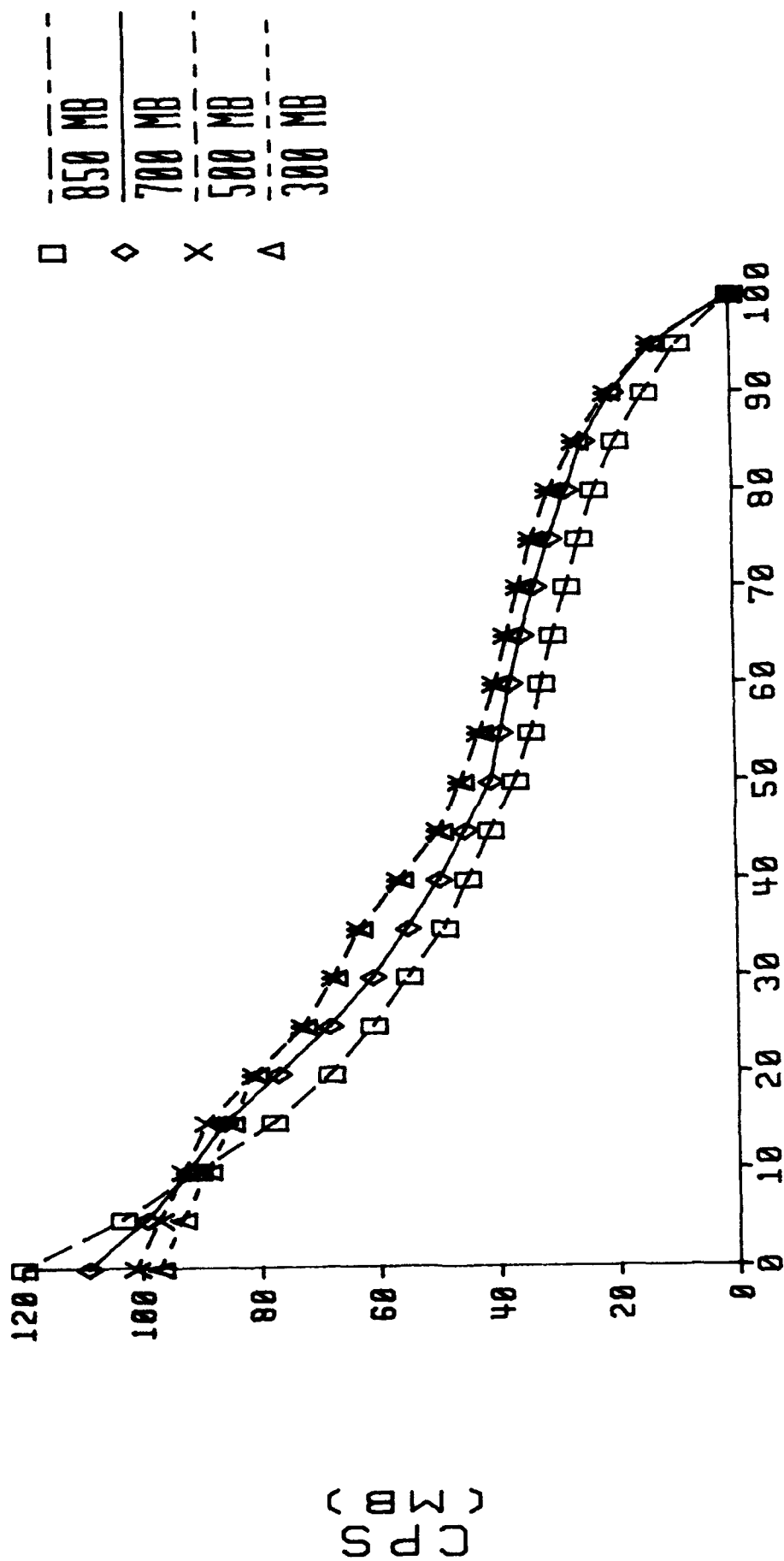


Figure 1
CLOUD AMOUNT (PERCENT)

The procedure used by Mitchell and Warburton was to use two different initial moisture fields, input them to the NMC GSM, convert the output moisture forecasts to cloud forecast and compare the results to 5LAYER cloud forecasts. One initial moisture field was taken from the 3DNEPH in the same way as 5LAYER. The second initial moisture field was the output of the global Hough analysis used operationally by NMC at the time.

The forecasts were compared using 20/20 scores and bias scores. The 20/20 score is the percentage of cloud forecast grid points verifying within 20% of the observed cloud amount. The bias is the mean forecast cloud minus the mean observed cloud. The 5LAYER outperformed both GSM approaches in 20/20 scores and showed minimal bias throughout the 48 hour forecast period. The GSM approaches both showed significant moist biases which reached their maxima at 24 hours and stayed relatively constant thereafter.

Two changes to the GSM forecasts yielded better results. The first was to ignore 1000 mb and 300 mb moisture. The second was to use the GSM initialized with 3DNEPH derived moisture to compute a GSM cloud forecast trend which was then added to the original 3DNEPH analysis. The use of the two changes improved the 20/20 scores to the point that it appeared that the GSM cloud forecasts could outperform 5LAYER forecasts after 12 hours, but some means of further reducing the layer bias needed to be found.

In 1984, AFGWC implemented a developmental version of their GSM. (The GSM became operational in October 1985 after the installation of the CRAY X-MP/12 supercomputer.) This in conjunction with the transition to the RTNEPH in August 1983 meant that investigation of Mitchell and Warburton could be expanded. The Phillips Laboratory (then called the Air Force Geophysics Laboratory (AFGL)) obtained archives of 5LAYER forecasts, AFGWC developmental GSM forecasts and RTNEPH verifying cloud analyses from AFGWC. The Phillips Laboratory had developed what was called the AFGL Baseline GSM which duplicated the AFGWC GSM but was modified to run on the CRAY-1/S at the Air Force Supercomputer Center at Kirtland AFB, New Mexico.

This follow-on investigation was conducted by Mitchell and Hahn¹⁰. The investigation included the AFGWC CPS-to-cloud curve approach plus the RH-to-cloud approaches of the NMC and the European Centre for Medium Range Weather Forecasts (ECMWF).

The NMC curves follow the approach of equation (1) in the following manner:

$$CL_k = (100/\pi) \{ \text{ARCCOS}[(M_k - RH_k)/A_k] \}, \quad (3)$$

$$M_k - A_k = RH_c \leq RH_k \leq RH_m = M_k + A_k$$

where M_k and A_k are empirical constants that vary vertically with pressure and

$$CL_k = 0 \text{ if } RH_k < RH_c \quad \text{and} \quad CL_k = 100 \text{ if } RH_k > RH_m$$

The NMC scheme is an example of one which uses $RH_m < 1$. The latter choice recognizes the possibility that a layer of overcast cloud may be thinner than the model layer, i.e. vertically subgrid in scale.

The ECMWF curves, also known as the Geleyn scheme, follow the approach of equation (2) in the following manner:

$$CL_k = \left[\frac{RH_k - RHC_k}{1 - RHC_k} \right]^2, \quad 0 \leq RHC_k \leq RH_k \leq 1 \quad (4)$$

$$\text{where } RHC_k = 1 - 2\sigma_k + 2\sigma_k^2 + 1.732\sigma_k(1 - 3\sigma_k + 2\sigma_k^2)$$

where $\sigma_k = P_k/P_*$, the ratio of the mid-layer pressure, P_k , to the surface pressure, P_*

In addition to the verification of the above schemes over the northern hemisphere extratropical grid used by 5LAYER (known as the NH octagon), these schemes were verified over the United States and Europe. The results of the verifications were disappointing, demonstrating that the existing schemes:

- (1) showed a very large spin-up (increase) in cloud amounts in the first twenty-four hours of the GSM forecast
- (2) showed unacceptably large positive and negative biases
- (3) did not surpass 5LAYER accuracy with any consistency whatsoever

The disappointing performance of the existing cloud forecast schemes led to the conclusion that a diagnostic humidity to cloud scheme for a given model (in this case the AFGWC GSM) must be developed specifically for that particular model. Also, the scheme must account for any bias in the model domain-mean humidity and the frequency distribution of humidity in the model's humidity forecast fields. This was because these two humidity properties:

- (1) showed significant change during a model's spin-up period
- (2) reached a model-preferred state after spin-up
- (3) varied with height
- (4) varied by geographic region

Because of the large number (6) of degrees of freedom in equations (1) or (2) an objective method of specifying them was needed. Of importance to this procedure was that the RTNEPH provided an objective, gridded, 3-D cloud analysis data base (as opposed to a satellite image or zonal average cloud climatology). Therefore, it was possible to determine frequency distributions of cloud amounts. It followed that relating GSM frequency distributions of humidity with RTNEPH frequency distributions of cloud amount could provide the necessary objective linkage.

A straightforward method whereby the two frequency distributions can be related is shown in Figure 2 (after Mitchell and Hahn¹⁰). The key to the linkage is the use of the cumulative percent frequency distributions of both cloud amount (bottom of Figure 2, part a) and relative humidity (bottom of Figure 2, part b). The mapping shown in Figure 2 is from cloud amount to relative humidity primarily to determine RHC_k , but the mapping can be done in reverse to transform a forecast relative humidity to a cloud forecast. In practice, the mapping results in a single relative humidity-to-cloud curve, a sample of which can be seen in Appendix A, Figure A-2. These curves vary by layer. At this point it becomes apparent that the curves follow the general form of equation (2). First, there is a curve for each layer as denoted by the k subscript. The y-axis specifies an input value of forecast RH while the x-axis corresponds to an output value of forecast cloud amount. There is a value of critical RH and maximum cloud RH for each layer. Finally, the exponent of non-linearity and functional form of the equation are determined by the mapping of the distributions of RH and cloud amount.

The results were encouraging. The objective scheme, now known as the cloud curve algorithm (CCA), reduced the bias when verified over the NH octagon but not when verified over the U.S. or Europe. This reflects the variability of the humidity distributions with geography mentioned above. The CCA can handle that variability, but that could not be tested in the Mitchell and Hahn effort because of the limited number of GSM forecast cases at hand.

In terms of skill as shown by total cloud 20/20 scores, 5LAYER was definitely superior in the 0 to 12 hour range. CCA was superior to any of the existing GSM schemes and sometimes outperformed 5LAYER at 24 hours and beyond over the U.S. and Europe. The superiority of 5LAYER in the 0 - 12 hour range was determined to be because of its direct access to RTNEPH analyses as its source of initial moisture information. The procedure is described in Section 1 above. The 5LAYER therefore has detailed initial moisture information over the entire extratropics. The GSM, on the other hand, has an RH analysis on the equivalent of a 200 nm grid spacing with input RH information only over land from RAOBs. This grid spacing is maintained throughout the forecast cycle. In addition, GSM errors are introduced in the conversion from spectral space to grid space and in the conversion from sigma layers to pressure levels. In the GSM postprocessing, these highly smoothed RH analyses and forecasts are interpolated to the same 100 nm spacing used by 5LAYER for the computation of RH-to-cloud curves and the conversion of RH forecasts to cloud forecasts.

The results were encouraging enough to warrant a second follow-on effort which is described below.

1.2 Description of the Current Experiment. The project described in this section was a 6.3 advanced development which continued the efforts of Mitchell and Warburton and Mitchell and Hahn. In that regard, it was intended to determine if CCA using the AFGWC GSM was skillful enough to be incorporated into the AFGWC cloud forecast operations. In addition, this advanced development sought to test the CCA extensions recommended by Mitchell and Hahn, namely:

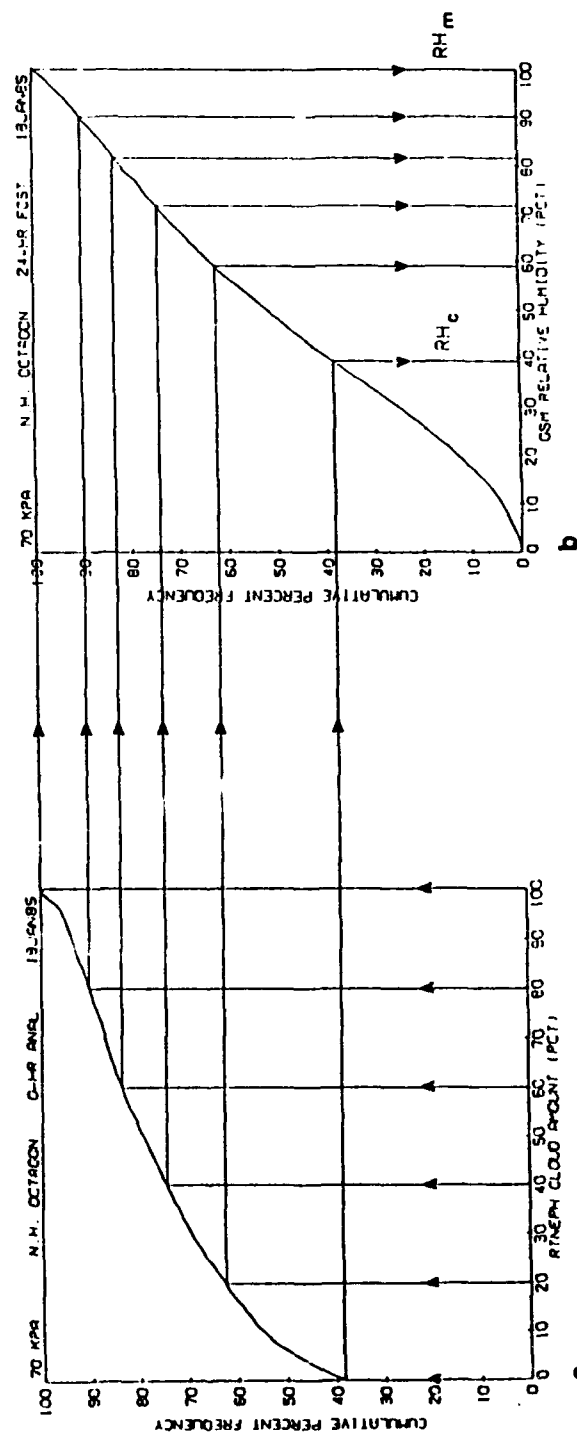
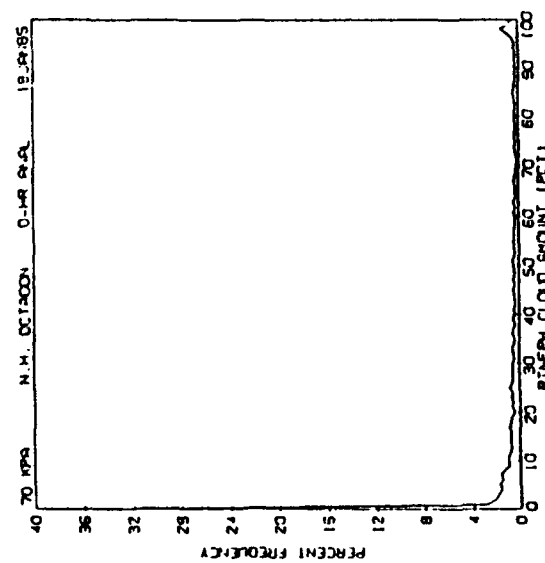
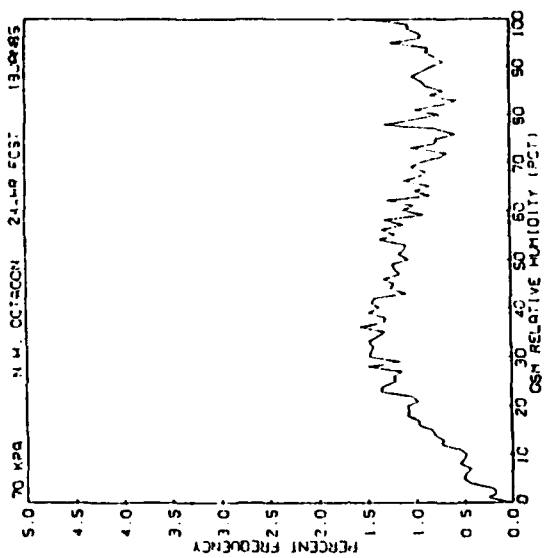


Figure 2

- (1) regional stratification (including land vs water)
- (2) use of a RH trending technique
- (3) real-time update of curves
- (4) output of GSM RH forecasts on sigma layers to reduce post-processing

The last item had to be deleted because AFGWC did not have the resources to generate the new data bases external to the GSM processing.

It is important to note that the CCA is an objective diagnostic cloud forecast scheme which can be used with any numerical weather prediction model. If a real-time cloud analysis model, say the RTNEPH, is available, then a real-time update of the relative humidity to cloud curves (or, more simply, cloud curves) is possible. The CCA approach is being used by other groups. The CCA approach was developed independently by Rikus and Hart¹¹. They developed their scheme for use with the Australian Bureau of Meteorology Research Centre GSM and the International Satellite Cloud Climatology Program (ISCCP) cloud profiles. Campana, et. al.¹² are investigating the use of CCA with the NMC GSM and RTNEPH analyses which are being shipped to NMC on a real-time basis via the shared processing network.

The original concept for this project specified a 3 season (9 month) quasi-production effort to run in parallel with the other cloud forecast models at AFGWC. Because of the large number of variations to be evaluated, the storage of cloud forecasts was a physical impossibility. Therefore, relative humidity forecast and cloud curves were stored. When a verifying cloud analysis became available, a cloud forecast was computed. It was kept long enough to verify then discarded. As a result, even though running in parallel with AFGWC operations, CCA forecasts were never seen by AFGWC operations personnel, but in special cases were archived and examined by development personnel.

However, during the July 1990 to April 1991 evaluation period, the decision was made by the Phillips Laboratory to evaluate additional variations in the CCA scheme. As result, a Phase II effort was conducted from July 1991 to December 1991.

The pilot study by Mitchell and Hahn was performed over the NH octagon, on 6 pressure levels (1000 mb, 850 mb, 700 mb, 500 mb, 400mb, and 300 mb), and for 5 forecast lengths (00, 12, 24, 36 and 48 hours). Given that one curve was computed for each combination of geographical region, pressure level and forecast length there were 30 curves involved.

The Phase I CCA effort evaluated numerous variations on the basic CCA approach. The GSM relative humidity forecasts on 6 pressure levels had to be compacted to 3 layers (low, middle, and high) to match the operationally available 100 nm grid cloud analyses and forecasts. Since the GSM is a global model, two hemispheric cloud analyses (northern and

southern) had to be synthesized using 5LAYER (extratropics) and TRONEW (tropics) RTNEPH-based analyses. The other variations that were developed and evaluated were:

- (1) application of real-time update of CCA curves
- (2) division of the world into 14 regions (areal stratification)
- (3) two candidate schemes for compacting 6 GSM output moist pressure levels into three layers
- (4) three candidate stacking schemes for computing total cloud from input low, middle and high layer clouds
- (5) use of a relative humidity trend approach in addition to the basic CCA methodology

In the Phase II effort, the superior Phase I configuration for both the basic and trended approaches were determined. Then the following variations were developed and evaluated:

- (1) further areal stratification
- (2) use of a diurnal correction similar to that used by 5LAYER
- (3) use of vertical velocity as an additional predictor

The procedure for computing a cloud curve is straightforward. For each cloud analysis, count the number of occurrences of each cloud amount value. In this project, the cloud amounts were stored in multiples of 10% (0%, 10%, 20%, ..., 100%). For each relative humidity forecast, count the number of occurrences of each relative humidity value. In this project, the relative humidities were available in 0.1% increments but were rounded to 1% increments. This counting procedure continues for a specified period and a running tally of occurrences is kept. Two counting periods were evaluated. Counts were kept for one week and 4 week periods. Then once a week, the frequency of occurrence distributions were transformed into cumulative frequency of occurrence distributions and then percent cumulative frequency of occurrence distributions. The respective percent cumulative frequency of occurrence distributions were then mapped to each other to form relative humidity to cloud and cloud to relative look-up tables. The reason for computing both will become clear in the discussion of the relative humidity trend approach. The curves based on one week counts were called weekly curves. The curves based on 4 week counts were called monthly curves.

One refinement to the procedure described above needs to be explained. The critical relative humidity values obtained in the mapping are usually no lower than 30% and can go as high as 90%. It is therefore desirable to expand the scale of moist relative humidity values since those are the ones associated with cloud formation. To do that, the transformation of RH to RH^* is used (Rasmussen¹³). It is given as:

$$RH^* = 1 - (1 - RH)^{1/2} \quad 0 \leq RH \leq 1 \quad (5)$$

The effect of the transformation is shown below (after Mitchell and Hahn^o):

<u>RH</u>	<u>RH*</u>
1.0	1.0
0.90	0.68
0.80	0.55
0.70	0.45
0.60	0.37
0.50	0.29
0.40	0.23
0.30	0.16
0.20	0.11
0.10	0.05
0.00	0.00

So while internal to the algorithm RH* is the variable being manipulated, all references in the text and all figures will be in terms of relative humidity.

Since humidity distributions vary by geographical region, the globe was divided into 14 regions. They were:

- (1) Entire Globe
- (2) Northern Hemisphere Extratropical
- (3) Global Tropical
- (4) Southern Hemisphere Extratropical
- (5) Northern Hemisphere Polar
- (6) Northern Hemisphere Mid-Latitude
- (7) Southern Hemisphere Mid-Latitude
- (8) Southern Hemisphere Polar
- (9) Northern Hemisphere Mid-Latitude Land
- (10) Northern Hemisphere Mid-Latitude Ocean
- (11) Southern Hemisphere Mid-Latitude Land
- (12) Southern Hemisphere Mid-Latitude Ocean
- (13) Tropical Land
- (14) Tropical Ocean

Curves were computed for each of the 14 regions. The 14 regions also constituted verification areas. That is, each global cloud forecast was verified over each verification area. The reason for this was that 3 global forecast scenarios were evaluated. The scenarios were defined as follows:

- (1) use only the global curve for the global forecast
- (2) use the polar, mid-latitude and tropical curves in combination to form the global forecast (regions 3, 5, 6, 7 & 8)
- (3) additionally divide the mid-latitude and tropical regions by land vs. ocean to form the global forecast (regions 5, 8, 9, 10, 11, 12, 13, & 14)

These procedures were needed to thoroughly investigate the effect of increasing areal stratification of curves.

Since a moist bias in the 1000 mb relative humidity in the AFGWC GSM had been identified and since Mitchell and Warburton had had success in ignoring 1000 mb moisture, a scheme to further evaluate the effect of the bias was incorporated. In the compaction from 6 pressure levels into three layers, two low layers were defined. Low layer L1 excluded 1000 mb relative humidity. From July 5, 1990 to August 29, 1990 it was excluded only over water. It was excluded everywhere after that. Low layer L2 included 1000 mb relative humidity.

One of the more vexing problems is the computation of total cloud from input layer cloud amounts. One facet of the problem is that depending on the horizontal orientation of the clouds in each layer, the total cloud for a given set of input layer cloud amounts can vary. Therefore, the total cloud can only be estimated. Three total cloud stacking schemes were evaluated: maximum overlap, random overlap, and tuned overlap. The details of computing each are given below:

To obtain a forecast of total cloud from a forecast of cloud cover at several layers, a vertical cloud stacking algorithm must be used. Cloud stacking algorithms usually fall into one of two categories, the assumptions of either maximum cloud overlap or random cloud overlap. In a more general algorithm applied here, taken from that used in the 5LAYER model, a free parameter referred to as the stacking factor R is used to compute maximum overlap, random overlap and, falling anywhere in-between the first two, a tuned overlap.

Given two cloud layers A and B with A denoting the largest, the cloud amount values can be divided by 100 to give fractions between 0 and 1. In this case they are respectively CA and CB, where $CA \geq CB$. If cloud presence in one layer is considered an event independent of cloud presence in the other layer, i.e., random vertical alignment, then the vertically superimposed overlap of the two layers is the product $CA*CB$. The total or combined sky cover fraction, CC, of the two layers is then given by:

$$CC = CA + CB - CA*CB \quad (6)$$

or equivalently,

$$CC = CA + (1 - CA)*CB \quad (7)$$

Equation (6) shows that CC can be viewed as the cloud fraction from layer A plus that part of cloud layer B randomly aligned over the clear area of layer A. Actual experience shows, however, that cloud presence in one layer is often positively correlated with cloud presence in another layer. The correlation is greater for smaller layer separation distances. To account for this observation, the stacking algorithm to be used in this project generalizes Eq. (6) by introducing a "stacking factor" R, such that,

$$CC = CA + (1 - CA) * CB * R, \quad (8)$$

where, $CA > CB$ and $0 < R < 1$

The two limiting cases of $R = 0$ and $R = 1$ yield the cloud amount, respectively, for maximum overlap ($CC = CA$) and random overlap ($1 \leq CC \leq CA$, where $CC = 1$ if $CA = 1$). Intermediate values of R give combined cloud amounts falling between these limiting values.

The application of the intermediate values of R is as follows:

High Layer.....	.	
	.	
Total
Middle Layer..	.	
	.	
Semi-Total.
	.	
Low Layer.....	.	

$$\text{Semi-Total CC} = CA + (1 - CA) * CB * R1 \quad (9)$$

Total CC = CA + (1 - CA)*CB*R2, if low > middle (10)

Total CC = CA + (1 - CA)*CB*R3, if middle > low (11)

In the limiting case of maximum overlap, $R_1 = R_2 = R_3 = 0$. In the case of random overlap, $R_1 = R_2 = R_3 = 1$. In the tuned overlap case, the values $R_1 = R_2 = R_3 = 0.55$ were determined during system testing by comparing CCA computed total cloud and TRONEW/5LAYER observed total cloud and adjusting R_1 , R_2 , and R_3 until the mean absolute difference was minimized.

Since there were two low layers (L1 and L2) and 3 stacking schemes, there were 6 total cloud forecasts. They were labeled as follows:

T1	low layer 1, maximum overlap
T2	low layer 1, random overlap
T3	low layer 1, tuned overlap
T4	low layer 2, maximum overlap
T5	low layer 2, random overlap
T6	low layer 2, tuned overlap

As cited above, one of the strengths of the 5LAYER is that it has access to global moisture information on a 25 nm grid by way of the RTNEPH. One of the weaknesses of the GSM is that it has moisture information only from RAOBs over land on a 200 nm grid. One of the approaches to mitigate this GSM weakness successfully tried by Mitchell and Warburton was the use of a cloud trend (see section 1.1). The

trending approach used in this effort is a relative humidity trend approach which tries to incorporate the initial relative humidity information inherent in the RTNEPH. The method is as follows:

- (1) From the N-hour GSM RH forecast subtract the 0-hour GSM RH analysis to compute an N-hour RH trend at each grid point and layer
- (2) Convert the 0-hour RTNEPH 100 nm cloud analysis to a 0-hour DH (derived humidity) analysis using the appropriate cloud to RH curve
- (3) Add the 0-hour RTNEPH DH analysis to the N-hour GSM RH trend to get an N-hour DH forecast
- (4) Convert the N-hour RTNEPH DH forecast to an N-hour cloud forecast using the appropriate RH to cloud curve

In Phase II, the focus shifted from a global forecast to a northern hemisphere forecast. This was done to allow further areal stratification without a major data base redesign. Four additional regions were added (see Figure 3):

- (1) North America Land
- (2) European Land
- (3) East Asia Land
- (4) North Africa/Middle East Land

The regions above were chosen by examining the 3DNEPH climatology for 1979 (Henderson-Sellers and Hughes¹⁴). One of the features that was important to consider is the persistent cloud minima over the Afro-Asia deserts which reaches its maximum extent in spring. The other areas were chosen by a subjective examination of the January and July climatologies.

One of the consequences of the lack of an advanced parameterization of physical processes in the AFGWC GSM is an inability to capture the effects of the diurnal solar heating cycle. This is due to a lack of PBL parameterizations over land and radiation parameterizations over both land and ocean. One approach to capturing this diurnal signal would be to further stratify curves by forecast valid time in addition to stratification by forecast length. This approach was not pursued because of the resources required to redesign the code and data bases. A second approach is the one used by 5LAYER, which is to keep track of the diurnal fluctuations in the RTNEPH cloud analyses for the preceding 48 hours. If a diurnal signal is found, it is applied to the current forecast cycle.

The impetus for including a diurnal correction in Phase II was the presence of a strong diurnal signature in the early Phase I results. An example of a strong diurnal signature can be seen in the persistence forecast skill scores shown in Figure I (Executive Summary). The strong peaking at 24, 48 and 72 hours is indicative of a strong diurnal persistence in the cloud cover. The fact that 5LAYER uses a diurnal

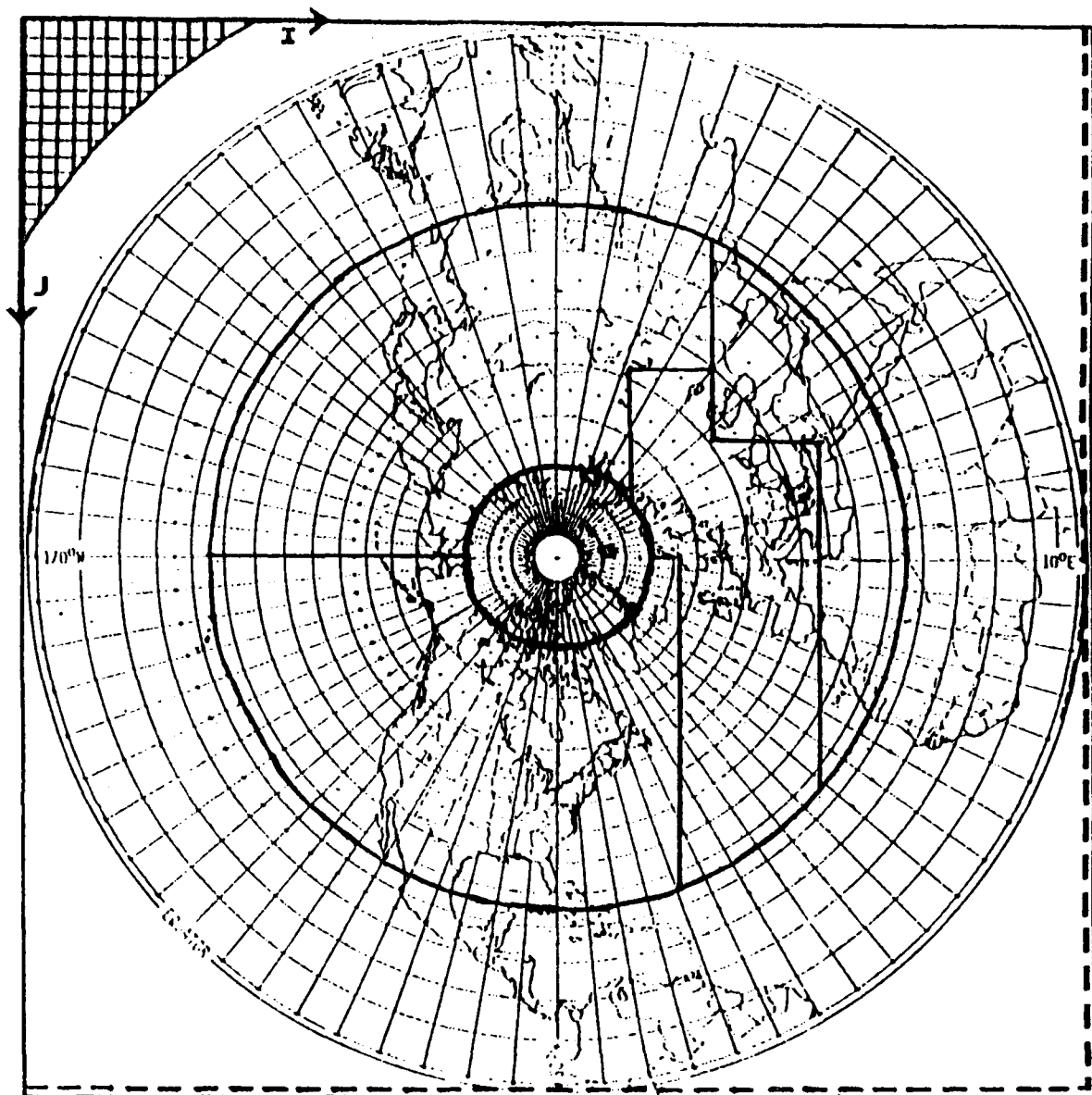
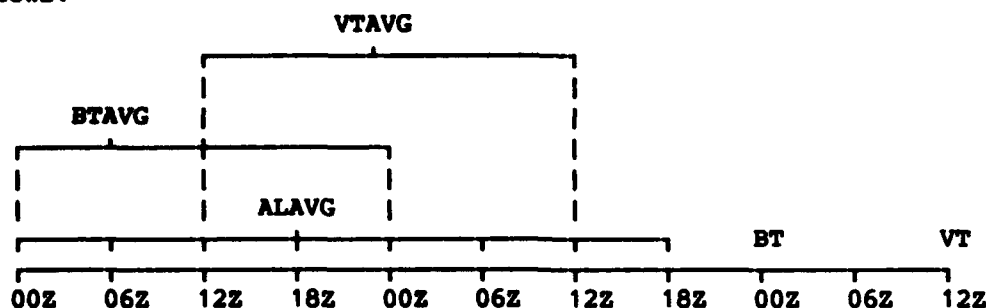


Figure 3

correction further strengthened the concept that a diurnal correction in the CCA would be of benefit. The diurnal correction is computed as follows:



The diagram above illustrates the case of a 12 hour cloud forecast valid at 12Z. There is a cloud analysis for the basetime (BT) of 00Z which will be denoted BTANAL. The procedure is to then average the two previous 00Z cloud analyses (on grid point by grid point basis) to obtain a basetime average analysis BTAvg. Similarly, since the forecast to be modified has a 12Z valid time, the two previous 12Z analyses to obtain a valid time average analysis VTAvg. In addition, the average of the eight analyses immediately prior to the 00Z base time is computed to obtain an average of all eight analyses ALAVG. The next step is to determine the degree of diurnal signal in the cloud analyses. If the difference between the cloud amount at a given grid point for BTANAL and BTAvg is zero, then the diurnal signal is strong and the diurnal correction is given a weight of 1. If the difference is 30% or greater, we conclude there is no diurnal correlation and the diurnal correction is given a weight of 0. For differences between 0% and 30%, the weight of the diurnal correction is determined by:

$$\text{WEIGHT} = 1 - (\text{ABS}(\text{BTANL} - \text{BTAvg})/30), 0 \leq \text{WEIGHT} \leq 1 \quad (12)$$

The diurnal correction DIUCOR for the 12Z is the product of the diurnal signal at 12Z over the previous 48 hours and the weight determined above. It is thus computed using the equation below at every grid point:

$$\text{DIUCOR} = \text{WEIGHT} * (\text{VTAvg} - \text{ALAVG}) \quad (13)$$

Therefore the final 12Z cloud forecast is computed by first applying the CCA technique and then adjusting it by adding in the diurnal correction DIUCOR on a grid point by grid point basis.

Finally, at the request of AFGWC vertical velocity was included as a secondary predictor of cloud formation. A study by Peterson and Hutchison¹⁰ concluded that the use of vertical velocity reduced the root-mean-squared difference between expected cloud and RTNEPH observed cloud. The incorporation of vertical velocity into the CCA scheme was accomplished by adding an additional stratification of curves based on whether the forecast vertical velocity was either up or down.

One more subject needs to be addressed before looking at the results of the development effort. Since this project sought to determine the viability of incorporating CCA cloud forecasts into AFGWC operations, the skill of CCA had to be determined in the same way that AFGWC tracks the

skill of its operational 5LAYER cloud forecast model. AFGWC computes a series of verification statistics based on a grid point to grid point comparison between cloud forecast arrays and verifying RTNEPH-based analysis arrays. If the satellite data input to the analysis was more than 4 hours old, it was not included in the verification.

The results of that grid point to grid point comparison over a given region and verification period are plotted in an 11 x 11 contingency matrix, or table. The x - axis is forecast cloud amount values 0, 10, 20, 30, ..., 100. The y - axis is analysis cloud amount values 0, 10, 20, 30, ..., 100. The result is a table with the form shown below:

	j	A _j												
A N A L Y S I S	11	100*	n _{1,11}		n _{5,11}						n _{11,11}			
	10	90*												
	9	80*												
	8	70*												
	7	60*												
	6	50*												
	5	40*	n _{1,5}		n _{5,5}						n _{11,5}			
	4	30*												
	3	20*												
	2	10*												
	1	0*	n _{1,1}		n _{5,1}						n _{11,1}			
			*	****	****	****	****	****	****	****	****	****	****	*
			0	10	20	30	40	50	60	70	80	90	100	F ₁
			1	2	3	4	5	6	7	8	9	10	11	i ₁
FORECAST														

The contingency table and its contents are described using the following variables:

$n_{i,j}$ = the number of grid points whose forecast and verifying cloud amounts correspond to the i,j element of the table

n_i = total number of grid points in forecast category i
 $= \sum_{j=1}^{11} n_{i,j}$

n_j = total number of grid points in analysis category j
 $= \sum_{i=1}^{11} n_{i,j}$

S = total number of grid points in the entire 11 x 11 array
 $= \sum_{j=1}^{11} \left[\sum_{i=1}^{11} n_{i,j} \right]$

c_{ij} = the chance that a given forecast will be in the i, j element of the array

$$= \frac{n_{ij}}{S}$$

F_i = $10*(i-1)$ = forecast cloud amount associated with category i

A_j = $10*(j-1)$ = analysis cloud amount associated with category j

A'_i = average analysis cloud amount of forecasts in forecast category i

As an aside, a similar contingency table could be computed with forecast RH vs observed cloud (as opposed to forecast cloud). Such an approach could be used in a 'poor-man' MOS approach.

The verification statistics fall into two general classes. The first is the percentage of grid points whose cloud forecasts satisfy some criteria within the table. In this report those statistics are presented in the range of 0 to 1. The second is those statistics which illustrate the mean difference, or error, between cloud forecasts and verifying cloud analyses. These are presented as whole numbers. The statistics to be calculated are discussed and their equation given below:

The 20/20 score is the percentage of forecasts verifying within 20% (two categories) of the observed cloud amount.

$$20/20 \text{ Score} = S_{20} = \frac{1}{S} \sum_{j=1}^J \sum_{i=j-2}^{j+2} n_{ij} \quad (14)$$

The chance 20/20 score is the chance percentage of forecasts verifying within 20% of the observed cloud amount.

$$\text{Chance } 20/20 \text{ Score} = C_{20} = \frac{1}{S} \sum_{j=1}^J \sum_{i=j-2}^{j+2} c_{ij} \quad (15)$$

The Heidike skill score is a ratio involving the 20/20 score and chance 20/20 score.

$$\text{Heidike Skill Score} = H = \frac{S_{20} - C_{20}}{1 - C_{20}} \quad (16)$$

Bias is the difference between the mean forecast cloud amount and the mean observed cloud amount averaged over an entire region over the entire verification period.

$$\begin{aligned}
 \text{Bias} &= \frac{1}{S} \sum_{j=1}^J \sum_{i=1}^I n_{ij} * (F_i - A_j) \\
 &= \frac{10}{S} \sum_{j=1}^J \sum_{i=1}^I n_{ij} * (i-j)
 \end{aligned} \tag{17}$$

RMSE is the root mean square error of the forecast cloud.

$$\begin{aligned}
 \text{RMSE} &= \left[\frac{1}{S} \sum_{j=1}^J \sum_{i=1}^I n_{ij} * (F_i - A_j)^2 \right]^{1/2} \\
 &= \left[\frac{100}{S} \sum_{j=1}^J \sum_{i=1}^I n_{ij} * (i-j)^2 \right]^{1/2}
 \end{aligned} \tag{18}$$

The chance RMSE is the RMSE error if the forecast were based solely on chance.

$$\begin{aligned}
 \text{Chance RMSE} &= \left[\frac{1}{S} \sum_{j=1}^J \sum_{i=1}^I c_{ij} * (F_i - A_j)^2 \right]^{1/2} \\
 &= \left[\frac{100}{S} \sum_{j=1}^J \sum_{i=1}^I c_{ij} * (i-j)^2 \right]^{1/2}
 \end{aligned} \tag{19}$$

The MAE is the mean absolute error of cloud forecasts.

$$\begin{aligned}
 \text{MAE} &= \frac{1}{S} \sum_{j=1}^{11} \left[\sum_{i=1}^{11} n_{ij} * \text{ABS}(F_i - A_j) \right] \\
 &= \frac{10}{S} \sum_{j=1}^{11} \left[\sum_{i=1}^{11} n_{ij} * \text{ABS}(i-j) \right] \quad (20)
 \end{aligned}$$

Sharpness is the percentage of cloud forecasts in the ranges 0% to 20% and 80% to 100%.

$$\text{Sharpness} = \sum_{j=1}^{11} \left[\frac{1}{S} \sum_{i=1}^3 n_{ij} + \sum_{i=9}^{11} n_{ij} \right] \quad (21)$$

Chance sharpness is the sharpness observed if the forecasts were based solely on chance.

$$\text{Chance Sharpness} = \sum_{j=1}^{11} \left[\frac{1}{S} \sum_{i=1}^3 c_{ij} + \sum_{i=9}^{11} c_{ij} \right] \quad (22)$$

It turns out that chance sharpness values are identical to the sharpness values and were not used.

The reliability is the sum of the weighted mean average errors for each forecast category (0%, 10%, ..., 100%) subtracted from 100.

$$\text{Reliability} = 100 - \sum_{i=1}^{11} \left[\frac{1}{S} \sum_{j=1}^{11} n_{ij} * \text{ABS}(F_i - A'_j) \right] \quad (23)$$

$$\text{where } A'_j = \frac{1}{n_j} \sum_{i=1}^{11} n_{ij} * A_j = \frac{10}{n_j} \sum_{i=1}^{11} n_{ij} * (j-1)$$

The bust score is the percentage of forecasts verifying 90% or more in error

$$\text{Bust Score} = \frac{1}{S} \left[\sum_{j=9} \left| \sum_{i=1}^3 n_{ij} \right| + \sum_{j=1}^3 \left| \sum_{i=9} n_{ij} \right| \right] \quad (24)$$

The experiment described above generated a large volume of verification statistics. As a result, data reduction was a formidable task. There were four global forecasts verified every 6 hours (global curve, latitude band curves, latitude band + land/ocean curves and the ECMWF Geleyn scheme). The global forecasts were verified over 14 areas. In addition, there were weekly and monthly versions of each curve. There were both the non-trended and trended approaches. There were 13 forecast lengths to verify. There were four layers to consider and 6 total cloud results to verify. Figure 4 shows a sample page of verification statistics. This page is for 1 scenario, 1 area, and 1 verification statistic. These statistics were computed weekly for each of four weeks in a 'month' and monthly for the entire four week verification period. The legend for Figure 4 is:

NT = non-trended
 TR = trended
 MM = monthly statistics (W1 would be week 1, etc)
 LY = 5LAYER
 PE = persistence
 L1 = CCA layer L1
 L2 = CCA layer L2
 LL = 5LAYER and persistence low layer
 MM = also used for middle layer
 HH = high layer
 W = indicates weekly curve
 M = indicates monthly curve
 T1 - T6 = indicates total cloud stacking schemes 1 through 6

The approach in the next section is to attempt to summarize the performance of CCA using snapshots of algorithm performance.

2. SUMMARY OF RESULTS.

This project had three main objectives:

- (1) To test variations in the CCA methodology to determine the superior configuration in the AFGWC GSM
- (2) To perform inter-model skill comparisons between CCA (using the AFGWC GSM) and AFGWC's current cloud forecast models (5LAYER in the extratropics and TRONEW in the tropics), persistence and diurnal persistence (which TRONEW uses)
- (3) To perform inter-model skill comparisons between CCA (using the AFGWC GSM) and the Geleyn scheme used operationally until May 1985 in the European Center for Medium Range Weather Forecasting (ECMWF) GSM to diagnose cloud for their radiation scheme (using the AFGWC GSM).

All of the objectives of the project were met. This discussion of the results is divided into four parts. The first part is a discussion of the relative humidity (RH) to cloud curves generated in the course of the development. The second is a discussion of the skill of the basic CCA scheme. The third part is a discussion of the effect of the use of the RH trend approach on the skill of the algorithm. The fourth part is a discussion of the shaded hemispheric display of cloud and relative humidity in Appendix I.

2.1 Cloud Curve Algorithm Relative Humidity to Cloud Curves.

One of the keys to understanding the significance of the cloud curve algorithm is to examine the nature of the curves derived and compare them to curves generated by another well-known, respected technique. In this case, the other scheme is the Geleyn scheme shown in Equation 4. The reason for including it in this study is to reinforce the notion that borrowing a scheme from another numerical weather prediction model is not a superior method of developing a cloud prediction scheme for the AFGWC GSM.

All the curves to be discussed are shown in Appendix A. The first curves shown (Figure A-1) are the ECMWF curves used in this project. The ECMWF scheme (like 5LAYER) has only one degree of freedom, namely the dependence of the critical relative humidity on the height (i.e., sigma) of the model layer. There is no dependence on region, forecast length or season. It is this inflexibility which leads to the large biases found in applying the ECMWF scheme to the AFGWC GSM. The low, middle and high layers used were designed to match the design of the layers in the 3 layer output of the verifying RTNEPH and the 5LAYER and TRONEW models. The layers were defined: low layer sigma = 0.8 to 1.0, middle layer sigma = 0.5 to 0.8 and high layer sigma = 0.0 to 0.5.

The next set of curves (Figure A-2) is a set of CCA curves that vary by layer. At this point it becomes apparent that the CCA curves follow the general form of equation (1). First, there is a curve for each layer as denoted by the k subscript. The y-axis specifies an input value of forecast RH while the x-axis corresponds to an output value of forecast cloud amount. There is a value of critical RH and maximum cloud RH for

each layer. The values of critical RH range from 42% to 74%. As with all CCA curves, the value of the maximum cloud RH turned out to be 100%. Finally, the exponent of non-linearity and functional form of the equation are determined by the mapping of the distributions of RH and cloud amount. In addition, unlike the ECMWF curves in Figure A-1 which are applied over the entire globe for every forecast length, the CCA curves in Figure A-2 are stratified by region and forecast length. The elegance of the CCA is that each of the degrees of freedom is solved objectively by the nature of the given forecast model RH and verifying cloud amount distributions.

One other subject of note involves an appreciation for information that the curves impart. There are times when the curves seem quite the same when there is in fact a large variation in their nature. The key is to maintain a horizontal orientation rather than the vertical one which the eye tends to take. For instance, in the variation by layer in Figure A-2 an input forecast of 75% RH yields:

- 2% cloud for the high layer (HH)
- 10% cloud for the low layer (L2)
- 25% cloud for the low layer (L1)
- 47% cloud for the middle layer (MM)

Therefore, it is the separation of the curves in the horizontal that is significant.

The last thing to note about the variation by layer in Figure A-2 is that both of the two low layers (L1 and L2) are shown. One result of the development is that the 1000 mb GSM moist bias had a significant negative impact on the CCA results. Note that L1 curves require less input RH than the L2 curves for a given cloud amount which is consistent with the fact that the L1 curves ignore the overly moist 1000 mb GSM RH. More skillful results came from using low layer L1. In the curve plots that follow, the low layer used is L1.

The next set of three plots (Figures A-3 to A-5) show the variability of weekly vs monthly curves (defined on page 10) for the low, middle and high layers. Weekly curves are preferred from the standpoint of responsiveness to changes in the GSM or RTNEPH models themselves. The concern was that weekly curves would be too sensitive to the synoptic situation of the week in which counts were being made which would distort the forecasts for the week during which the curve was used. Despite the fact that the weekly and monthly curves appear virtually identical, in those regions of the curves with flat slopes there can be as much as a 5% difference in cloud amount for the same input RH (see the plot for the low layer with an input RH of 65%). However, over the course of the experimentation, the differences averaged out. The various skill scores showed that both weekly and monthly curves showed virtually the same skill. In phase II, bi-weekly curves were used to ensure an adequate statistical sample over the mid-latitude land sub-regions.

Next, we look at curve variability by forecast length with plots for each layer (Figures A-6 to A-8). Included in the plots are curves for 00, 24 and 48 hour forecasts, a plot of the appropriate ECMWF curve, and a forecast length time averaged curve. The time averaged curve used

combined counts for the 12 through 60 (in 6 hour increments), 72, and 96 hour forecasts. One of the original intents of the project was to use a forecast scenario based on the use of the time averaged curve. However, the scenario had to be dropped because owing to the large number of scenarios being tested the machine time being used for the development was beginning to impact AFGWC operations.

The plot for the low layer (Figure A-6) dramatically shows that a degree of freedom for equation (1) is the forecast length. The low layer curves reflect a model spin-up out to 48 hours with the greatest spin-up occurring in the first 24 hours. The similarity of the 48 hour and time averaged curve indicate that the model spin-up has been completed and the model preferred state has been reached. The middle layer (Figure A-7) shows a spin-up of only 24 hours with the primary difference being at higher relative humidities. Both the low and high layer reflect the spin-up primarily in the values of the critical RH. Finally, the high layer (Figure A-8) shows a significant spin-up only in the first 24 hours. With respect to the ECMWF curves, the only similarity is with the 00 hour high level curve. Again, even though the vertical separations between some curves is significant, the important distinction is the horizontal separation. The 70% critical RH for the ECMWF low layer curve yields cloud amounts of from 60% to 65% for the CCA curves. The model spin-up seen in these curves was also found by Krishnamurti et. al.¹⁶ in their comparison of cloud cover forecasts from several global models to ISCCP data sets.

The significance of the real-time update of the curves is shown in the variability by season for each layer (Figures A-9 to A-11). The most variability for Northern Hemisphere Mid-Latitude Land is found in the low layer (Figure A-9) with a critical RH of 58% in August yielding 30% to 35% cloud in April. The other layers show less though significant variability. The ECMWF curve for the low layer is very different from the CCA curves. The differences for the middle (Figure A-10) and high (Figure A-11) layers are smaller but significant.

The variability of the curves by region are shown by the next six plots (Figures A-12 to A-17). There are two plots for each layer. For the Northern Hemisphere, NH Mid-Latitude, NH Tropics and NH Mid-Latitude Ocean, the low and middle layers show the most difference in the critical RH's but converge for RH greater than 70%. In the high layer, they diverge between the more similar critical RH values and 100%. For NH Mid-Latitude Land and its sub-regions, the curves start with similar values of critical RH and have varying tendencies to diverge. The ECMWF curves show the most difference from the CCA curves in the low layer with decreasing degrees of difference at the middle and high layers.

The final two sets of plots show that the curves do vary with the consideration of vertical velocity in both summer (Figures A-18, A-19 and A-20) and winter (Figures A-21, A-22 and A-23). The differences are the ones that are expected, i.e., upward vertical velocity yields larger cloud amounts than downward vertical velocity for a given forecast RH value. Stated another way, we expect more sub-grid RH variability within a grid volume, and hence more fractional cloud, when vertical velocity is upwards. Not considering vertical velocities gives values in between.

The purpose of the section has been to demonstrate that there are potentially large differences among CCA curves and between CCA and ECMWF curves. What has been presented here has only been a limited sample. With four layers, 13 forecast lengths, 14 regions, weekly vs monthly curves and 36 weekly curve updates, there were 52,416 curves generated during Phase I. In an operational application, only the few most skillful scenarios would be chosen for implementation.

Of course, the discussion above is superfluous if there is no skill imparted. That is the subject of the following discussion.

2.2 Basic Algorithm Skill Scores.

The skill of a cloud forecast scheme is determined by performing a grid point by grid point comparison between the forecast cloud amount and the observed cloud amount at each layer and for total cloud. The results of that comparison are entered into a contingency table as shown on page 17. Running totals are maintained over the course of a week or a month. The verification statistics used are defined in pages 17 - 21. The results presented here are based on 4 week long verification periods. These CCA skill scores refer to the skill of the CCA when used with the AFGWC GSM.

One of the statistics important to both radiation modelers and operational weather forecasters is the bias, the mean cloud averaged over a time and space domain. An acceptable bias is $\pm 5\%$ cloud.

One of the key results of this project is that for a given verification area, the bias for that area can be substantially reduced by computing a curve for that specific area. That is, even though the hallmark of the CCA scheme is its ability to minimize layer cloud biases, those biases apply to the entire domain over which counts were accumulated to generate the curves. Verification over a sub-domain may yield a substantial bias. The potential for large sub-region biases motivates stratification of curves into smaller regions.

Bias, 20/20, reliability and RMSE scores for the Northern Hemisphere Mid-Latitude Ocean for the period 17 Jan 91 to 13 Feb 91 are shown in Appendix B. The first plot is for the low layer (Figure B-1). The global, latitude band and land/ocean curves are defined on page 11. Note that using the global curves yields biases that range from -25% to -30% . Using the latitude band curves decreases the bias to the range -18% to -22% . Using a curve computed specifically for the NH Mid-Latitude Ocean region reduces the bias to an acceptable level, i.e. between 0% and 5% . The 5LAYER bias starts out at an acceptable level but dries to unacceptable biases with increasing forecast lengths. The ECMWF bias averages out at -50% . It was because of the large ECMWF biases that the Geleyn scheme was not included in Phase II. Even though the CCA is designed to reduce the layer bias, it is probably not possible to achieve a 0% layer bias. That is because the layer cloud inputs to the cloud curves are available only in 10% increments. The second factor is that the contingency table results are stored in 10% increments.

The next three plots are for the middle layer (Figure B-2), high layer (Figure B-3) and total cloud (Figure B-4). They all show the same

worst to best progression: ECMWF, global curve, latitude band curve, region specific curve with 5LAYER biases (except for the high layer) starting small and increasing with forecast length. Given that the layer biases will not be strictly 0 even with a region specific curve, there will be a non-zero total cloud bias. The total cloud bias is dependent on the ability of the numerical prediction model to maintain the correct vertical stacking of relative humidity and how independent each cloud layer is from the others. The total cloud bias scores for both persistence and 5LAYER are shown in the next plot (Figure B-5). The 5LAYER shows a tendency to dry out over the forecast period. The tendency of the persistence to maintain a nearly zero bias, as expected was noted throughout the project even over the smallest verification area.

The skillfulness of region specific curves is shown also in the last three plots. The graphs of the total cloud 20/20 score (Figure B-6), reliability (Figure B-7) and RMSE (Figure B-8) show the same worst to best progression with the improvements in skill being significant as one progresses from a global curve to a region specific curve. 5LAYER skill starts out initially very high but rapidly decreases with increasing forecast length.

Bias, 20/20, reliability and RMSE scores for Northern Hemisphere Mid-Latitude Land are shown in Appendix C (Figures C-1 to C-8). While the worst to best progression is not as straightforward as the Mid-Latitude Ocean case, the region specific curve definitely gives the best low layer (Figure C-1) and total cloud (Figure C-4) biases. For the middle layer (Figure C-2), the global curve sometimes has the least bias. While for the high layer (Figure C-3) all the curves have acceptable bias values. The 5LAYER biases (again with the exception of the high layer) show a pattern of drying with increasing forecast length, however, the extremes of bias values are smaller than for Mid-Latitude Ocean. This illustrates a result that was seen often in the course of the development, i.e., the region specific curve may not always give the least bias in a specific circumstance. However, what was found was that the extremes of bias values were much smaller for region specific curves. Also, the majority of the region specific curve biases were within the acceptable range. A comparison with the total cloud persistence and 5LAYER biases (Figure C-5) shows that the CCA values are competitive.

The 20/20, reliability, and RMSE scores do not show the nice clear-cut superiority for region specific curves that was seen in the Mid-Latitude Ocean case. In fact, the ECMWF 20/20 (Figure C-6) scores are slightly better than the region specific curve score, but are less skillful in terms of reliability (Figure C-7) and RMSE (Figure C-8). The 5LAYER skill scores again start very high and decrease sharply with increasing forecast lengths. So, to expand the conclusion stated above, increased regional stratification of curves does reduce the extremes of bias values but is not sufficient to guarantee superior skill. Other extensions of the scheme must be utilized to achieve consistently superior skill. The ability of the CCA scheme to achieve low bias values in mean monthly layer and total cloud amounts was also seen by Sheu and Curry¹⁷ in their comparison of several RH-to-cloud diagnostic schemes.

The results above were determined in Phase I. The land/ocean curve stratification was carried over into Phase II as the Phase I baseline. The variations tested in Phase II were: increased regional stratification, a diurnal correction, and the inclusion of vertical velocity as a predictor. These are described in section 1.2.

The 20/20 scores for the period 01 Aug 91 to 28 Aug 91 are shown in Appendix D. The 20/20 scores for European Land (Figure D-1) stay better than 60% through 48 hours where it beats 5LAYER by 11 percentage points. The next plot (Figure D-2) shows the relative skill of the Phase II variations. The notation PH 1 BASE denotes the Phase I baseline. RGN CURVES denotes the use of the mid-latitude land subregions. This regional stratification was used with both diurnal correction (DIU COR) and vertical velocity (VERT VEL) and their combination (DC AND VV). The increased regional stratification yielded the same skill as the Phase I baseline. The use of vertical velocity actually decreased the skill slightly. Not surprisingly for the warm season, the use of a diurnal correction yielded the most increase in skill. The increase due to the diurnal correction was greatest for European Land. The skill over European Land appears due to the fact that Europe has the most dense observation network. This leads to a more accurate specification of the initial GSM moisture and therefore more accurate relative humidity forecasts. The dense surface observations also improve the quality of the RTNEPH cloud analysis which improves the quality of the cloud curves and the reliability of the verification.

The skill of CCA compared to 5LAYER decreases in the progression through East Asia Land (Figure D-3) and North America Land (Figure D-4) to North African/Middle Eastern Land (Figure D-5). Even 5LAYER loses to persistence (Figure D-5) after 12 hours. The CCA skill progression by region appears linked to the density of the observation network over each region. The composite CCA skill over Mid-Latitude Land (Figure D-6) as a whole still exceeds that of 5LAYER; but over Mid-Latitude Ocean (Figure D-7) the apparent impact of the lack of moisture observations in the GSM initial state is apparent. The CCA skill compared to diurnal persistence in the Tropics, both land (Figure D-8) and ocean (Figure D-9), is dismal. This is consistent with the fact that the region is dominated by convection and dynamic models are skillful only in the vicinity of moving tropical disturbances. Over Tropical Land diurnal persistence clearly beats persistence which validates the use of diurnal persistence in the TRONEW model. This is particularly true with the AFGWC GSM in which the contribution of convective processes is substantially suppressed compared to other models (Yang et. al.'89).

Moving to the autumn (Appendix E), the 20/20 scores for 24 Oct 91 to 24 Nov 91 for European Land (Figure E-1) stay above 60% out to 36 hours and exceed those of 5LAYER by 9 percentage points at 48 hours. The next plot (Figure E-2) shows that the primary improvement over the Phase I baseline is due to the use of a region specific curve. The addition of a diurnal correction gives the greatest skill. Again the use of vertical velocity decreases the skill. It appears that the binary vertical velocity stratification should be replaced with three or more stratifications. Peterson and Hutchison² used 5 categories: strong up, up, neutral, down and strong down. Unfortunately, the Autumn CCA skill over Europe is not representative of the other land subregions (Figures

E-3 to E-5). As a result, CCA can do no better than parity with 5LAYER over Mid-Latitude Land (Figure E-6) after 24 hours. CCA beats 5LAYER at 42 hours over the Mid-Latitude Ocean (Figure E-7). This apparently can be attributed to increased moisture information in the GSM over ocean areas due to the movement of synoptic scale systems from land to ocean. The CCA performance in the tropics (Figures E-8 and E-9) continues to be dismal.

The superior performance of CCA with respect to 5LAYER over European Land in the Autumn is reflected in other skill scores (Appendix F). The CCA bias (Figure F-1) is no worse than 3%, while that of 5LAYER approaches -8%.

The sharpness is the 'binary-ness' of the cloud forecasts, that is, the percentage of cloud forecasts in the 0% to 20% and 80% to 100% cloud amount ranges. There is a range of sharpness values inherent to a given grid spacing. The sharpness appropriate to a given situation is reflected in the sharpness values associated with persistence. The plot of sharpness values for CCA (Figure F-2) shows them to be consistent with the persistence values. This means that CCA skill is not the result of smoothing, i.e., the practice of improving cloud forecast skill by forcing cloud forecasts into the 20% to 80% range.

In terms of the other skill scores for European Land in the Autumn (reliability (Figure F-3), RMSE (Figure F-4), bust score (Figure F-5), Heidike skill score (Figure F-6) and mean absolute error (Figure F-7)), CCA consistently surpasses 5LAYER at the 12 hour point. This success in terms of multiple skill scores indicates that the CCA truly is a skillful objective diagnostic cloud forecast technique. We again emphasize that the skill of the CCA is highly dependent on the skill of the GSM relative humidity forecasts.

Moving to the winter (Appendix G), the 20/20 scores for 16 Jan 92 to 12 Feb 92 for European Land (Figure G-1) show a significant decline from the summer and autumn scores. Figure G-2 shows that there was still an increase in skill over the Phase I baseline due to the use of a region specific curve. The addition of a diurnal correction makes no significant difference, while the use of the binary vertical velocity scheme decreases the skill. The winter skill of the CCA over the other land sub-regions (Figures G-3 to G-5) is the same to less than that of the autumn skill. As a result, CCA can not even achieve parity with 5LAYER over Mid-Latitude Land (Figure G-6). The Mid-Latitude Ocean (Figure G-7) skill improves slightly to beat 5LAYER at 36 hours. The winter tropical skill (Figures G-8 and G-9) improves over the autumn skill, but still does not beat diurnal persistence. It is not clear why winter skill over Mid-Latitude Land decreases while skill over Mid-Latitude Ocean increases.

2.3 Effect of the Relative Humidity Trend Technique.

One variation which has not been discussed yet is the effect of the relative humidity trending technique on the skill of the CCA. The autumn 20/20 scores for European Land, N H Mid-Latitude Land and N H Mid-Latitude Ocean are repeated in Appendix H with the trended scores.

As described in section 1.2, the trending technique is a poor-man attempt to incorporate RTNEPH derived moisture information into the GSM RH forecast. The fact that the trended technique is less skillful than the basic technique over both European Land (Figure H-1) and Mid-Latitude Land (Figure H-2) indicates that the RTNEPH doesn't add sufficient additional moisture information. On the other hand, the trended technique outperforms SLAYER after 18 hours over Mid-Latitude Ocean (Figure H-3). This tends to confirm that the lack of relative humidity observations over the oceans handicaps the GSM RH forecast skill over the oceans.

The problem, as seen in the next two plots, is that the trending technique generates large positive biases over both land (Figure H-4) and ocean (Figure H-5). We found that the positive bias is due to the use of RH^* within the algorithm. Hand calculations which used RH-to-cloud curves and an RH trend gave less cloud than the use of RH^* -to-cloud curves and an RH^* trend. This is a reasonable occurrence given that RH^* is a non-linear transform which expands the moist end of the RH spectrum. The reason for the sharp increase in bias in the first 24 hours is due to the fact that the 0-hour forecast is 'perfect' due to its use of an RTNEPH derived moisture analysis. As the model spins up to its preferred state, the effect of the RH^* non-linearity increases.

2.4 Shaded Hemispheric Displays of Relative Humidity and Clouds.

Appendix I contains shaded hemispheric displays of relative humidity and clouds. The six figures are 24 hour forecasts valid 06Z, 23 October 1990. The legend for the six figures is:

N (or S) for Northern or Southern Hemisphere
 24 for 24 hour forecast
 L1 (or L2, MM, HH) for the layer of the atmosphere
 RH (or DH) for GSM RH forecast or RTNEPH derived humidity
 NT (or TR) for non-trended or trended forecast
 ANAL for the verifying analysis

Black = 0% cloud and White = 100% cloud.

All the displays are polar stereographic. For the Northern Hemisphere the North Pole is at the center of the circle. Details of the landmass orientation can be seen in Figure 3. For the Southern Hemisphere, the South Pole is at the center of the circle as is Antarctica. South America is a little to the right of the 'top' of the circle. Africa is slightly 'down' from the extreme right of the circle. Australia is slightly to the left 2/3 of the way between the center of the circle and 'bottom' of the circle.

After 24 hours, the GSM has largely completed the spin-up to its model preferred moisture distribution. This can be seen in the distinct moist frontal bands and post-frontal dry 'tongues'. The persistent cloud free area over North Africa and the Middle East is evident in both the CCA RH and cloud displays and the verifying RTNEPH. Also, the decrease in the mean areal cloud amount with height especially at the high layer is evident in both the CCA and RTNEPH displays.

In comparing the RH displays to the DH displays, it is evident that the DH displays have a much brighter appearance. This indicates the moist bias which has crept into the trended forecast. The less smoothed appearance of the trended forecast reflects the use of RTNEPH derived moisture.

One of the concerns that arises from using regional stratifications of curves is that shaded displays would have artificially induced boundaries. The October 1990 figures show a sharp discontinuity between the extratropics and the tropics. There does not appear to be any discontinuities associated with separate land and ocean curves either in the tropics or the mid-latitudes. Cloud displays of Phase II forecasts do not show any discontinuities due to mid-latitude land subregion curves.

The hardcopy figures in this report can only hint at the detail available when displayed on a high resolution video terminal. In addition, the ability to construct time sequence loops reveals that tropical systems move from east to west and mid-latitude systems move from west to east as one would expect and in a manner similar to the verifying RTNEPH displays.

3. CONCLUSIONS AND RECOMMENDATIONS

This project had three main objectives:

- (1) To test variations in the CCA methodology to determine the superior algorithm configuration in the AFGWC GSM
- (2) To perform inter-model skill comparisons between CCA (using the AFGWC GSM) and AFGWC's current cloud forecast models (5LAYER in the extratropics and TRONEW in the tropics), persistence and diurnal persistence (which TRONEW uses)
- (3) To perform inter-model skill comparisons between CCA (using the AFGWC GSM) and the Geleyn scheme used until May 1985 in the European Center for Medium Range Weather Forecasting (ECMWF) GSM to diagnose cloud for their radiation scheme (using the AFGWC GSM)

The following variations in the CCA methodology showed the most skill:

- (1) In compacting GSM RH values on 6 pressure levels to three layers (low,middle,high), the 1000 mb values are ignored because of a moist bias, especially over the low-latitude oceans.
- (2) In computing a total cloud amount from input low, middle and high cloud amounts, a tuned overlap works best in the extratropics while a random overlap works best in the tropics.
- (3) Increasing regional stratification of curves yielded the most skill. In the final phase, curves were computed for: European Land, East Asia Land, North American Land, North Africa/Middle East Land, Northern Hemisphere Mid-Latitude Ocean, Northern Hemisphere Tropical Land and Northern Hemisphere Tropical Ocean.
- (4) CCA showed little sensitivity to the length of the frequency of occurrence accumulation period. In the final phase, an accumulation period of two weeks was used to ensure an adequate sample over small regions.
- (5) The incorporation of a diurnal correction similar to that used by 5LAYER yielded increased skill in the summer over land.
- (6) The incorporation of a binary (up or down) vertical velocity stratification did not yield increased skill. Future tests should use a three category stratification: strong up, strong down, and weak.
- (7) Once a week real-time update of the curves reflected the seasonal changes in RH and cloud amount distributions which sometimes resulted in large variations in the amount of cloud associated with a given input RH value.
- (8) An RH trend approach which tried to capture the RH information contained in the RTNEPH cloud analysis yielded in general more skill over ocean areas, but showed an unexpectedly high moist bias.

The cloud forecast skill of CCA (using the AFGWC GSM) compared to 5LAYER and TRONEW (i.e., diurnal persistence) varied by season and region

of the world. The table below shows the forecast length at which CCA outperformed 5LAYER (extratropics) or TRONEW (tropics) based on the 20/20 score for total cloud (- indicates CCA did worse than either 5LAYER or TRONEW at all forecast lengths):

<u>Region</u>	<u>1 Aug 91</u> <u>to</u> <u>28 Aug 91</u>	<u>24 Oct 91</u> <u>to</u> <u>20 Nov 91</u>	<u>16 Jan 92</u> <u>to</u> <u>12 Feb 92</u>
European Land	12 hours	12 hours	36 hours
East Asia Land	12 hours	-	-
North America Land	18 hours	-	-
North Africa/ Middle East Land	-	-	-
Northern Hemisphere			
Mid-Latitude Land	12 hours	-	-
Mid-Latitude Ocean	-	42 hours	36 Hours
Tropical Land	-	-	-
Tropical Ocean	-	-	-

Note that CCA did well over Northern Hemisphere Mid-Latitude Land in the summer, but performance dropped off in the autumn and winter. Over Northern Hemisphere Mid-Latitude Ocean the performance was poor in the summer but increased slightly in the autumn and winter. Performance in the tropics was uniformly poor. This is similar to AFGWC's experience which leads them to use diurnal persistence in the tropics rather than 5LAYER.

The inter-model comparison between CCA and 5LAYER was heavily slanted toward 5LAYER. The 5LAYER uses as its initial condition a detailed RTNEPH cloud analysis on a 25 nm grid which is smoothed to a 100 nm grid. The cloud analysis is converted to a moisture analysis, advected along a forecast trajectory and converted back to a cloud forecast. The 5LAYER therefore has detailed moisture information linked to cloud cover over the entire extratropics. In this comparison, it was verifying RTNEPH cloud analyses against which the cloud forecasts (CCA and 5LAYER) were evaluated.

In contrast to the 5LAYER, the AFGWC GSM (regardless of the choice of cloud forecast scheme) suffers from the following major disadvantages:

- (1) No RTNEPH cloud analysis information (or any other cloud information) is used to derive the GSM initial moisture analysis
- (2) The GSM spatial resolution is poor
- (3) The GSM has many pre- and post-processing interpolation steps

The GSM uses as its initial conditions an RH analysis on the equivalent of a 200 nm grid spacing with input RH information from RAOBs which are generally available only over land. This coarse spatial resolution is maintained throughout the forecast cycle. In addition, errors are introduced in the conversion from spectral space to grid space and in the conversion from sigma layers to pressure levels in GSM pre- and post-processing interpolation steps. These highly smoothed GSM RH

analyses and forecasts are interpolated to the same 100 nm grid used by 5LAYER for the computation of RH-to-cloud curves and the conversion of RH forecasts to cloud forecasts for verification against the 100 nm grid RTNEPH. Given the circumstances, it is surprising that the CCA shows as much skill as it does when used with the AFGWC GSM.

A fairer comparison between CCA in the AFGWC GSM and 5LAYER would require:

- (1) Executing the GSM at much higher spatial resolution
- (2) Outputting the GSM RH forecast directly on GSM sigma-level surfaces
- (3) Utilizing the RTNEPH directly in deriving the GSM initial moisture analysis

Furthermore, a more advanced GSM with state-of-the-art parameterized physical processes should be used ,e.g., the Phillips Laboratory Advanced Physics Global Spectral Model. The above recommended efforts were significantly beyond the resources available for this study.

The table below shows the forecast length at which CCA outperformed persistence based on the 20/20 score for total cloud (- indicates CCA did worse than persistence at all forecasts lengths):

<u>Region</u>	<u>1 Aug 91</u> <u>to</u> <u>28 Aug 91</u>	<u>24 Oct 91</u> <u>to</u> <u>20 Nov 91</u>	<u>16 Jan 92</u> <u>to</u> <u>12 Feb 92</u>
European Land	6 hours	6 hours	30 hours
East Asia Land	6 hours	12 hours	-
North America Land	6 hours	12 hours	(mixed)
North Africa/ Middle East Land	-	(mixed)	30 hours
Northern Hemisphere			
Mid-Latitude Land	6 hours	12 hours	-
Mid-Latitude Ocean	54 hours	-	30 hours
Tropical Land	-	-	-
Tropical Ocean	-	-	-

In the inter-model comparison between the CCA and Geleyn schemes, the CCA scheme was consistently more skillful than the Geleyn (ECMWF) scheme, which gave large negative cloud biases.

Another NWP model being used at AFGWC is the Relocatable Window Model (RWM) and is a more suitable candidate for comparing CCA to 5LAYER. It was not used in this study because it was not sufficiently ready. It is a higher resolution model used to provide forecasts over smaller forecast areas called windows. These forecast areas are chosen based on the needs of military operations and are usually over land. The RWM is an excellent candidate for the use of CCA. It is a grid point model which gets its initial RH analysis guess from the GSM. However, the RH analysis update is performed on the small RWM grid spacing on the RWM sigma layers. This avoids the pre- and post-processing errors found in

the GSM and may give CCA the detailed RH information it needs. CCA should therefore perform much better in the RWM than in the GSM especially if the RTNEPH cloud analysis could be used as a data source for the RWM initial moisture analysis. Presently, the cloud forecast scheme being used by the RWM is borrowed from the Swedish Limited Area Model (SLAM). The scheme is a linear one similar to that of Smagorinski'. Based on the performance of the Geleyn scheme in the GSM, CCA should perform much better than the SLAM scheme in the RWM.

One forecast scheme which was not considered was the Model Output Statistics (MOS). The MOS approach requires that a model be run for at least two years in order to derive the proper MOS equations for forecasting the predictand in a particular region. Once the equations are derived, major changes to the physics of the NWP cannot be changed without forcing the derivation of a new set of MOS equations. The CCA curves, on the other hand, can adjust to the changed model physics within the length of the frequency of occurrence accumulation period, i.e. two weeks as determined in this study.

REFERENCES

1. Smagorinski, J. (1960) *The Physics of Precipitation*, Geophysical Monograph No. 5, AGU, p.71.
2. Geleyn, J.-F. (1981) *Some diagnostics of the cloud/radiation interaction in the ECMWF forecasting model*, ECMWF Workshop on Radiation and Cloud-Radiation Interaction in Numerical Modeling, 15-17 October 1980, European Centre for Medium Range Weather Forecasts, Reading, Berkshire, U.K. pp 135-162.
3. Crum, T.D. (1987) *AFGWC Cloud Forecast Models*, AFGWC/TN-87-001, Air Force Global Weather Central, Offutt AFB, NE, pp 1.
4. Kiess, R. and Cox, W. (1988) *The AFGWC Automated Real-time Cloud Analysis Model*, AFGWC/TN-88-001, Air Force Global Weather Central, Offutt AFB, NE, pp 1.
5. Stobie, J.G. (1986) *AFGWC's Advanced Weather Analysis and Prediction System (AWAPS)*, AFGWC/TN-86-001, Air Force Global Weather Central, Offutt AFB, NE, pp 1-1.
6. Sela, J. (1980) Spectral modeling at the National Meteorological Center. *Mon. Wea. Rev.*, 108:1279-1292.
7. Slingo, J. (1987) The development and verification of a cloud prediction scheme for the ECMWF model, *Q. J. R. Met. Soc.*, 113:899-927.
8. Mitchell, K. and Warburton, J. (1983) *A comparison of cloud forecasts derived from the NMC and AFGWC operational hemisphere forecasts of moisture*, Proceedings of AMS Sixth Conference on Numerical Weather Prediction, 6-9 June 1983, Omaha, NE, pp 66-73.
9. Edson, H. (1965) *Numerical Cloud and Icing Forecasts*, Scientific Services Technical Note 13, 3rd Weather Wing, Offutt AFB, NE, pp. 44.
10. Mitchell, K. and Hahn, D. (1989) *Development of a cloud forecast scheme for the GL Baseline Global Spectral Model*. GL-TR-89-0343, Geophysics Laboratory, Hanscom AFB, MA (ADA231595)
11. Rikus, L. and Hart, T. (1988) *The development and refinement of a diagnostic cloud parameterization scheme for the BMRC Global Model*. In Proceedings of the International Radiation Symposium (IRS 88), Lille, France, 18 - 24 August 1988.
12. Campana, K., Mitchell, K., Yang, S., Hou, Y., and Stowe, L. (1991) *Validation and improvement of cloud parameterization at the National Meteorological Center*, Proceedings of the AMS 9th conference on Numerical Weather Prediction, October 14 - 19, 1991, Denver, CO.

13. Rasmussen, G. (1982) *Some techniques for the objective analysis of humidity for regional scale numerical weather prediction*. Ph. D. thesis, NCAR/CT-67, National Center for Atmospheric Research, Boulder, CO.
14. Henderson-Sellers, A. and Hughes, N. (1985) 1979 3D-Nephanalysis global total cloud amount climatology. *Bulletin of the American Meteorological Society*. Volume 66, Number 6, June 1985, pp. 626-627.
15. Peterson, R. and Hutchison, K. (1990) *Cloud Models Enhancement Project Final Report*. TASC-TR-5773-2. The Applied Sciences Corporation, Reading, MA.
16. Krishnamurti, T. N., Bedi, H. S., Ingles, K., Weiner, A., Kuma, K., Campana, K., Kimoto, M. (1988) *Comparison of Cloud Cover from Global Models and ISCCP Data Sets*. Report prepared for the Fourth Session of the CAS/JSC-WGNE, Toronto, September 16-30, 1988.
17. Sheu, R., and Curry, J. (1992) Interactions between North Atlantic Clouds and the Large-Scale Environment. *Mon. Wea. Rev.*, 120:261 - 278.
18. Yang, C. H., Mitchell, K., Norquist, D. and Yee, S. (1989) *Diagnostics for and Evaluation of New Physical Parameterization Schemes for Global NWP Models*. GL-TR-89-0158, Geophysics Laboratory, Hansom AFB, MA. ADA228033

LIST OF ACRONYMS

AFGWC	Air Force Global Weather Central
AWAPS	Advanced Weather Analysis and Prediction System
CCA	Cloud Curve Algorithm
CPS	Condensation Pressure Spread
DH	Derived Humidity (derived from RTNEPH cloud)
ECMWF	European Centre for Medium Range Weather Forecasts
ISCCP	International Satellite Cloud Climatology Program
GSM	Global Spectral Model
MAE	Mean Absolute Error
MOS	Model Output Statistics
NWP	Numerical Weather Prediction
PBL	Planetary Boundary Layer
RH	Relative Humidity
RMSE	Root Mean Square Error
RWM	Relocatable Window Model
SLAM	Swedish Limited Area Model

APPENDIX A:

PLOTS OF RELATIVE HUMIDITY TO CLOUD CURVES

LIST OF FIGURES

- Figure A-1. Relative Humidity to Cloud Curves for Low, Middle and High Layers Computed Using the European Centre For Medium Range Weather Forecasts Geleyn Scheme (Equation 4).
- Figure A-2. Cloud Curve Algorithm Relative Humidity to Cloud Curves for Low Layer L1, Low Layer L2, Middle Layer (MM), and High Layer (HH) Computed On 01 August 1990 Over For 24-Hour Northern Hemisphere Mid-Latitude Cloud Forecasts.
- Figure A-3. Cloud Curve Algorithm Relative Humidity to Cloud Curves for Weekly and Monthly Accumulation Periods Computed On 01 August 1990 Over For 24-Hour Low Layer Northern Hemisphere Mid-Latitude Cloud Forecasts.
- Figure A-4. Cloud Curve Algorithm Relative Humidity to Cloud Curves for Weekly and Monthly Accumulation Periods Computed On 01 August 1990 Over For 24-Hour Middle Layer Northern Hemisphere Mid-Latitude Cloud Forecasts.
- Figure A-5. Cloud Curve Algorithm Relative Humidity to Cloud Curves for Weekly and Monthly Accumulation Periods Computed On 01 August 1990 Over For 24-Hour High Layer Northern Hemisphere Mid-Latitude Cloud Forecasts.
- Figure A-6. Cloud Curve Algorithm Relative Humidity to Cloud Curves for 00, 24, and 48 Hour Forecast Lengths, and a Time Average (TIME AVG) of 12 Through 96 Hour Forecast Lengths, and Relative Humidity to Cloud Curves Computed Using the European Centre For Medium Range Weather Forecasts Geleyn Scheme (Equation 4) Computed On 01 January 1991 for Low Layer Northern Hemisphere Mid-Latitude Cloud Forecasts.
- Figure A-7. Cloud Curve Algorithm Relative Humidity to Cloud Curves for 00, 24, and 48 Hour Forecast Lengths, and a Time Average (TIME AVG) of 12 Through 96 Hour Forecast Lengths, and Relative Humidity to Cloud Curves Computed Using the European Centre For Medium Range Weather Forecasts Geleyn Scheme (Equation 4) Computed On 01 January 1991 for Middle Layer Northern Hemisphere Mid-Latitude Cloud Forecasts.
- Figure A-8. Cloud Curve Algorithm Relative Humidity to Cloud Curves for 00, 24, and 48 Hour Forecast Lengths, and a Time Average (TIME AVG) of 12 Through 96 Hour Forecast Lengths, and Relative Humidity to Cloud Curves Computed Using the European Centre For Medium Range Weather Forecasts Geleyn Scheme (Equation 4) Computed On 01 January 1991 for High Layer Northern Hemisphere Mid-Latitude Cloud Forecasts.

- Figure A-9. Cloud Curve Algorithm Relative Humidity to Cloud Curves Computed On August 1, 1990; October 24, 1990; January 16, 1991 and April 10, 1991 and Relative Humidity to Cloud Curves Computed Using the European Centre For Medium Range Weather Forecasts Geleyn Scheme (Equation 4) For 24 Hour Low Layer Northern Hemisphere Mid-Latitude Cloud Forecasts.
- Figure A-10. Cloud Curve Algorithm Relative Humidity to Cloud Curves Computed On August 1, 1990; October 24, 1990; January 16, 1991 and April 10, 1991 and Relative Humidity to Cloud Curves Computed Using the European Centre For Medium Range Weather Forecasts Geleyn Scheme (Equation 4) For 24 Hour Middle Layer Northern Hemisphere Mid-Latitude Cloud Forecasts.
- Figure A-11. Cloud Curve Algorithm Relative Humidity to Cloud Curves Computed On August 1, 1990; October 24, 1990; January 16, 1991 and April 10, 1991 and Relative Humidity to Cloud Curves Computed Using the European Centre For Medium Range Weather Forecasts Geleyn Scheme (Equation 4) For 24 Hour High Layer Northern Hemisphere Mid-Latitude Cloud Forecasts.
- Figure A-12. Cloud Curve Algorithm Relative Humidity to Cloud Curves For The Northern Hemisphere, Northern Hemisphere Mid-Latitudes, Northern Hemisphere Tropics and Northern Hemisphere Mid-Latitude Oceans and Relative Humidity to Cloud Curves Computed Using the European Centre For Medium Range Weather Forecasts Geleyn Scheme (Equation 4) Computed On 28 August 1991 for 24 Hour Low Layer Cloud Forecasts.
- Figure A-13. Cloud Curve Algorithm Relative Humidity to Cloud Curves For Northern Hemisphere Mid-Latitude Land, North America Land, European Land, and North Africa/Middle East Land and Relative Humidity to Cloud Curves Computed Using the European Centre For Medium Range Weather Forecasts Geleyn Scheme (Equation 4) Computed On 28 August 1991 for 24 Hour Low Layer Cloud Forecasts.
- Figure A-14. Cloud Curve Algorithm Relative Humidity to Cloud Curves For The Northern Hemisphere, Northern Hemisphere Mid-Latitudes, Northern Hemisphere Tropics and Northern Hemisphere Mid-Latitude Oceans and Relative Humidity to Cloud Curves Computed Using the European Centre For Medium Range Weather Forecasts Geleyn Scheme (Equation 4) Computed On 28 August 1991 for 24 Hour Middle Layer Cloud Forecasts.

- Figure A-15.** Cloud Curve Algorithm Relative Humidity to Cloud Curves For Northern Hemisphere Mid-Latitude Land, North America Land, European Land, and North Africa/Middle East Land and Relative Humidity to Cloud Curves Computed Using the European Centre For Medium Range Weather Forecasts Geleyn Scheme (Equation 4) Computed On 28 August 1991 for 24 Hour Middle Layer Cloud Forecasts.
- Figure A-16.** Cloud Curve Algorithm Relative Humidity to Cloud Curves For The Northern Hemisphere, Northern Hemisphere Mid-Latitudes, Northern Hemisphere Tropics and Northern Hemisphere Mid-Latitude Oceans and Relative Humidity to Cloud Curves Computed Using the European Centre For Medium Range Weather Forecasts Geleyn Scheme (Equation 4) Computed On 28 August 1991 for 24 Hour High Layer Cloud Forecasts.
- Figure A-17.** Cloud Curve Algorithm Relative Humidity to Cloud Curves For Northern Hemisphere Mid-Latitude Land, North America Land, European Land, and North Africa/Middle East Land and Relative Humidity to Cloud Curves Computed Using the European Centre For Medium Range Weather Forecasts Geleyn Scheme (Equation 4) Computed On 28 August 1991 for 24 Hour High Layer Cloud Forecasts.
- Figure A-18.** Cloud Curve Algorithm Relative Humidity to Cloud Curves Computed Without Considering Vertical Velocity (NO VERT) and Computed For Upward and Downward Vertical Velocity and Relative Humidity to Cloud Curves Computed Using the European Centre For Medium Range Weather Forecasts Geleyn Scheme (Equation 4) Computed On 28 August 1991 for 24 Hour Low Layer Northern Hemisphere Mid-Latitude Land Cloud Forecasts.
- Figure A-19.** Cloud Curve Algorithm Relative Humidity to Cloud Curves Computed Without Considering Vertical Velocity (NO VERT) and Computed For Upward and Downward Vertical Velocity and Relative Humidity to Cloud Curves Computed Using the European Centre For Medium Range Weather Forecasts Geleyn Scheme (Equation 4) Computed On 28 August 1991 for 24 Hour Middle Layer Northern Hemisphere Mid-Latitude Land Cloud Forecasts.
- Figure A-20.** Cloud Curve Algorithm Relative Humidity to Cloud Curves Computed Without Considering Vertical Velocity (NO VERT) and Computed For Upward and Downward Vertical Velocity and Relative Humidity to Cloud Curves Computed Using the European Centre For Medium Range Weather Forecasts Geleyn Scheme (Equation 4) Computed On 28 August 1991 for 24 Hour High Layer Northern Hemisphere Mid-Latitude Land Cloud Forecasts.

- Figure A-21. Cloud Curve Algorithm Relative Humidity to Cloud Curves Computed Without Considering Vertical Velocity (NO VERT) and Computed For Upward and Downward Vertical Velocity and Relative Humidity to Cloud Curves Computed Using the European Centre For Medium Range Weather Forecasts Geleyn Scheme (Equation 4) Computed On 12 February 1992 for 24 Hour Low Layer Northern Hemisphere Mid-Latitude Land Cloud Forecasts.
- Figure A-22. Cloud Curve Algorithm Relative Humidity to Cloud Curves Computed Without Considering Vertical Velocity (NO VERT) and Computed For Upward and Downward Vertical Velocity and Relative Humidity to Cloud Curves Computed Using the European Centre For Medium Range Weather Forecasts Geleyn Scheme (Equation 4) Computed On 12 February 1992 for 24 Hour Middle Layer Northern Hemisphere Mid-Latitude Land Cloud Forecasts.
- Figure A-23. Cloud Curve Algorithm Relative Humidity to Cloud Curves Computed Without Considering Vertical Velocity (NO VERT) and Computed For Upward and Downward Vertical Velocity and Relative Humidity to Cloud Curves Computed Using the European Centre For Medium Range Weather Forecasts Geleyn Scheme (Equation 4) Computed On 12 February 1992 for 24 Hour High Layer Northern Hemisphere Mid-Latitude Land Cloud Forecasts.

ECMWF CURVES BY LAYER

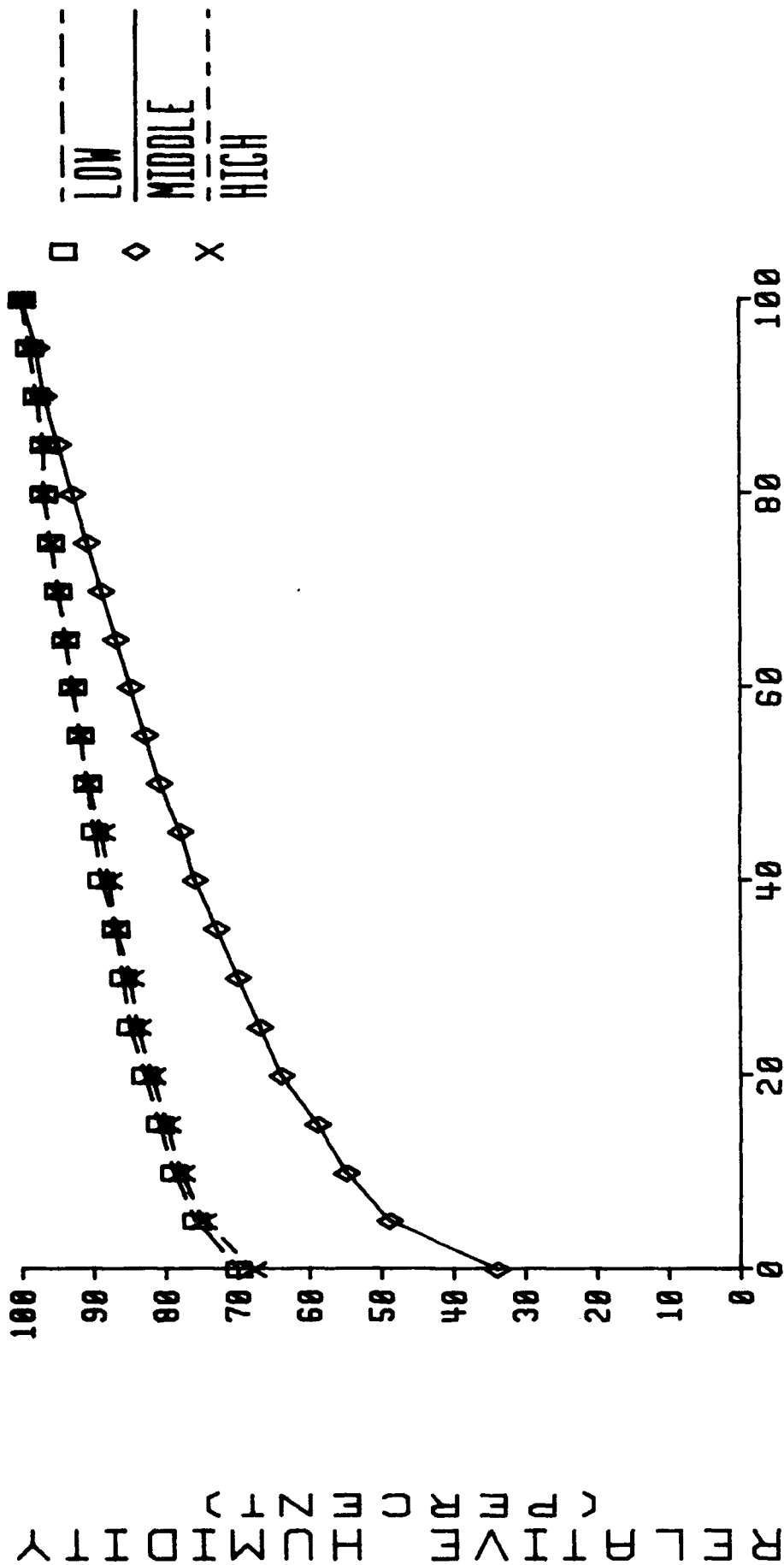
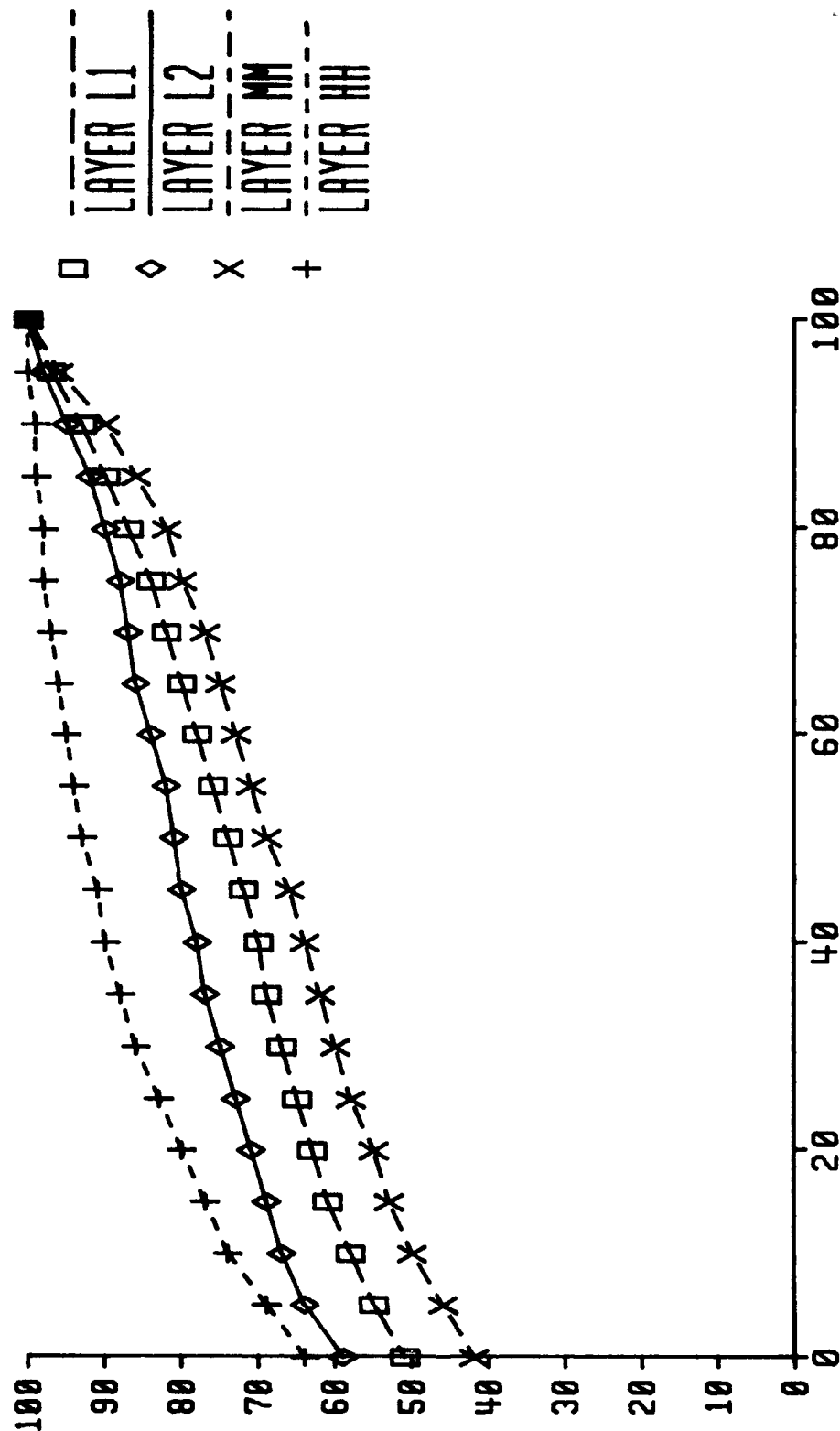


Figure A-1
CLOUD AMOUNT (PERCENT)

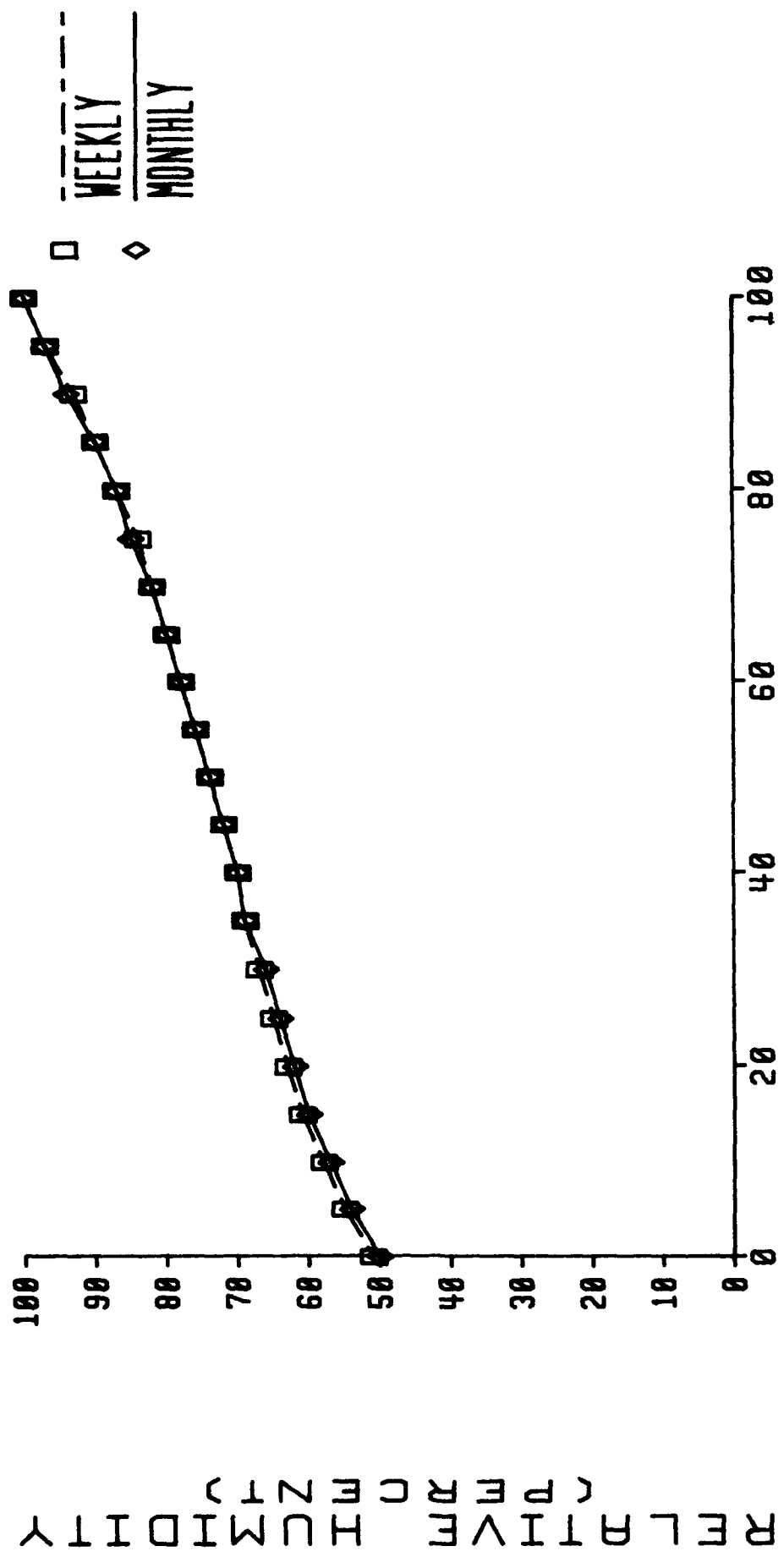
CCA CURVES BY LAYER
01AUC90 NH MID-LAT 24 HR

RELATIVE HUMIDITY
(PERCENT)



CLOUD AMOUNT (PERCENT)
Figure A-2

WEEKLY VS MONTHLY (LOW)
01AUG90 NH MID-LAT 24 HR



CLOUD AMOUNT (PERCENT)
Figure A-3

WEEKLY VS MONTHLY (MID)
01 AUG 90 NH MID-LAT 24 HR

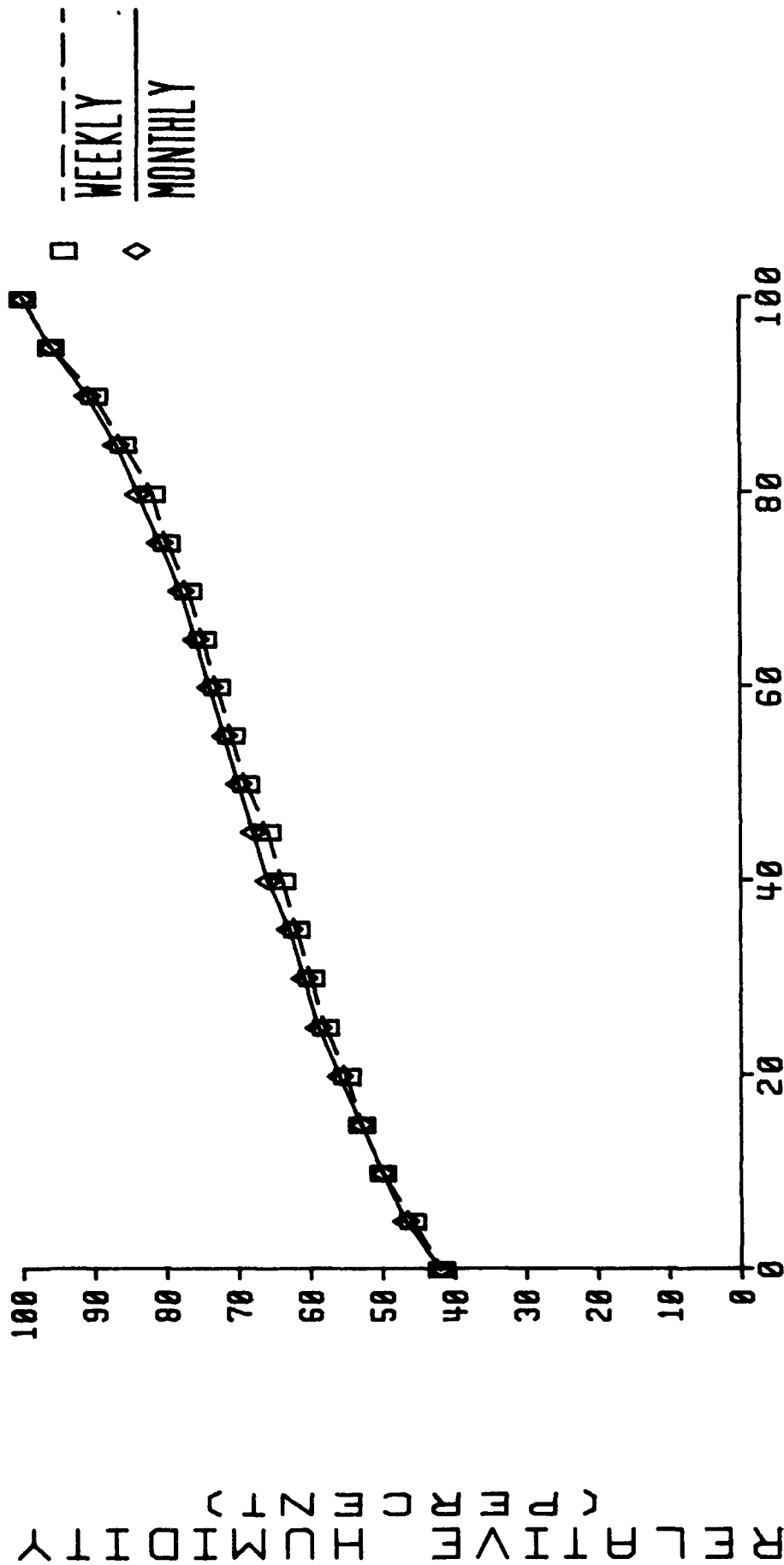
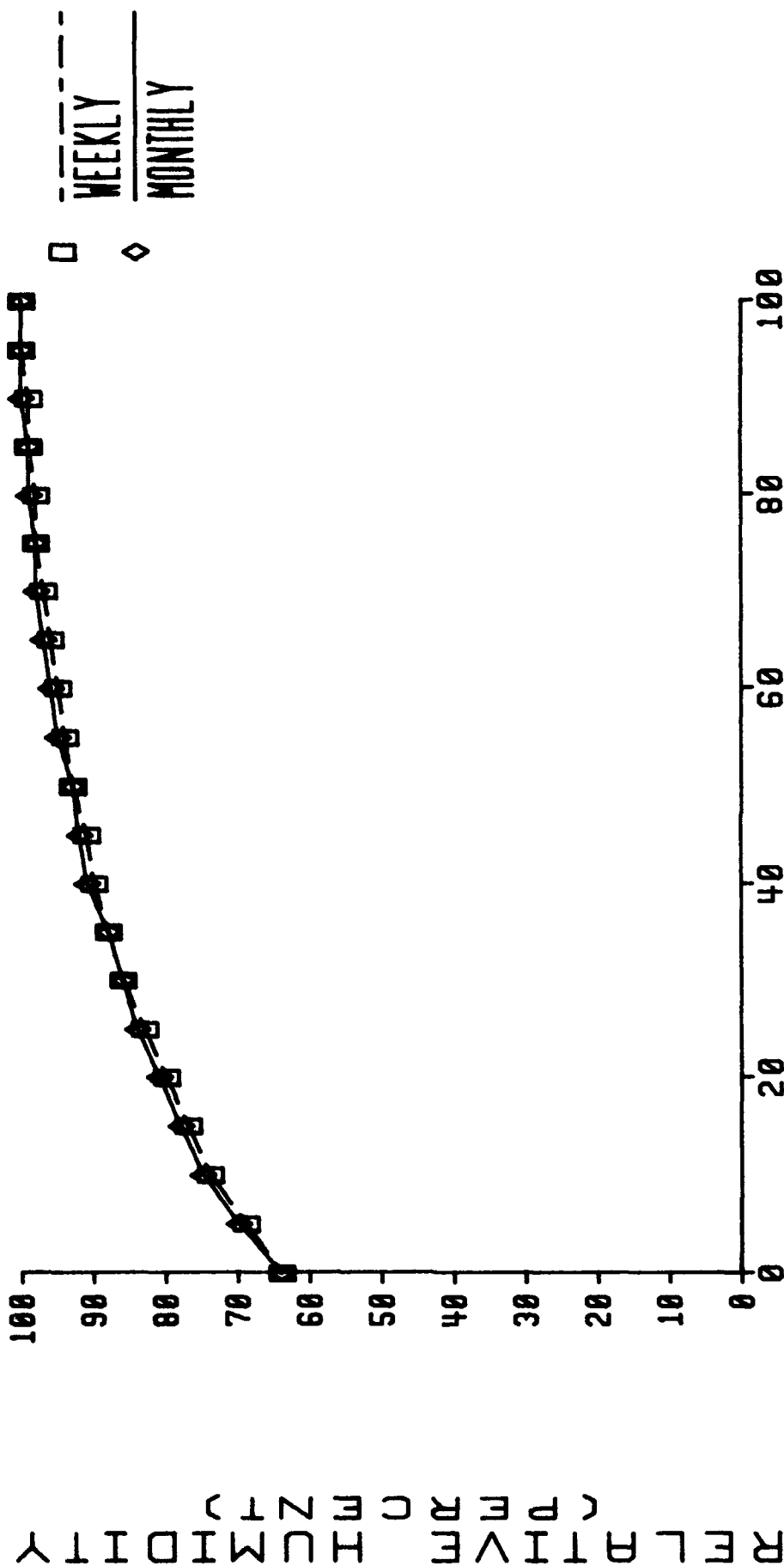


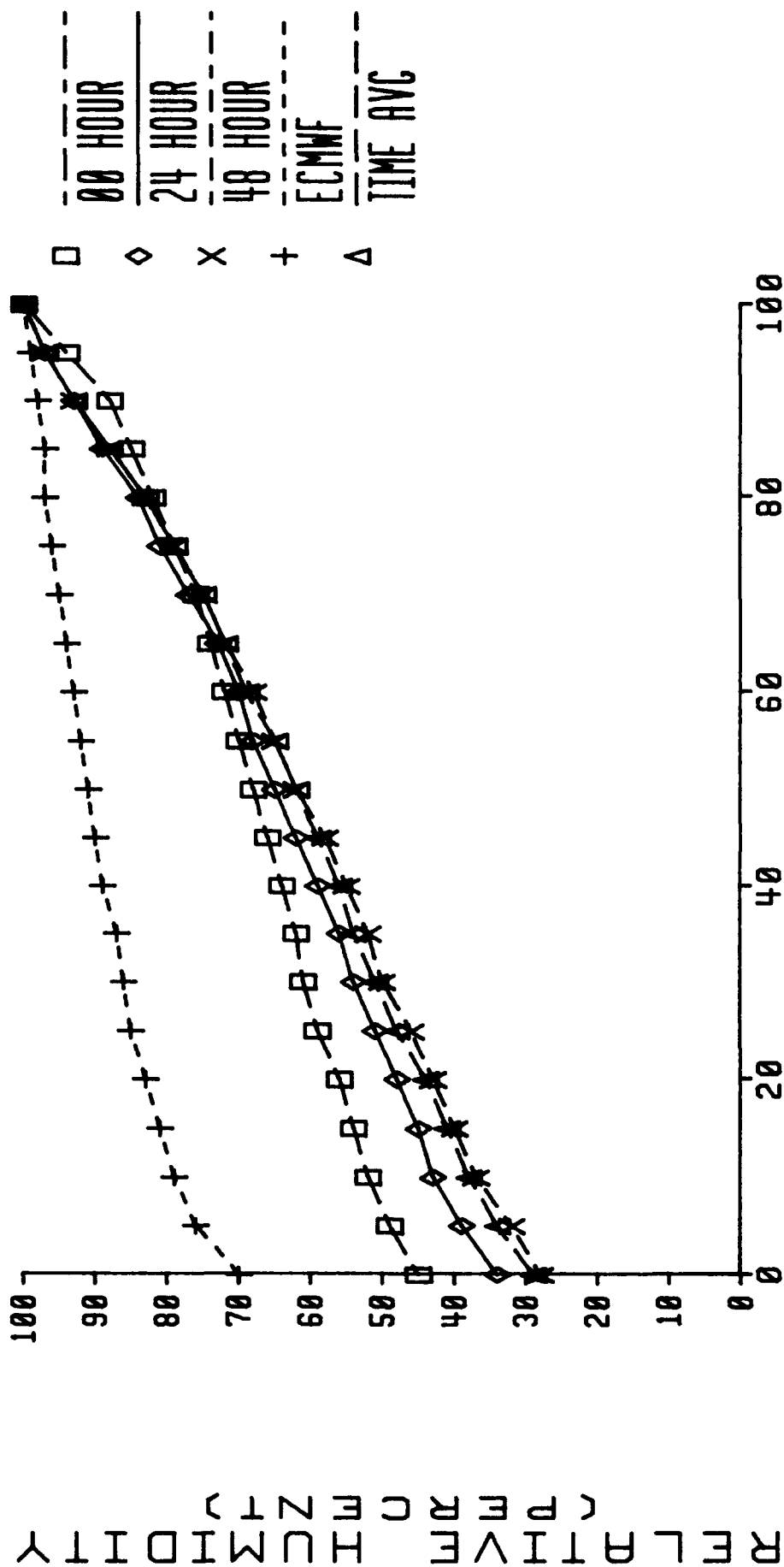
Figure A-4

WEEKLY VS MONTHLY (HIGH)
01AUG90 NH MID-LAT 24 HR



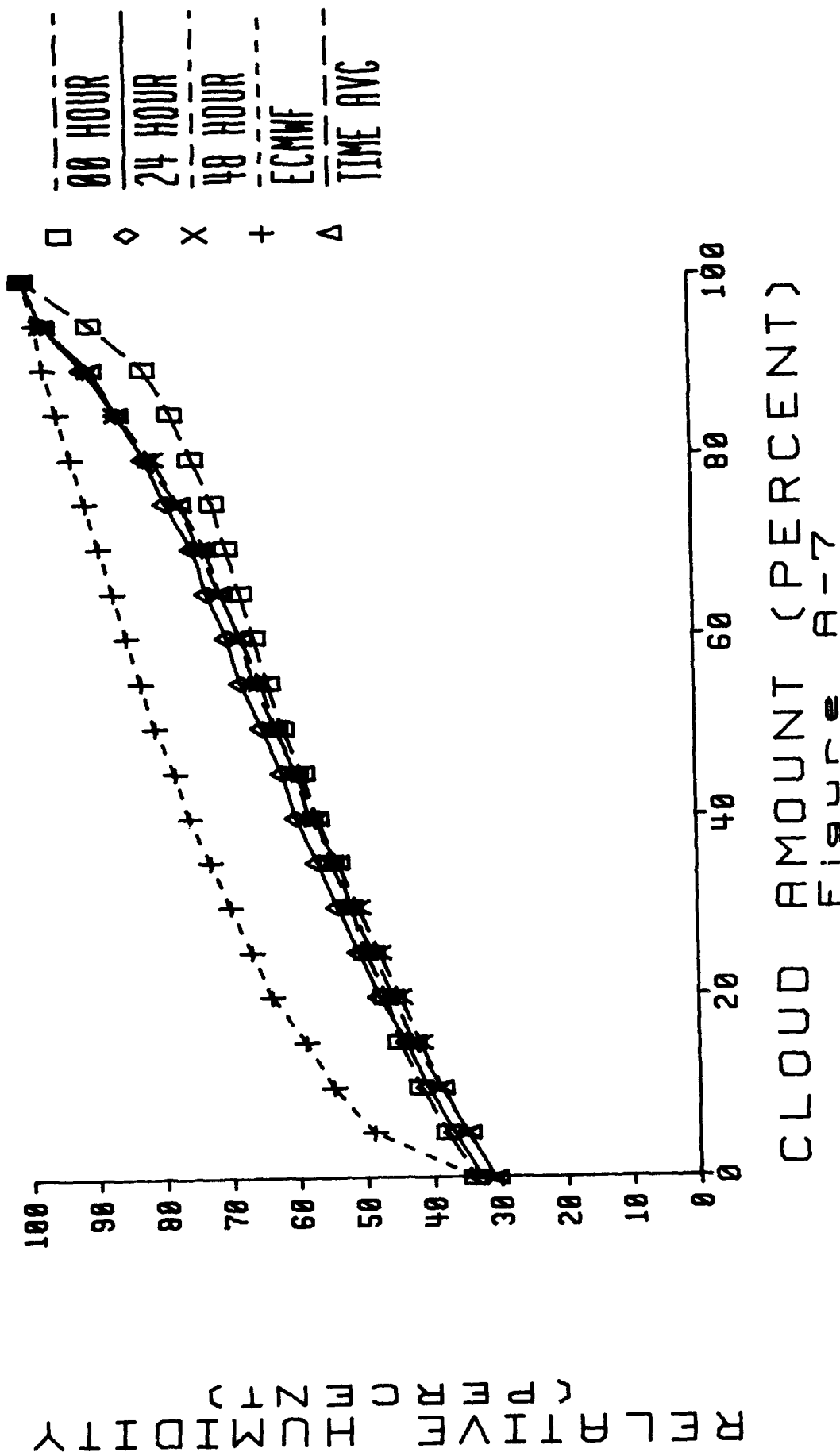
CLOUD AMOUNT (PERCENT)
Figure A-5

CURVES - FORECAST LENGTH 01/16/91 NH MID-LAT LOW



CLOUD AMOUNT (PERCENT)
Figure A-6

CURVES - FORECAST LENGTH 01/16/91 NH MID-LAT MID



CLOUD AMOUNT (PERCENT)
Figure A-7

CURVES - FORECAST LENGTH 01/16/91 NH MID-LAT HIGH

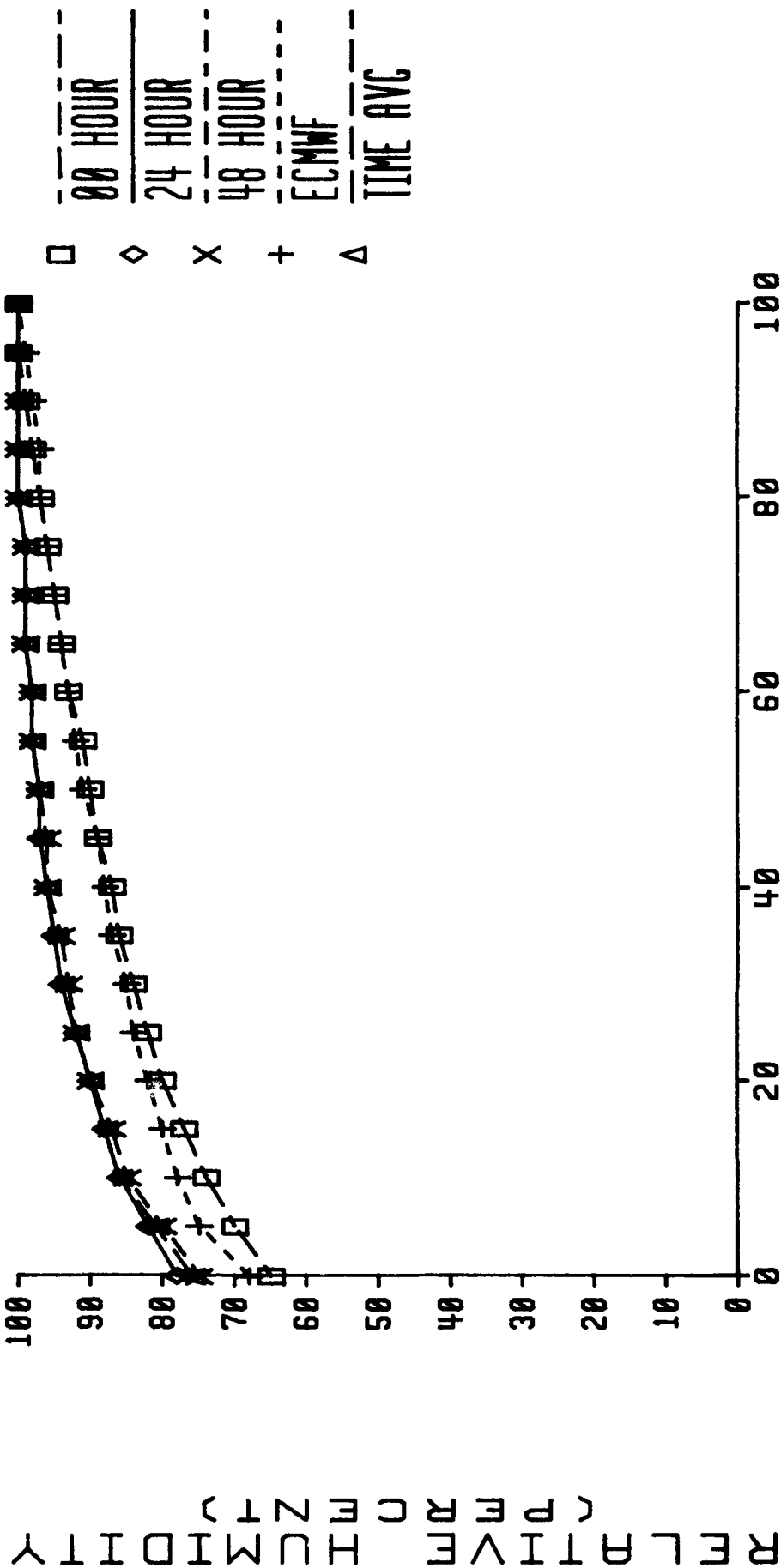
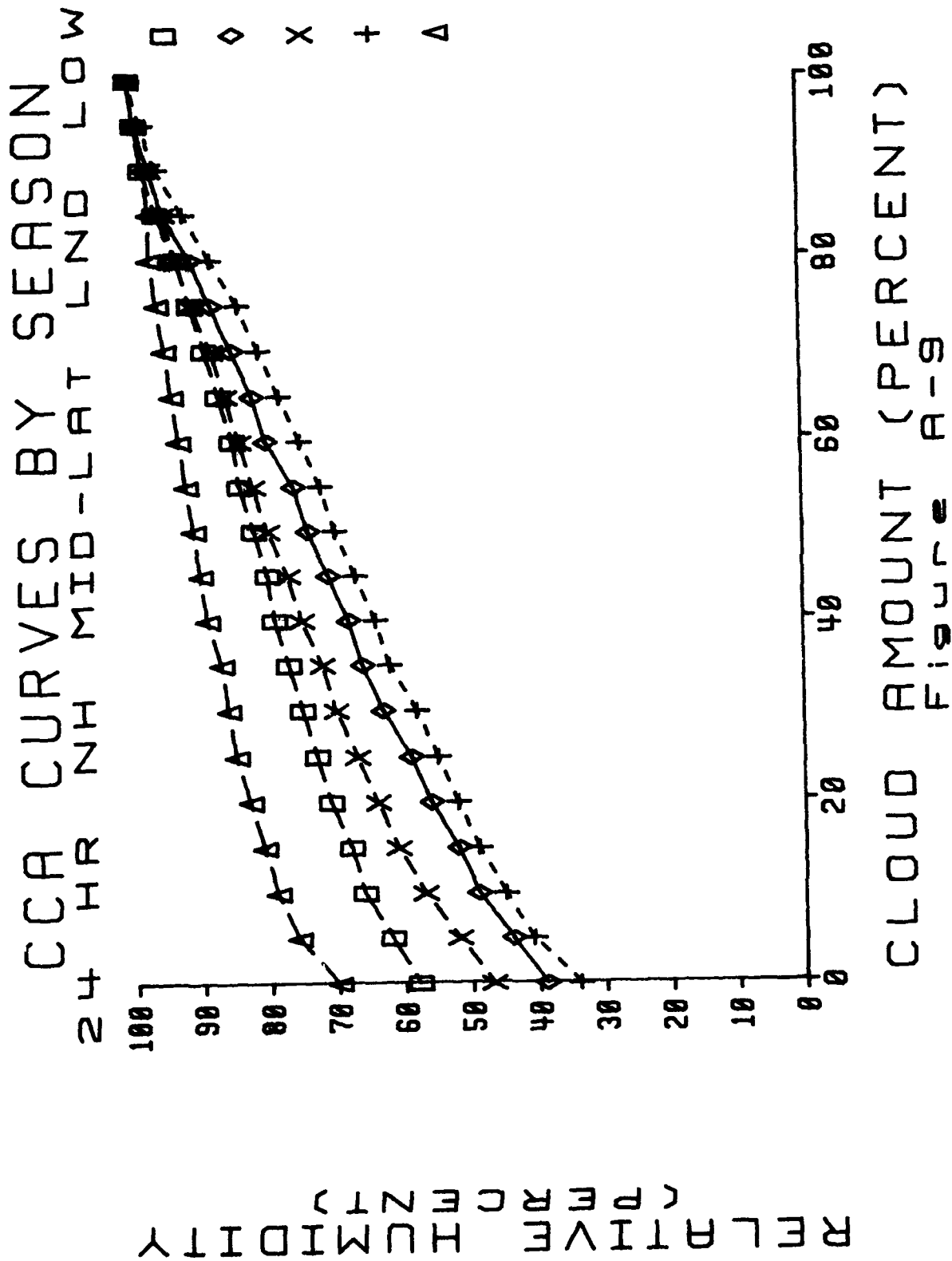
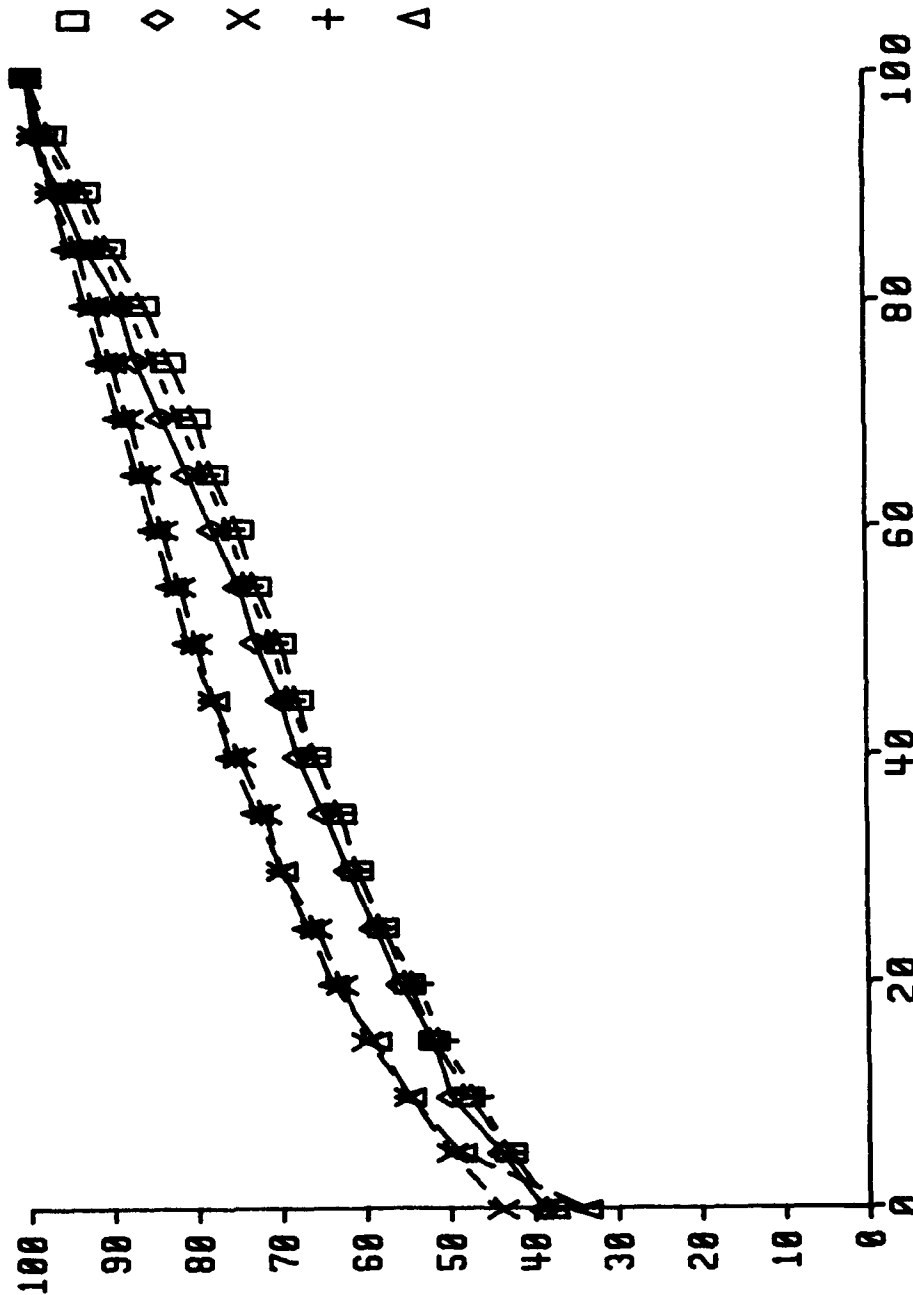


Figure A-8
CLOUD AMOUNT (PERCENT)



CCA CURVES BY SEASON 24 HR NH MID-LAT LND MID

RELATIVE HUMIDITY (PERCENT)

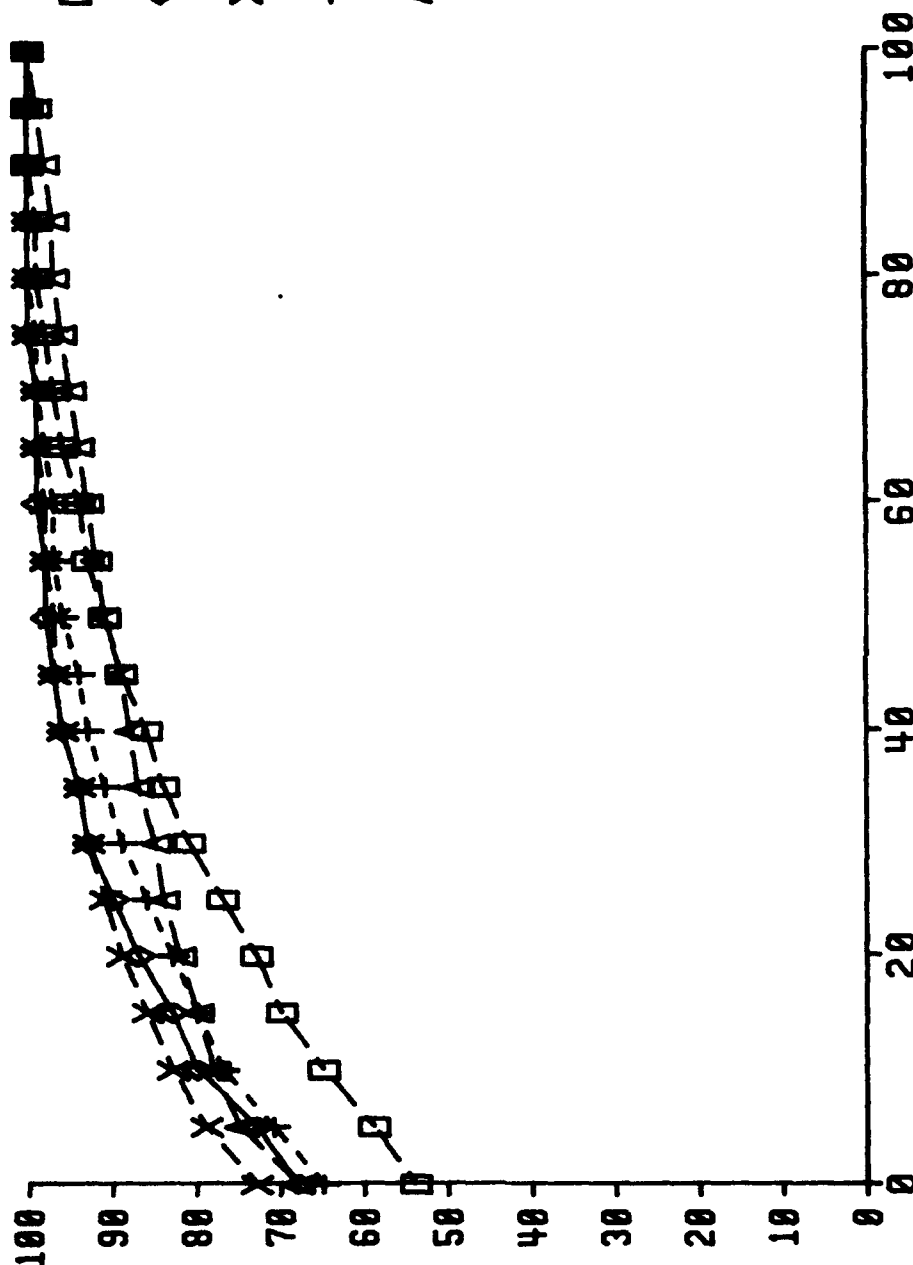


CLOUD AMOUNT (PERCENT)

Figure A-10

CCA CURVES BY SEASON 24HR NH MID-LAT LND HIGH

RELATIVE HUMIDITY
(PERCENT)



CLOUD AMOUNT (PERCENT)

Figure A-11

CCA CURVES BY REGION

28 AUG 91 24 HR LOW

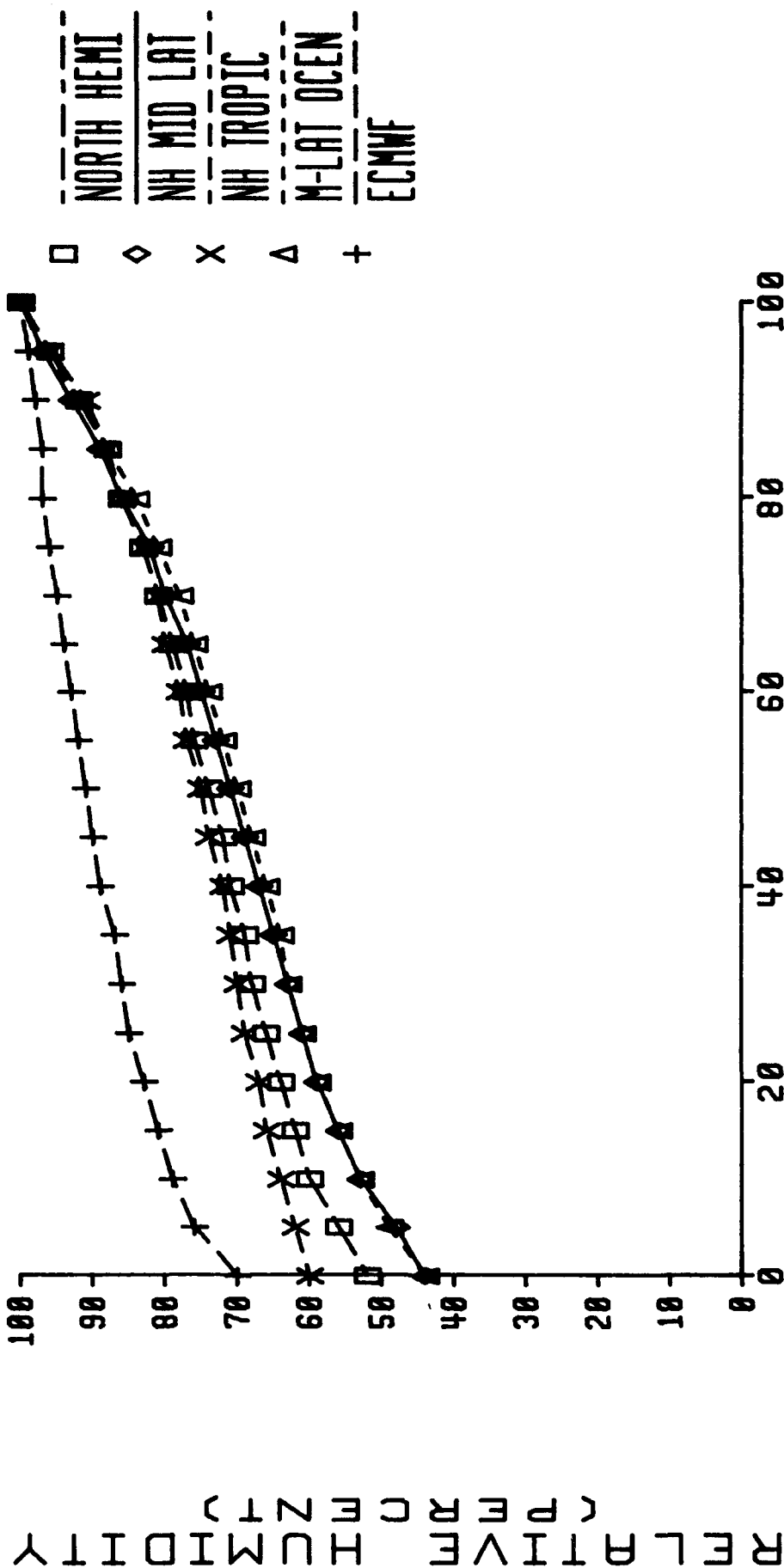


Figure A-12

CCA CURVES BY REGION

28 AUG 91 24 HR LOW

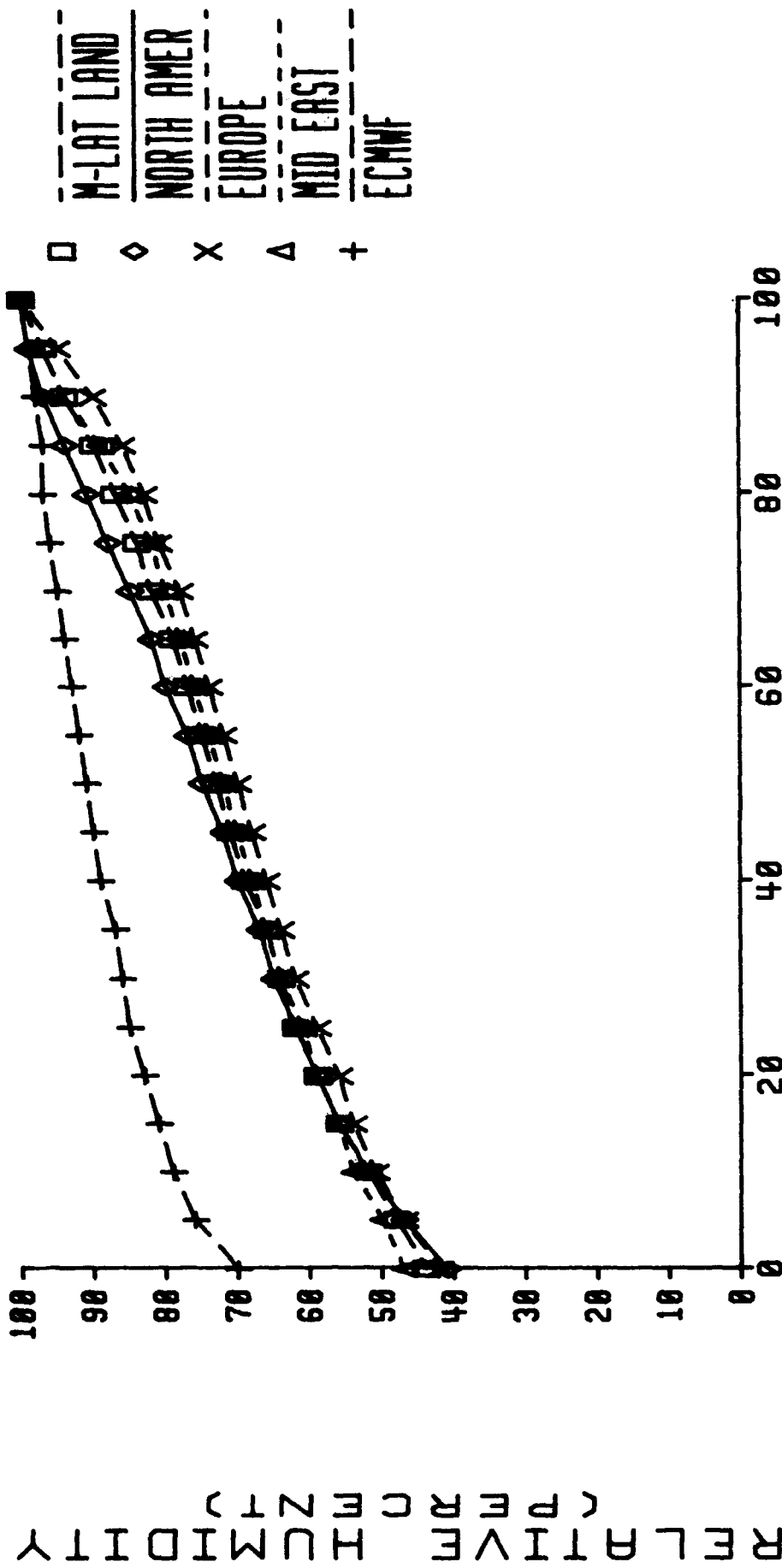
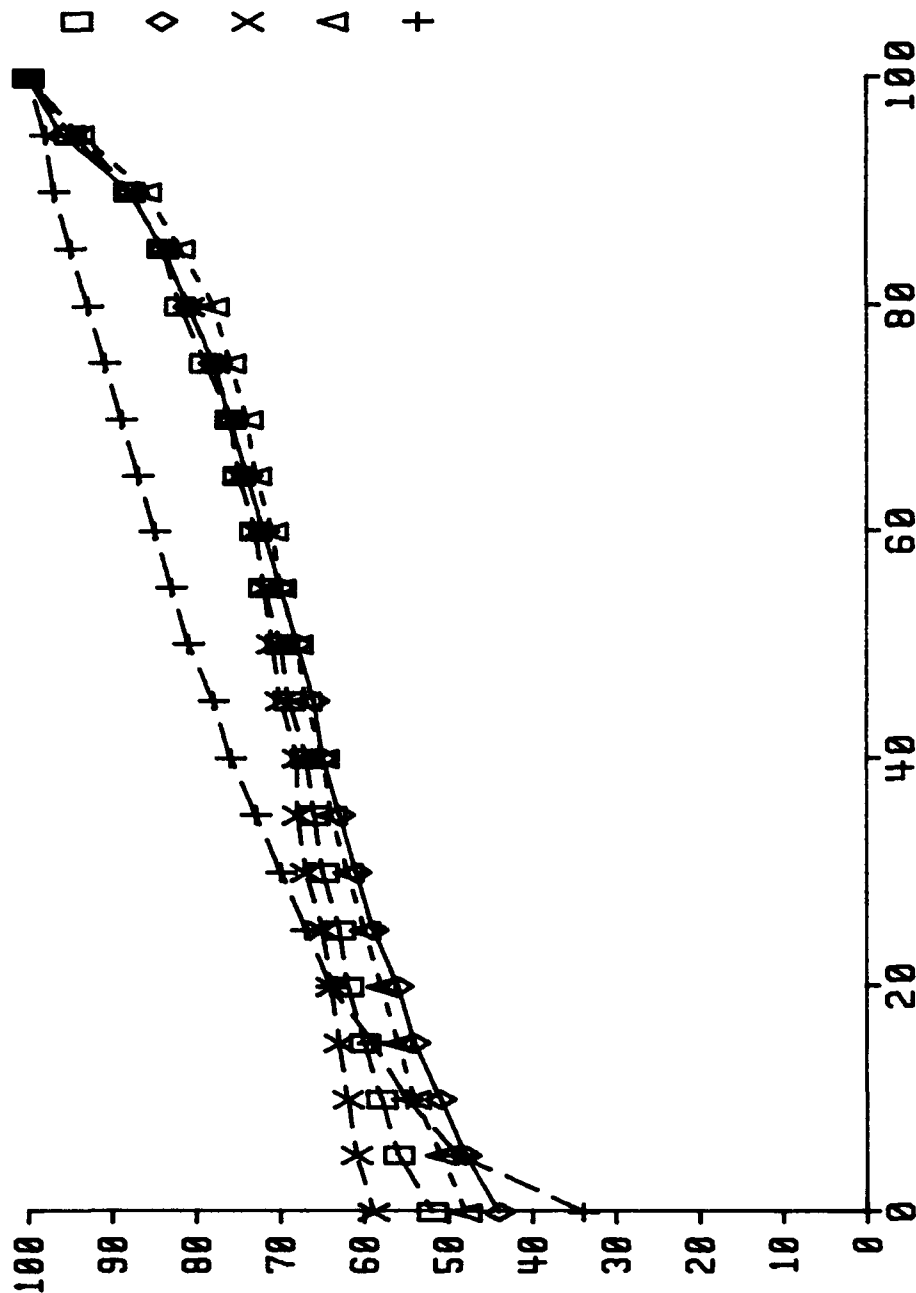


Figure A-13

CCA CURVES BY REGION 28 AUG 91 24 HR MIDDLE

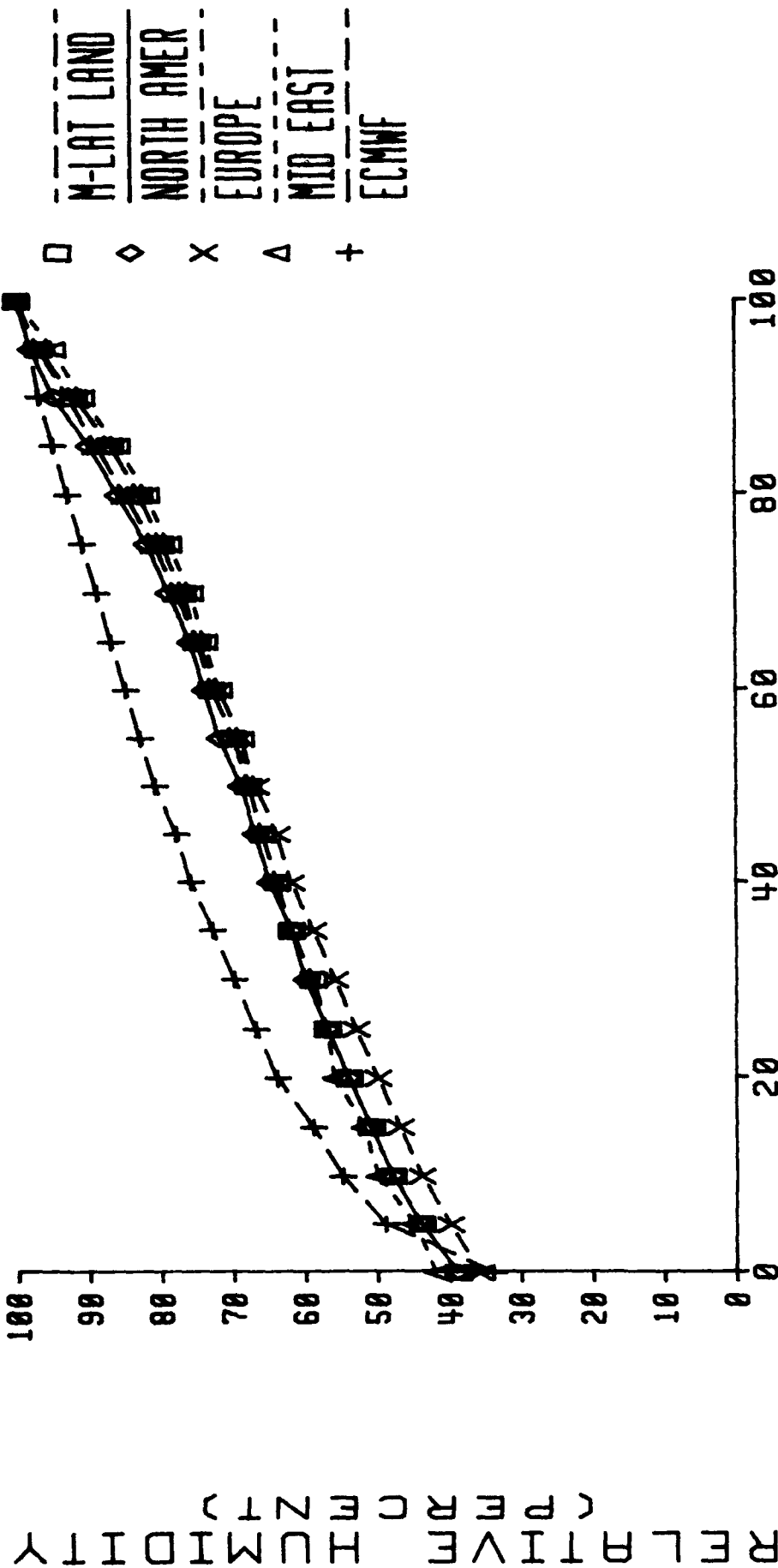
RELATIVE HUMIDITY (PERCENT)



CLOUD AMOUNT (PERCENT)

Figure A-14

CCA CURVES BY REGION 28 AUG 91 24 HR MIDDLE



CLOUD AMOUNT (PERCENT)
Figure A-15

CCA CURVES BY REGION

28 AUG 91 24 HOUR HIGH

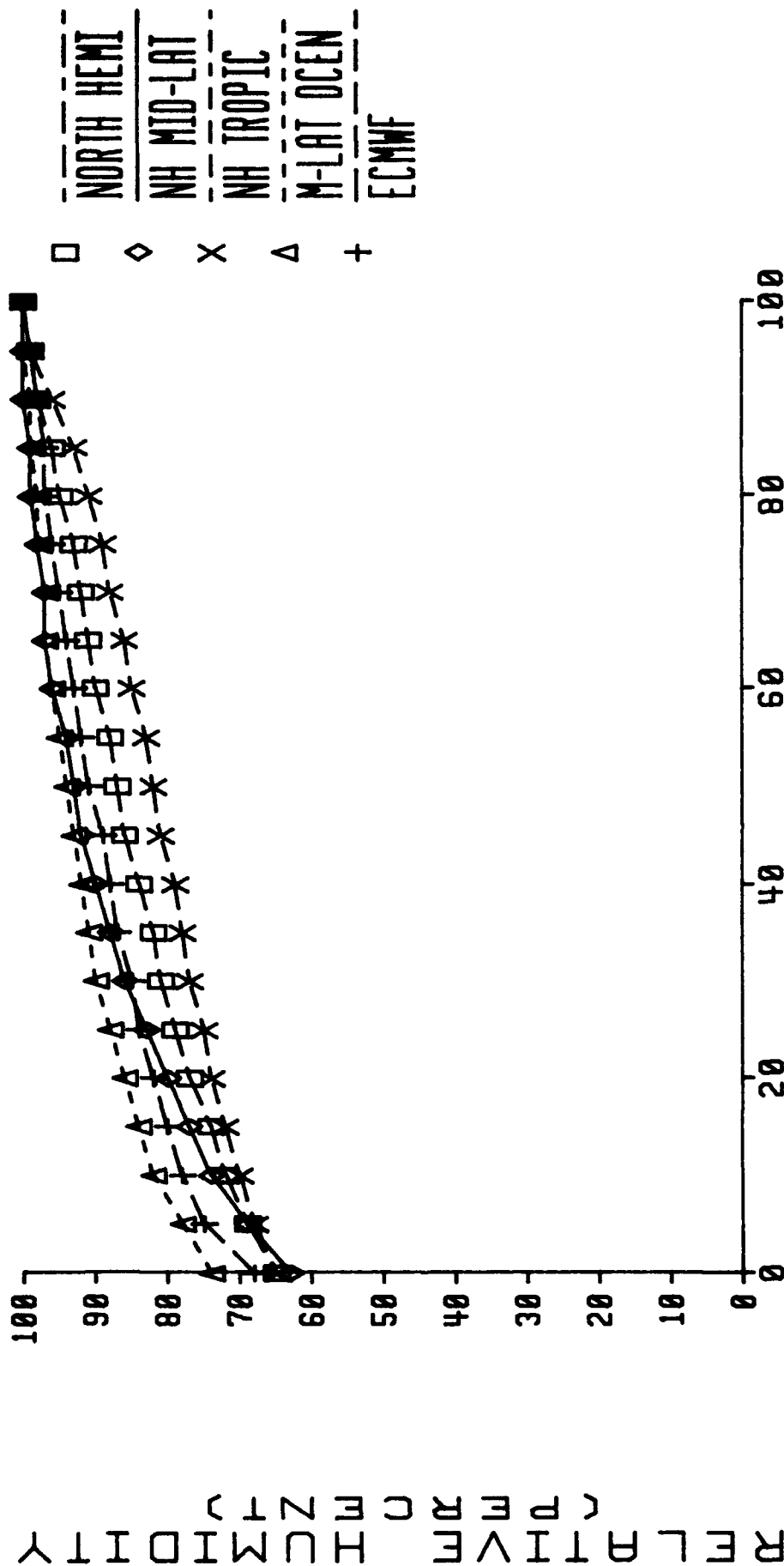
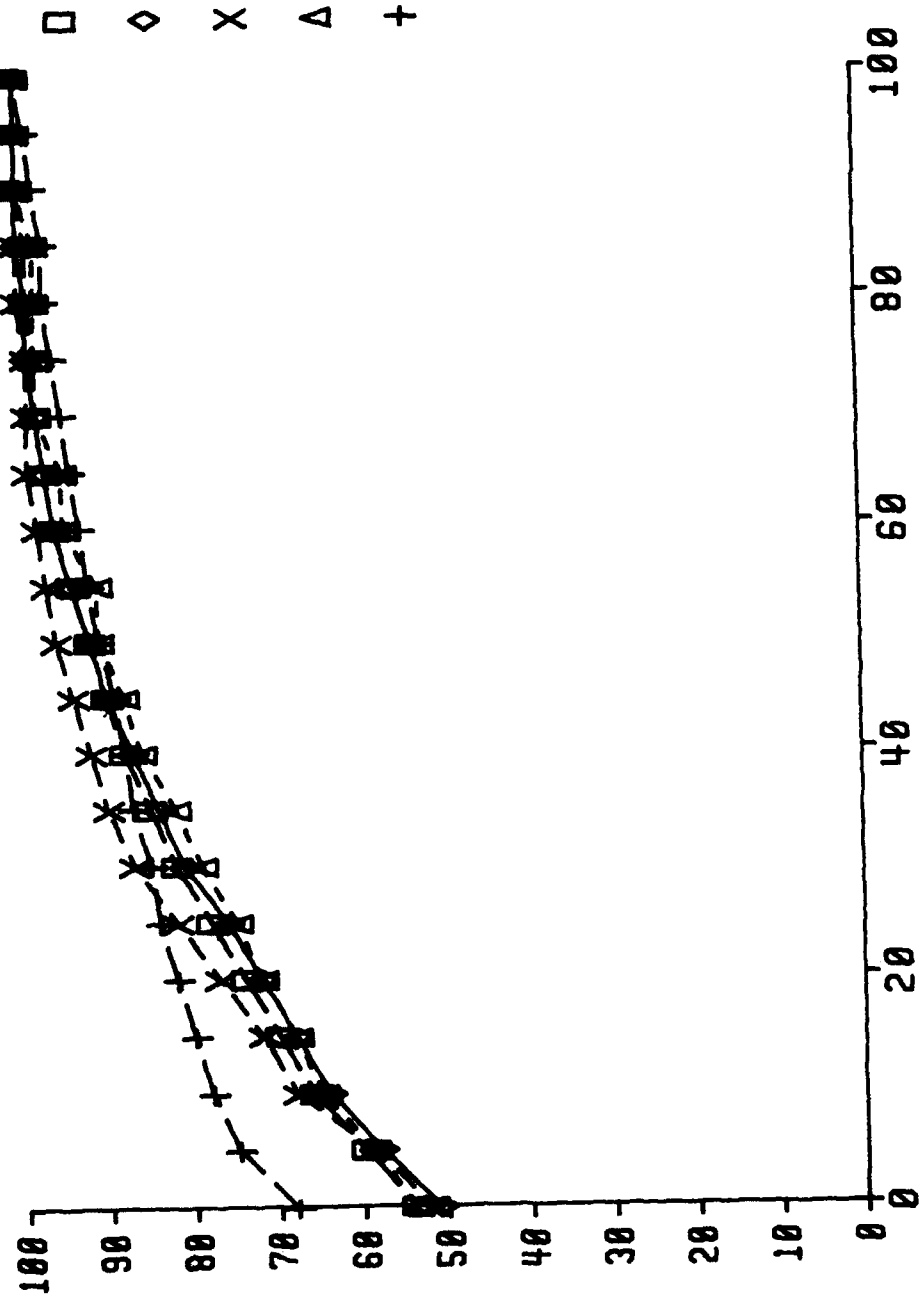


Figure A-16

CCA CURVES BY REGION
28 AUG 91 24 HOUR HIGH

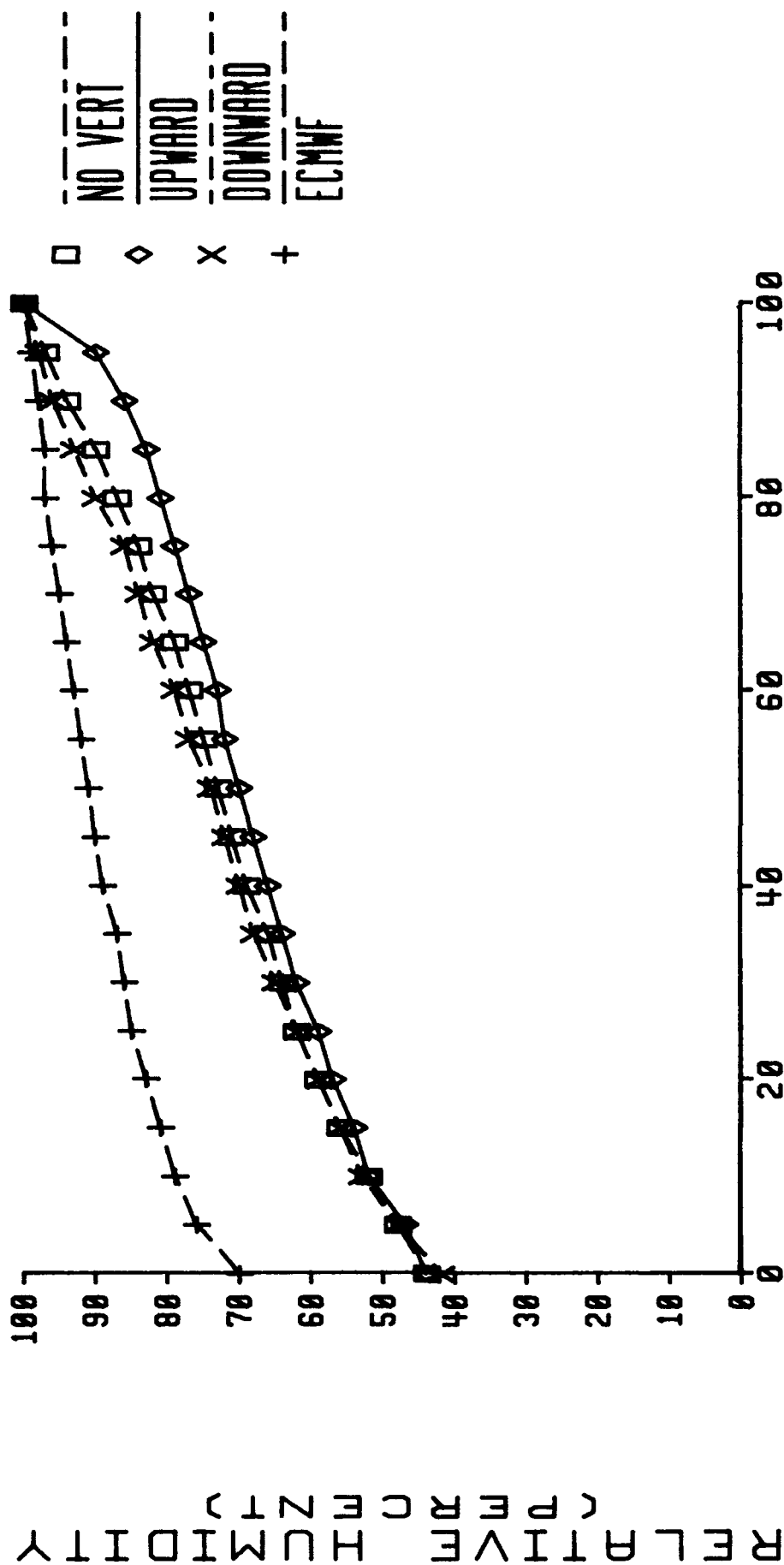
RELATIVE HUMIDITY (%)



CLOUD AMOUNT (PERCENT)
Figure A-17

M-LAT LAND
NORTH AMER
EUROPE
MID EAST
ECMWF

N H MID-LATITUDE LAND
28 AUG 91 24 HR LOW



CLOUD AMOUNT (PERCENT)
Figure A-18

NH MID-LATITUDE LAND
 28 AUG 91 24 HR MIDDLE

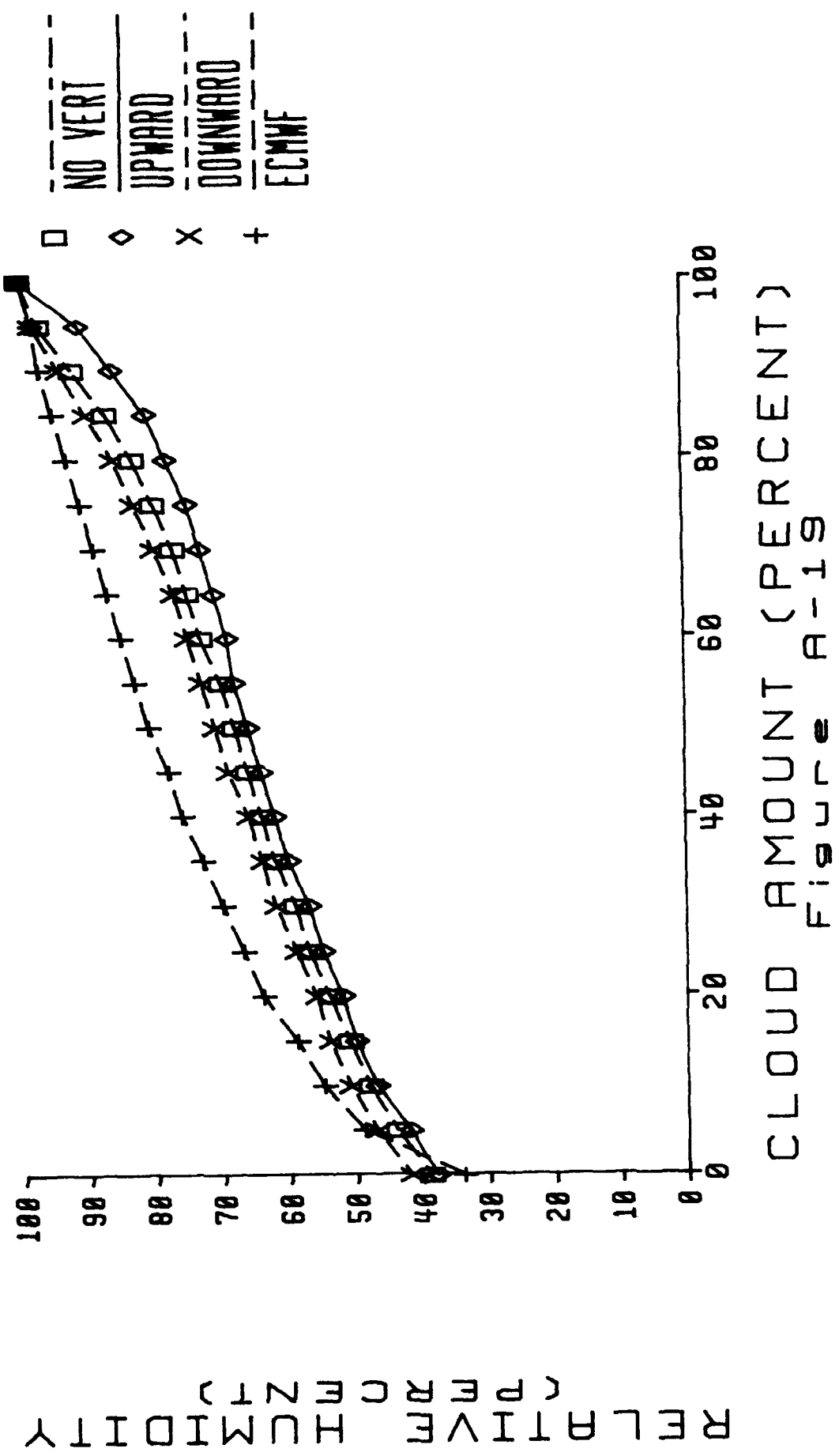
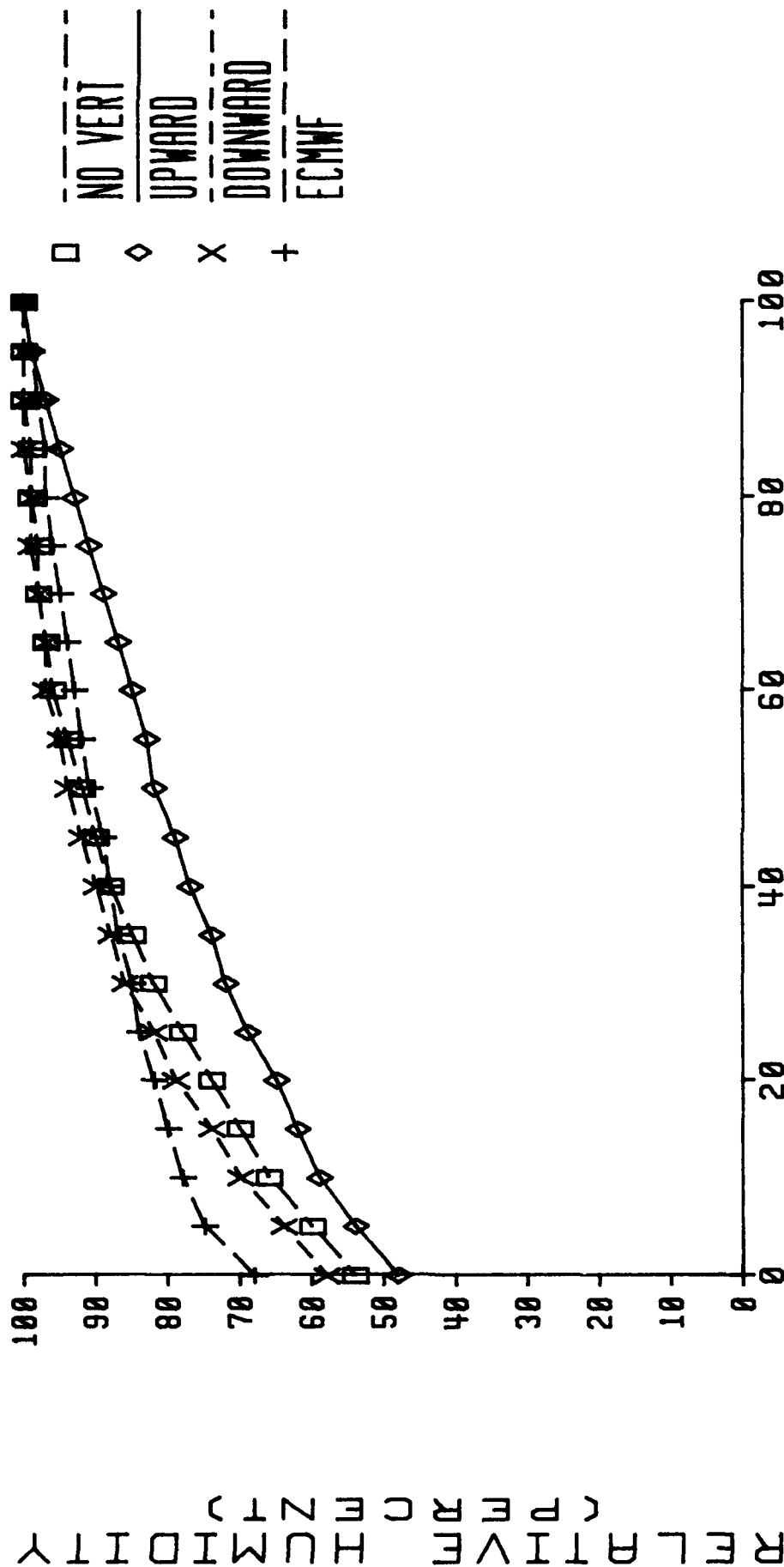


Figure A-19

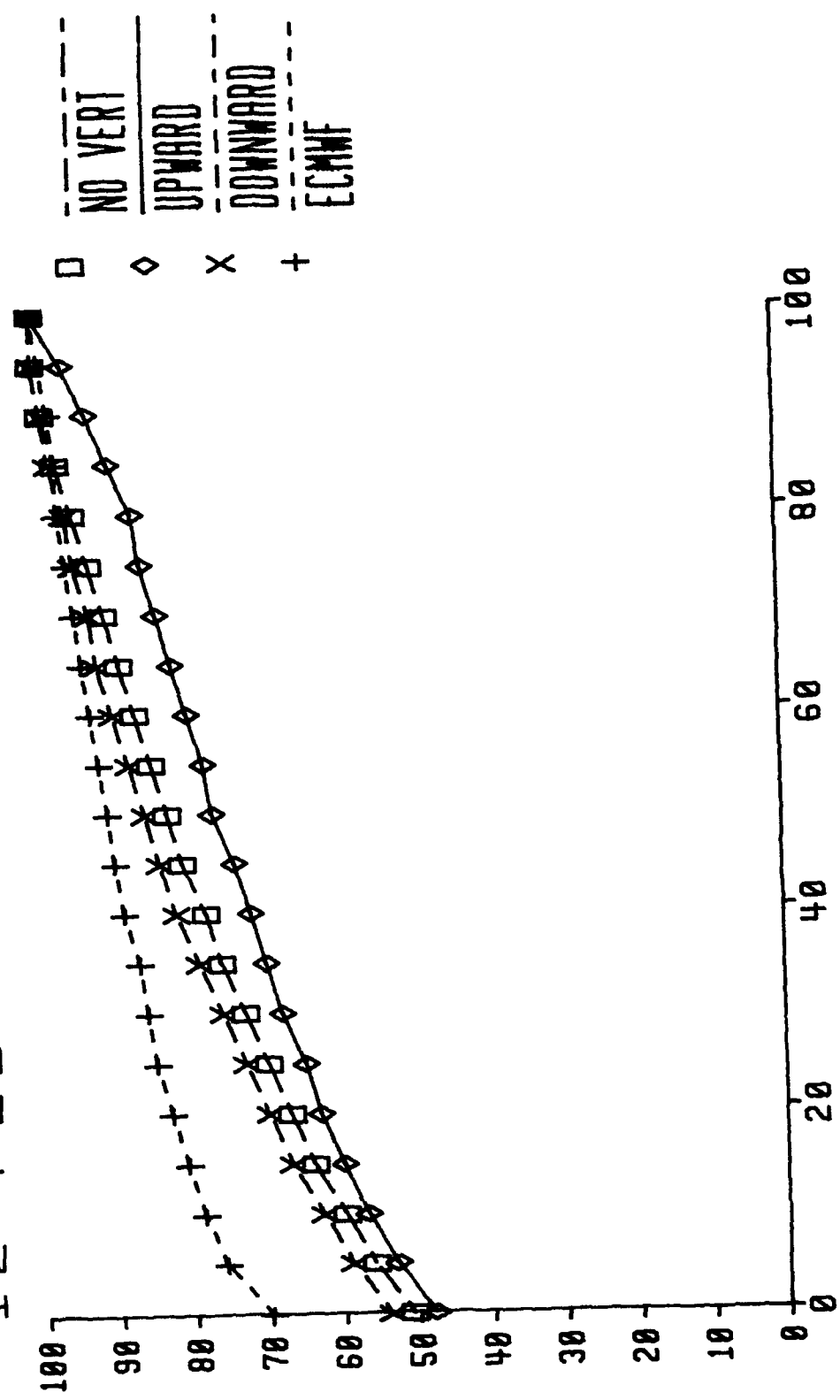
28 AUG 91 24 HOUR HIGH



CLOUD AMOUNT (PERCENT)
Figure A-20

N H MID-LATITUDE LAND
12 FEB 92 24 HR LOW

RELATIVE HUMIDITY
(PERCENT)



CLOUD AMOUNT (PERCENT)
Figure A-21

12 FEB 92 24 HR LAND MIDDLE

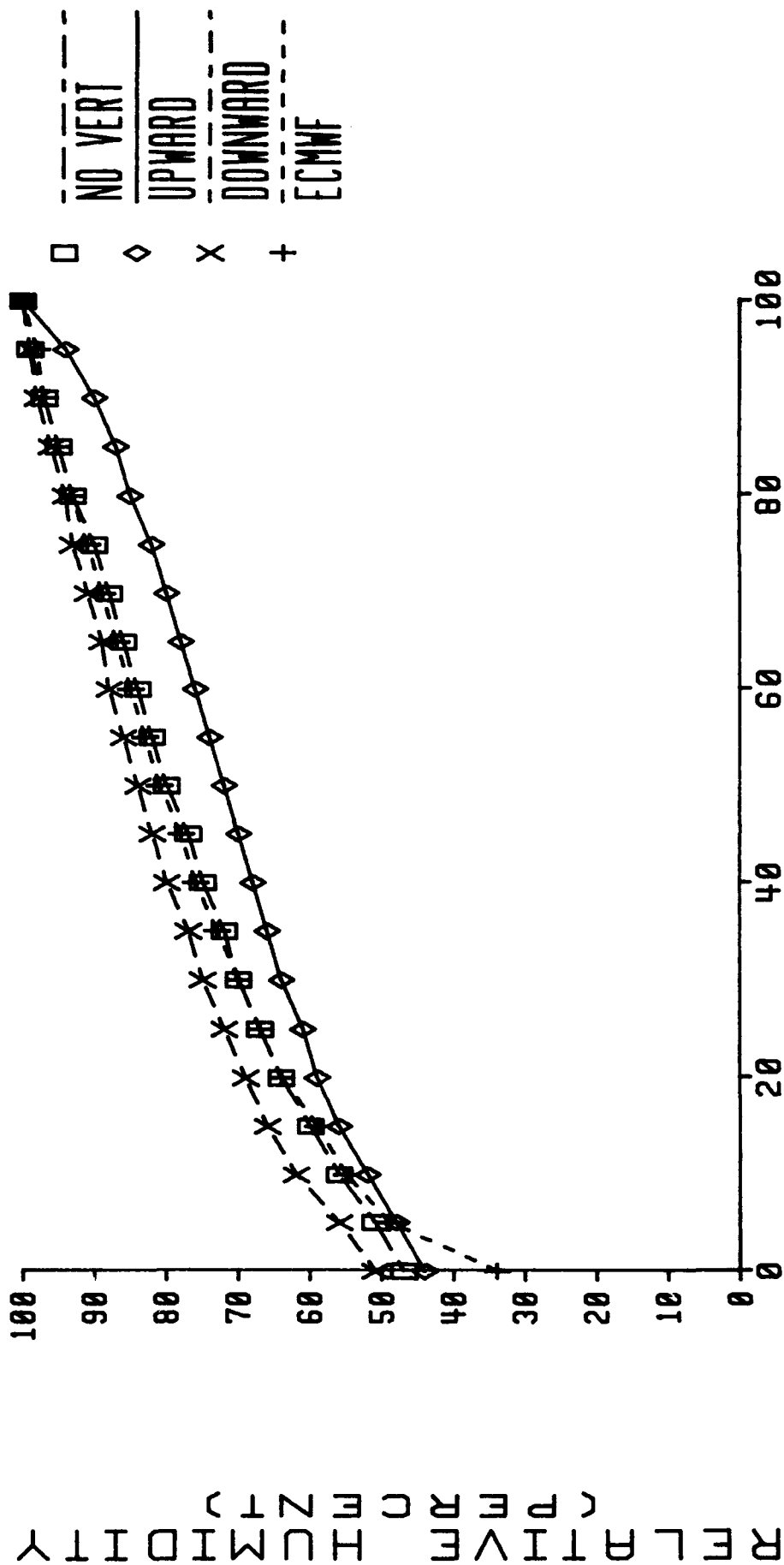
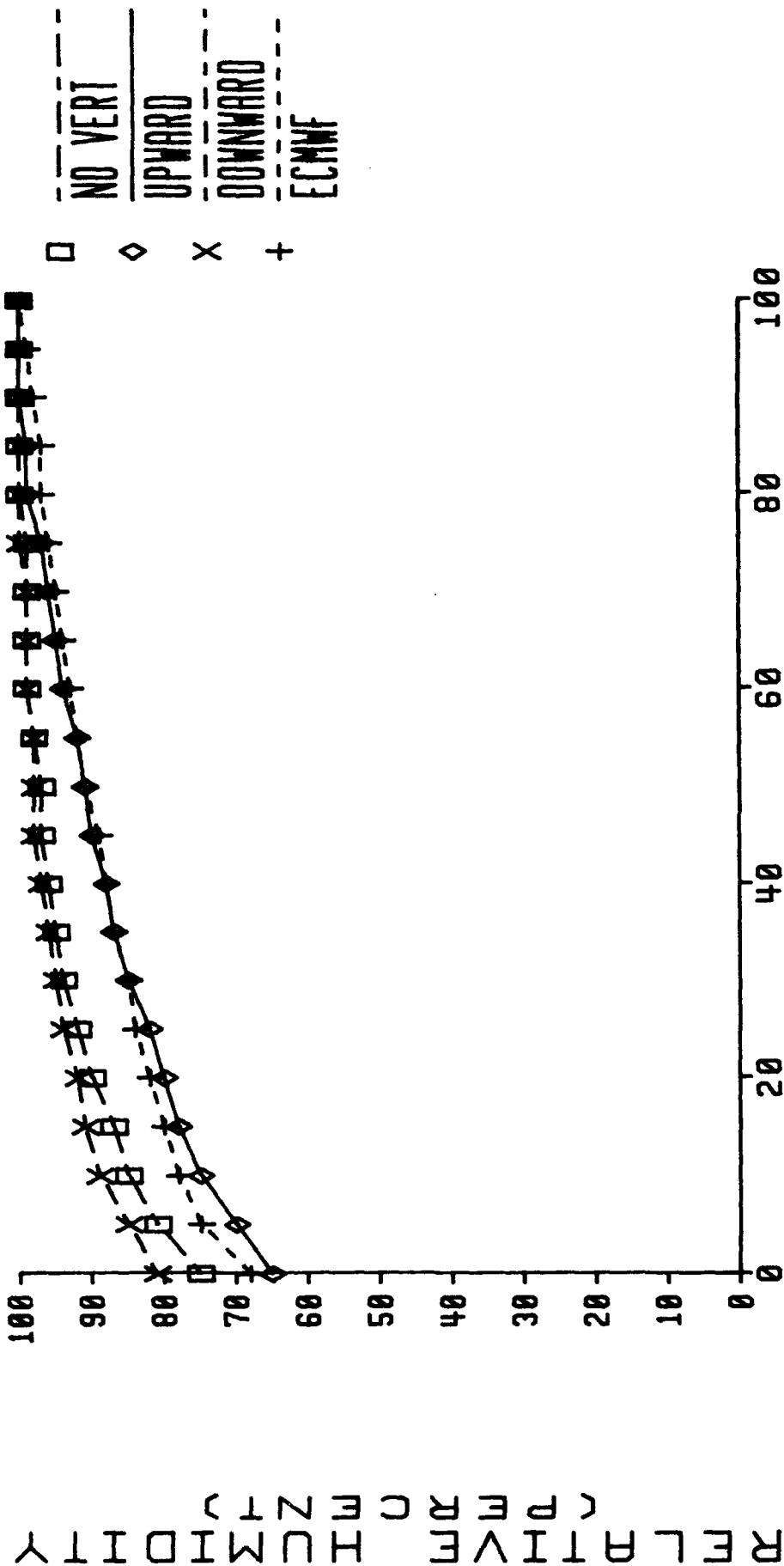


Figure A-22

N H MID-LATITUDE LAND HIGH
12 FEB 92 24 HR



CLOUD AMOUNT (PERCENT)
Figure A-23

APPENDIX B:

PLOTS OF VERIFICATION STATISTICS

FOR NORTHERN HEMISPHERE MID-LATITUDE OCEAN

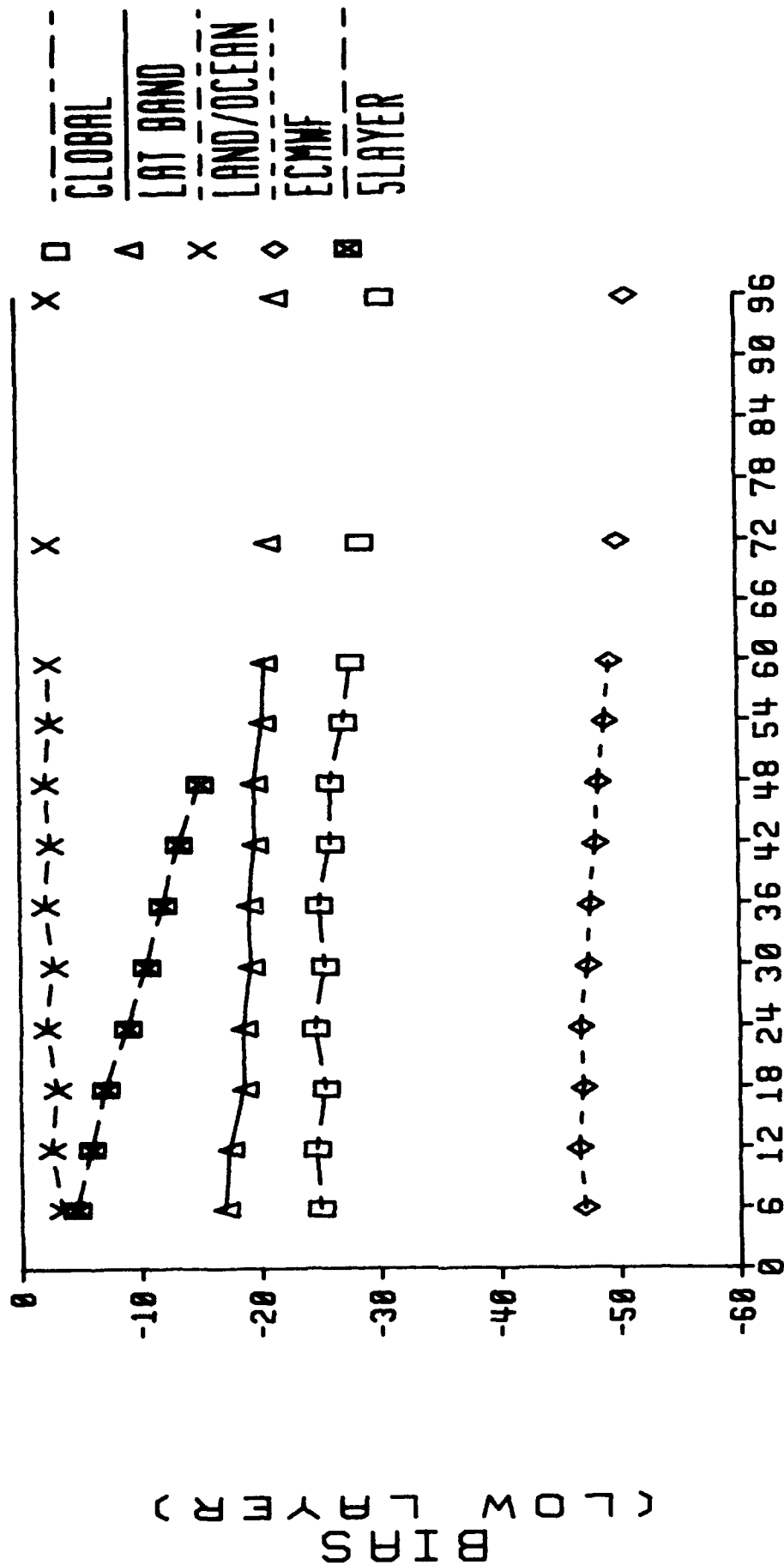
17 JAN 91 TO 13 FEB 91

LIST OF FIGURES

- Figure B-1.** BIAS Scores for Cloud Forecasts Computed by the 5LAYER Model (to 48 hours only), Computed Using Cloud Curve Algorithm Global Curves, Northern Hemisphere Mid-Latitude Curves, and Northern Hemisphere Mid-Latitude Ocean Curves and Cloud Forecasts Computed Using the European Centre for Medium Range Weather Forecasts Curves (Figure A-1) For 6 to 60, 72 and 96 Hour Low Layer Forecasts Verified Over Northern Hemisphere Mid-Latitude Ocean During the Period from 17 January 1991 to 13 February 1991.
- Figure B-2.** BIAS Scores for Cloud Forecasts Computed by the 5LAYER Model (to 48 hours only), Computed Using Cloud Curve Algorithm Global Curves, Northern Hemisphere Mid-Latitude Curves, and Northern Hemisphere Mid-Latitude Ocean Curves and Cloud Forecasts Computed Using the European Centre for Medium Range Weather Forecasts Curves (Figure A-1) For 6 to 60, 72 and 96 Hour Middle Layer Forecasts Verified Over Northern Hemisphere Mid-Latitude Ocean During the Period from 17 January 1991 to 13 February 1991.
- Figure B-3.** BIAS Scores for Cloud Forecasts Computed by the 5LAYER Model (to 48 hours only), Computed Using Cloud Curve Algorithm Global Curves, Northern Hemisphere Mid-Latitude Curves, and Northern Hemisphere Mid-Latitude Ocean Curves and Cloud Forecasts Computed Using the European Centre for Medium Range Weather Forecasts Curves (Figure A-1) For 6 to 60, 72 and 96 Hour High Layer Forecasts Verified Over Northern Hemisphere Mid-Latitude Ocean During the Period from 17 January 1991 to 13 February 1991.
- Figure B-4.** BIAS Scores for Cloud Forecasts Computed by the 5LAYER Model (to 48 hours only), Computed Using Cloud Curve Algorithm Global Curves, Northern Hemisphere Mid-Latitude Curves, and Northern Hemisphere Mid-Latitude Ocean Curves and Cloud Forecasts Computed Using the European Centre for Medium Range Weather Forecasts Curves (Figure A-1) For 6 to 60, 72 and 96 Hour Total Cloud Forecasts Verified Over Northern Hemisphere Mid-Latitude Ocean During the Period from 17 January 1991 to 13 February 1991.
- Figure B-5.** BIAS Scores for Cloud Forecasts Computed by the 5LAYER Model (to 48 hours only), by Using Persistence (to 72 hours only) and by Using Cloud Curve Algorithm Northern Hemisphere Mid-Latitude Ocean Curves For 6 to 60, 72 and 96 Hour Total Cloud Forecasts Verified Over Northern Hemisphere Mid-Latitude Ocean During the Period from 17 January 1991 to 13 February 1991.

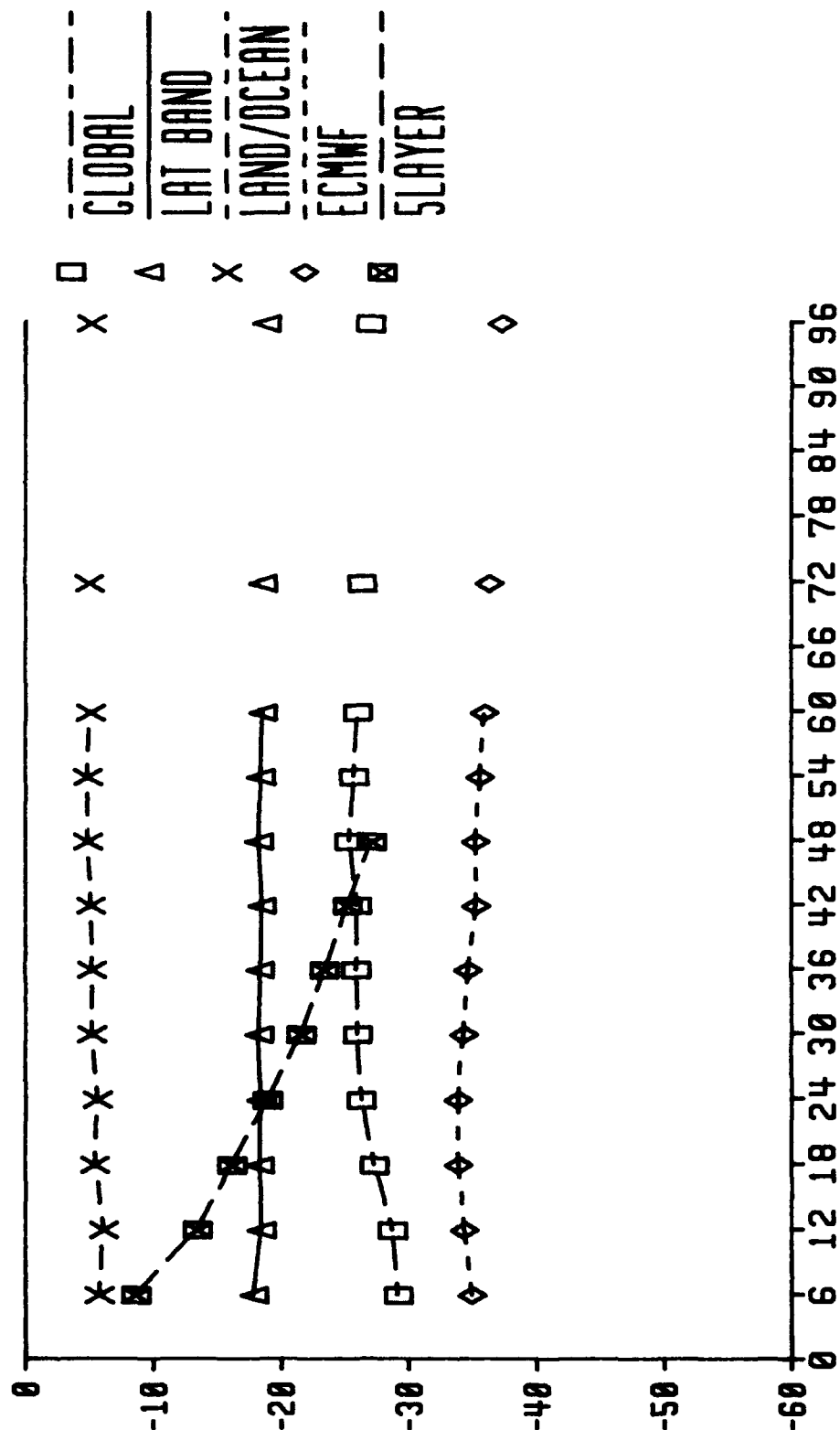
- Figure B-6. 20/20 Scores for Cloud Forecasts Computed by the 5LAYER Model (to 48 hours only), Computed Using Cloud Curve Algorithm Global Curves, Northern Hemisphere Mid-Latitude Curves, and Northern Hemisphere Mid-Latitude Ocean Curves and Cloud Forecasts Computed Using the European Centre for Medium Range Weather Forecasts Curves (Figure A-1) For 6 to 60, 72 and 96 Hour Total Cloud Forecasts Verified Over Northern Hemisphere Mid-Latitude Ocean During the Period from 17 January 1991 to 13 February 1991.
- Figure B-7. RELIABILITY Scores for Cloud Forecasts Computed by the 5LAYER Model (to 48 hours only), Computed Using Cloud Curve Algorithm Global Curves, Northern Hemisphere Mid-Latitude Curves, and Northern Hemisphere Mid-Latitude Ocean Curves and Cloud Forecasts Computed Using the European Centre for Medium Range Weather Forecasts Curves (Figure A-1) For 6 to 60, 72 and 96 Hour Total Cloud Forecasts Verified Over Northern Hemisphere Mid-Latitude Ocean During the Period from 17 January 1991 to 13 February 1991.
- Figure B-8. RMSE Scores for Cloud Forecasts Computed by the 5LAYER Model (to 48 hours only), Computed Using Cloud Curve Algorithm Global Curves, Northern Hemisphere Mid-Latitude Curves, and Northern Hemisphere Mid-Latitude Ocean Curves and Cloud Forecasts Computed Using the European Centre for Medium Range Weather Forecasts Curves (Figure A-1) For 6 to 60, 72 and 96 Hour Total Cloud Forecasts Verified Over Northern Hemisphere Mid-Latitude Ocean During the Period from 17 January 1991 to 13 February 1991.

N H MID-LAT OCEAN
17 JAN 91 - 13 FEB 91



FORECAST LENGTH (HOURS)
Figure B-1

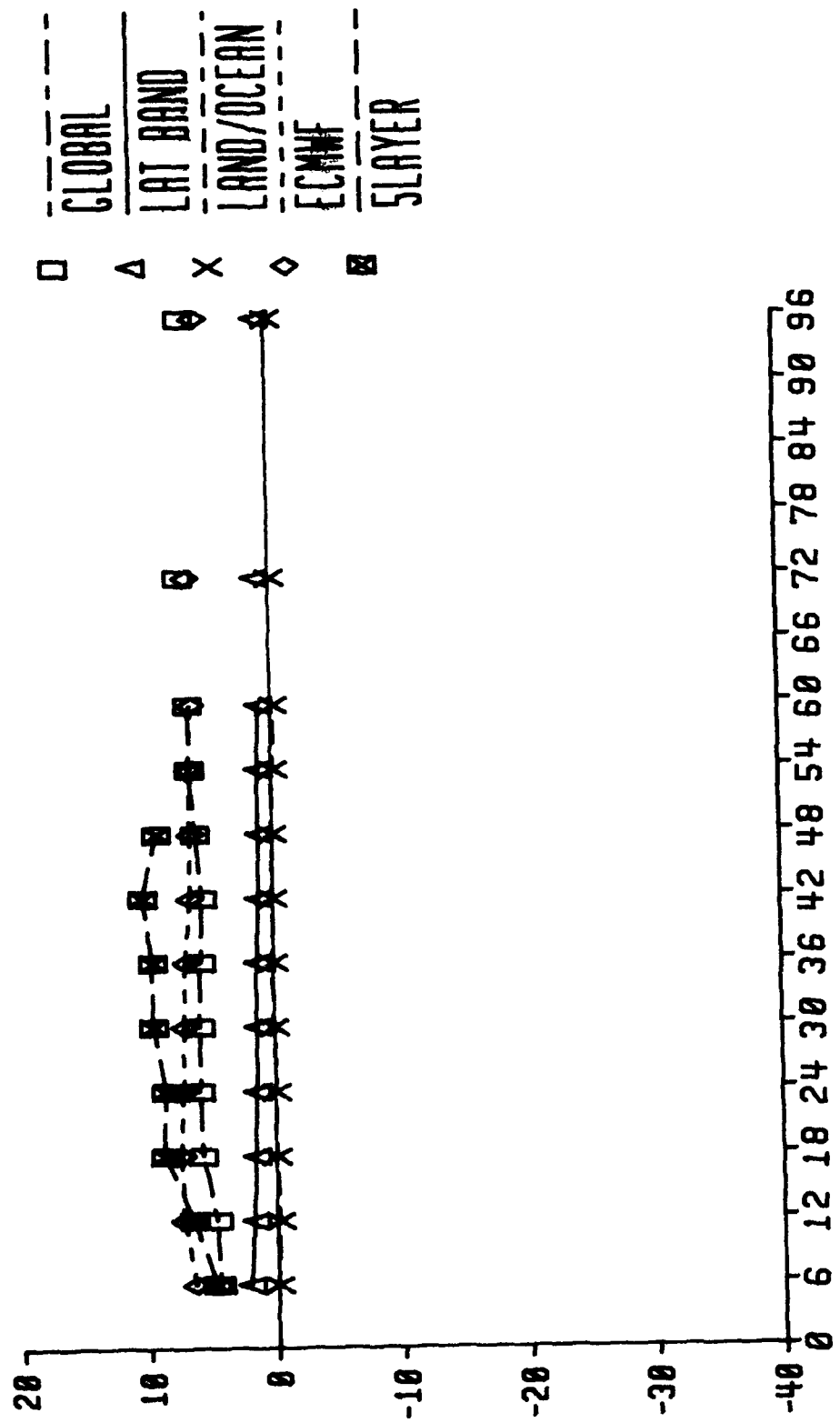
17 JAN 91 - 13 FEB 91



FORECAST LENGTH (HOURS)
Figure B-2

B I A S
(M I D D L E L A Y E R)

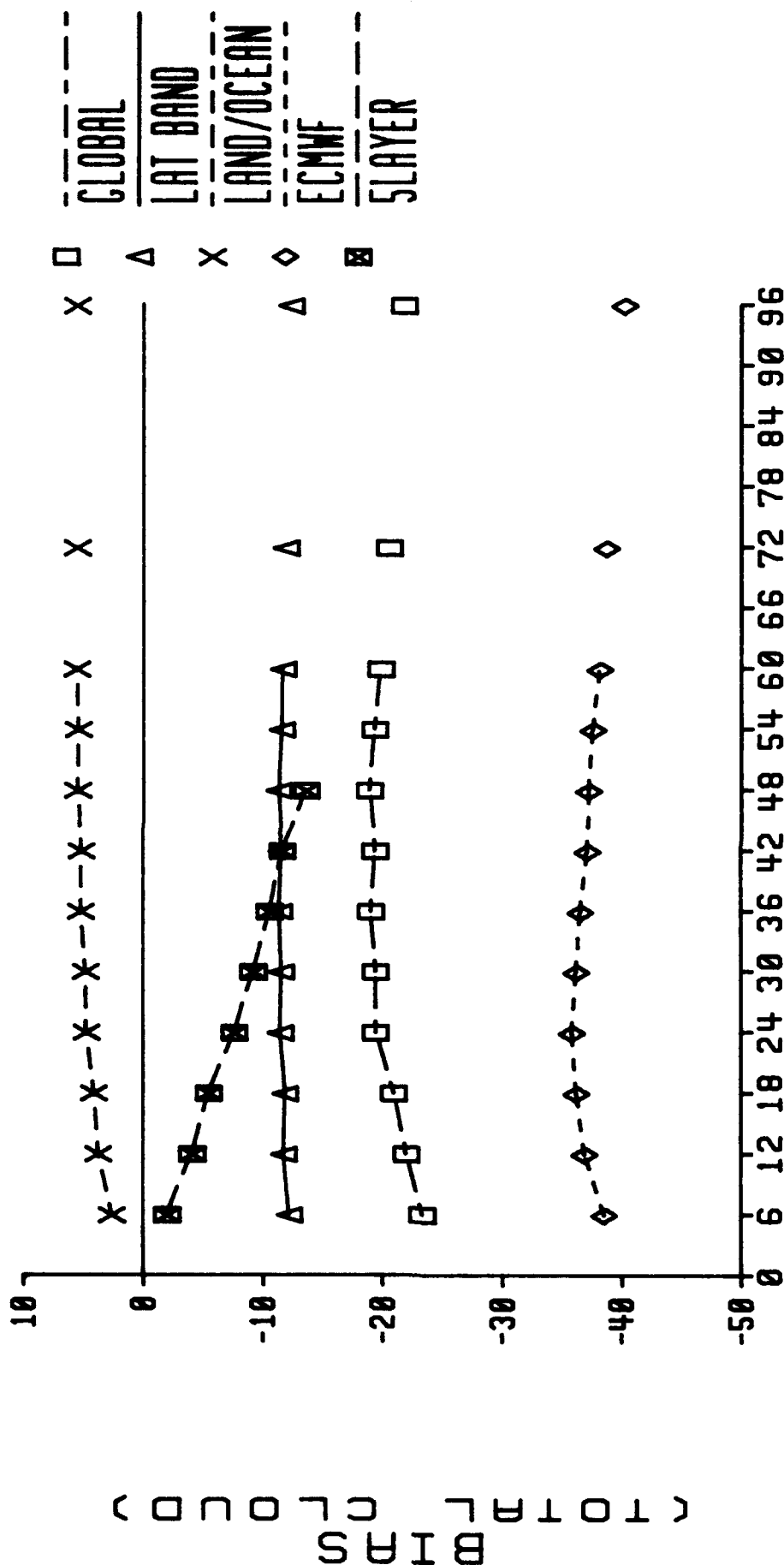
17 N H MID-LAT OCEAN 91 - 13 FEB 91



FORECAST LENGTH (HOURS)
Figure B-3

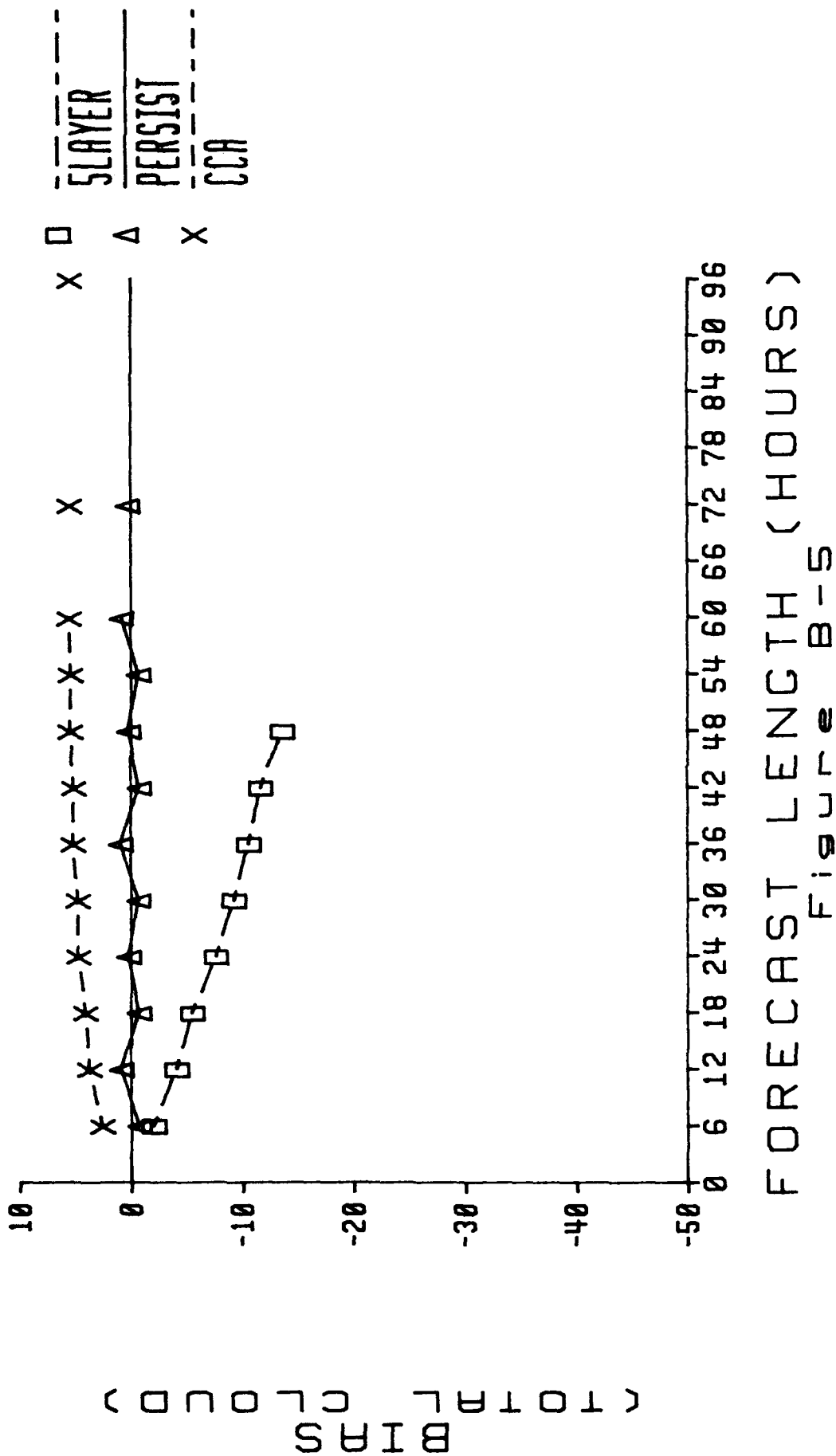
(HOURS)
SLAYER
ECMWF

N H MID-LAT OCEAN
17 JAN 91 - 13 FEB 91



FORECAST LENGTH (HOURS)
Figure B-4

17 N H MID-LAT OCEAN 91 13 FEB 91



N H MID-LAT OCEAN 17 JAN 91 - 13 FEB 91

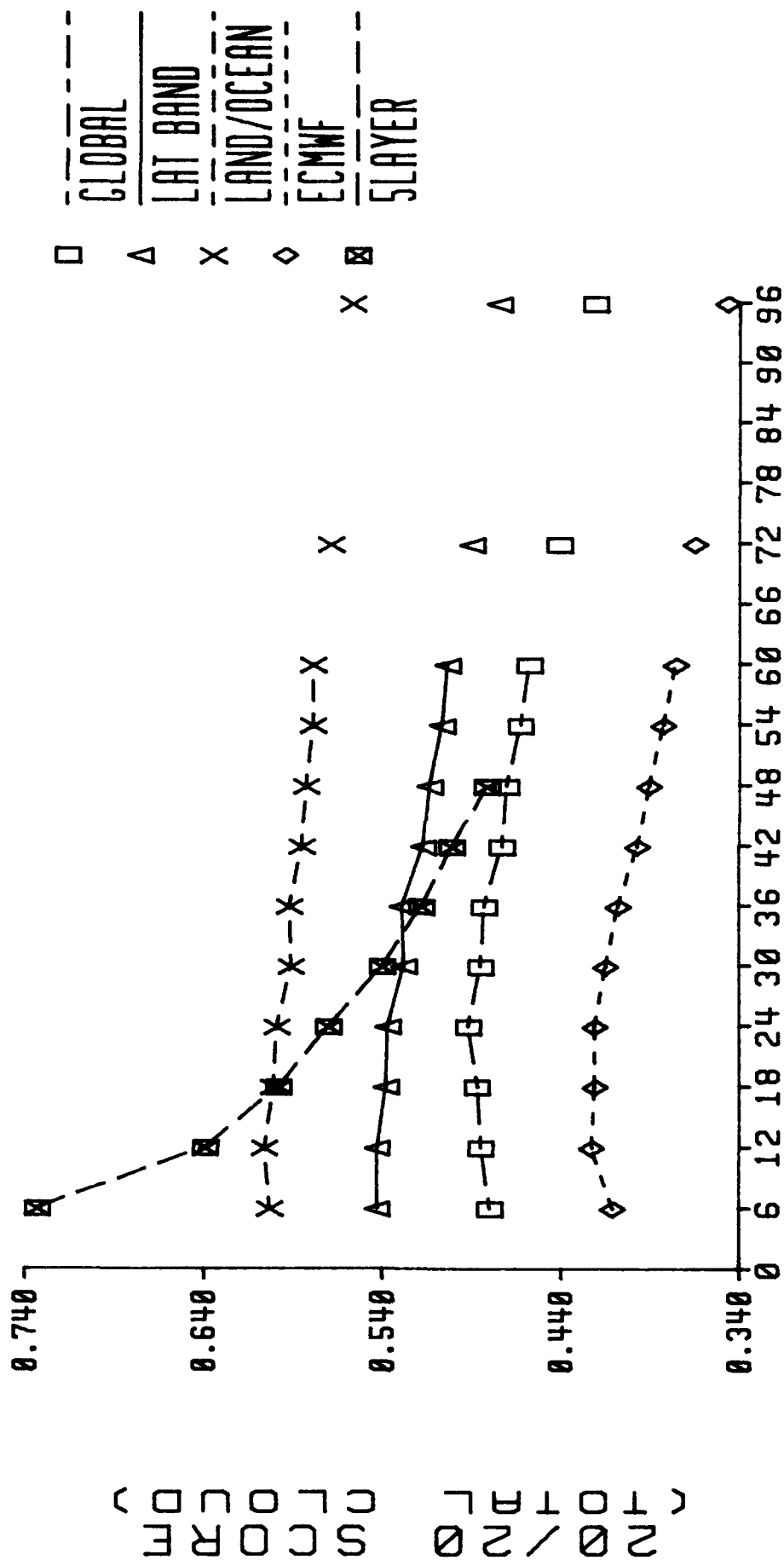


Figure B-6

17 JAN 91 - 13 FEB 91

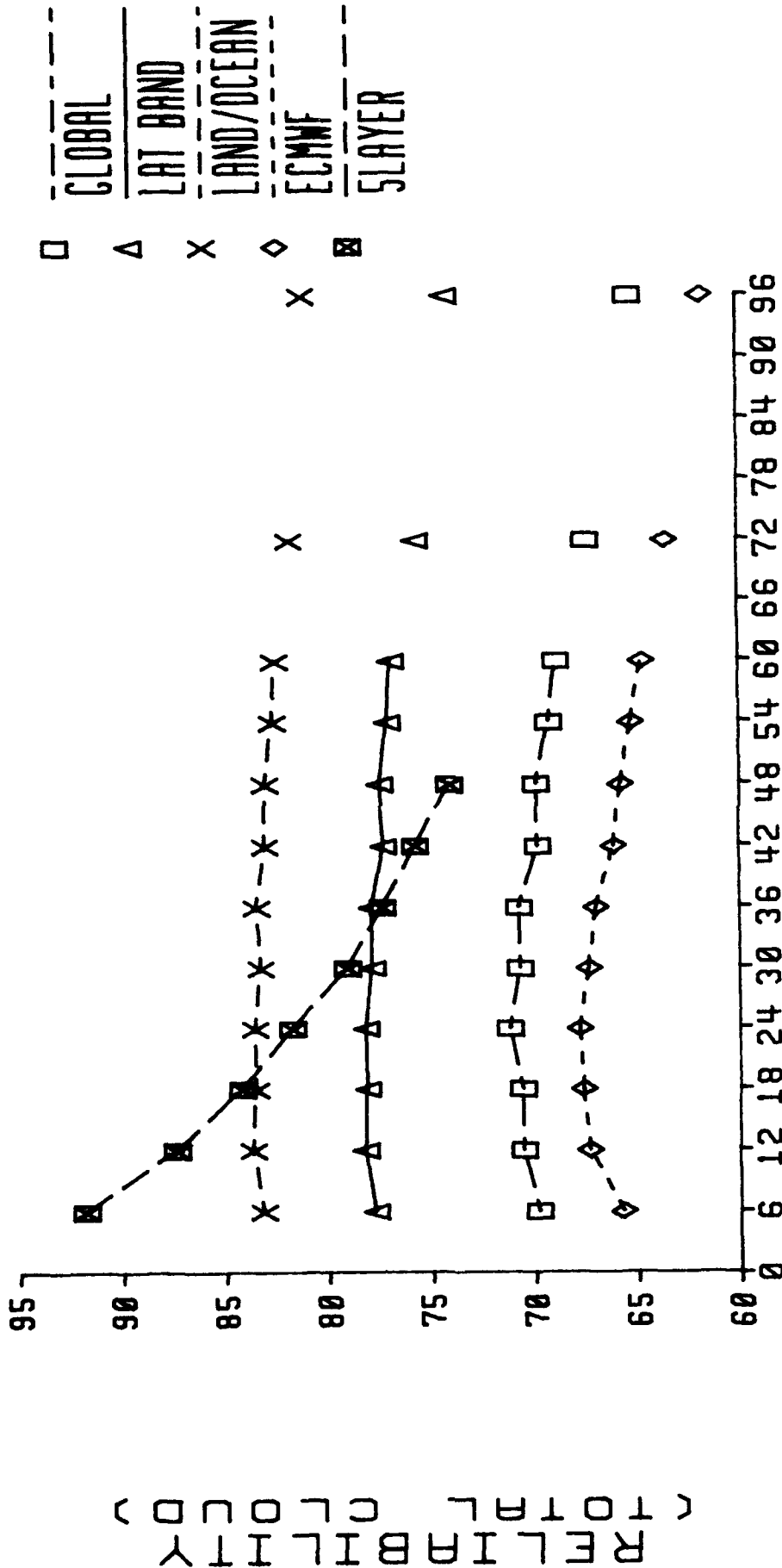
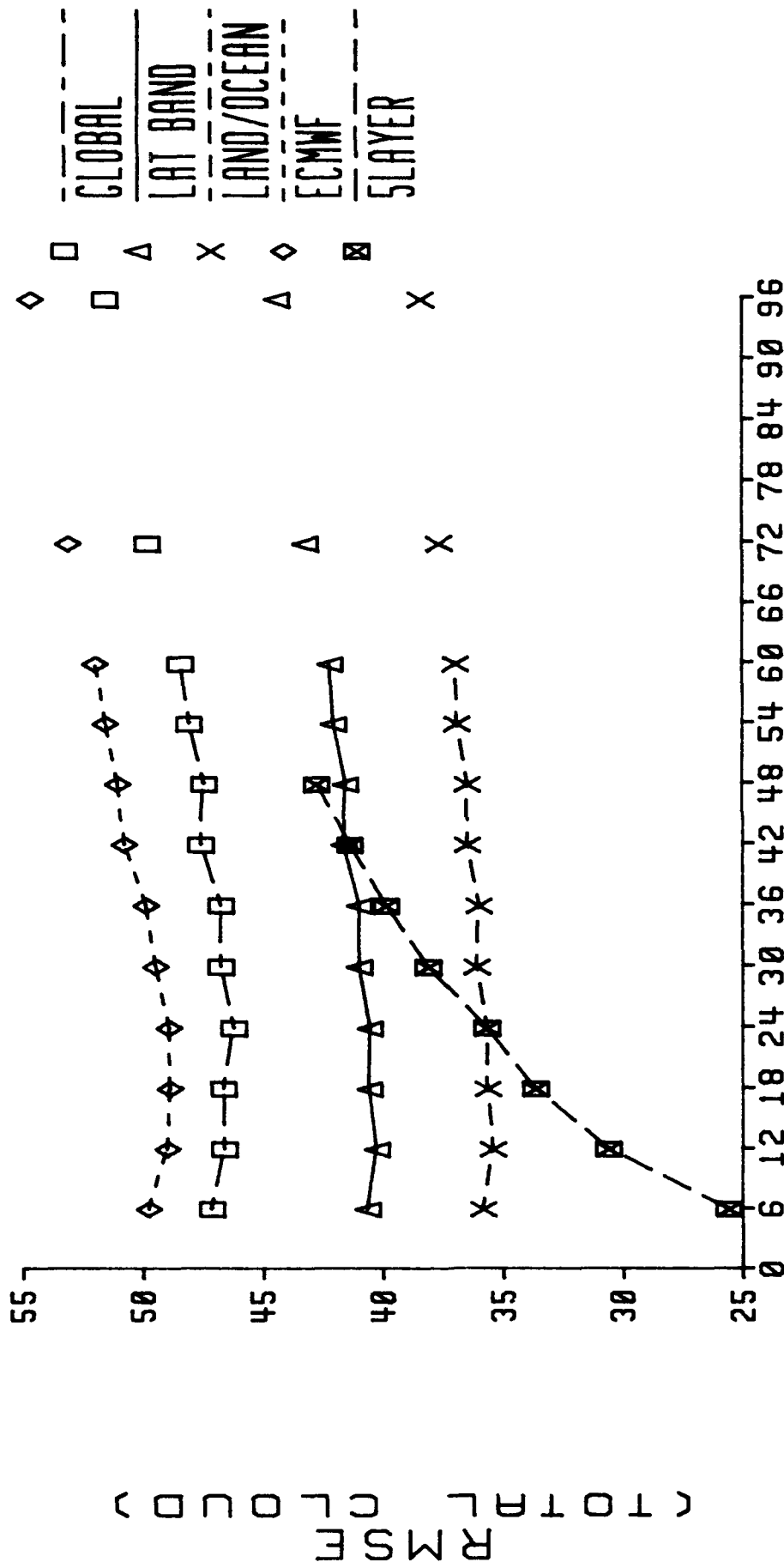


Figure B-7

N H MID-LAT OCEAN

17 JAN 91 - 13 FEB 91



FORECAST LENGTH (HOURS)
Figure B-8

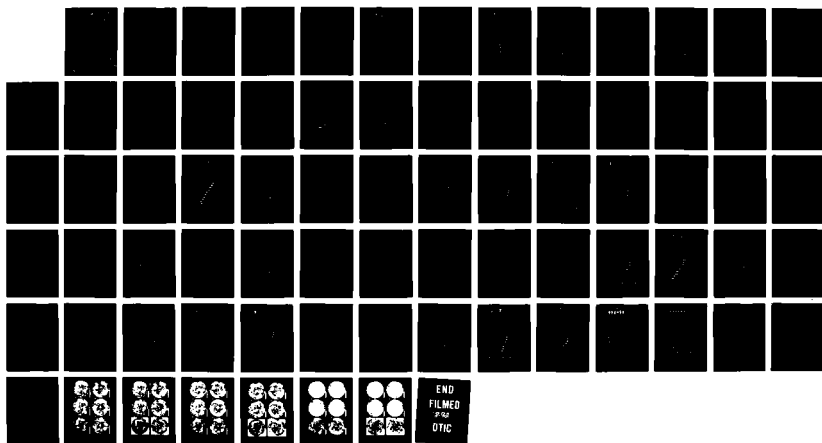
AD-A254 918

CLOUD CURVE ALGORITHM TEST PROGRAM(U) COMPUTER DATA
SYSTEMS INC FORT WORTH TX R N TRAPNELL 28 FEB 92
PL*-TR-92-2052

2/2

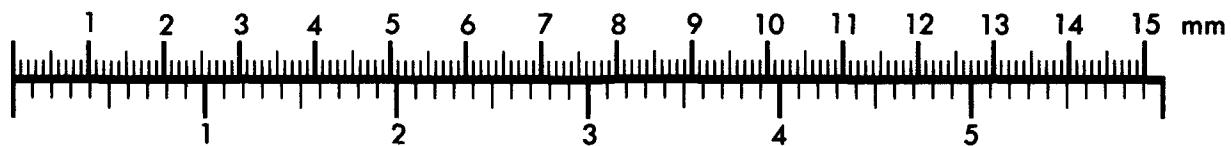
UNCLASSIFIED

NL

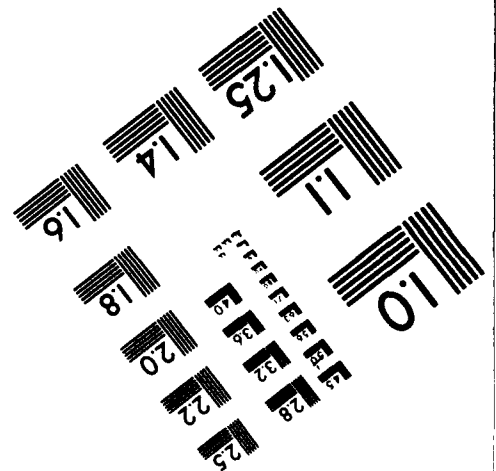




301/587-8202



MANUFACTURED TO AIIM STANDARDS
BY APPLIED IMAGE, INC.



This page intentionally left blank

APPENDIX C:

PLOTS OF VERIFICATION STATISTICS

FOR NORTHERN HEMISPHERE MID-LATITUDE LAND

17 JAN 91 TO 13 FEB 91

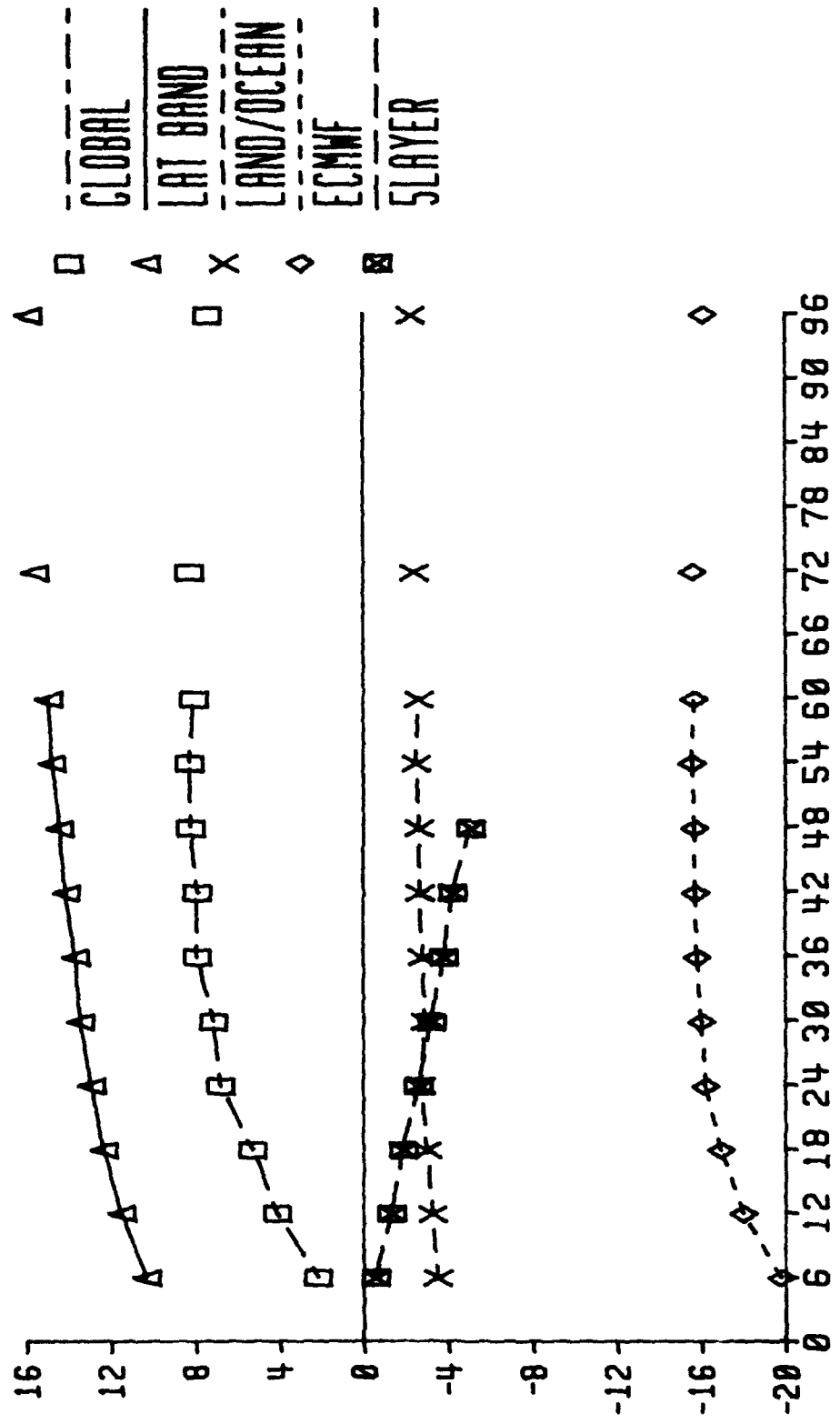
LIST OF FIGURES

- Figure C-1. BIAS Scores for Cloud Forecasts Computed by the 5 LAYER Model (to 48 hours only), Computed Using Cloud Curve Algorithm Global Curves, Northern Hemisphere Mid-Latitude Curves, and Northern Hemisphere Mid-Latitude Land Curves and Cloud Forecasts Computed Using the European Centre for Medium Range Weather Forecasts Curves (Figure A-1) For 6 to 60, 72 and 96 Hour Low Layer Forecasts Verified Over Northern Hemisphere Mid-Latitude Land During the Period from 17 January 1991 to 13 February 1991.
- Figure C-2. BIAS Scores for Cloud Forecasts Computed by the 5 LAYER Model (to 48 hours only), Computed Using Cloud Curve Algorithm Global Curves, Northern Hemisphere Mid-Latitude Curves, and Northern Hemisphere Mid-Latitude Land Curves and Cloud Forecasts Computed Using the European Centre for Medium Range Weather Forecasts Curves (Figure A-1) For 6 to 60, 72 and 96 Hour Middle Layer Forecasts Verified Over Northern Hemisphere Mid-Latitude Land During the Period from 17 January 1991 to 13 February 1991.
- Figure C-3. BIAS Scores for Cloud Forecasts Computed by the 5 LAYER Model (to 48 hours only), Computed Using Cloud Curve Algorithm Global Curves, Northern Hemisphere Mid-Latitude Curves, and Northern Hemisphere Mid-Latitude Land Curves and Cloud Forecasts Computed Using the European Centre for Medium Range Weather Forecasts Curves (Figure A-1) For 6 to 60, 72 and 96 Hour High Layer Forecasts Verified Over Northern Hemisphere Mid-Latitude Land During the Period from 17 January 1991 to 13 February 1991.
- Figure C-4. BIAS Scores for Cloud Forecasts Computed by the 5 LAYER Model (to 48 hours only), Computed Using Cloud Curve Algorithm Global Curves, Northern Hemisphere Mid-Latitude Curves, and Northern Hemisphere Mid-Latitude Land Curves and Cloud Forecasts Computed Using the European Centre for Medium Range Weather Forecasts Curves (Figure A-1) For 6 to 60, 72 and 96 Hour Total Cloud Forecasts Verified Over Northern Hemisphere Mid-Latitude Land During the Period from 17 January 1991 to 13 February 1991.
- Figure C-5. BIAS Scores for Cloud Forecasts Computed by the 5 LAYER Model (to 48 hours only), by Using Persistence (to 72 hours only) and by Using Cloud Curve Algorithm Northern Hemisphere Mid-Latitude Land Curves For 6 to 60, 72 and 96 Hour Total Cloud Forecasts Verified Over Northern Hemisphere Mid-Latitude Land During the Period from 17 January 1991 to 13 February 1991.

- Figure C-6. 20/20 Scores for Cloud Forecasts Computed by the 5 LAYER Model (to 48 hours only), Computed Using Cloud Curve Algorithm Global Curves, Northern Hemisphere Mid-Latitude Curves, and Northern Hemisphere Mid-Latitude Land Curves and Cloud Forecasts Computed Using the European Centre for Medium Range Weather Forecasts Curves (Figure A-1) For 6 to 60, 72 and 96 Hour Total Cloud Forecasts Verified Over Northern Hemisphere Mid-Latitude Land During the Period from 17 January 1991 to 13 February 1991.
- Figure C-7. RELIABILITY Scores for Cloud Forecasts Computed by the 5 LAYER Model (to 48 hours only), Computed Using Cloud Curve Algorithm Global Curves, Northern Hemisphere Mid-Latitude Curves, and Northern Hemisphere Mid-Latitude Land Curves and Cloud Forecasts Computed Using the European Centre for Medium Range Weather Forecasts Curves (Figure A-1) For 6 to 60, 72 and 96 Hour Total Cloud Forecasts Verified Over Northern Hemisphere Mid-Latitude Land During the Period from 17 January 1991 to 13 February 1991.
- Figure C-8. RMSE Scores for Cloud Forecasts Computed by the 5 LAYER Model (to 48 hours only), Computed Using Cloud Curve Algorithm Global Curves, Northern Hemisphere Mid-Latitude Curves, and Northern Hemisphere Mid-Latitude Land Curves and Cloud Forecasts Computed Using the European Centre for Medium Range Weather Forecasts Curves (Figure A-1) For 6 to 60, 72 and 96 Hour Total Cloud Forecasts Verified Over Northern Hemisphere Mid-Latitude Land During the Period from 17 January 1991 to 13 February 1991.

17 JAN 91 - 13 FEB 91

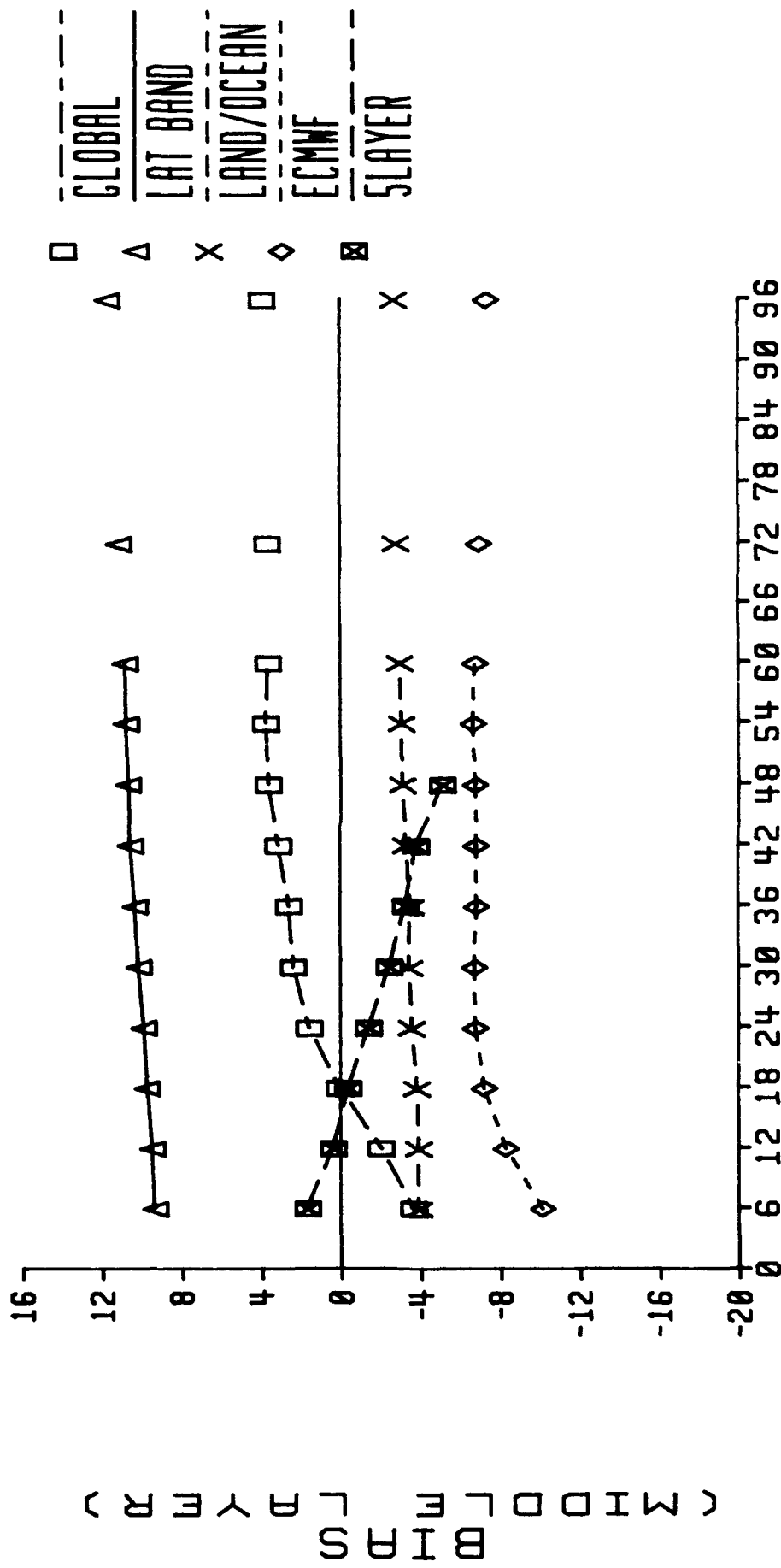
N H MID-LAT LAND



FORECAST LENGTH (HOURS)

Figure C-1

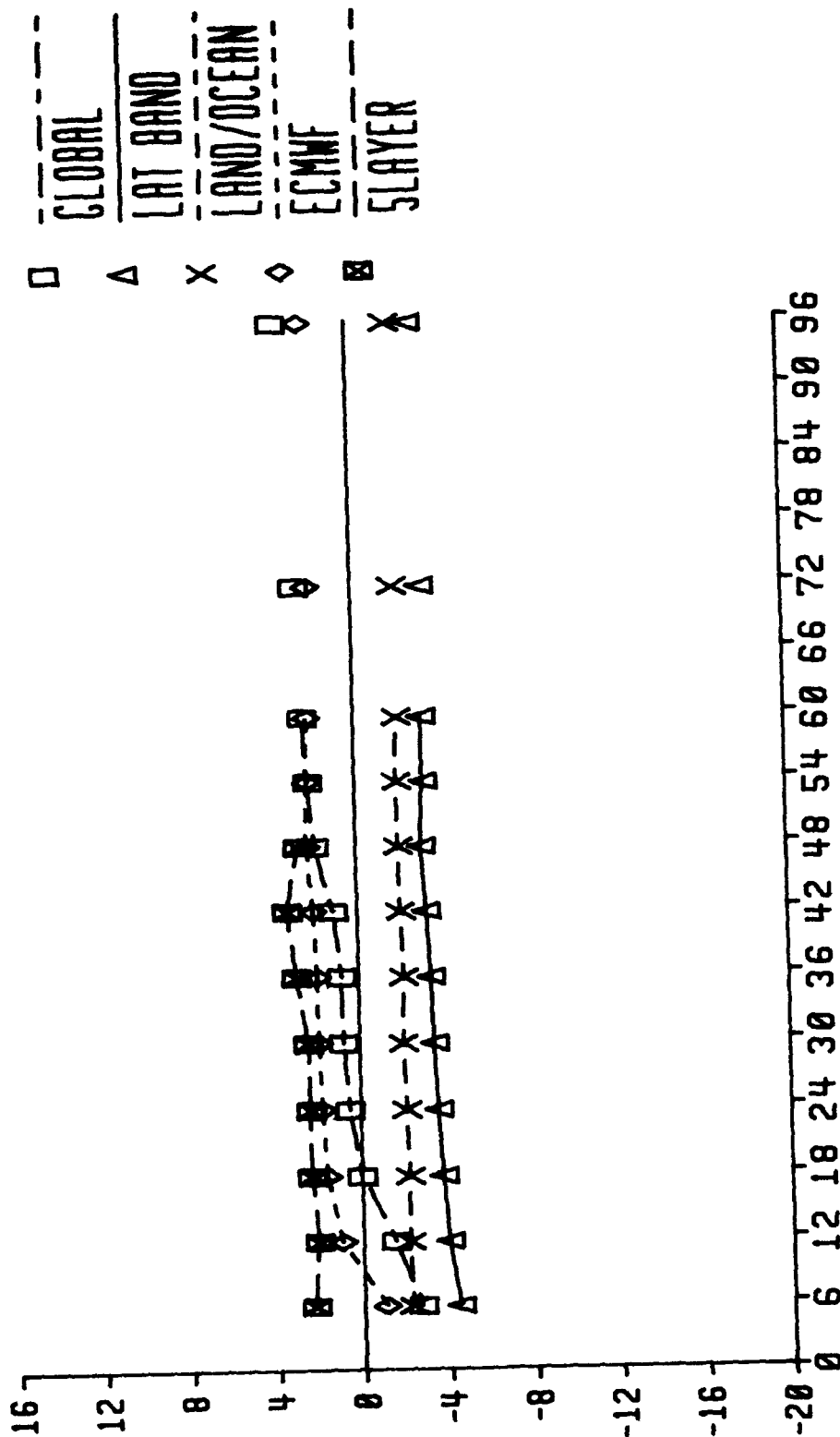
17 JAN 91 - 13 FEB 91



FORECAST LENGTH (HOURS)
Figure C-2

(HIGH
BINS
SLYFR)

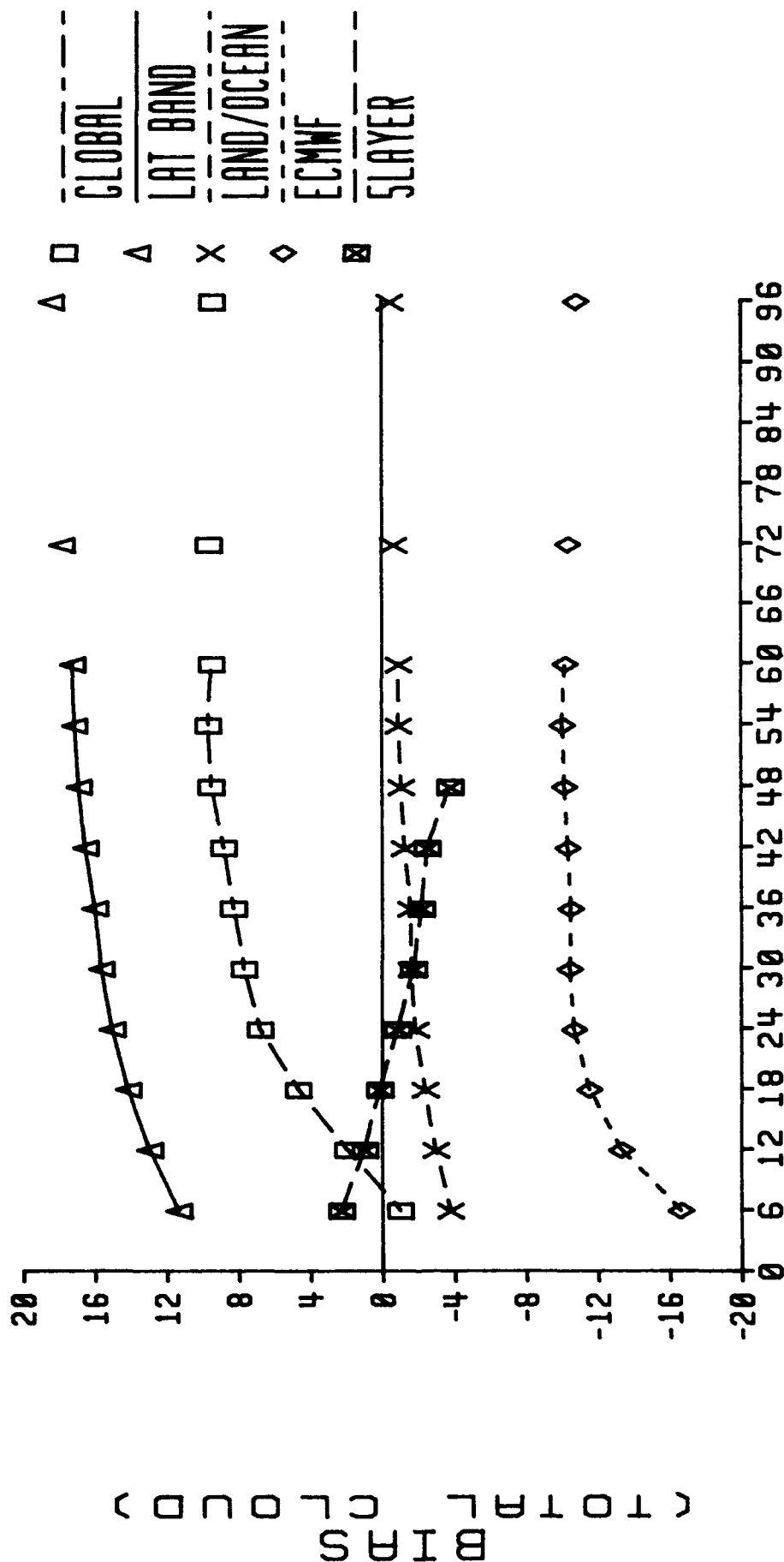
17 N H MID-LAT LAND 91 - 13 FEB 91



FORECAST LENGTH (HOURS)
Figure C-3

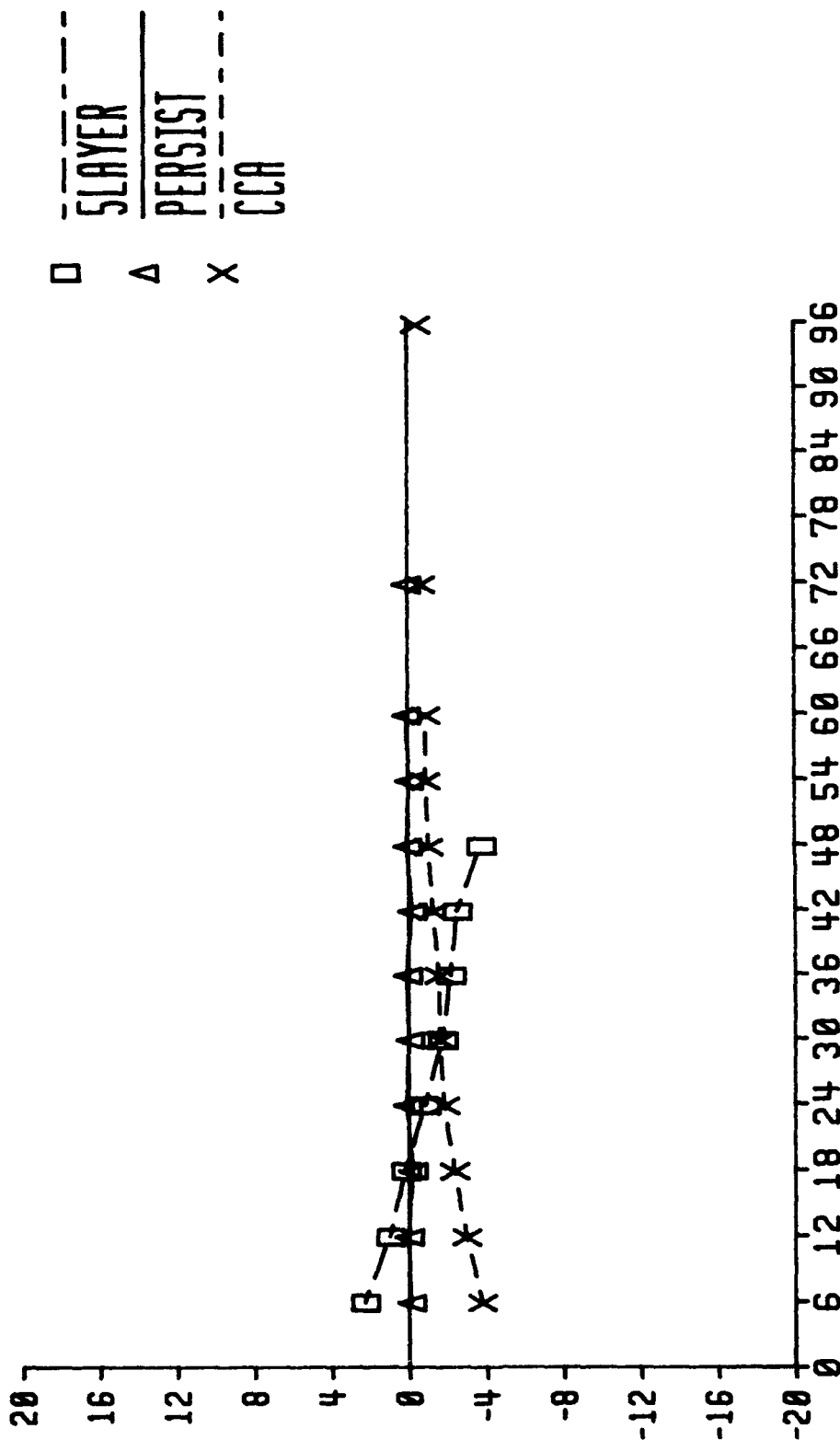
N H MID-LAT LAND

17 JAN 91 - 13 FEB 91



FORECAST LENGTH (HOURS)
Figure C-4

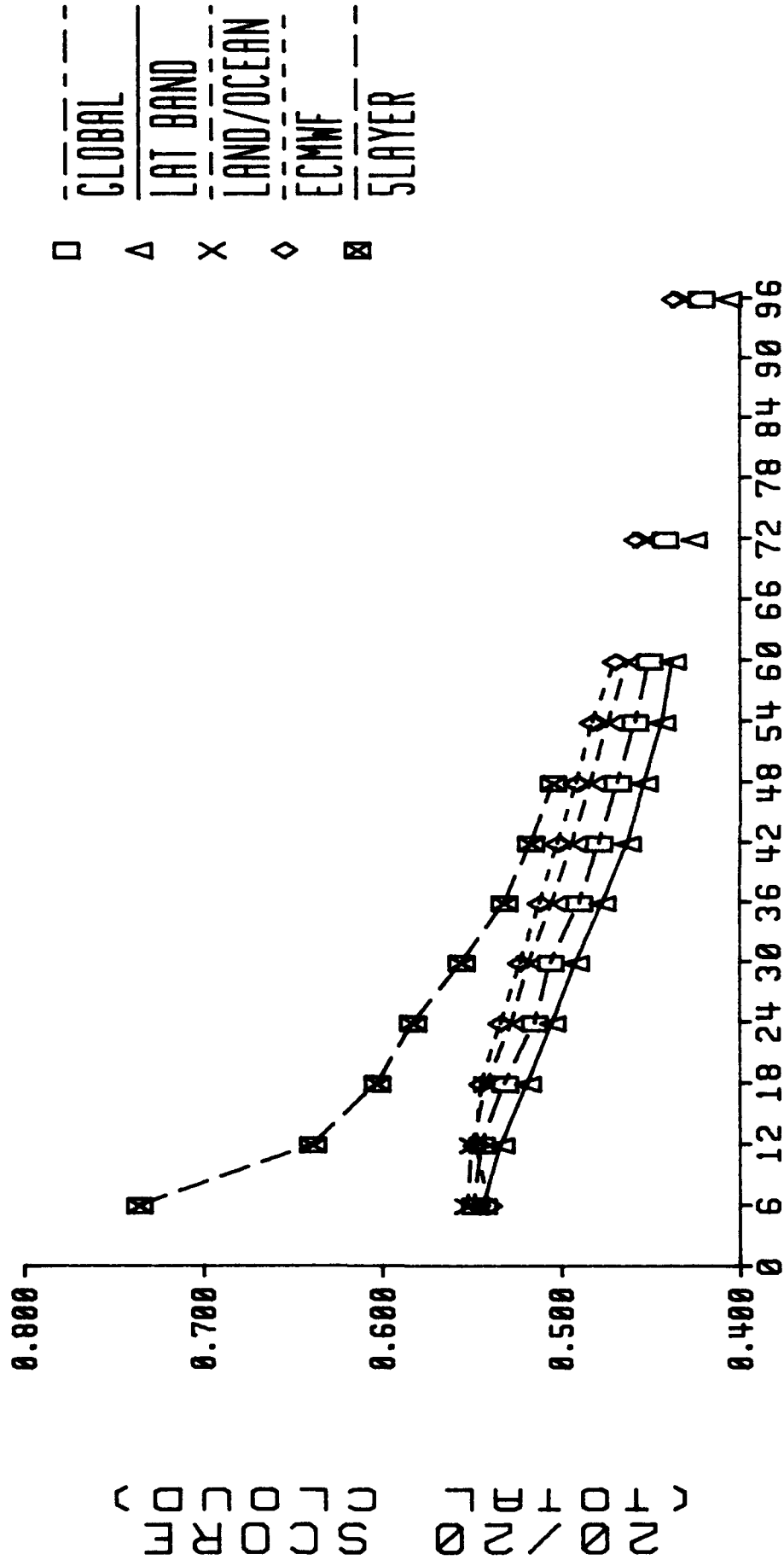
N H MID-LAT LAND 17 JAN 91 - 13 FEB 91



FORECAST LENGTH (HOURS)
Figure C-5

(TOTAL BINS CLOUD)

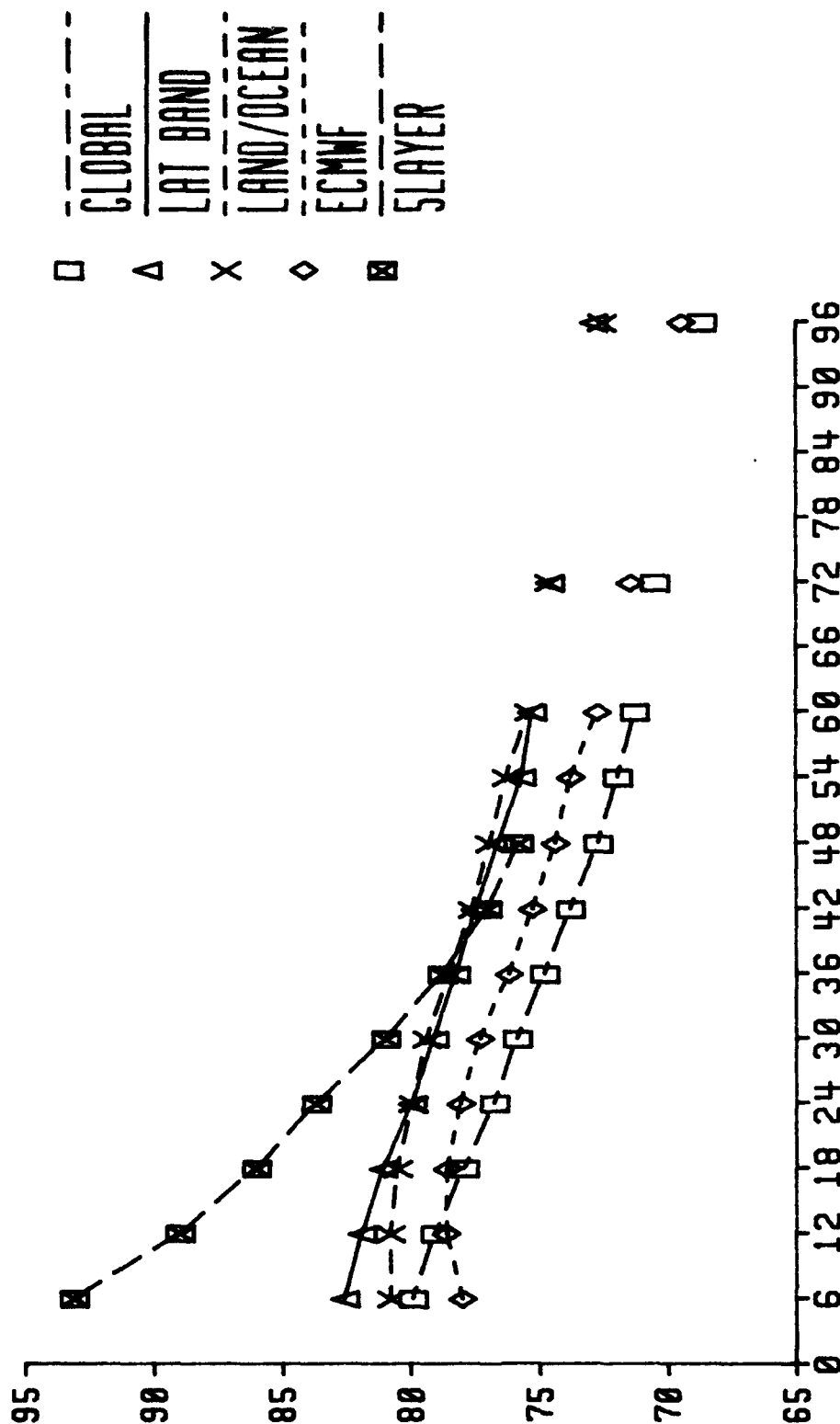
N H MID-LAT LAND 17 JAN 91 - 13 FEB 91



FORECAST LENGTH (HOURS)
Figure C-6

N H MID-LAT LAND

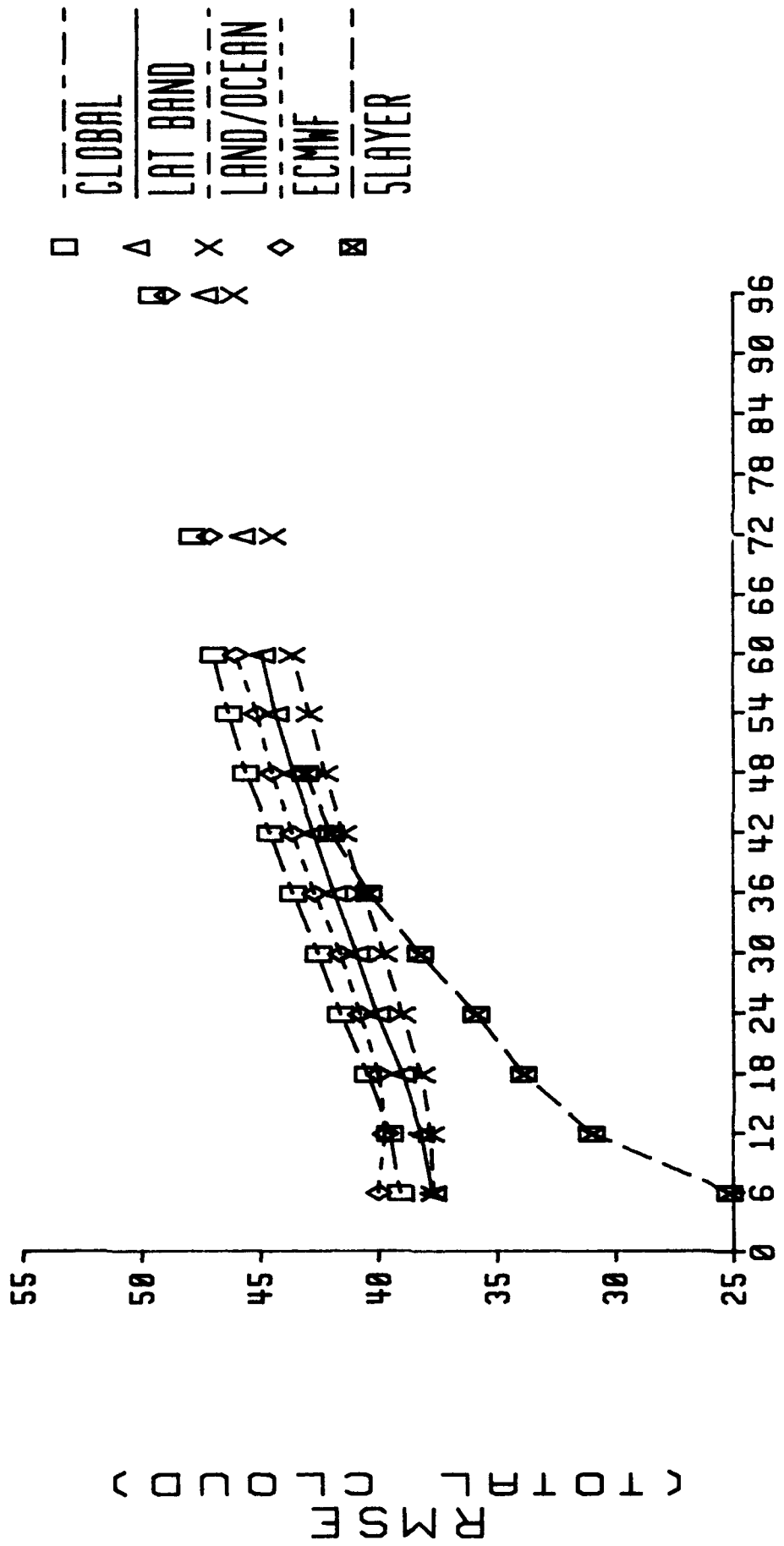
17 JAN 91 - 13 FEB 91



FORECAST LENGTH (HOURS)
Figure C-7

N H MID-LAT LAND

17 JAN 91 - 13 FEB 91



FORECAST LENGTH (HOURS)
Figure C-8

This page intentionally left blank

APPENDIX D:

PLOTS OF 20/20 SCORES

FOR THE PERIOD

01 AUG 91 TO 28 AUG 91

LIST OF FIGURES

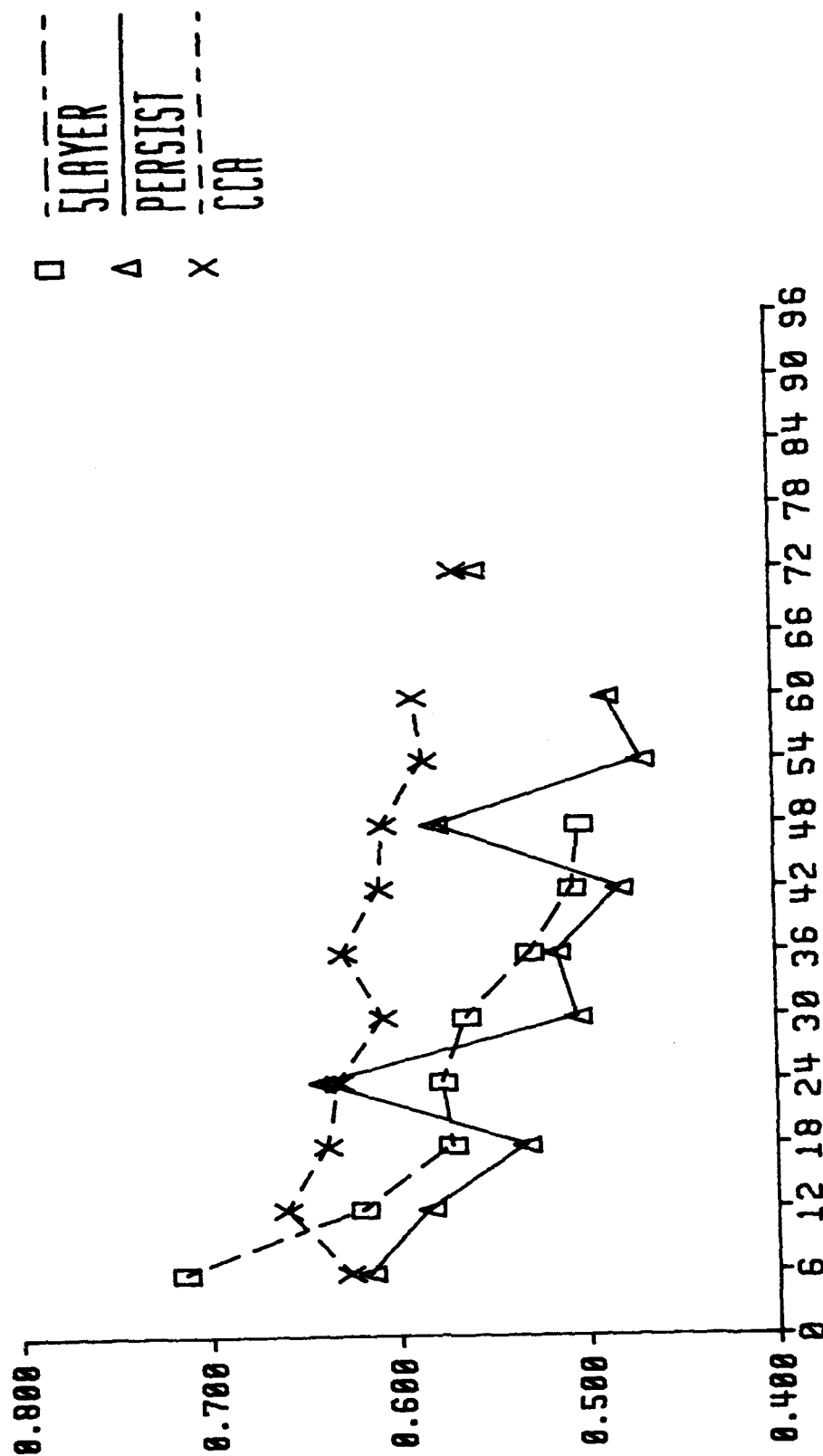
- Figure D-1. 20/20 Scores for Cloud Forecasts Computed by the 5LAYER Model (to 48 hours only), by Using Persistence and by Using Cloud Curve Algorithm European Land Curves For 6 to 60 and 72 Hour Total Cloud Forecasts Verified Over European Land During the Period from 01 August 1991 to 28 August 1991.
- Figure D-2. 20/20 Scores for Cloud Forecasts Computed by Using Cloud Curve Algorithm Northern Hemisphere Mid-Latitude Land Curves (Phase I Baseline), European Land Curves (Region Curves), European Land Curves with Diurnal Correction (to 72 hour only), European Land Curves with Vertical Velocity (to 60 hours only), and European Land Curves with both Diurnal Correction and Vertical Velocity (to 60 hour only) for 6 to 60, 72 and 96 Hour Total Cloud Forecasts Verified Over European Land During the Period from 01 August 1991 to 28 August 1991.
- Figure D-3. 20/20 Scores for Cloud Forecasts Computed by the 5LAYER Model (to 48 hours only), by Using Persistence and by Using Cloud Curve Algorithm East Asia Land Curves For 6 to 60 and 72 Hour Total Cloud Forecasts Verified Over East Asia Land During the Period from 01 August 1991 to 28 August 1991.
- Figure D-4. 20/20 Scores for Cloud Forecasts Computed by the 5LAYER Model (to 48 hours only), by Using Persistence and by Using Cloud Curve Algorithm North America Land Curves For 6 to 60 and 72 Hour Total Cloud Forecasts Verified Over North America Land During the Period from 01 August 1991 to 28 August 1991.
- Figure D-5. 20/20 Scores for Cloud Forecasts Computed by the 5LAYER Model (to 48 hours only), by Using Persistence and by Using Cloud Curve Algorithm North Africa/Middle East Land Curves For 6 to 60 and 72 Hour Total Cloud Forecasts Verified Over North Africa/Middle East Land During the Period from 01 August 1991 to 28 August 1991.
- Figure D-6. 20/20 Scores for Cloud Forecasts Computed by the 5LAYER Model (to 48 hours only), by Using Persistence and by Using Cloud Curve Algorithm Northern Hemisphere Mid-Latitude Regional Land Curves For 6 to 60 and 72 Hour Total Cloud Forecasts Verified Over Northern Hemisphere Mid-Latitude Land During the Period from 01 August 1991 to 28 August 1991.
- Figure D-7. 20/20 Scores for Cloud Forecasts Computed by the 5LAYER Model (to 48 hours only), by Using Persistence and by Using Cloud Curve Algorithm Northern Hemisphere Mid-Latitude Ocean Curves For 6 to 60 and 72 Hour Total Cloud Forecasts Verified Over Northern Hemisphere Mid-Latitude Ocean During the Period from 01 August 1991 to 28 August 1991.

Figure D-8. 20/20 Scores for Cloud Forecasts Computed by Using Diurnal Persistence and Persistence and by Using Cloud Curve Algorithm Northern Hemisphere Tropical Land Curves For 6 to 60 and 72 Hour Total Cloud Forecasts Verified Over Northern Hemisphere Tropical Land During the Period from 01 August 1991 to 28 August 1991.

Figure D-9. 20/20 Scores for Cloud Forecasts Computed by Using Diurnal Persistence and Persistence and by Using Cloud Curve Algorithm Northern Hemisphere Tropical Ocean Curves For 6 to 60 and 72 Hour Total Cloud Forecasts Verified Over Northern Hemisphere Tropical Ocean During the Period from 01 August 1991 to 28 August 1991.

EUROPEAN LAND

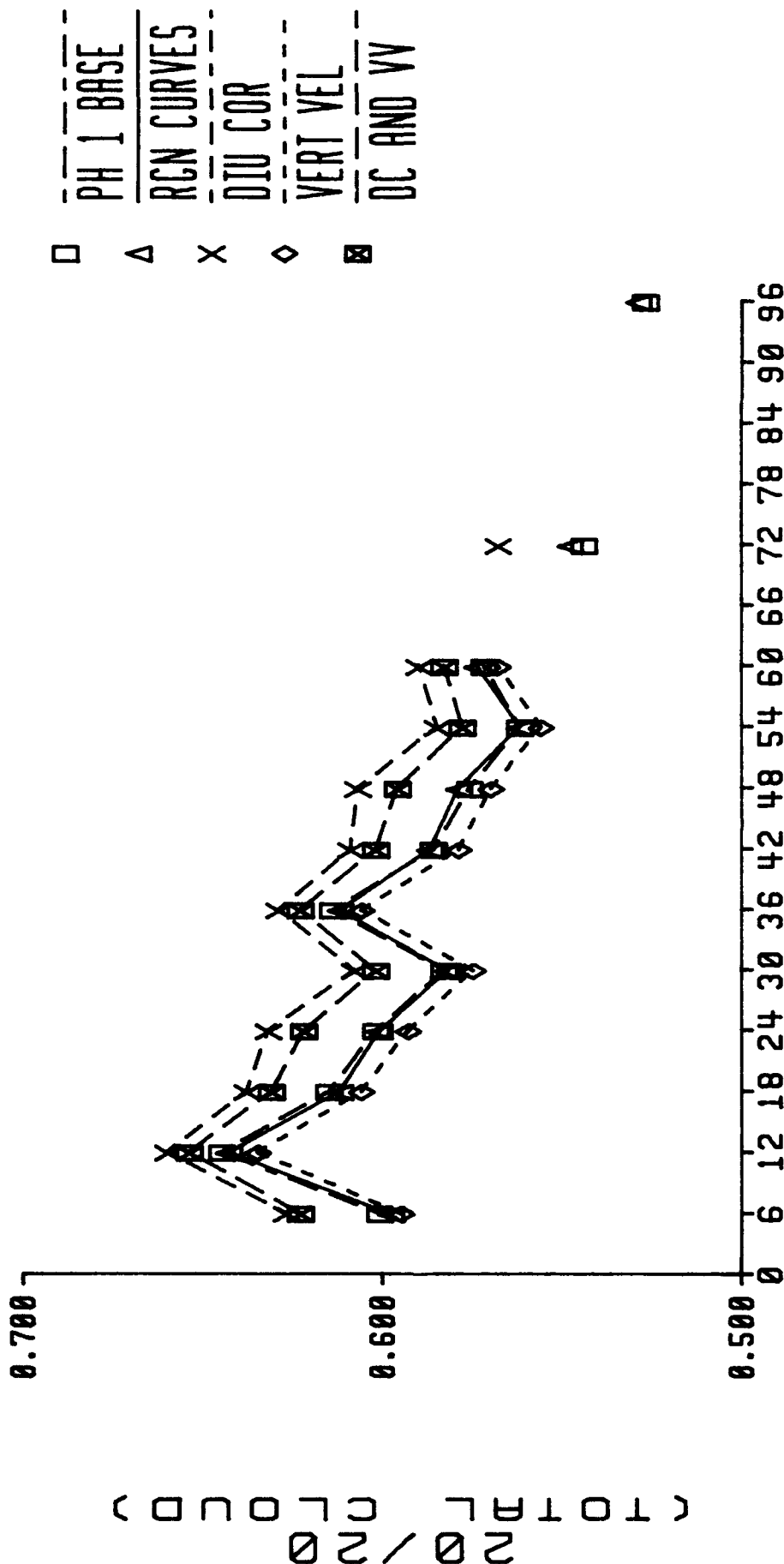
20/20 SCORE (TOTAL CLOUD)



FORECAST LENGTH (HOURS)

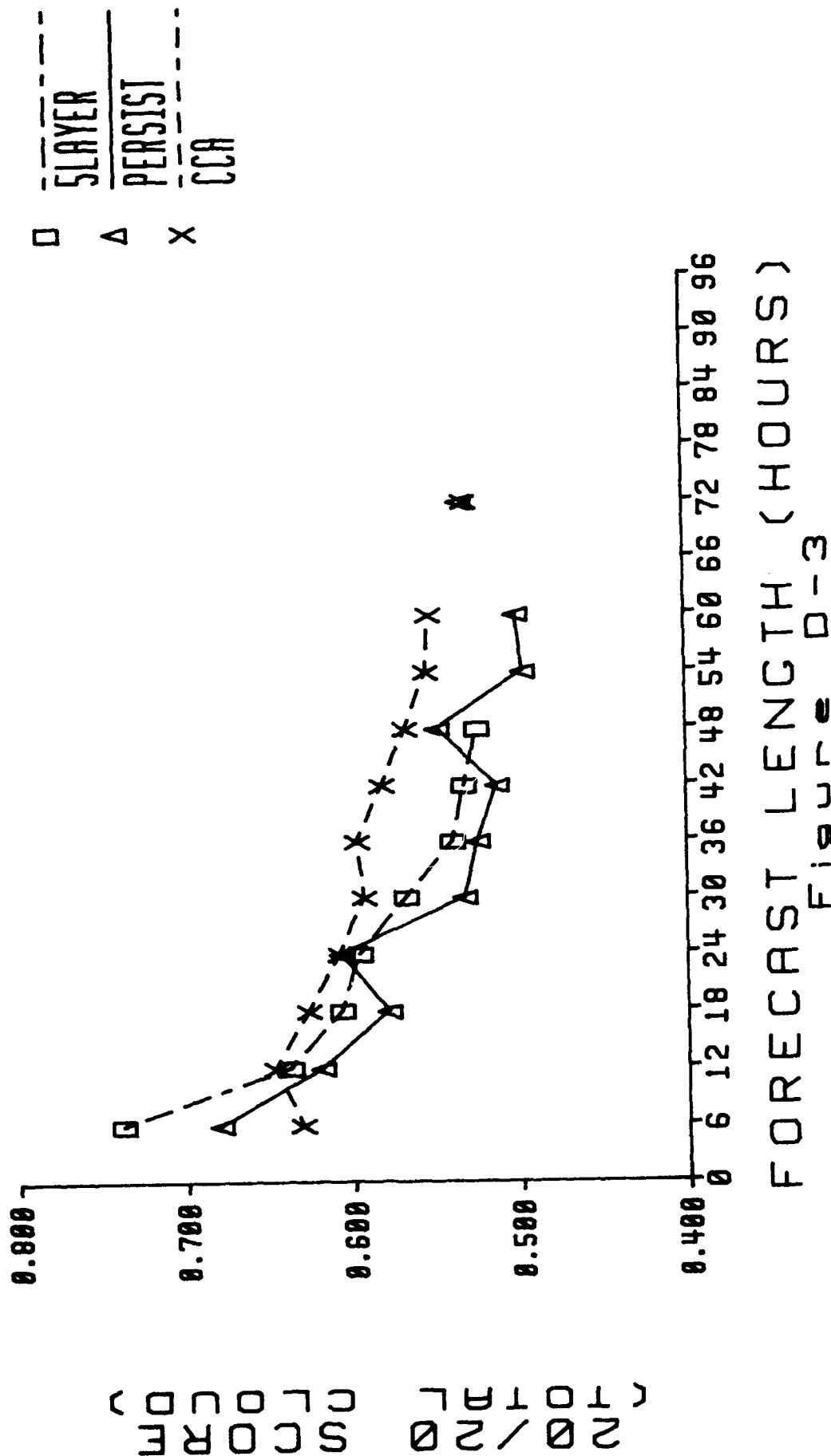
SLAYER
PERSIST
CCA

EUROPEAN LAND 01 AUG 91 TO 28 AUG 91



FORECAST LENGTH (HOURS)
Figure D-2

01 AUG 91 TO 28 AUG 91 EAST ASIA LAND



01 AUG 91 TO 28 AUG 91 NORTH AMERICA LAND

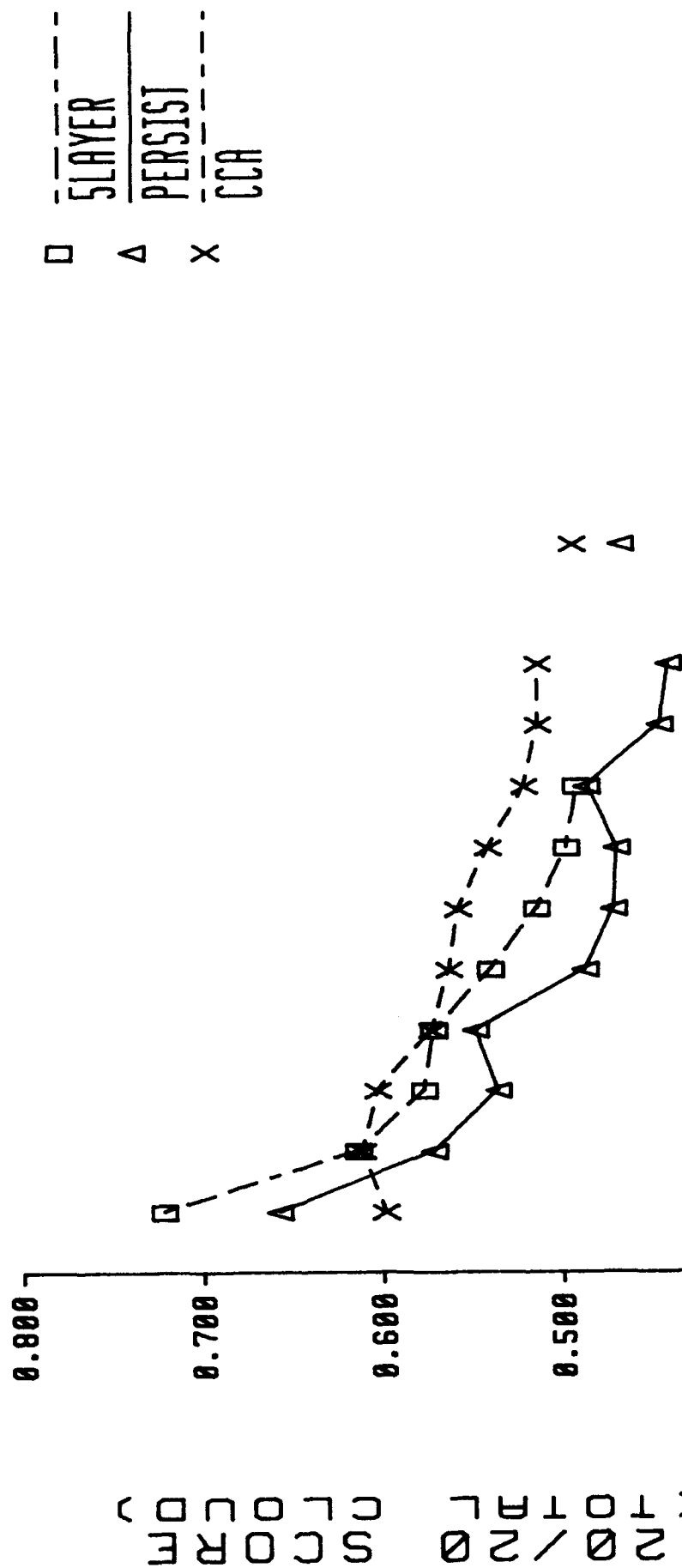


Figure D-4

N AFR/MID EAST LAND 01 AUG 91 TO 28 AUG 91

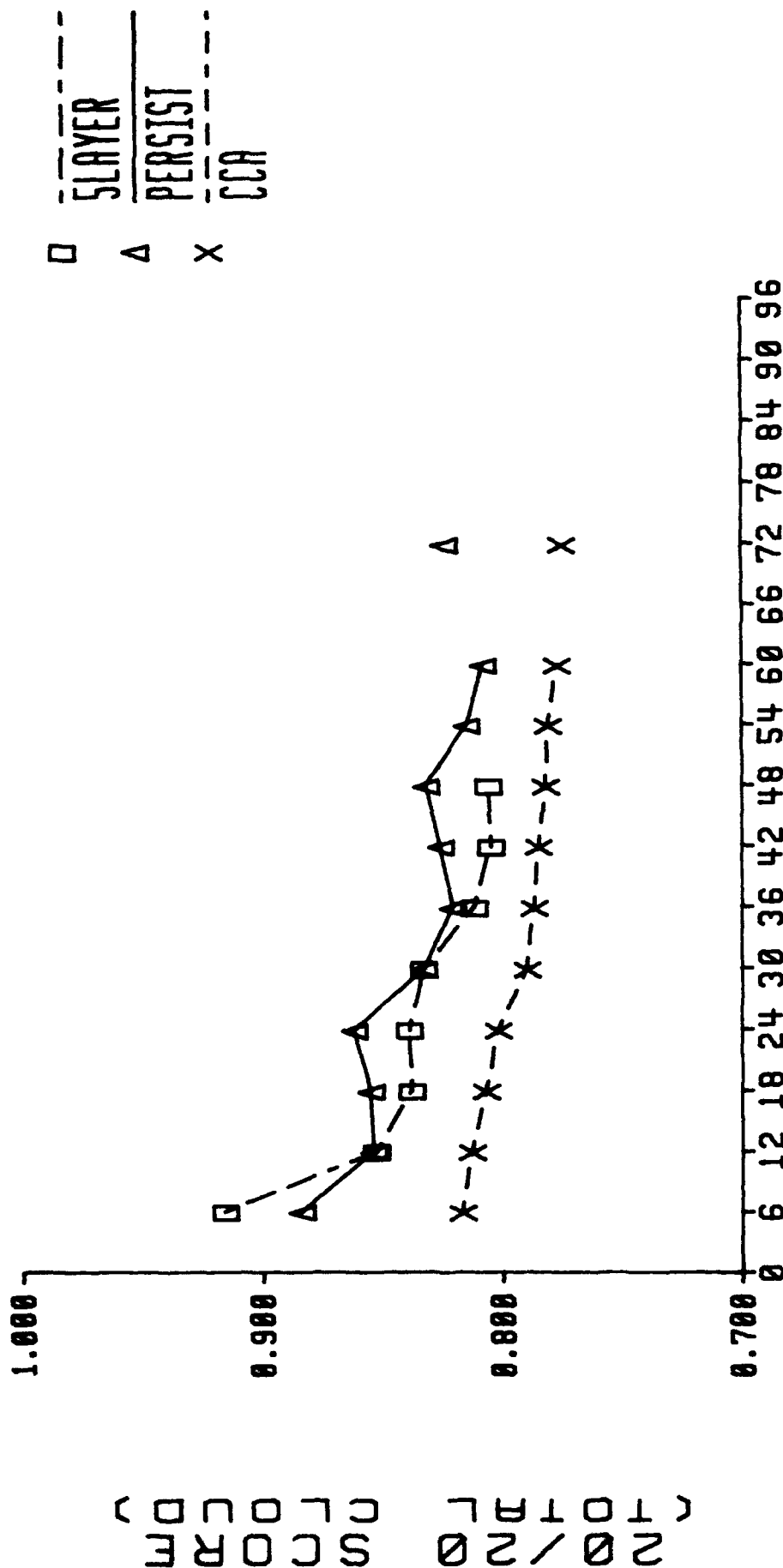
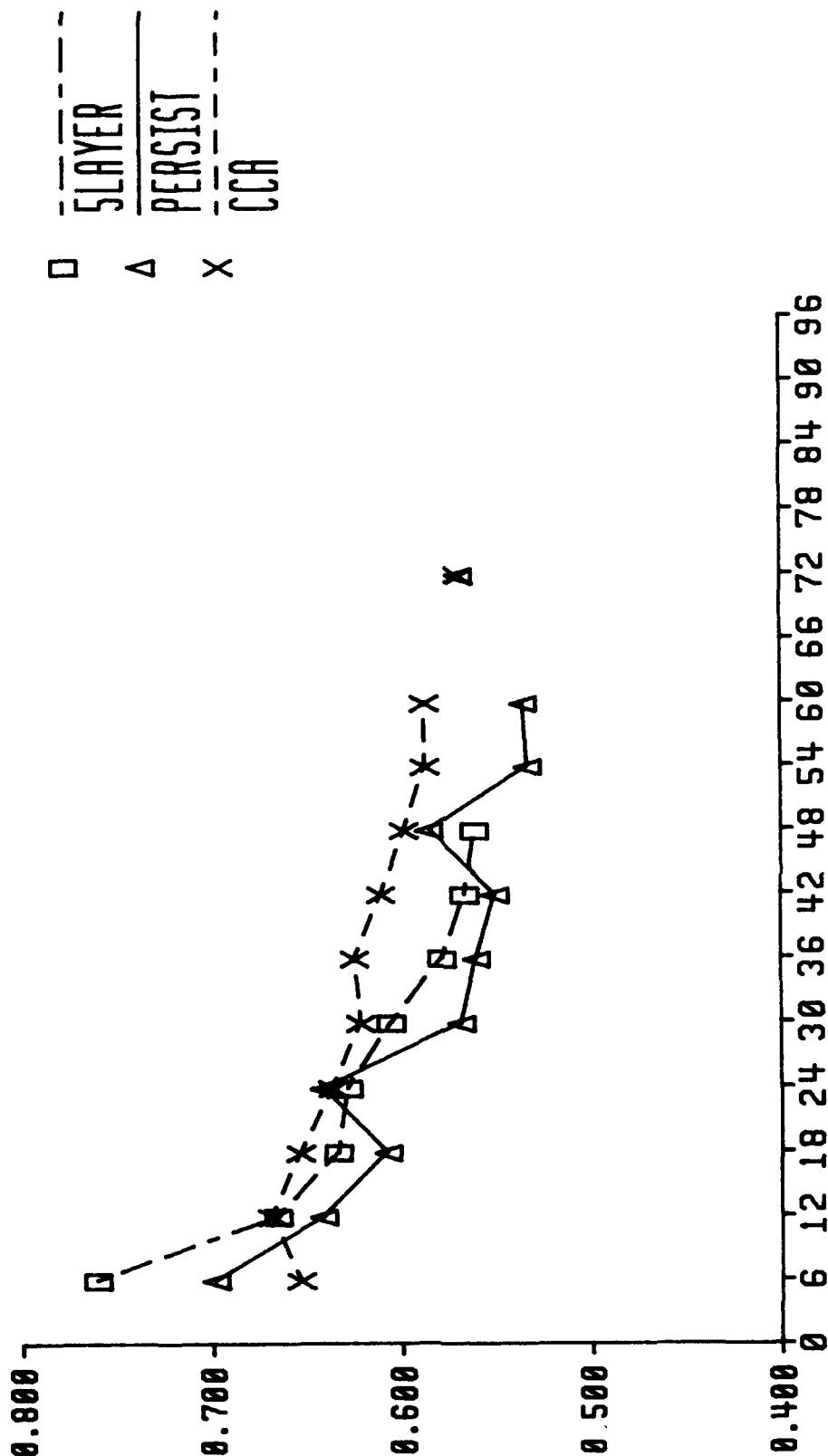


Figure D-5

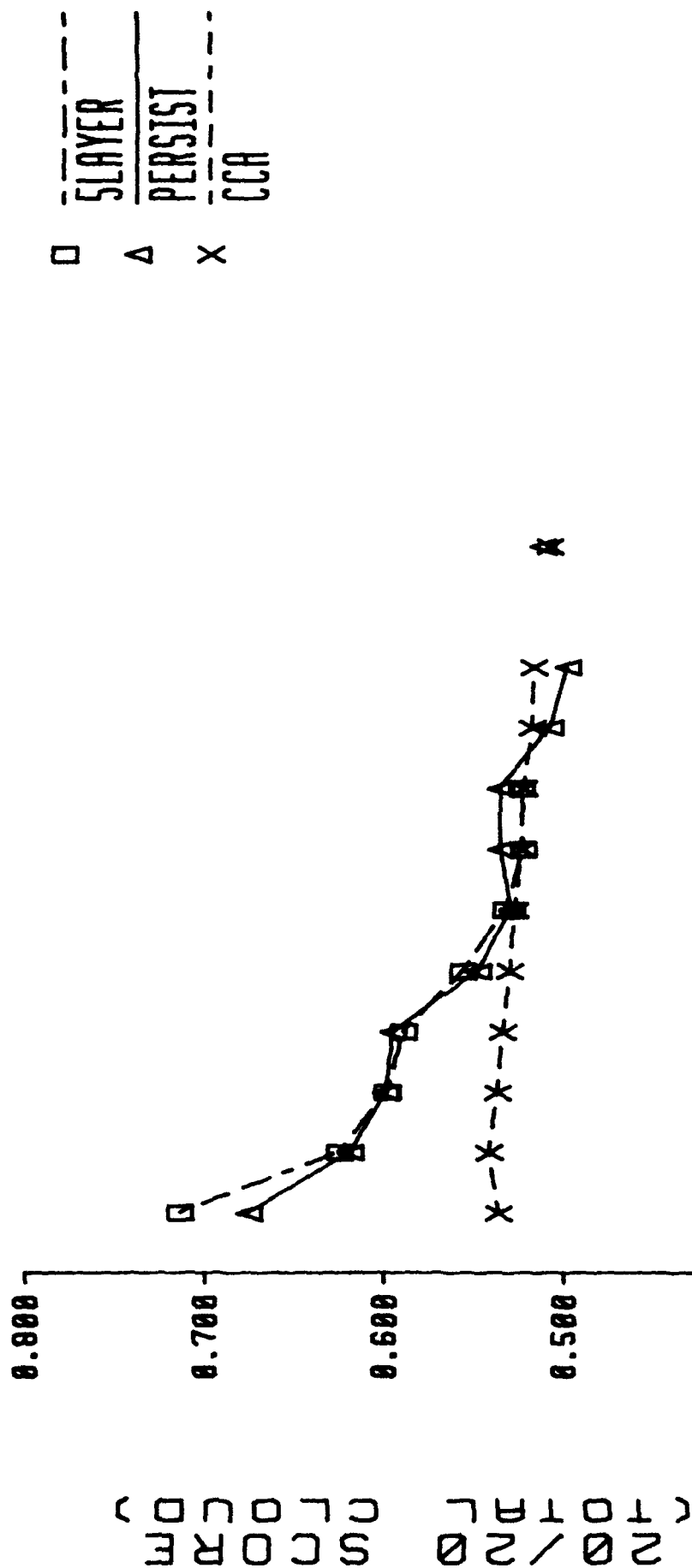
01 AUG 91 N H MID-LAT LAND 91

(20/20 SCORE)



FORECAST LENGTH (HOURS)
Figure D-6

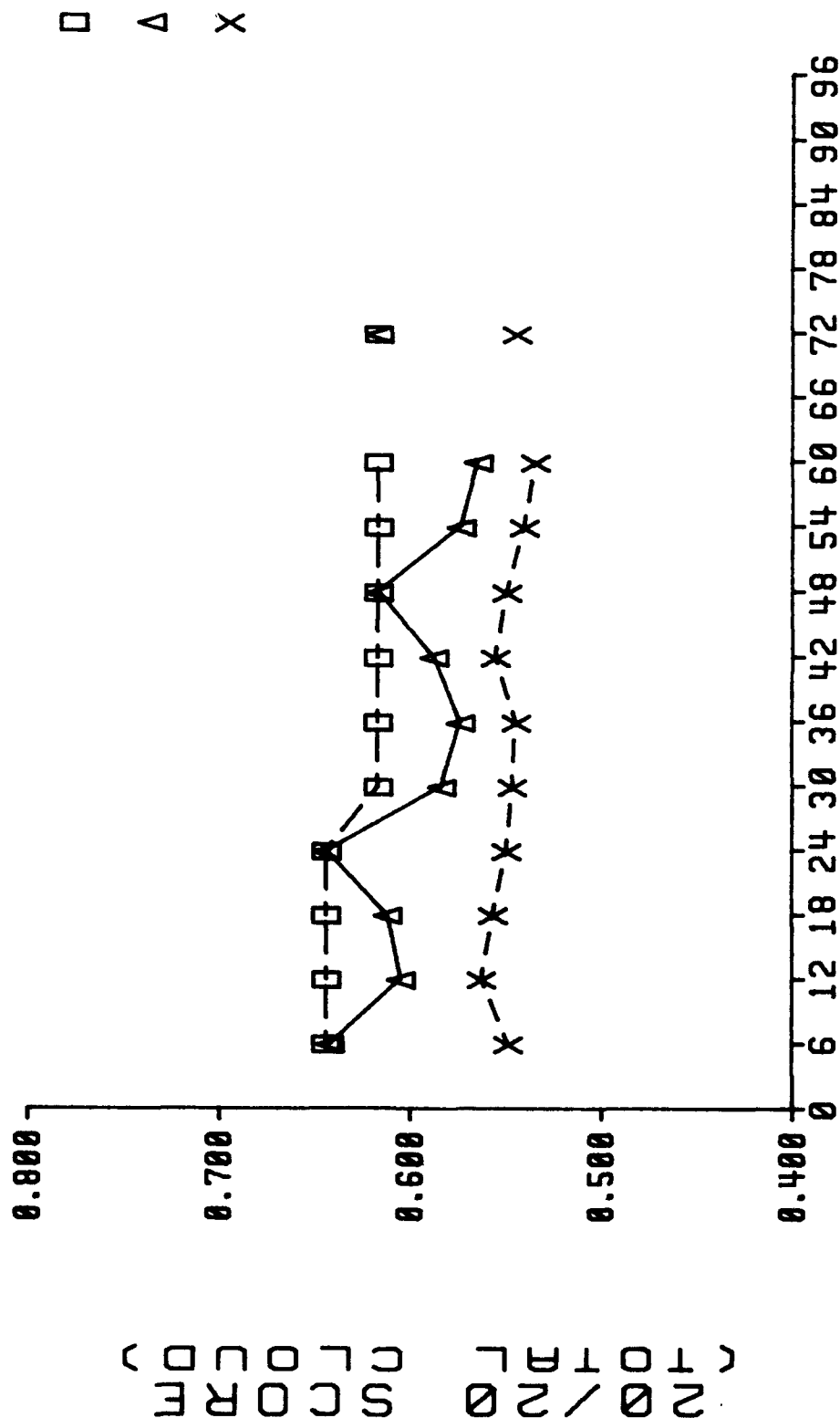
01 AUG 91 TO 28 AUG 91 N H MID-LAT OCEAN



FORECAST LENGTH (HOURS)

Figure D-7

01 AUG 91 TO 28 AUG 91 N H TROPICAL LAND



FORECAST LENGTH (HOURS)
Figure D-8

N H TROPICAL OCEAN 91

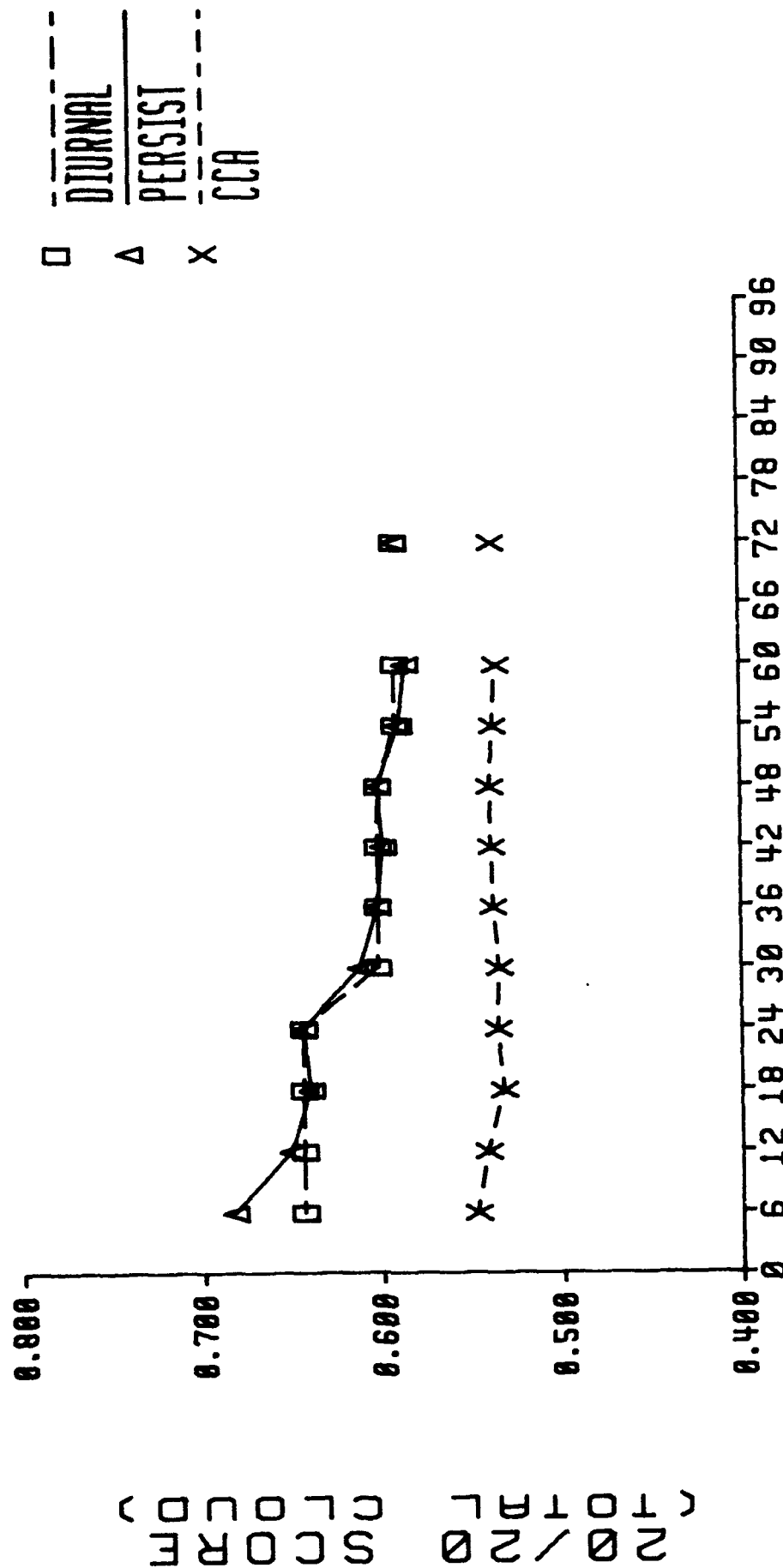


Figure D-9

APPENDIX E:

PLOTS OF 20/20 SCORES

FOR THE PERIOD

24 OCT 91 TO 20 NOV 91

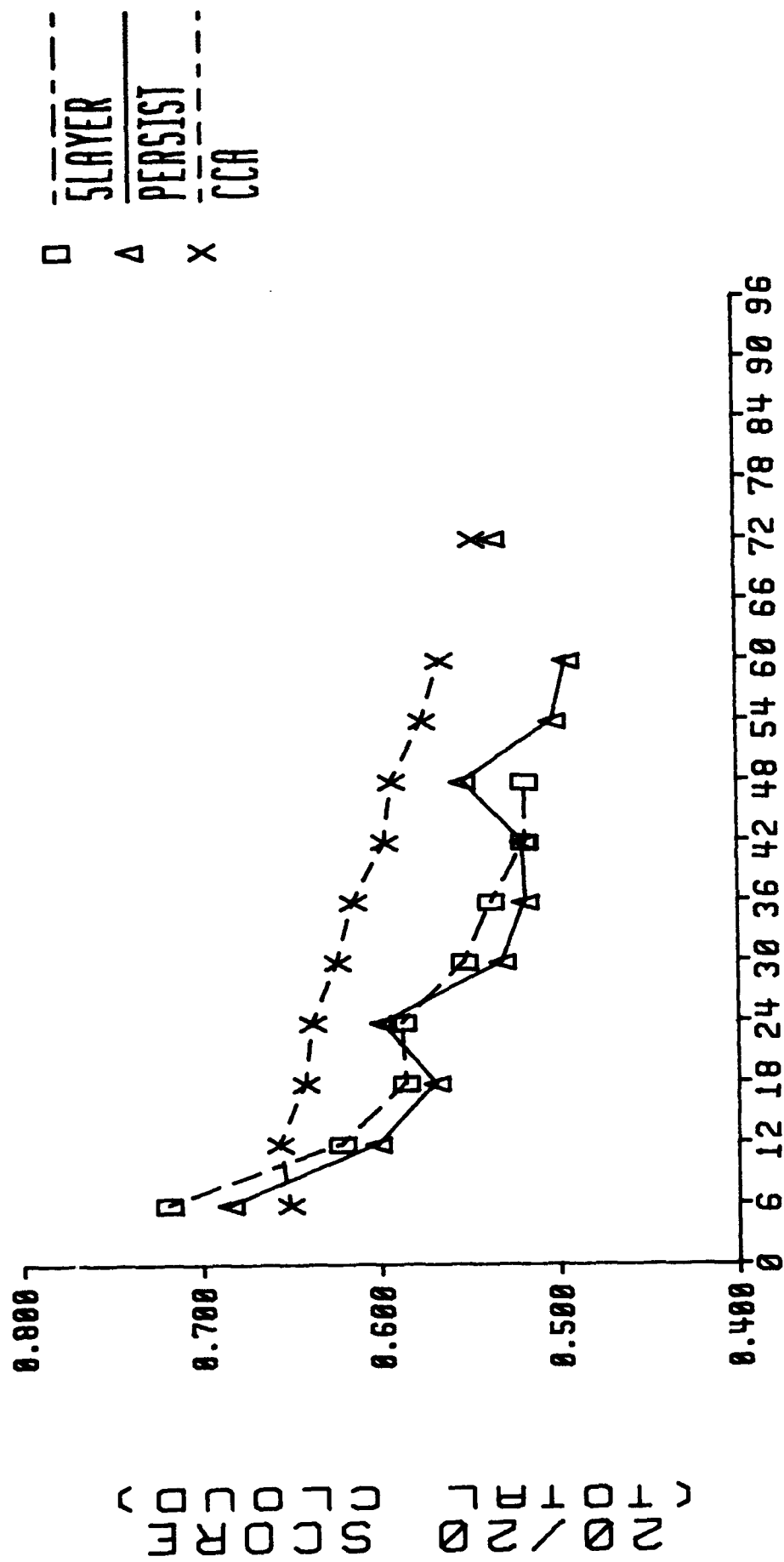
LIST OF FIGURES

- Figure E-1. 20/20 Scores for Cloud Forecasts Computed by the 5LAYER Model (to 48 hours only), by Using Persistence and by Using Cloud Curve Algorithm European Land Curves For 6 to 60 and 72 Hour Total Cloud Forecasts Verified Over European Land During the Period from 24 October 1991 to 20 November 1991.
- Figure E-2. 20/20 Scores for Cloud Forecasts Computed by Using Cloud Curve Algorithm Northern Hemisphere Mid-Latitude Land Curves (Phase I Baseline), European Land Curves (Region Curves), European Land Curves with Diurnal Correction (to 72 hour only), European Land Curves with Vertical Velocity (to 60 hours only), and European Land Curves with both Diurnal Correction and Vertical Velocity (to 60 hour only) for 6 to 60, 72 and 96 Hour Total Cloud Forecasts Verified Over European Land During the Period from 24 October 1991 to 20 November 1991.
- Figure E-3. 20/20 Scores for Cloud Forecasts Computed by the 5LAYER Model (to 48 hours only), by Using Persistence and by Using Cloud Curve Algorithm East Asia Land Curves For 6 to 60 and 72 Hour Total Cloud Forecasts Verified Over East Asia Land During the Period from 24 October 1991 to 20 November 1991.
- Figure E-4. 20/20 Scores for Cloud Forecasts Computed by the 5LAYER Model (to 48 hours only), by Using Persistence and by Using Cloud Curve Algorithm North America Land Curves For 6 to 60 and 72 Hour Total Cloud Forecasts Verified Over North America Land During the Period from 24 October 1991 to 20 November 1991.
- Figure E-5. 20/20 Scores for Cloud Forecasts Computed by the 5LAYER Model (to 48 hours only), by Using Persistence and by Using Cloud Curve Algorithm North Africa/Middle East Land Curves For 6 to 60 and 72 Hour Total Cloud Forecasts Verified Over North Africa/Middle East Land During the Period from 24 October 1991 to 20 November 1991.
- Figure E-6. 20/20 Scores for Cloud Forecasts Computed by the 5LAYER Model (to 48 hours only), by Using Persistence and by Using Cloud Curve Algorithm Northern Hemisphere Mid-Latitude Regional Land Curves For 6 to 60 and 72 Hour Total Cloud Forecasts Verified Over Northern Hemisphere Mid-Latitude Land During the Period from 24 October 1991 to 20 November 1991.
- Figure E-7. 20/20 Scores for Cloud Forecasts Computed by the 5LAYER Model (to 48 hours only), by Using Persistence and by Using Cloud Curve Algorithm Northern Hemisphere Mid-Latitude Ocean Curves For 6 to 60 and 72 Hour Total Cloud Forecasts Verified Over Northern Hemisphere Mid-Latitude Ocean During the Period from 24 October 1991 to 20 November 1991.

Figure E-8. 20/20 Scores for Cloud Forecasts Computed by Using Diurnal Persistence and Persistence and by Using Cloud Curve Algorithm Northern Hemisphere Tropical Land Curves For 6 to 60 and 72 Hour Total Cloud Forecasts Verified Over Northern Hemisphere Tropical Land During the Period from 24 October 1991 to 20 November 1991.

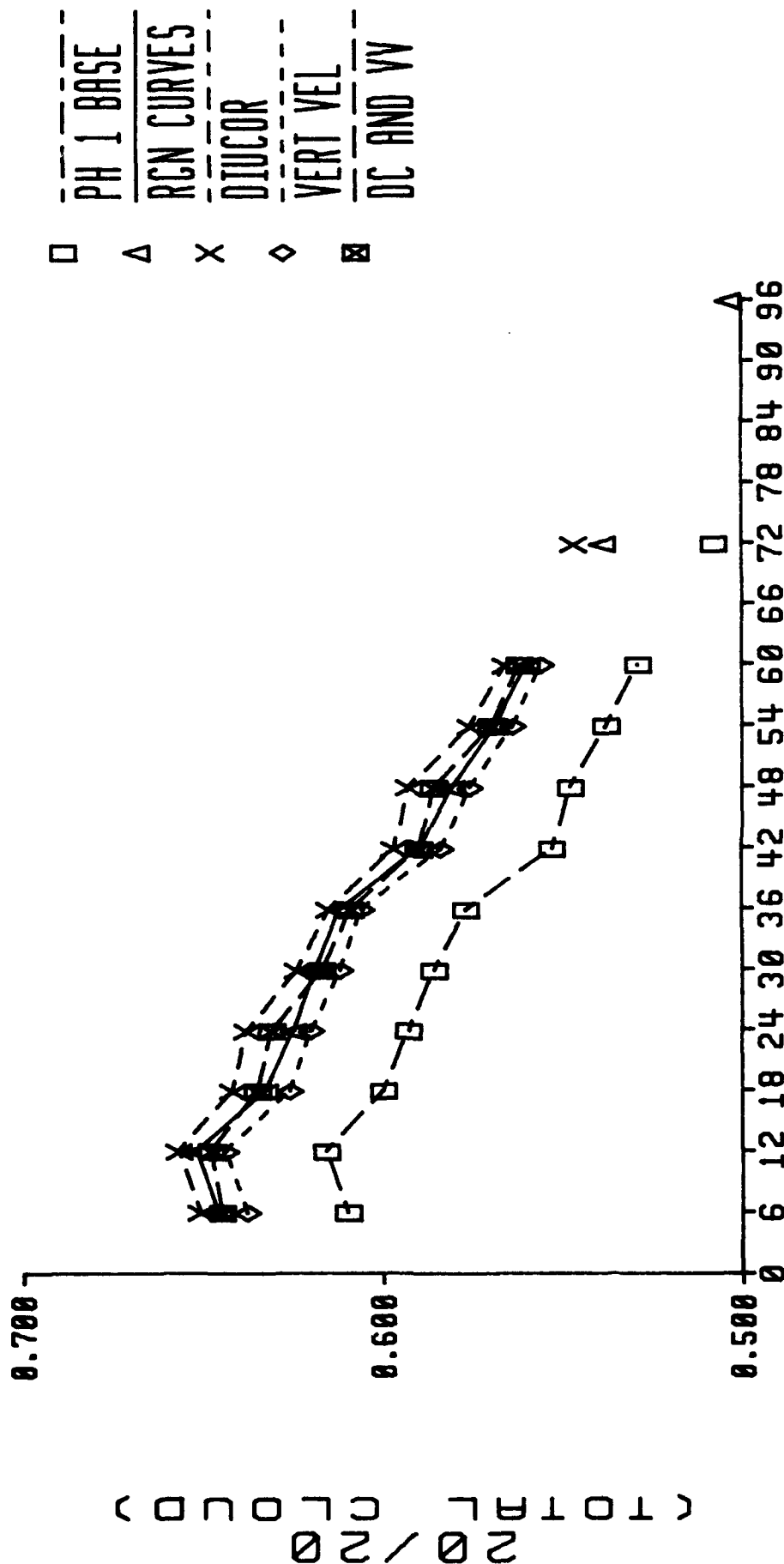
Figure E-9. 20/20 Scores for Cloud Forecasts Computed by Using Diurnal Persistence and Persistence and by Using Cloud Curve Algorithm Northern Hemisphere Tropical Ocean Curves For 6 to 60 and 72 Hour Total Cloud Forecasts Verified Over Northern Hemisphere Tropical Ocean During the Period from 24 October 1991 to 20 November 1991.

EUROPEAN LAND 24 OCT 91 TO 20 NOV 91



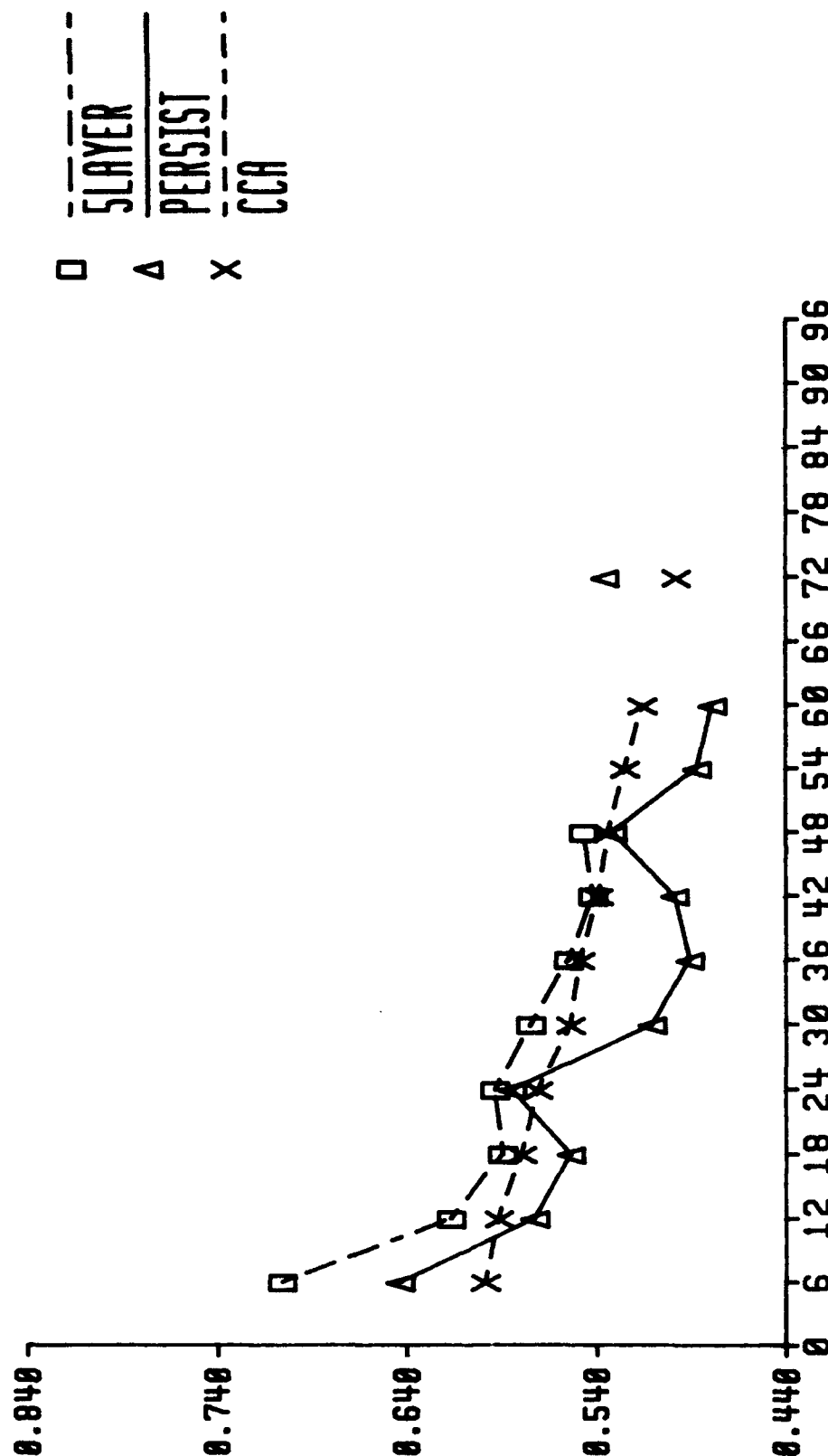
FORECAST LENGTH (HOURS)
Figure E-1

24 OCT 91 TO 20 NOV 91



FORECAST LENGTH (HOURS)
Figure E-2

EAST ASIA LAND 20 NOV 91



FORECAST LENGTH (HOURS)
Figure E-3

(20/20) SCORE

24 OCT 91 TO 20 NOV 91 NORTH AMERICA LAND

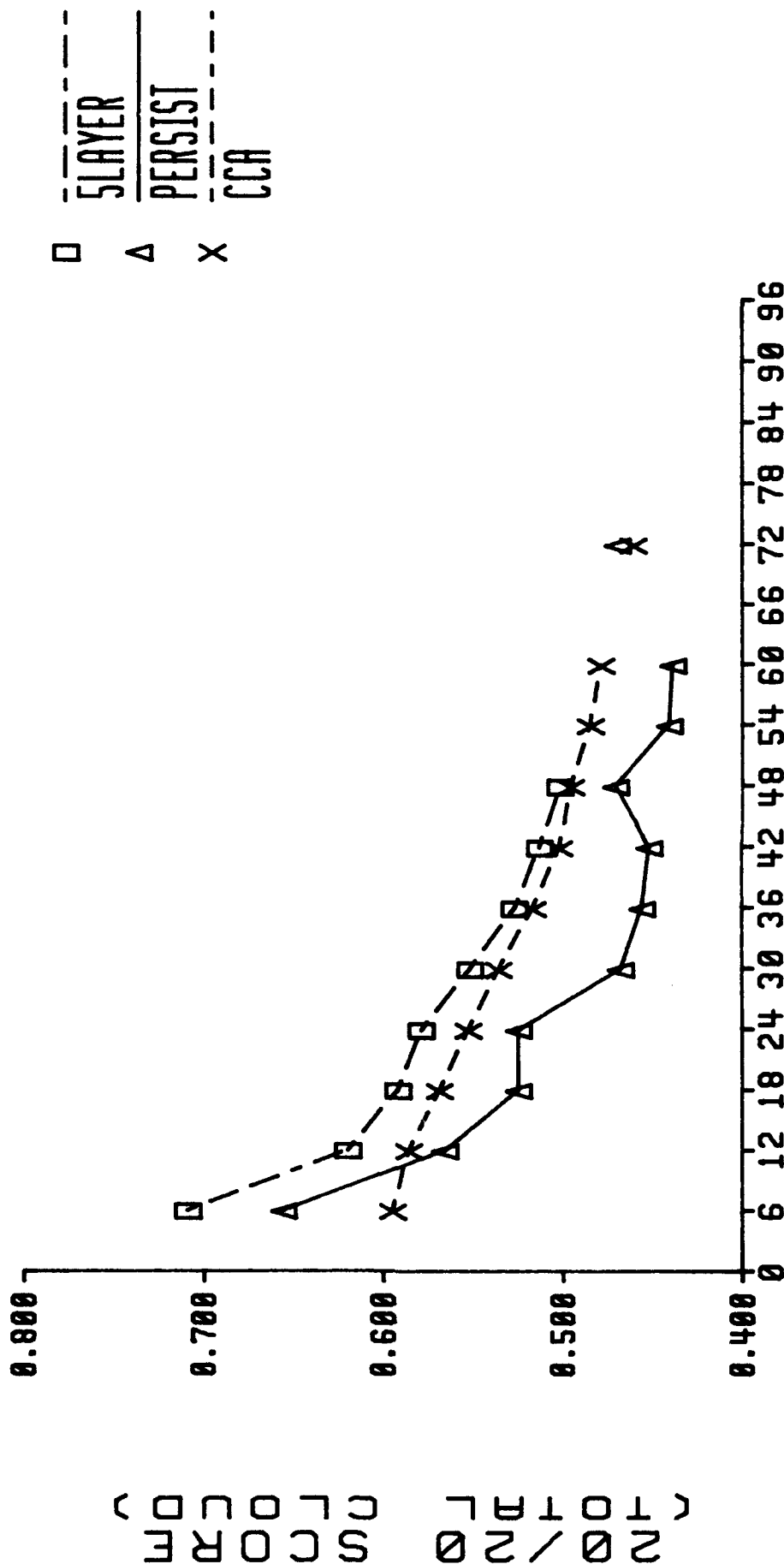


Figure E-4
FORECAST LENGTH (HOURS)

N AFR/MID EAST LAND
24 OCT 91 TO 20 NOV 91

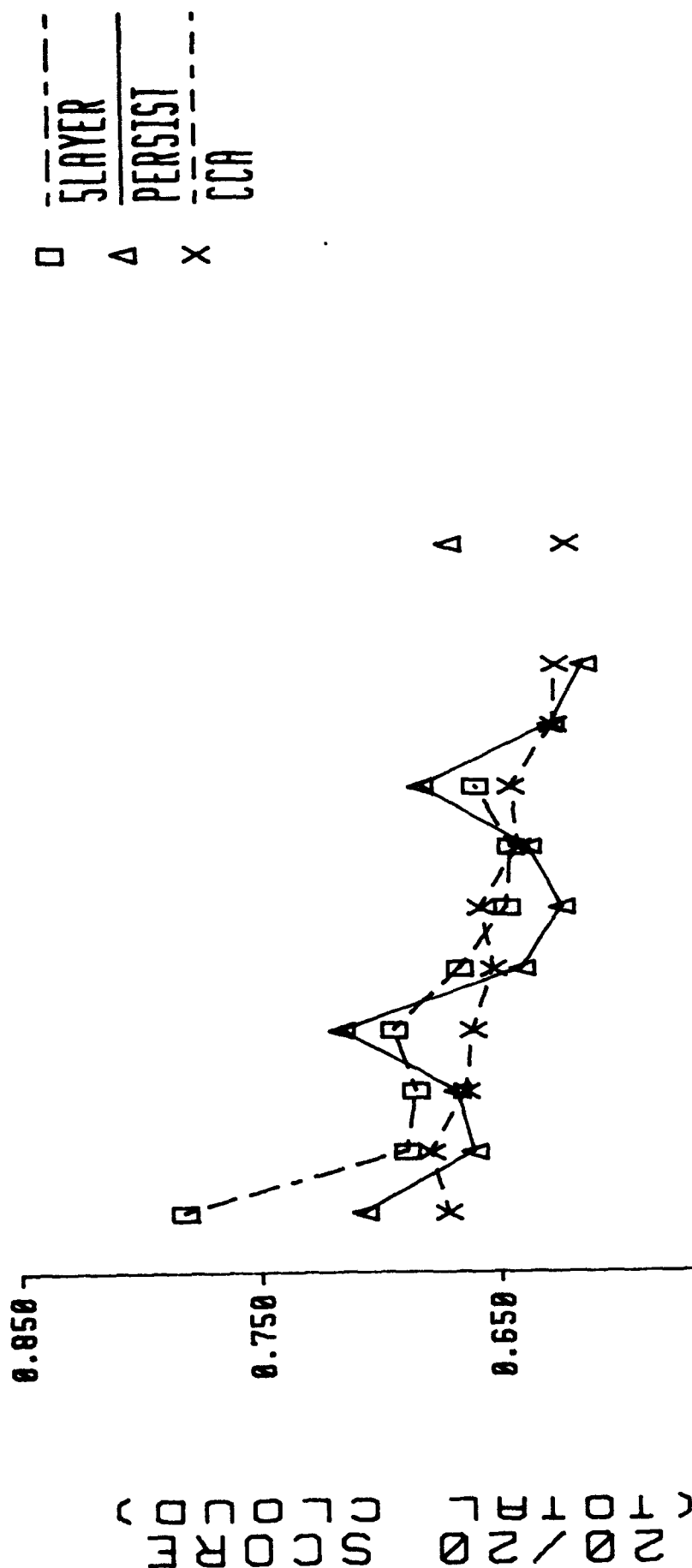
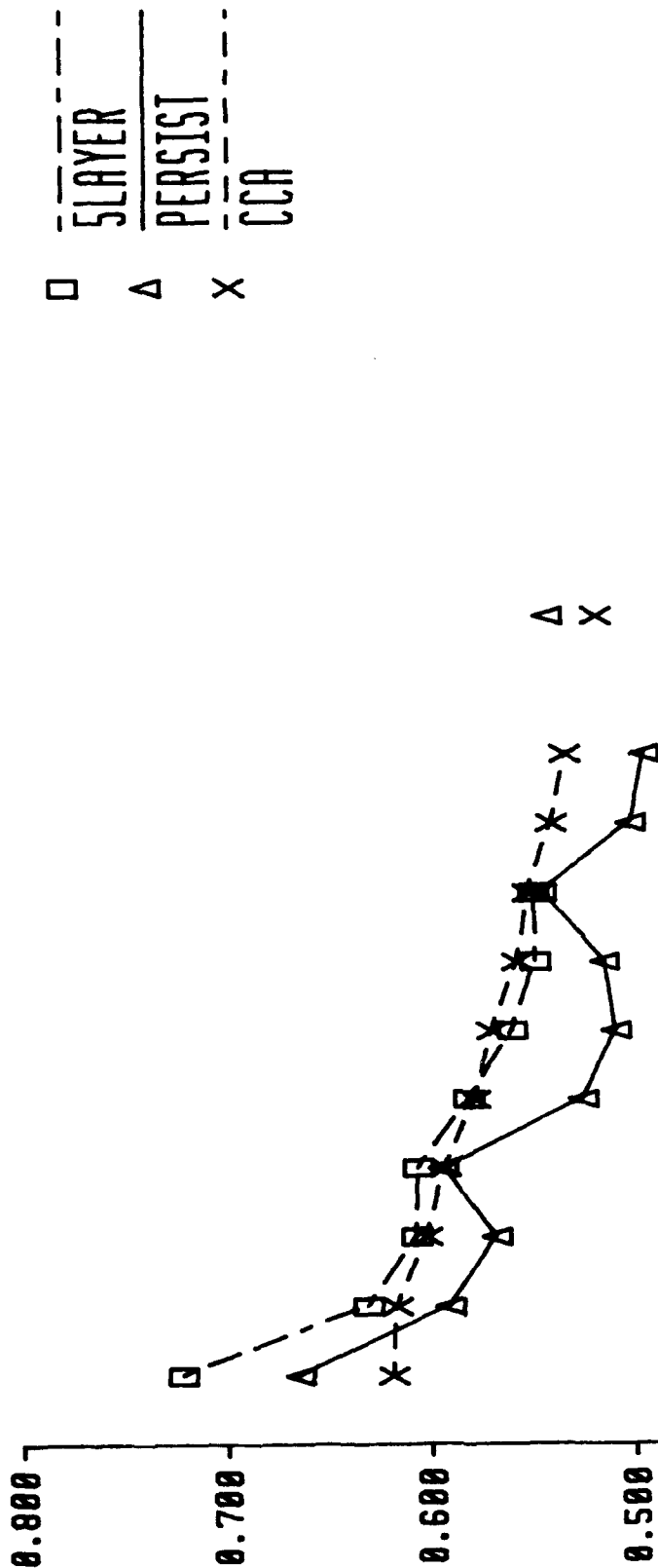


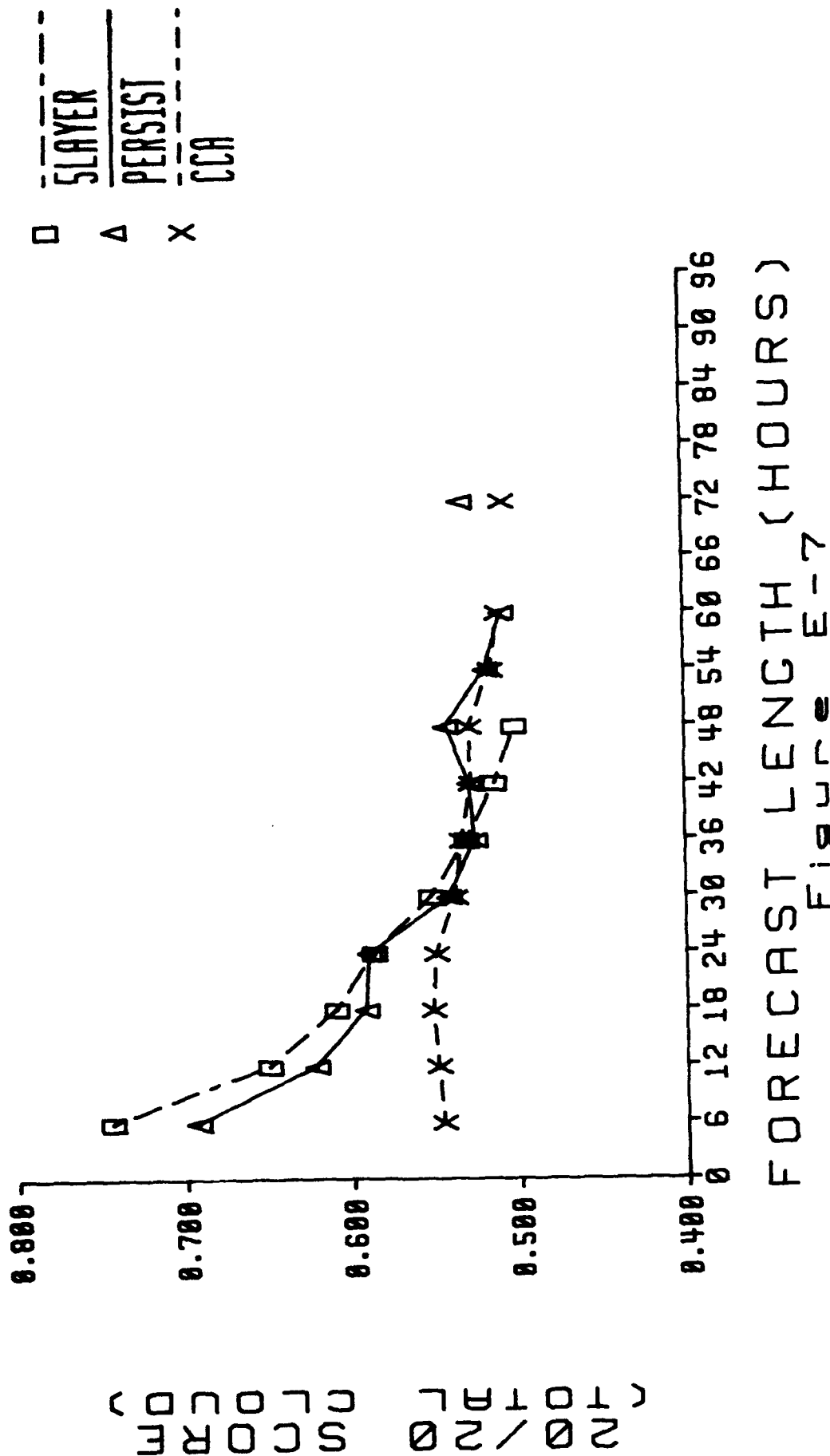
Figure E-5

N H MID-LAT LAND 91 24 OCT 91 TO 20 NOV 91

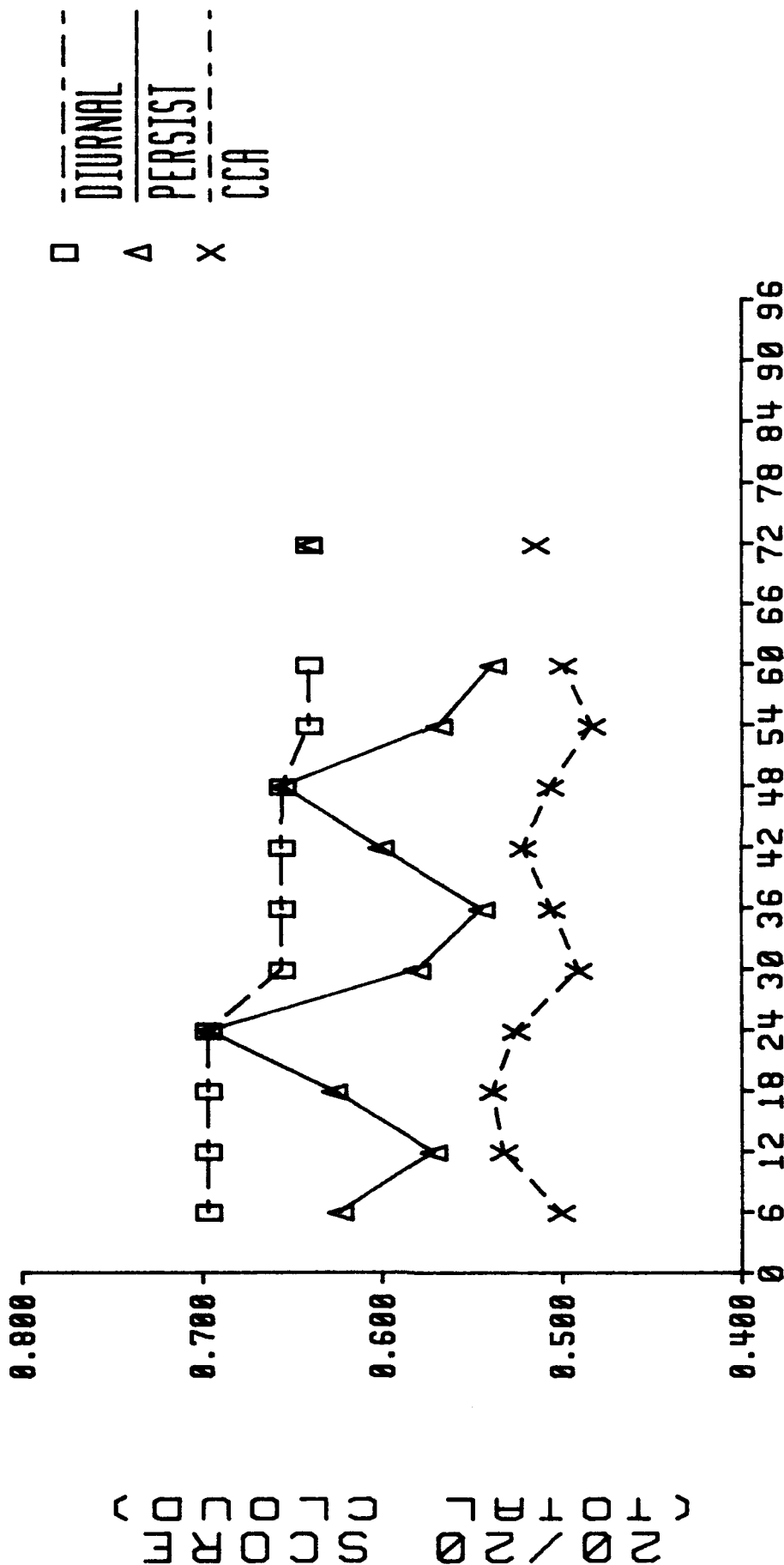


FORECAST LENGTH (HOURS)
Figure E-6

24 OCT 91 TO 20 NOV 91 N H MID-LAT OCEAN

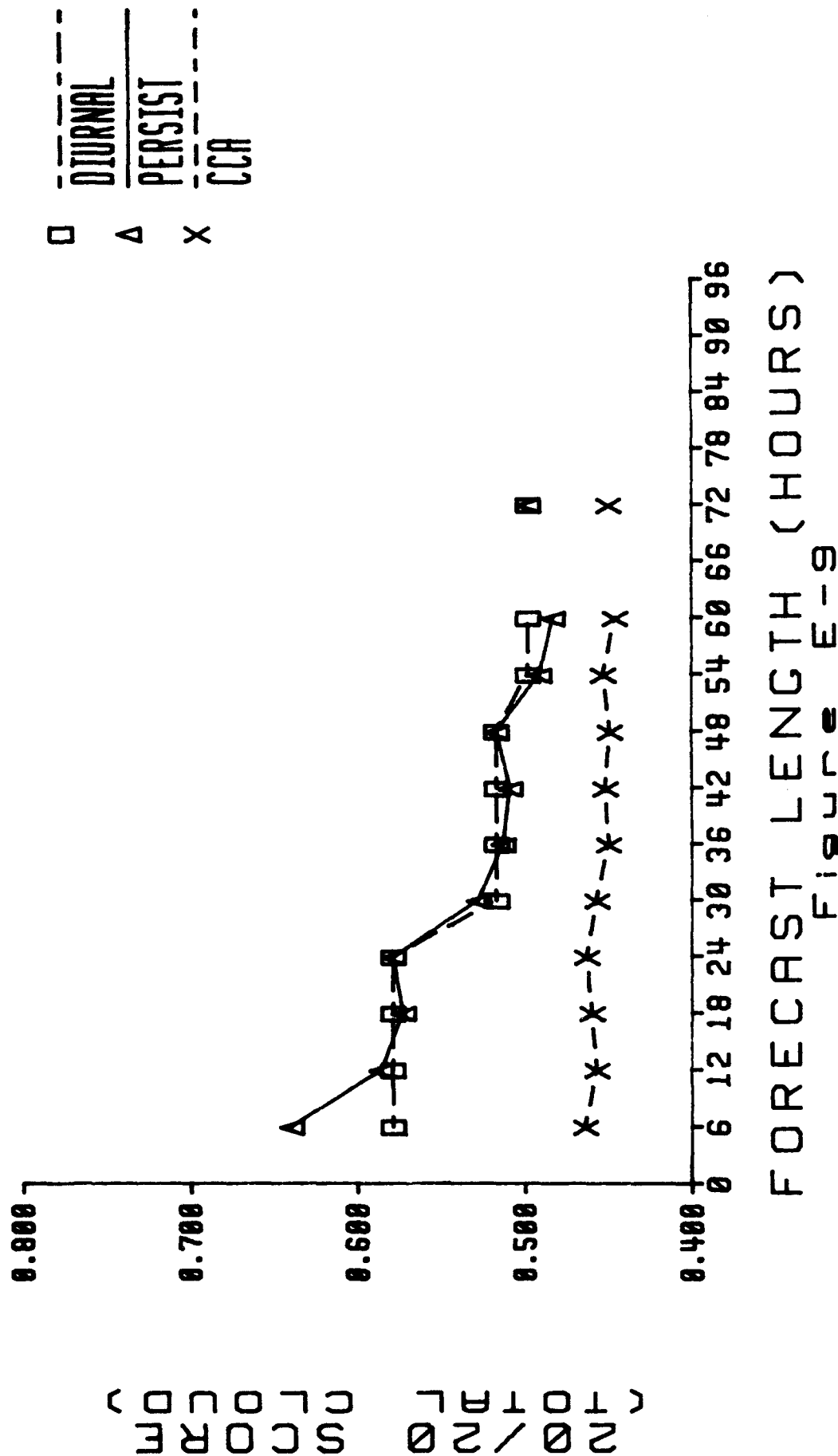


N H TROPICAL LAND 24 OCT 91 TO 20 NOV 91



FORECAST LENGTH (HOURS)
Figure E-8

24 OCT 91 TO 20 NOV 91 N H TROPICAL OCEAN



FORECAST LENGTH (HOURS)

Figure E-9

APPENDIX F:

PLOTS OF VERIFICATION STATISTICS

FOR EUROPEAN LAND

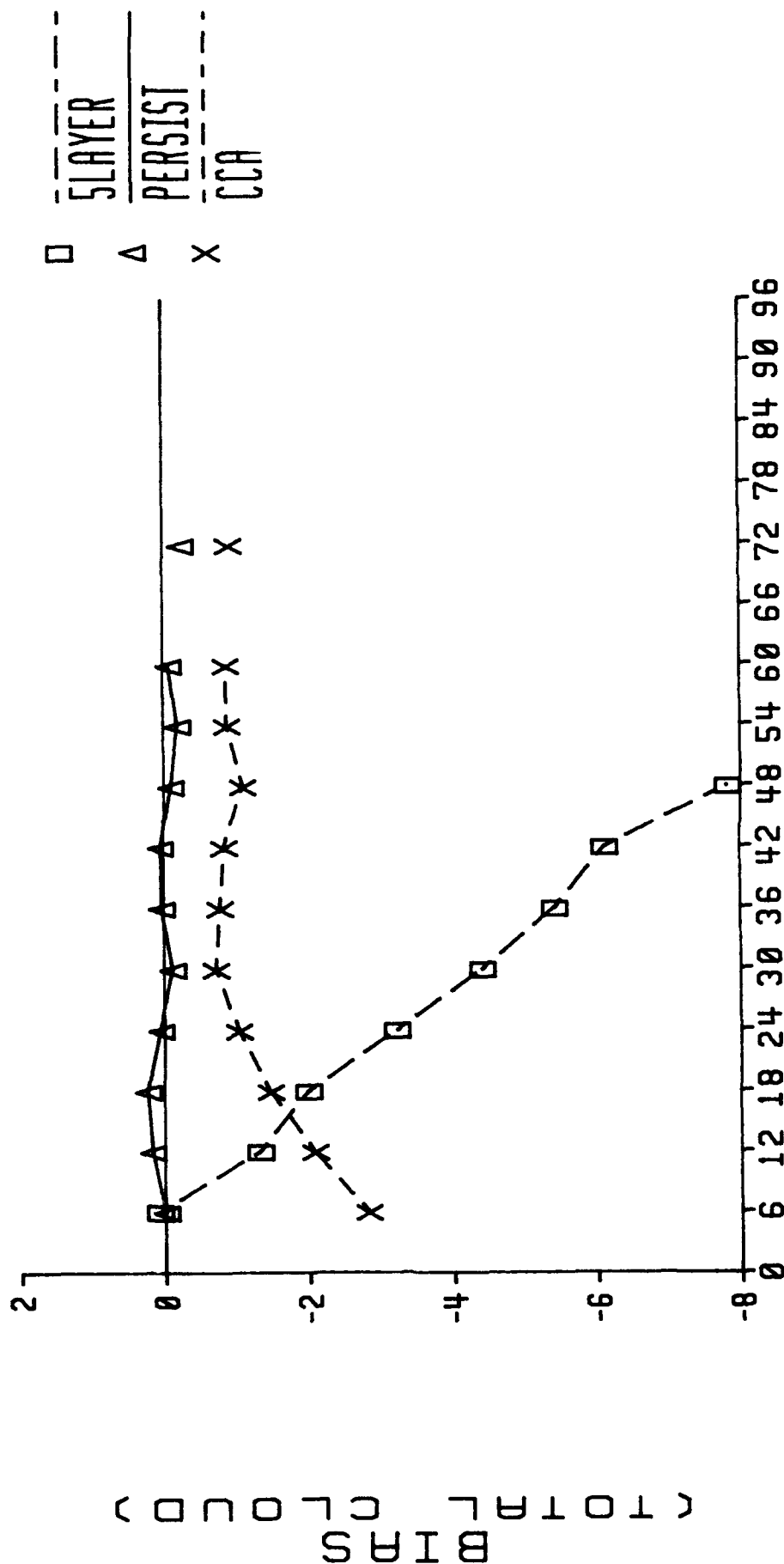
FOR THE PERIOD

24 OCT 91 TO 20 NOV 91

LIST OF FIGURES

- Figure F-1.** BIAS Scores for Cloud Forecasts Computed by the 5LAYER Model (to 48 hours only), by Using Persistence and by Using Cloud Curve Algorithm European Land Curves For 6 to 60 and 72 Hour Total Cloud Forecasts Verified Over European Land During the Period from 24 October 1991 to 20 November 1991.
- Figure F-2.** Sharpness Scores for Cloud Forecasts Computed by the 5LAYER Model (to 48 hours only), by Using Persistence and by Using Cloud Curve Algorithm European Land Curves For 6 to 60 and 72 Hour Total Cloud Forecasts Verified Over European Land During the Period from 24 October 1991 to 20 November 1991.
- Figure F-3.** Reliability Scores for Cloud Forecasts Computed by the 5LAYER Model (to 48 hours only), by Using Persistence and by Using Cloud Curve Algorithm European Land Curves For 6 to 60 and 72 Hour Total Cloud Forecasts Verified Over European Land During the Period from 24 October 1991 to 20 November 1991.
- Figure F-4.** RMSE Scores for Cloud Forecasts Computed by the 5LAYER Model (to 48 hours only), by Using Persistence and by Using Cloud Curve Algorithm European Land Curves For 6 to 60 and 72 Hour Total Cloud Forecasts Verified Over European Land During the Period from 24 October 1991 to 20 November 1991.
- Figure F-5.** Bust Scores for Cloud Forecasts Computed by the 5LAYER Model (to 48 hours only), by Using Persistence and by Using Cloud Curve Algorithm European Land Curves For 6 to 60 and 72 Hour Total Cloud Forecasts Verified Over European Land During the Period from 24 October 1991 to 20 November 1991.
- Figure F-6.** Heideke Skill Scores for Cloud Forecasts Computed by the 5LAYER Model (to 48 hours only), by Using Persistence and by Using Cloud Curve Algorithm European Land Curves For 6 to 60 and 72 Hour Total Cloud Forecasts Verified Over European Land During the Period from 24 October 1991 to 20 November 1991.
- Figure F-7.** MAE Scores for Cloud Forecasts Computed by the 5LAYER Model (to 48 hours only), by Using Persistence and by Using Cloud Curve Algorithm European Land Curves For 6 to 60 and 72 Hour Total Cloud Forecasts Verified Over European Land During the Period from 24 October 1991 to 20 November 1991.

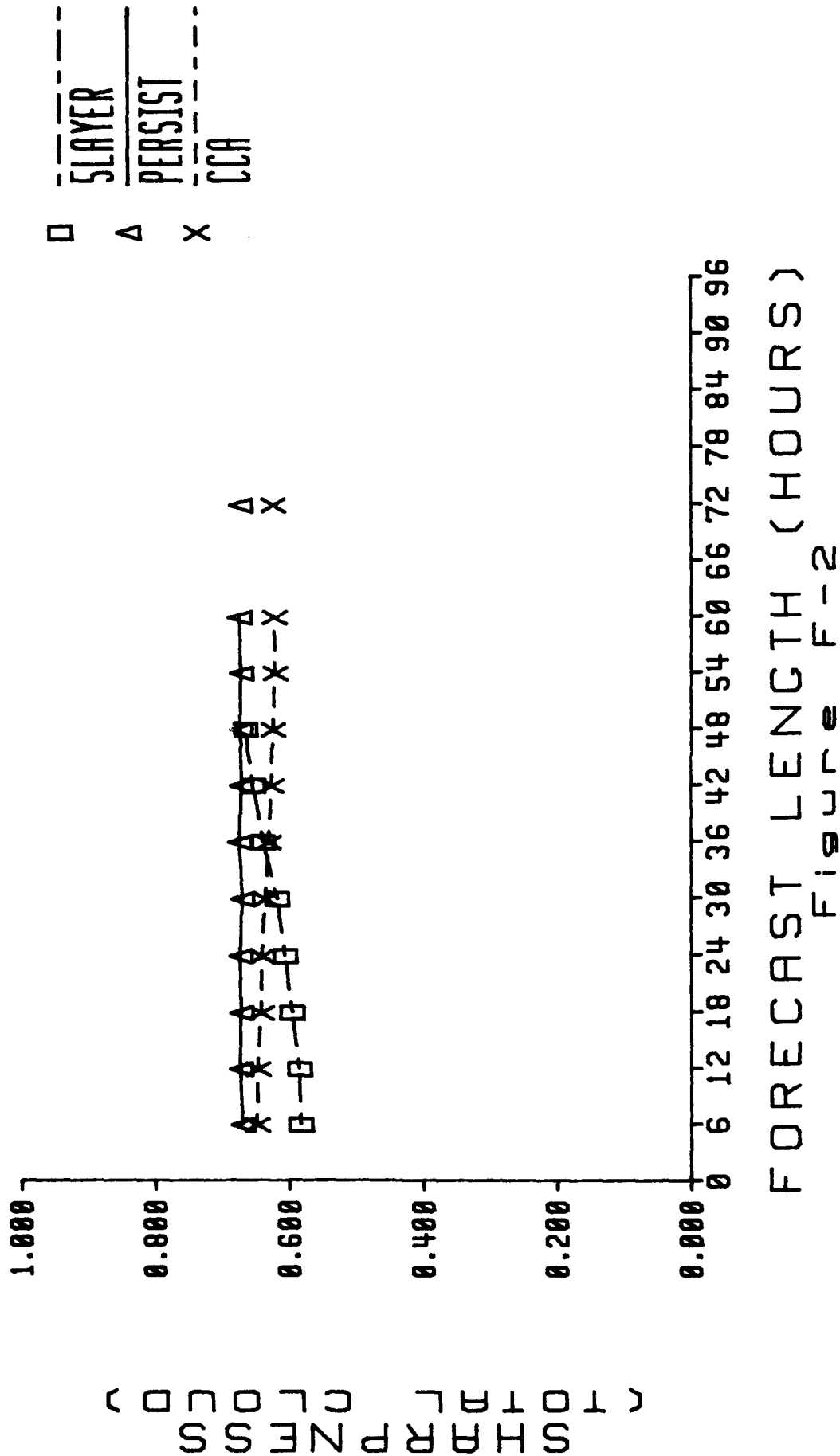
24 OCT 91 TO 20 NOV 91



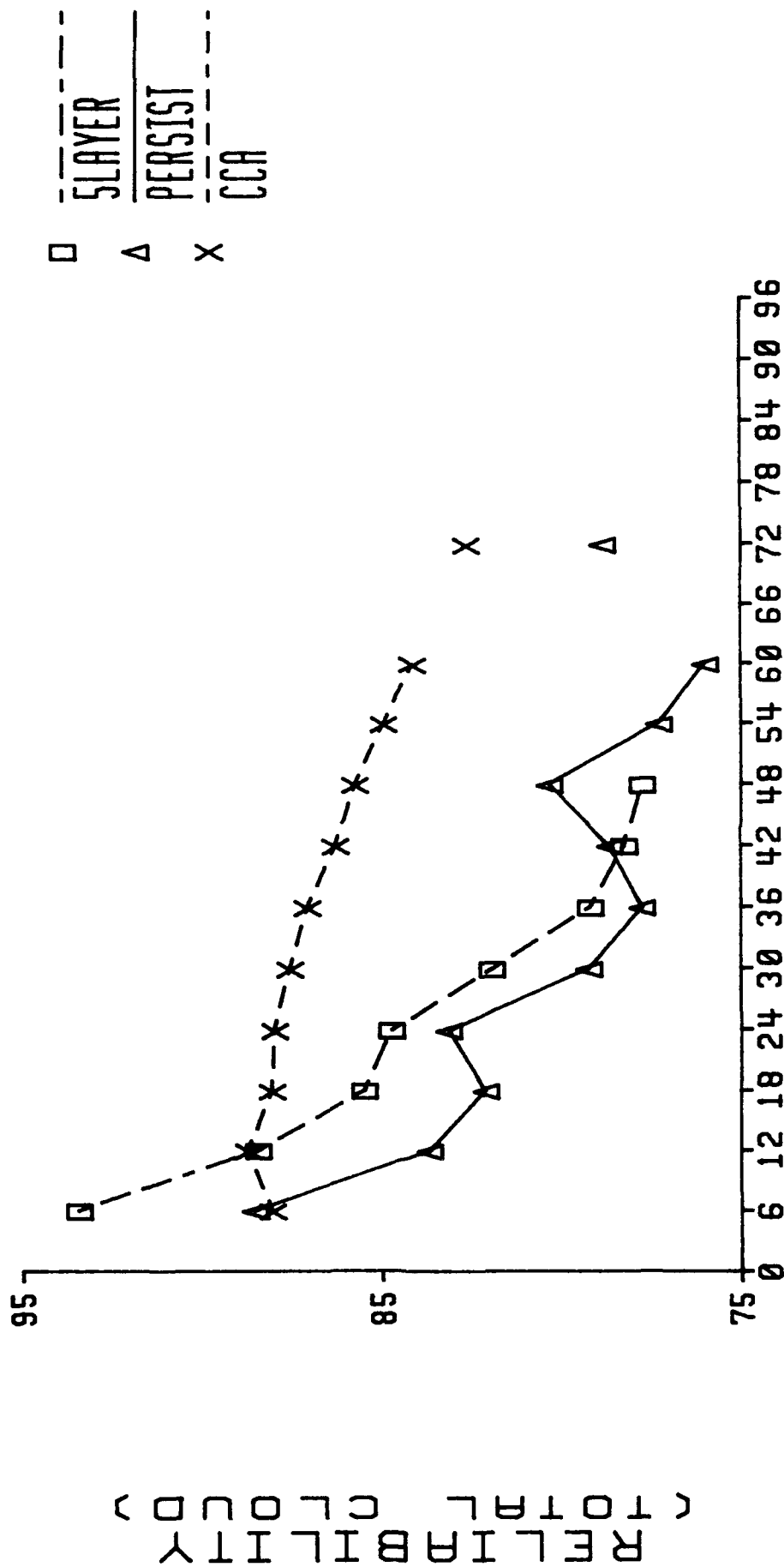
FORECAST LENGTH (HOURS)

Figure F-1

EUROPEAN LAND 24 OCT 91 TO 20 NOV 91

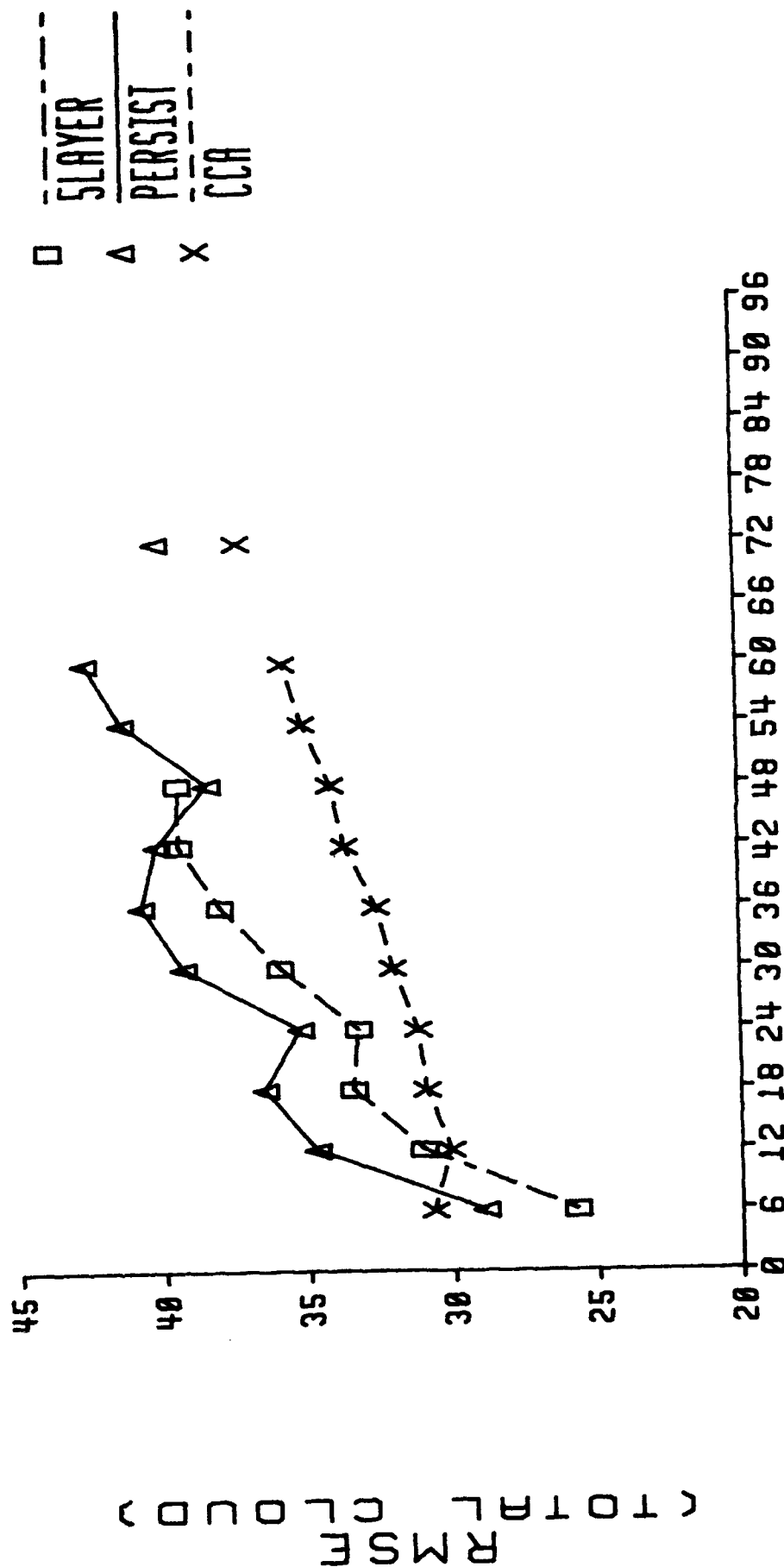


EUROPEAN LAND 24 OCT 91 TO 20 NOV 91



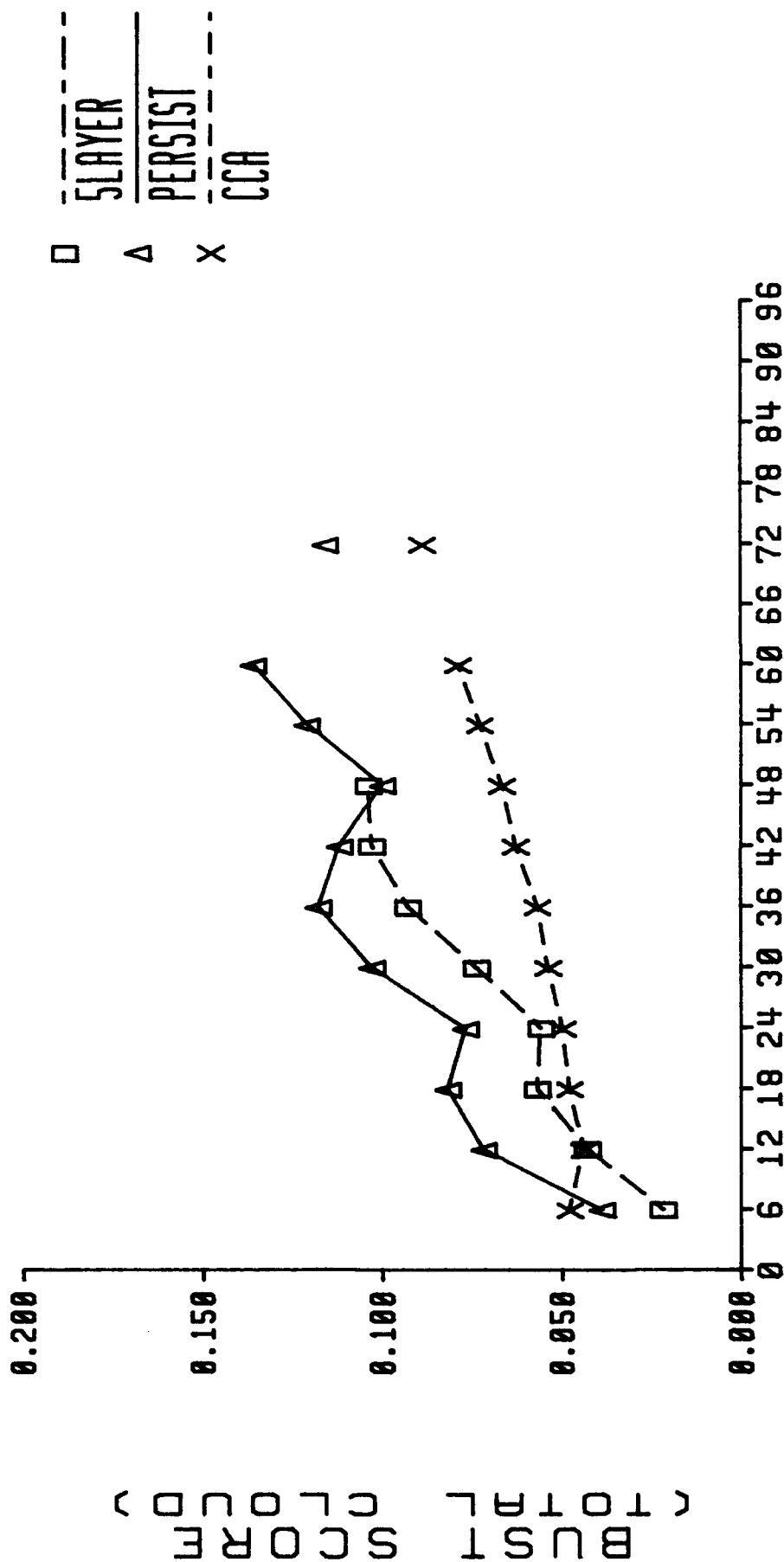
FORECAST LENGTH (HOURS)
Figure F-3

24 OCT 91 TO 20 NOV 91



FORECAST LENGTH (HOURS)
Figure F-4

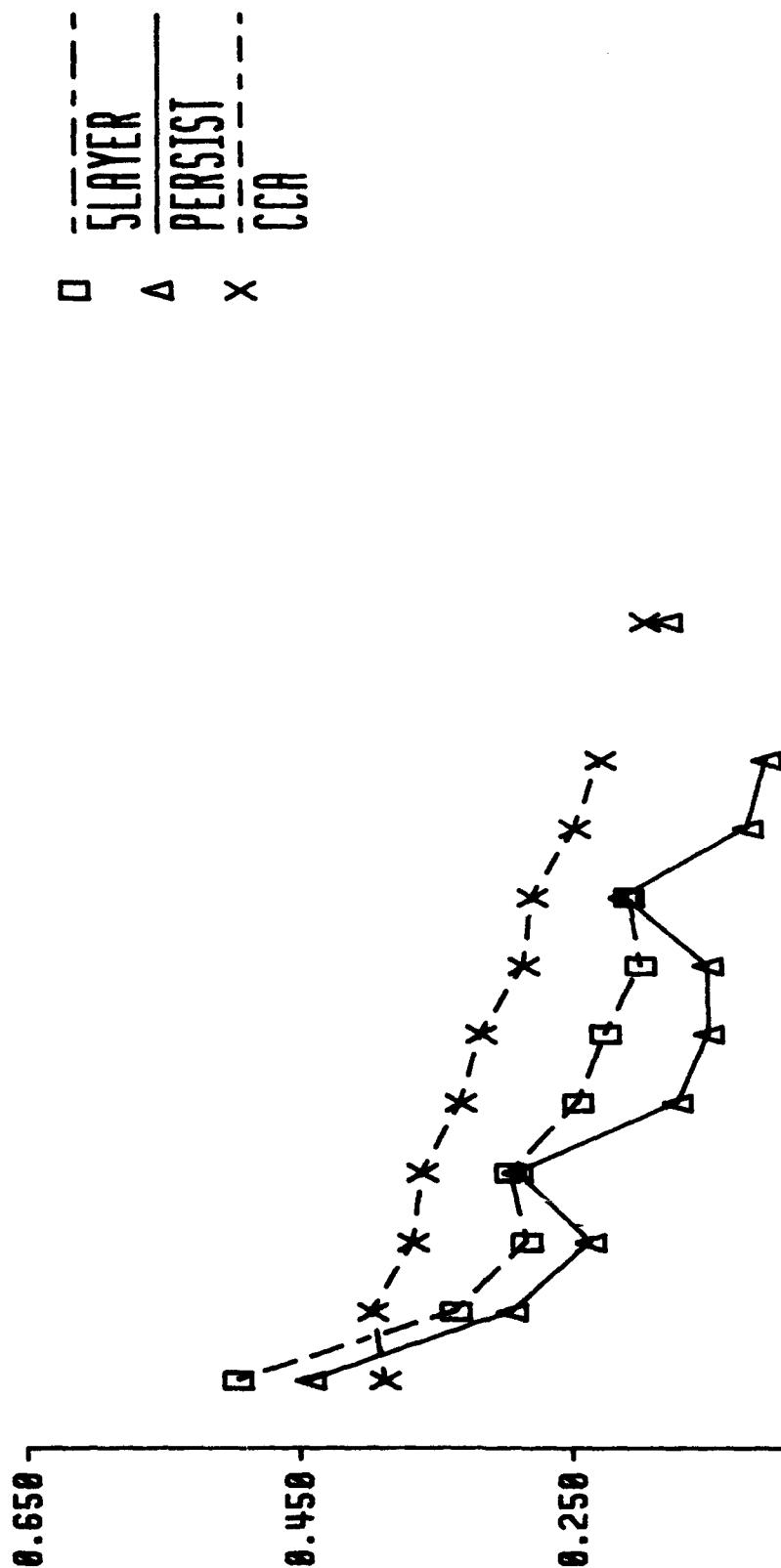
EUROPEAN LAND 24 OCT 91 TO 20 NOV 91



FORECAST LENGTH (HOURS)
Figure F-5

EUROPEAN LAND 24 OCT 91 TO 20 NOV 91

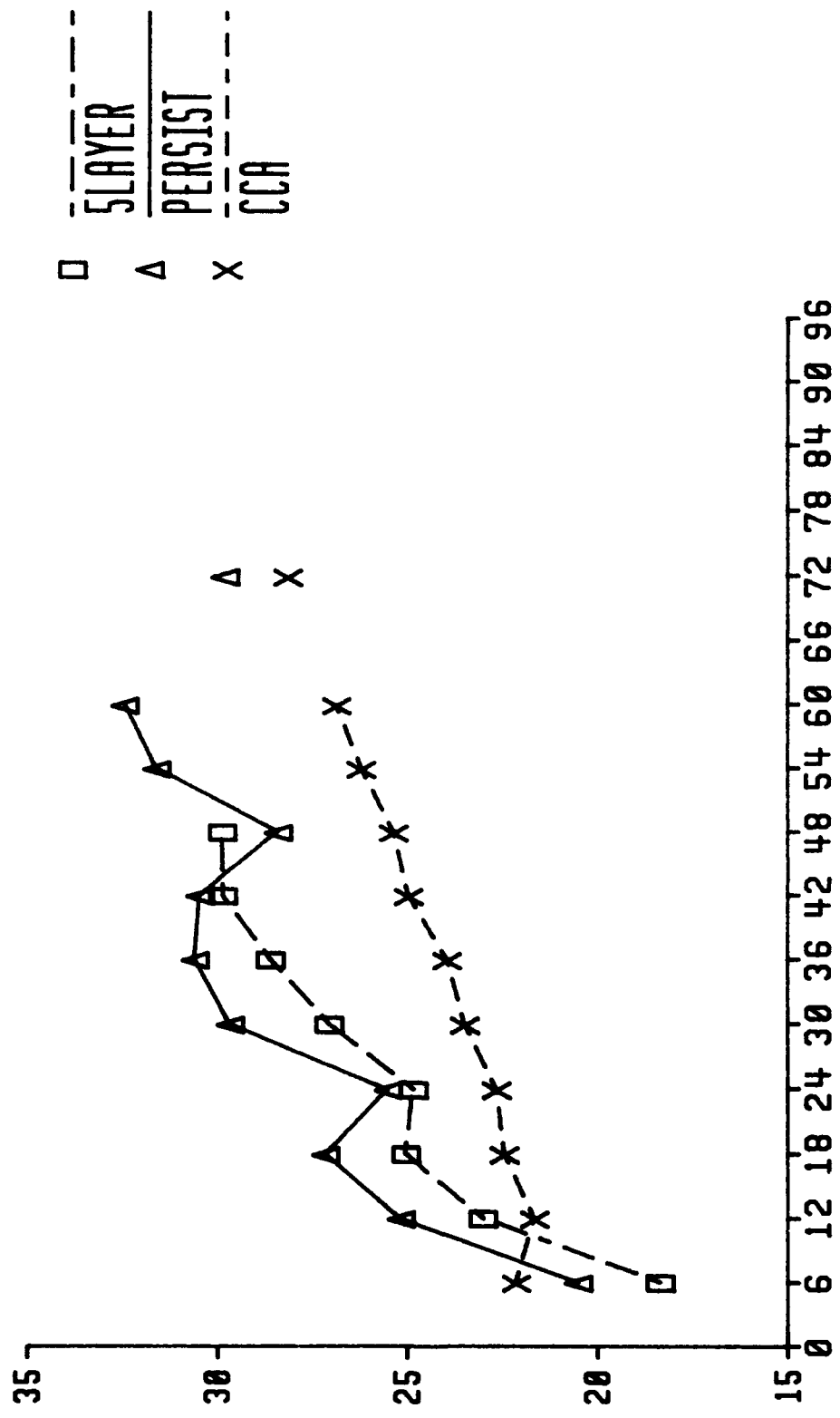
FIELD OF VIEW SKILL LOSS TO CORRECTION



FORECAST LENGTH (HOURS)
Figure F-6

24 OCT 91 TO 20 NOV 91

MEAN TOTAL CLOUD ERROR



FORECAST LENGTH (HOURS)
Figure F-7

This page intentionally left blank

APPENDIX G:

PLOTS OF 20/20 SCORES

FOR THE PERIOD

16 JAN 92 TO 12 FEB 92

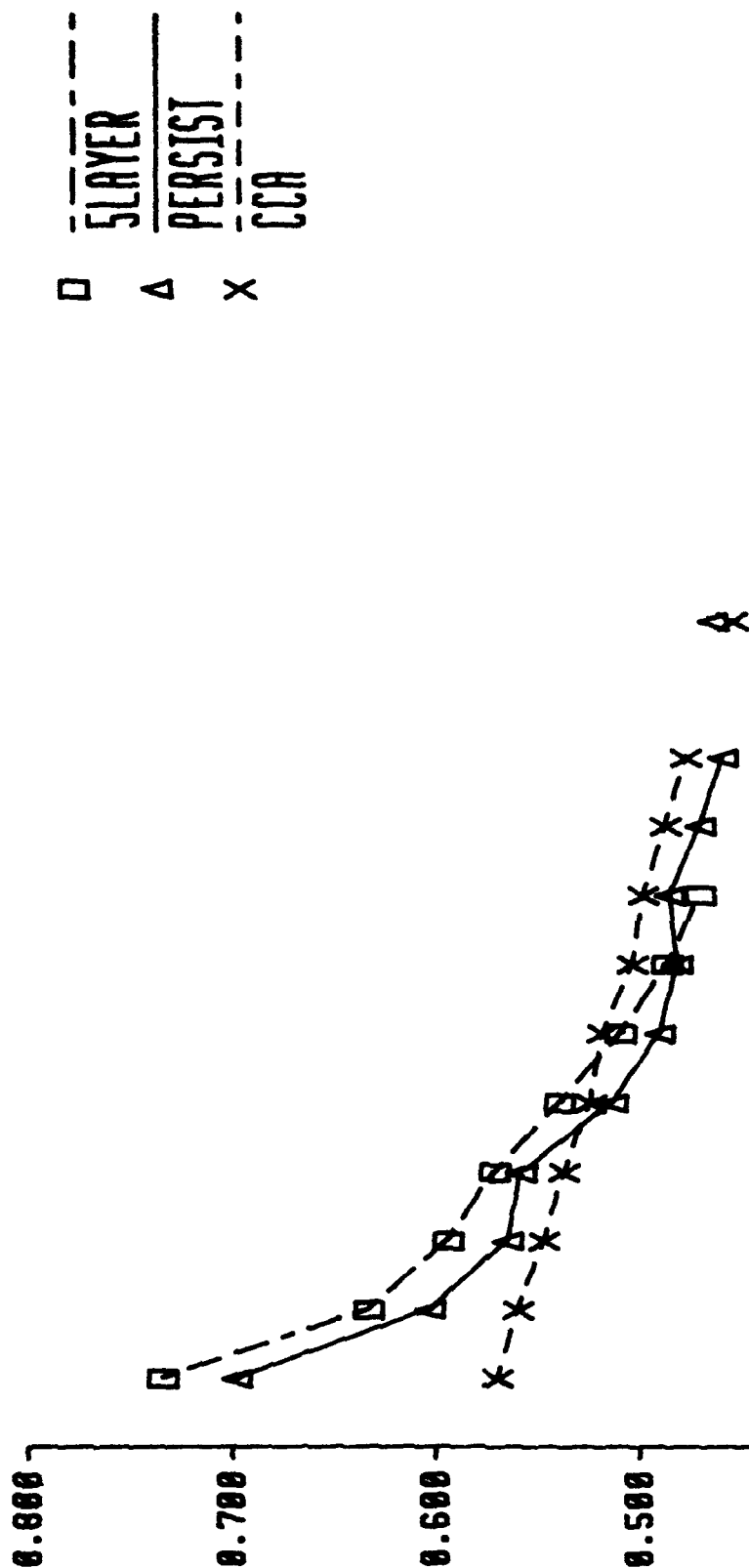
LIST OF FIGURES

- Figure G-1.** 20/20 Scores for Cloud Forecasts Computed by the 5LAYER Model (to 48 hours only), by Using Persistence and by Using Cloud Curve Algorithm European Land Curves For 6 to 60 and 72 Hour Total Cloud Forecasts Verified Over European Land During the Period from 16 January 1992 to 12 February 1992.
- Figure G-2.** 20/20 Scores for Cloud Forecasts Computed by Using Cloud Curve Algorithm Northern Hemisphere Mid-Latitude Land Curves (Phase I Baseline), European Land Curves (Region Curves), European Land Curves with Diurnal Correction (to 72 hour only), European Land Curves with Vertical Velocity (to 60 hours only), and European Land Curves with both Diurnal Correction and Vertical Velocity (to 60 hour only) for 6 to 60, 72 and 96 Hour Total Cloud Forecasts Verified Over European Land During the Period from 16 January 1992 to 12 February 1992.
- Figure G-3.** 20/20 Scores for Cloud Forecasts Computed by the 5LAYER Model (to 48 hours only), by Using Persistence and by Using Cloud Curve Algorithm East Asia Land Curves For 6 to 60 and 72 Hour Total Cloud Forecasts Verified Over East Asia Land During the Period from 16 January 1992 to 12 February 1992.
- Figure G-4.** 20/20 Scores for Cloud Forecasts Computed by the 5LAYER Model (to 48 hours only), by Using Persistence and by Using Cloud Curve Algorithm North America Land Curves For 6 to 60 and 72 Hour Total Cloud Forecasts Verified Over North America Land During the Period from 16 January 1992 to 12 February 1992.
- Figure G-5.** 20/20 Scores for Cloud Forecasts Computed by the 5LAYER Model (to 48 hours only), by Using Persistence and by Using Cloud Curve Algorithm North Africa/Middle East Land Curves For 6 to 60 and 72 Hour Total Cloud Forecasts Verified Over North Africa/Middle East Land During the Period from 16 January 1992 to 12 February 1992.
- Figure G-6.** 20/20 Scores for Cloud Forecasts Computed by the 5LAYER Model (to 48 hours only), by Using Persistence and by Using Cloud Curve Algorithm Northern Hemisphere Mid-Latitude Regional Land Curves For 6 to 60 and 72 Hour Total Cloud Forecasts Verified Over Northern Hemisphere Mid-Latitude Land During the Period from 16 January 1992 to 12 February 1992.
- Figure G-7.** 20/20 Scores for Cloud Forecasts Computed by the 5LAYER Model (to 48 hours only), by Using Persistence and by Using Cloud Curve Algorithm Northern Hemisphere Mid-Latitude Ocean Curves For 6 to 60 and 72 Hour Total Cloud Forecasts Verified Over Northern Hemisphere Mid-Latitude Ocean During the Period from 16 January 1992 to 12 February 1992.

Figure G-8. 20/20 Scores for Cloud Forecasts Computed by Using Diurnal Persistence and Persistence and by Using Cloud Curve Algorithm Northern Hemisphere Tropical Land Curves For 6 to 60 and 72 Hour Total Cloud Forecasts Verified Over Northern Hemisphere Tropical Land During the Period from 16 January 1992 to 12 February 1992 .

Figure G-9. 20/20 Scores for Cloud Forecasts Computed by Using Diurnal Persistence and Persistence and by Using Cloud Curve Algorithm Northern Hemisphere Tropical Ocean Curves For 6 to 60 and 72 Hour Total Cloud Forecasts Verified Over Northern Hemisphere Tropical Ocean During the Period from 16 January 1992 to 12 February 1992 .

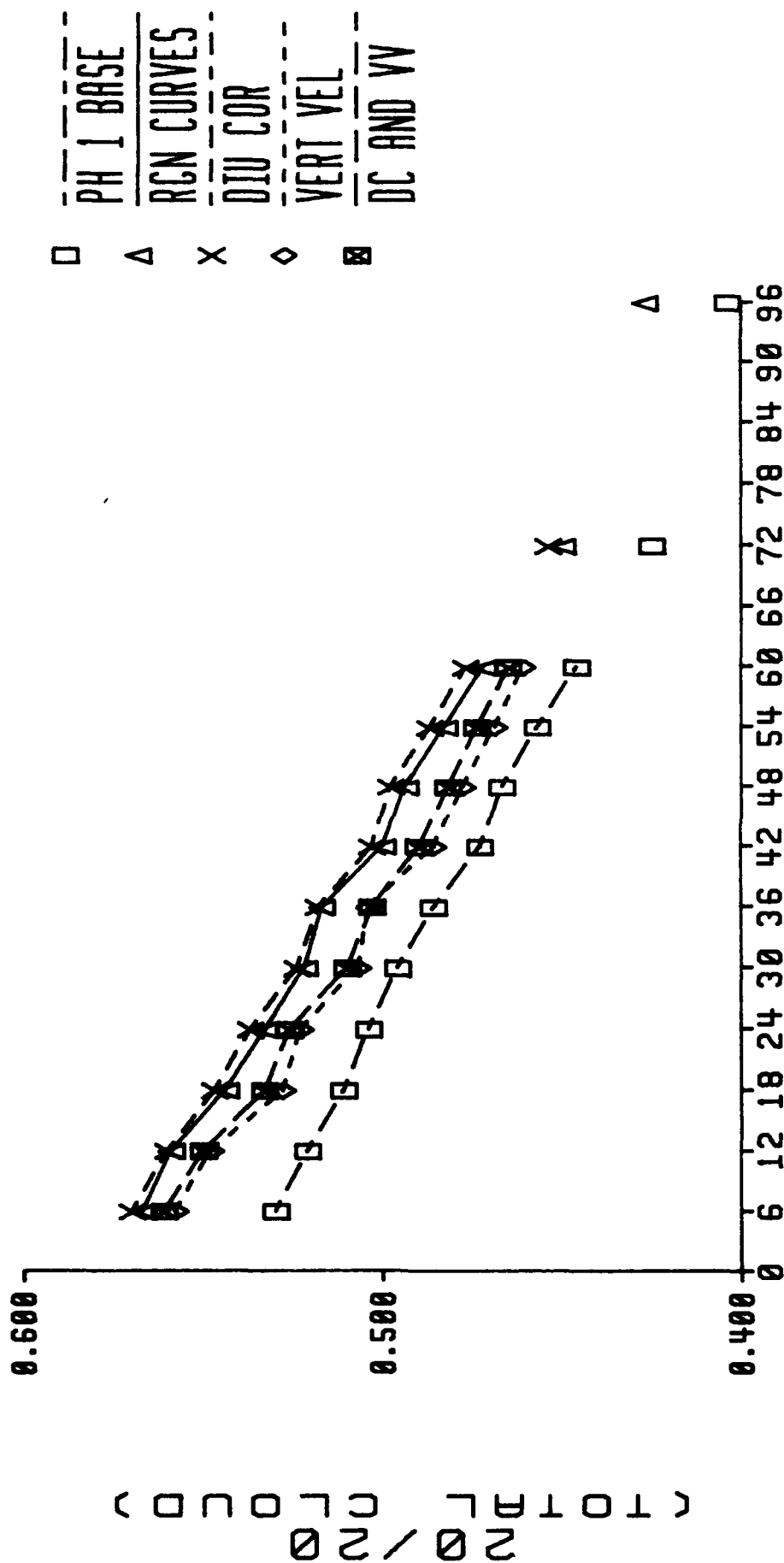
EUROPEAN LAND 16 JAN 92 TO 12 FEB 92



FORECAST LENGTH (HOURS)
Figure C-1

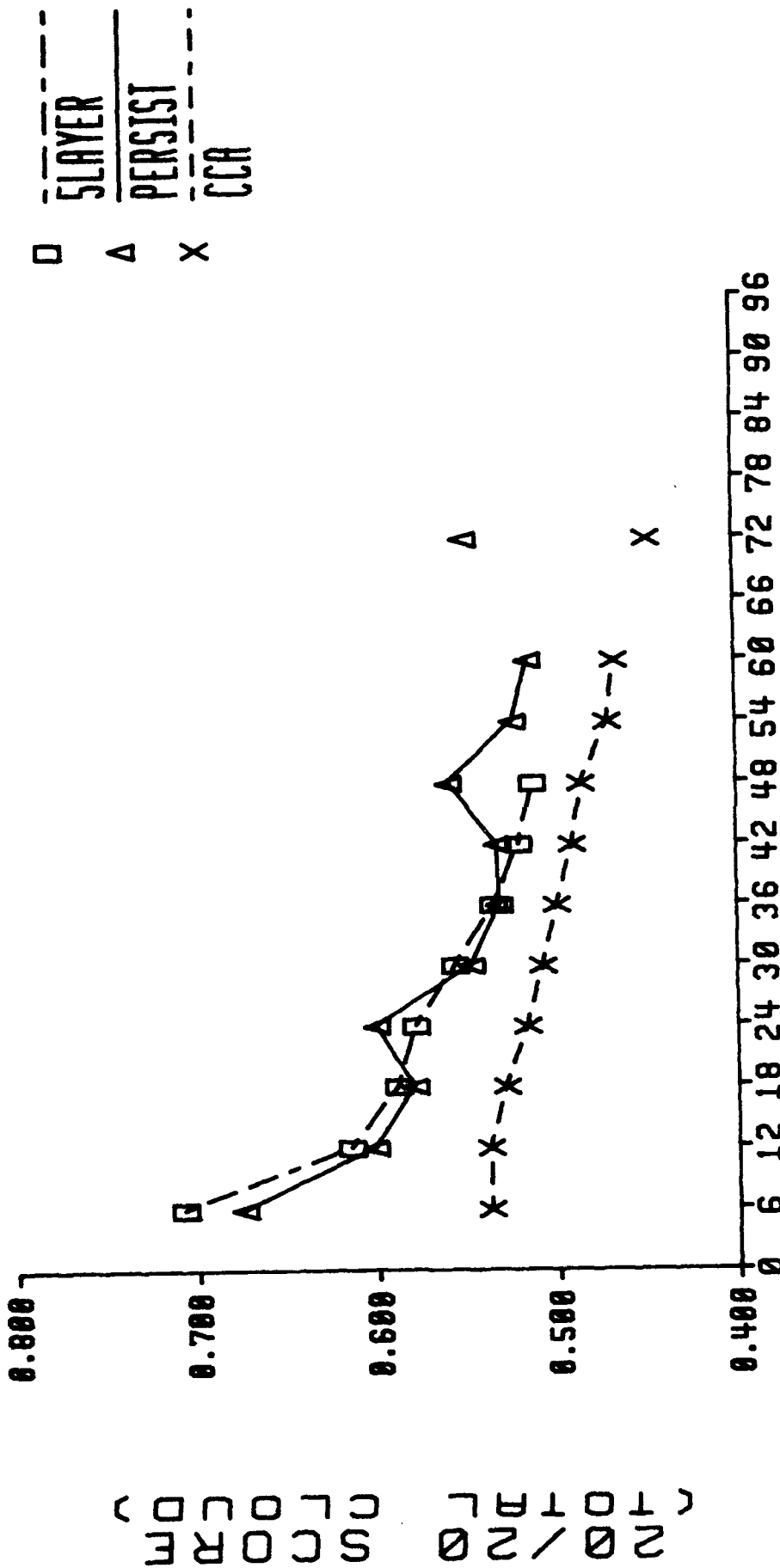
(20/20 SLCCF)
(20/20 SLCCF)

EUROPEAN LAND 16 JAN 92 TO 12 FEB 92



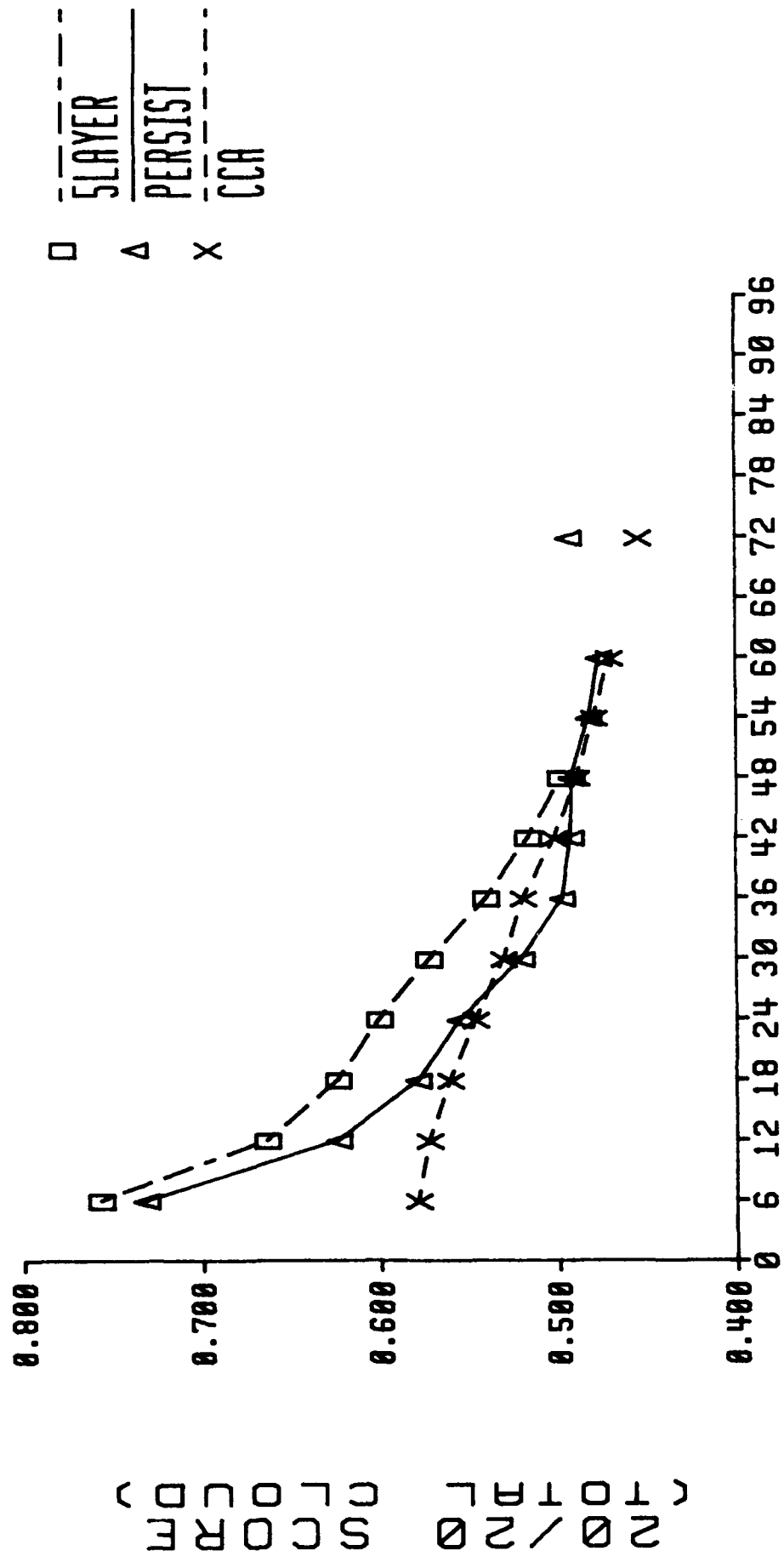
FORECAST LENGTH (HOURS)
Figure C-2

EAST ASIA LAND 12 FEB 92



FORECAST LENGTH (HOURS)
Figure C-3

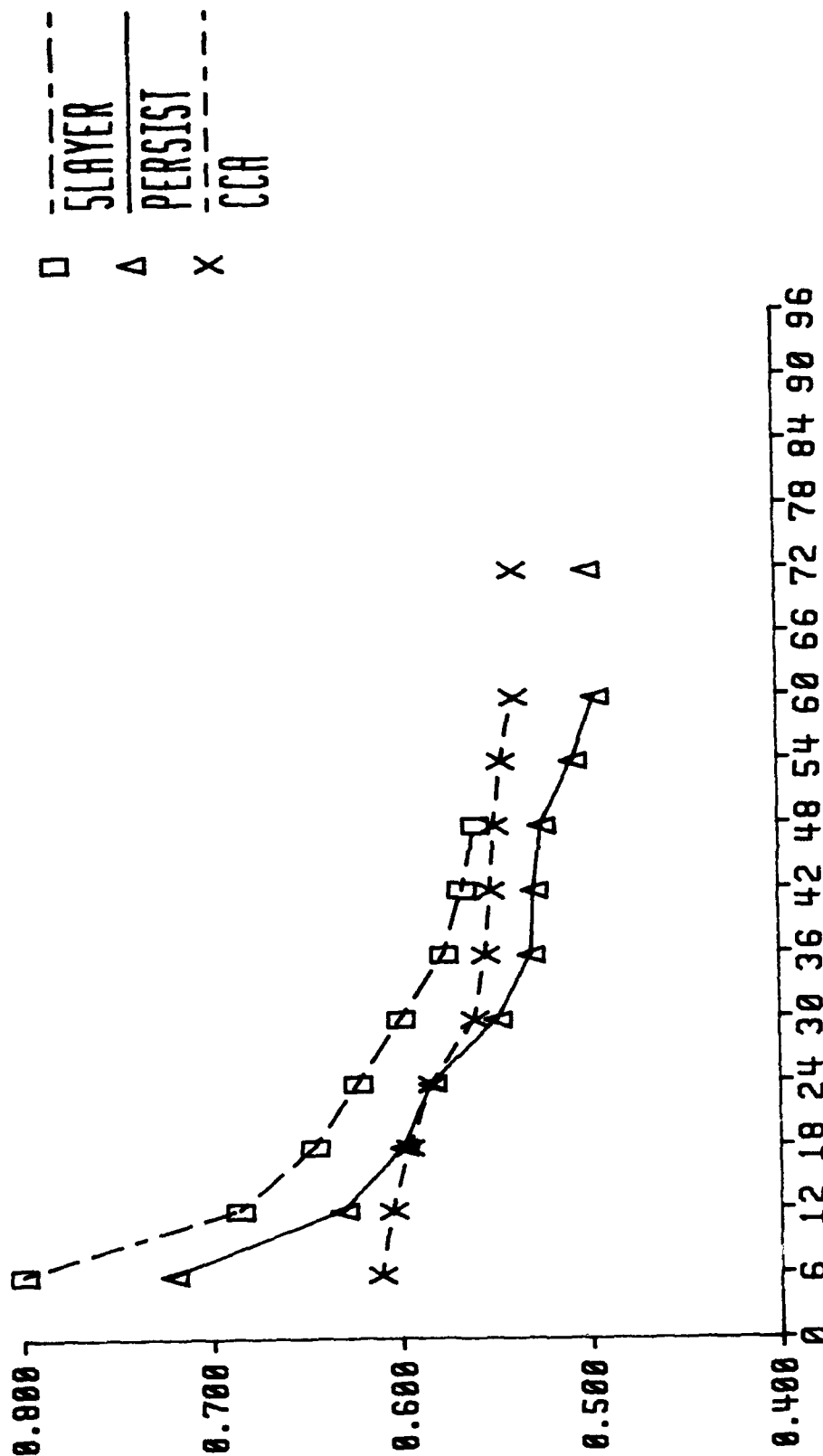
16 NORTH AMERICA LAND 92 TO 12 FEB 92



FORECAST LENGTH (HOURS)
Figure C-4

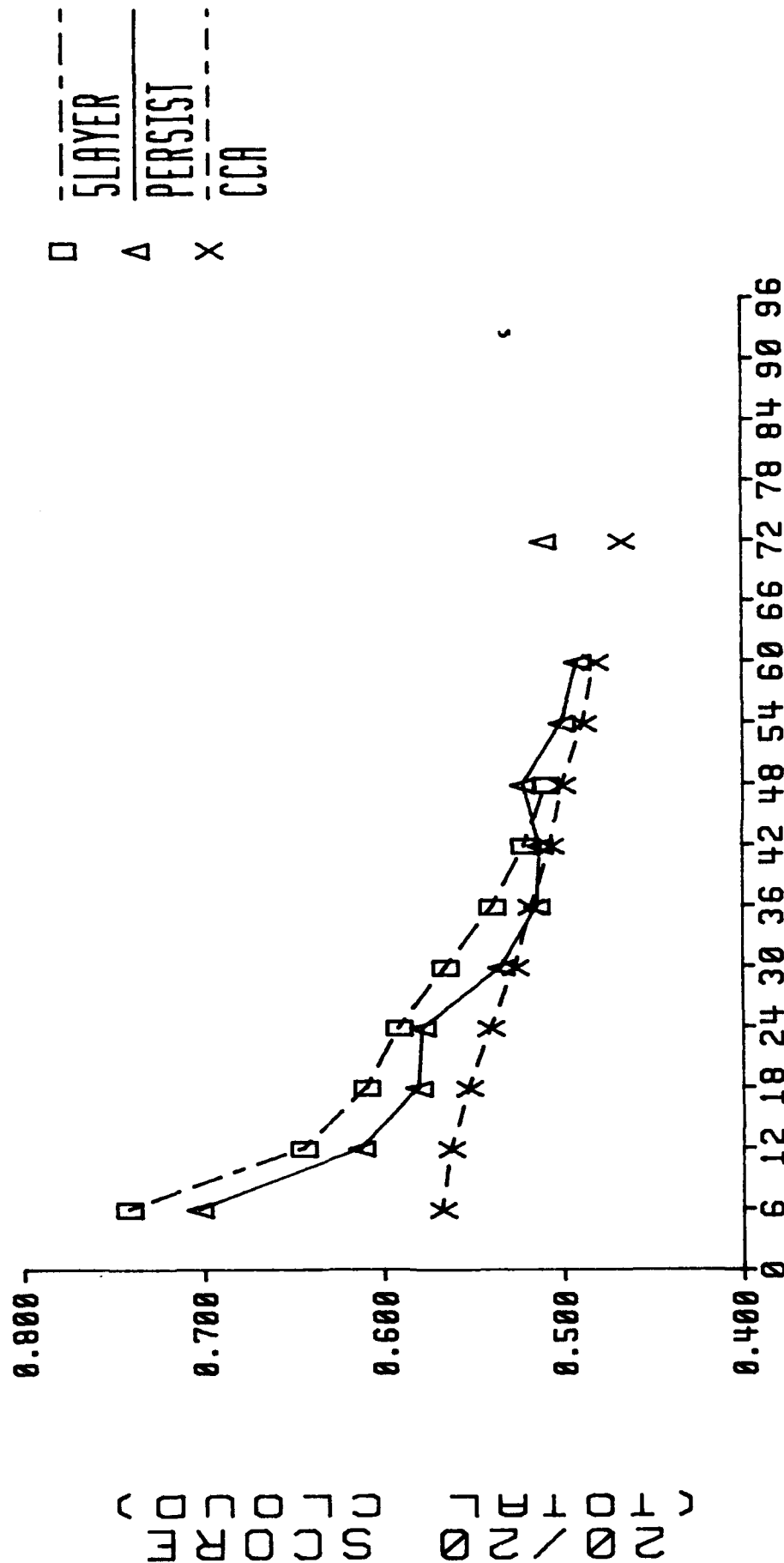
16 JAN 92 TO 12 FEB 92
N AFR/MID EAST LAND

20/20 SCORE (TOTAL CLOUD)



FORECAST LENGTH (HOURS)

16 JAN 92 TO 12 FEB 92



FORECAST LENGTH (HOURS)
Figure C-6

16 JAN 92 TO 12 FEB 92

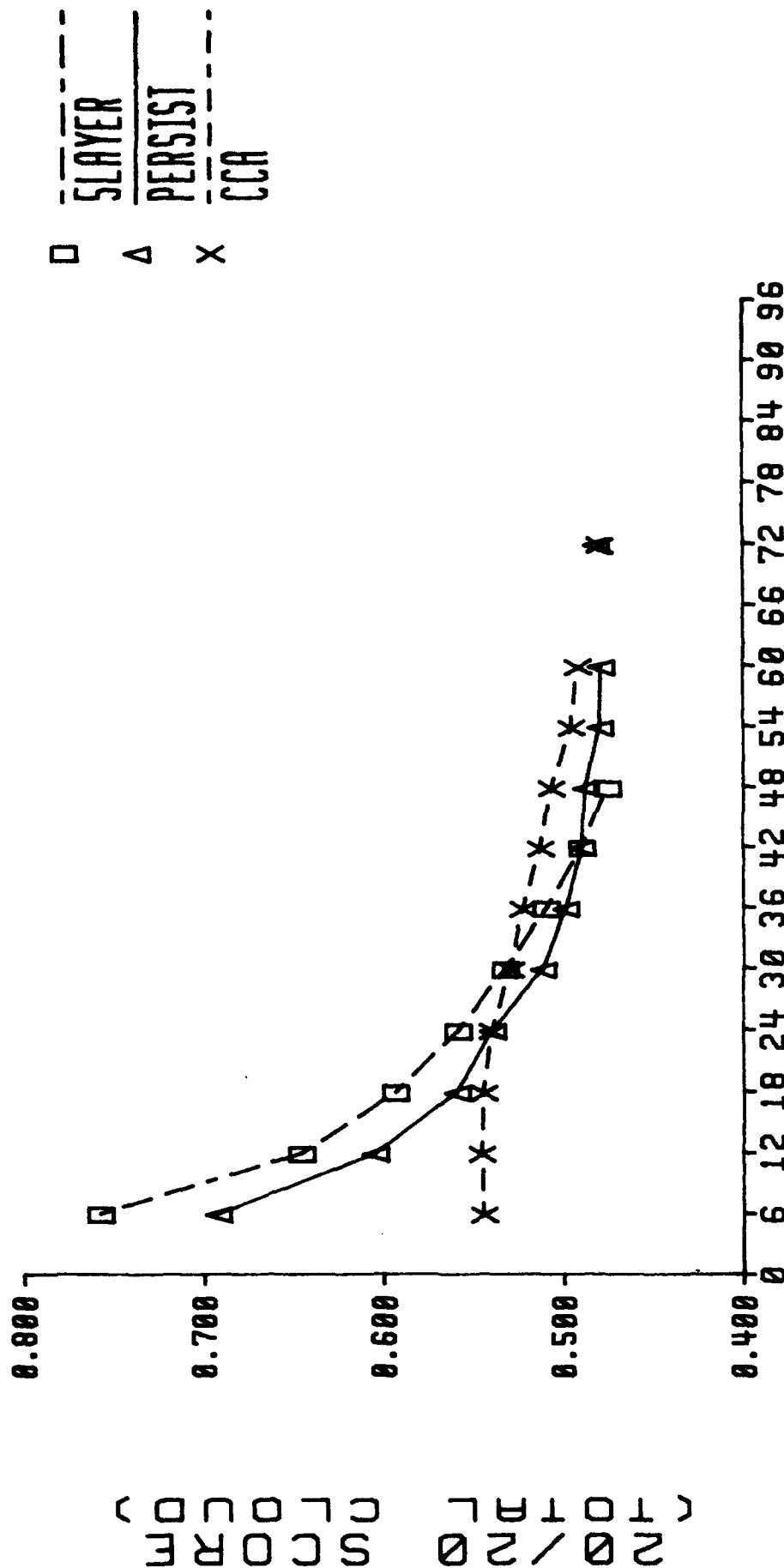
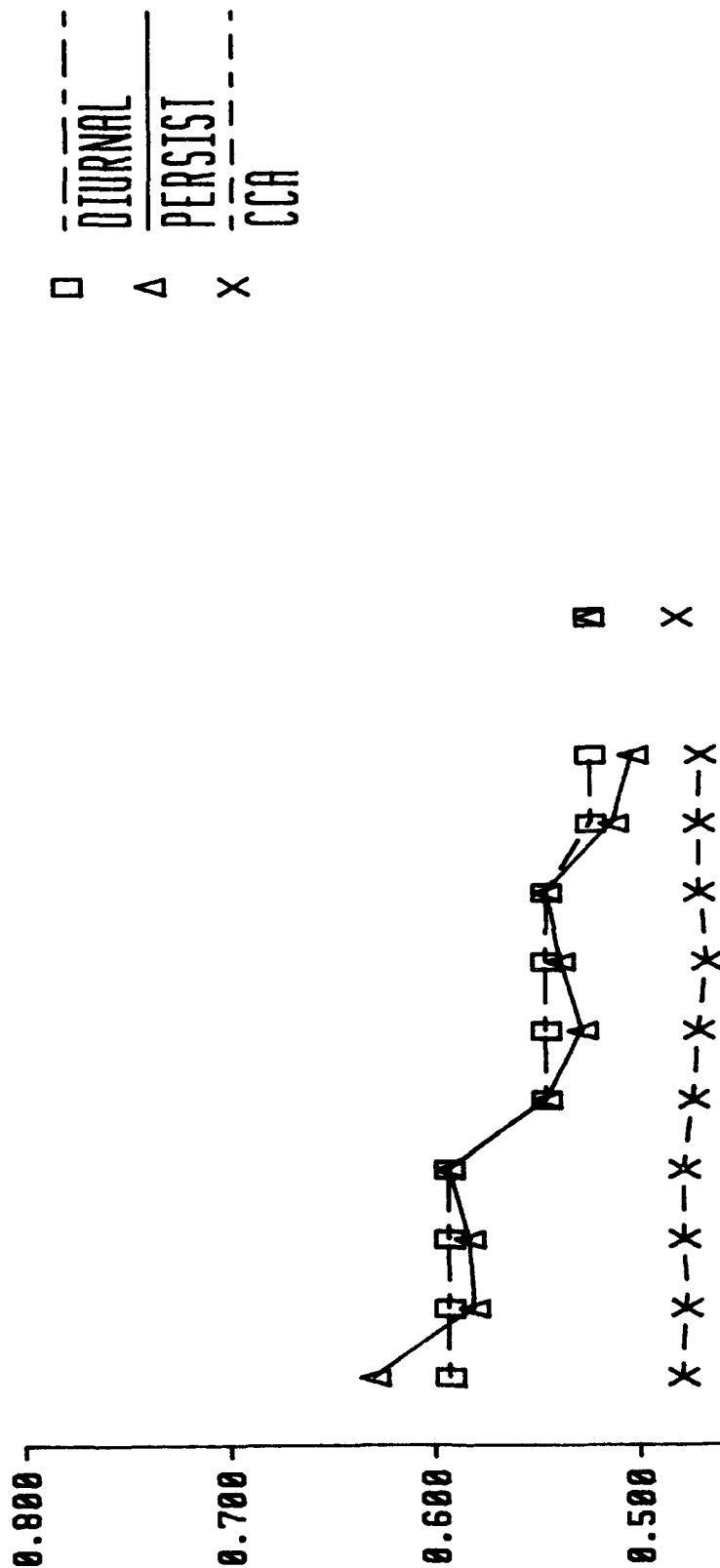


Figure C-7

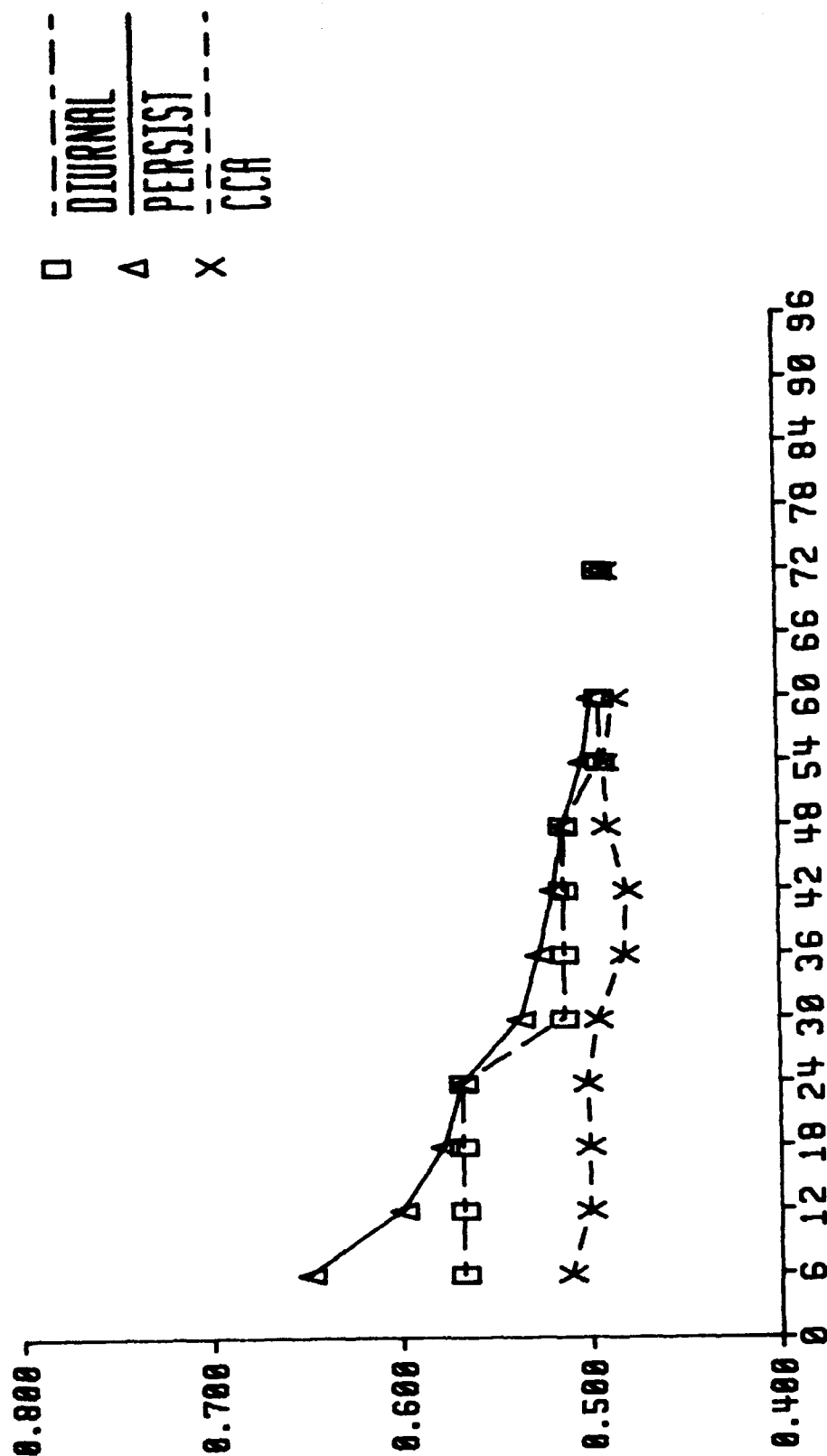
16 JAN 92 TO 12 FEB 92



FORECAST LENGTH (HOURS)
Figure C-8

FORECAST LENGTH (HOURS)

16 N H TROPICAL OCEAN 12 FEB 92



FORECAST LENGTH (HOURS)
Figure C-9

(20/20) SCORING

APPENDIX H:

PLOTS OF 20/20 SCORES

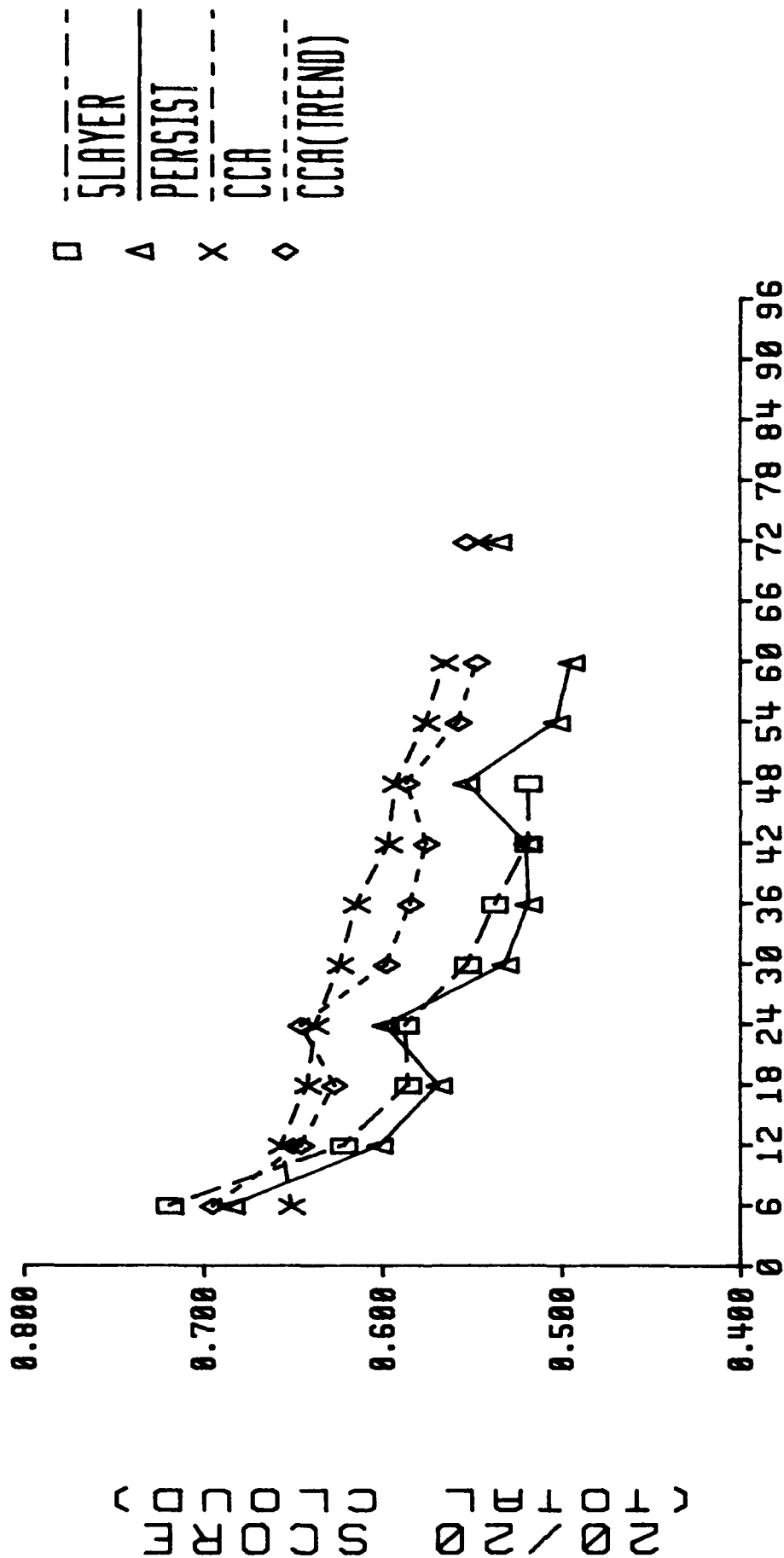
SHOWING THE EFFECTS OF THE

RELATIVE HUMIDITY TRENDING TECHNIQUE

LIST OF FIGURES

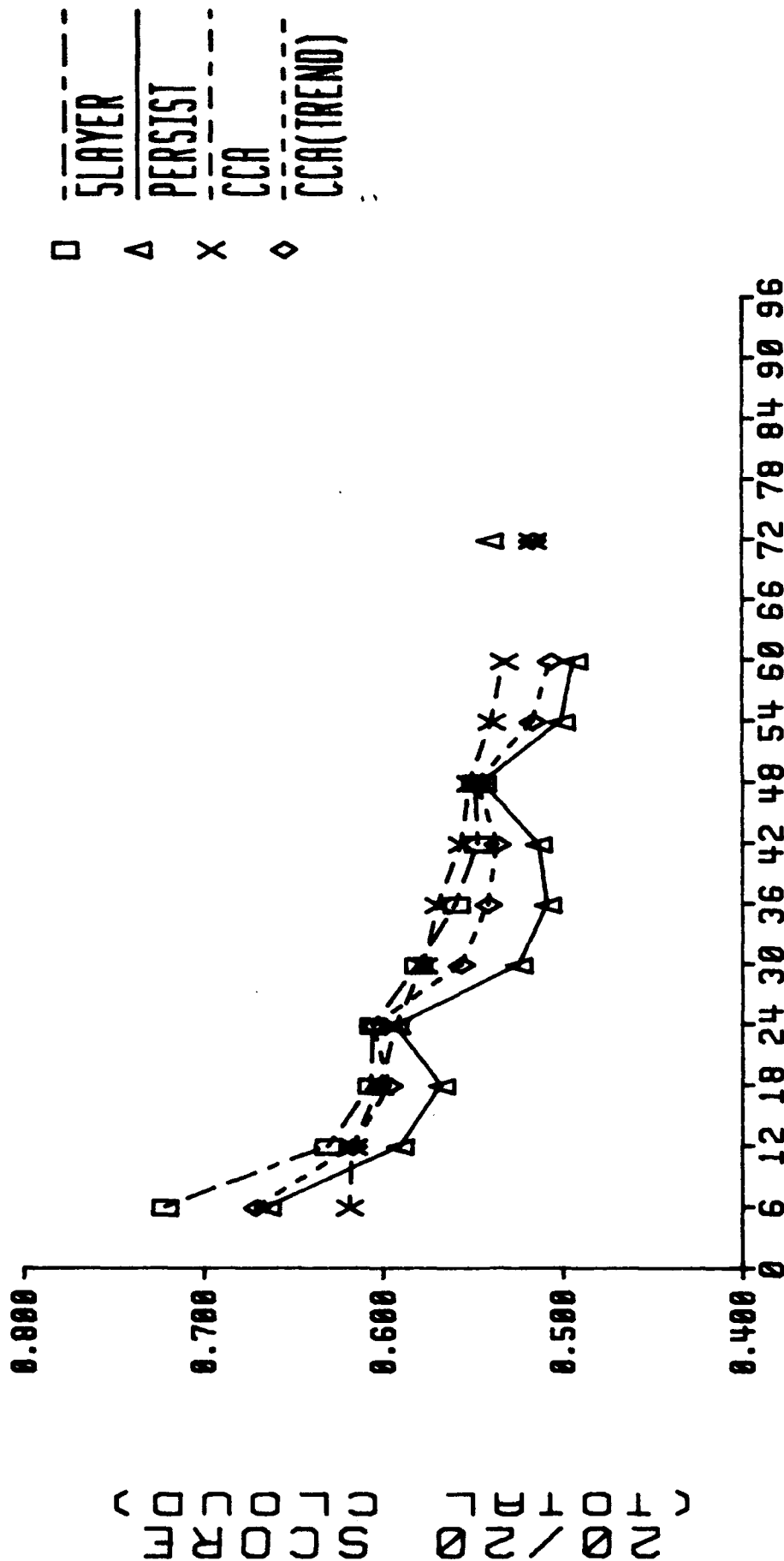
- Figure H-1.** 20/20 Scores for Cloud Forecasts Computed by the 5LAYER Model (to 48 hours only), by Using Persistence and by Using Cloud Curve Algorithm European Land Curves (Using both the Standard and RH Trending Techniques) For 6 to 60 and 72 Hour Total Cloud Forecasts Verified Over European Land During the Period from 24 October 1991 to 20 November 1991.
- Figure H-2.** 20/20 Scores for Cloud Forecasts Computed by the 5LAYER Model (to 48 hours only), by Using Persistence and by Using Cloud Curve Algorithm Northern Hemisphere Mid-Latitude Land Curves (Using both the Standard and RH Trending Techniques) For 6 to 60 and 72 Hour Total Cloud Forecasts Verified Over Northern Hemisphere Mid-Latitude Land During the Period from 24 October 1991 to 20 November 1991.
- Figure H-3.** 20/20 Scores for Cloud Forecasts Computed by the 5LAYER Model (to 48 hours only), by Using Persistence and by Using Cloud Curve Algorithm Northern Hemisphere Mid-Latitude Ocean Curves (Using both the Standard and RH Trending Techniques) For 6 to 60 and 72 Hour Total Cloud Forecasts Verified Over Northern Hemisphere Mid-Latitude Ocean During the Period from 24 October 1991 to 20 November 1991.
- Figure H-4.** BIAS Scores for Cloud Forecasts Computed Using Cloud Curve Algorithm Northern Hemisphere Mid-Latitude Land Curves with the RH Trending Technique and the Six Total Cloud Vertical Stacking Schemes (See page 13) For 6 to 60 and 72 Hour Total Cloud Forecasts Verified Over Northern Hemisphere Mid-Latitude Land During the Period from 24 October 1991 to 20 November 1991.
- Figure H-5.** BIAS Scores for Cloud Forecasts Computed Using Cloud Curve Algorithm Northern Hemisphere Mid-Latitude Ocean Curves with the RH Trending Technique and the Six Total Cloud Vertical Stacking Schemes (See page 13) For 6 to 60 and 72 Hour Total Cloud Forecasts Verified Over Northern Hemisphere Mid-Latitude Ocean During the Period from 24 October 1991 to 20 November 1991.

EUROPEAN LAND 24 OCT 91 TO 20 NOV 91



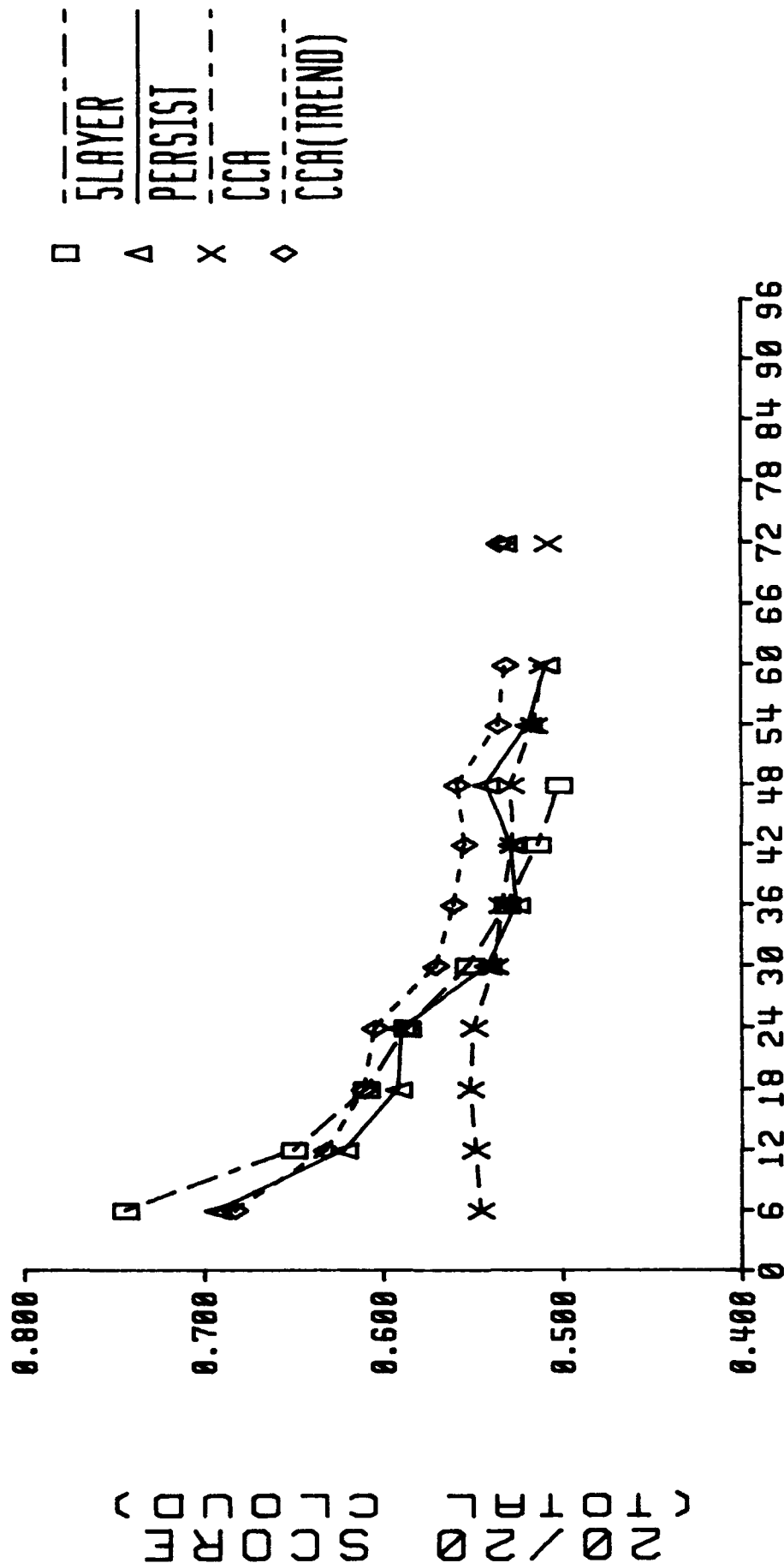
FORECAST LENGTH (HOURS)
Figure H-1

N H MID-LAT LAND 91
24 OCT 91 TO 20 NOV 91



FORECAST LENGTH (HOURS)
Figure H-2

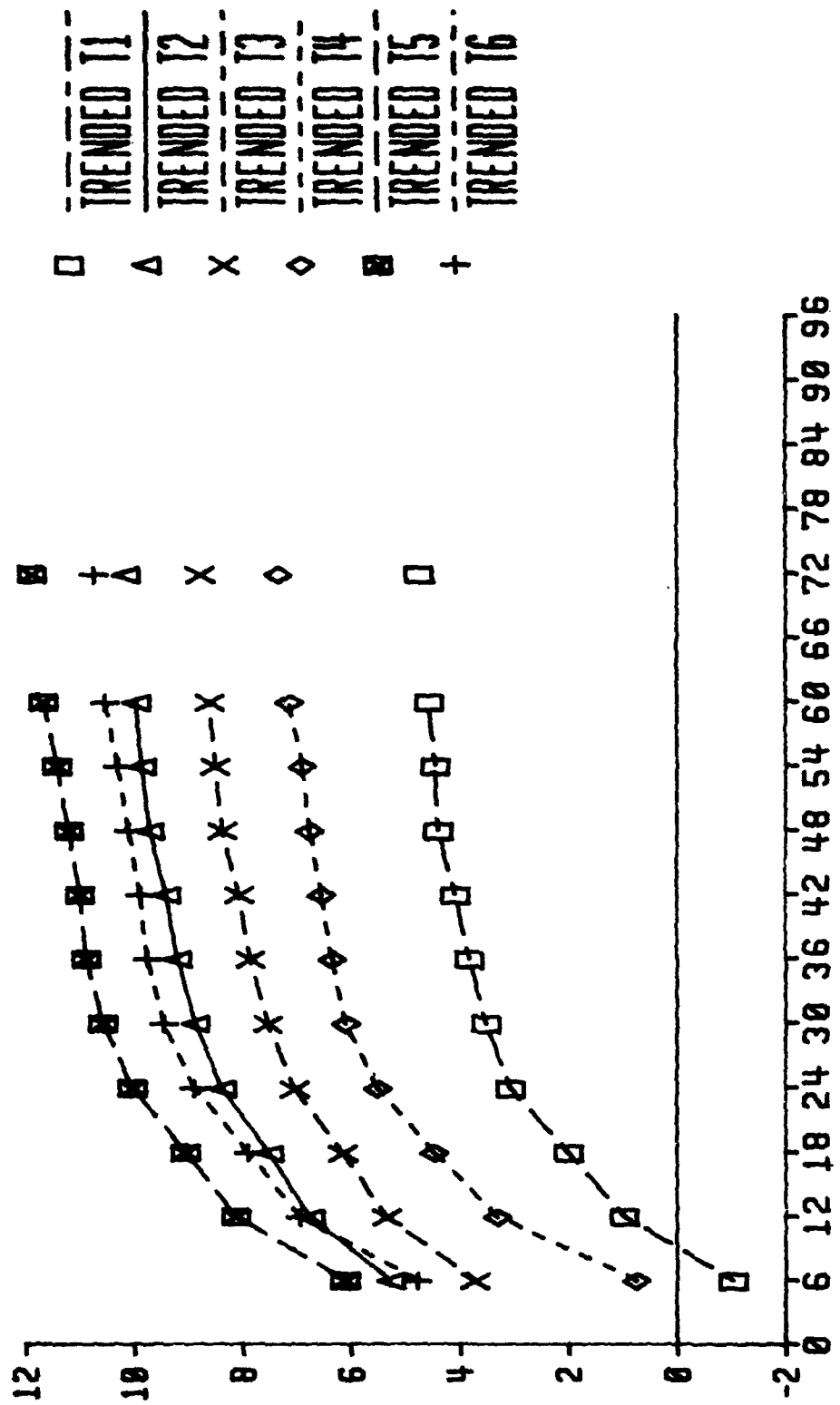
N H MID-LAT OCEAN 24 OCT 91 TO 20 NOV 91



FORECAST LENGTH (HOURS)
Figure H-3

17 JAN 91 - 13 FEB 91

N H MID-LAT LAND

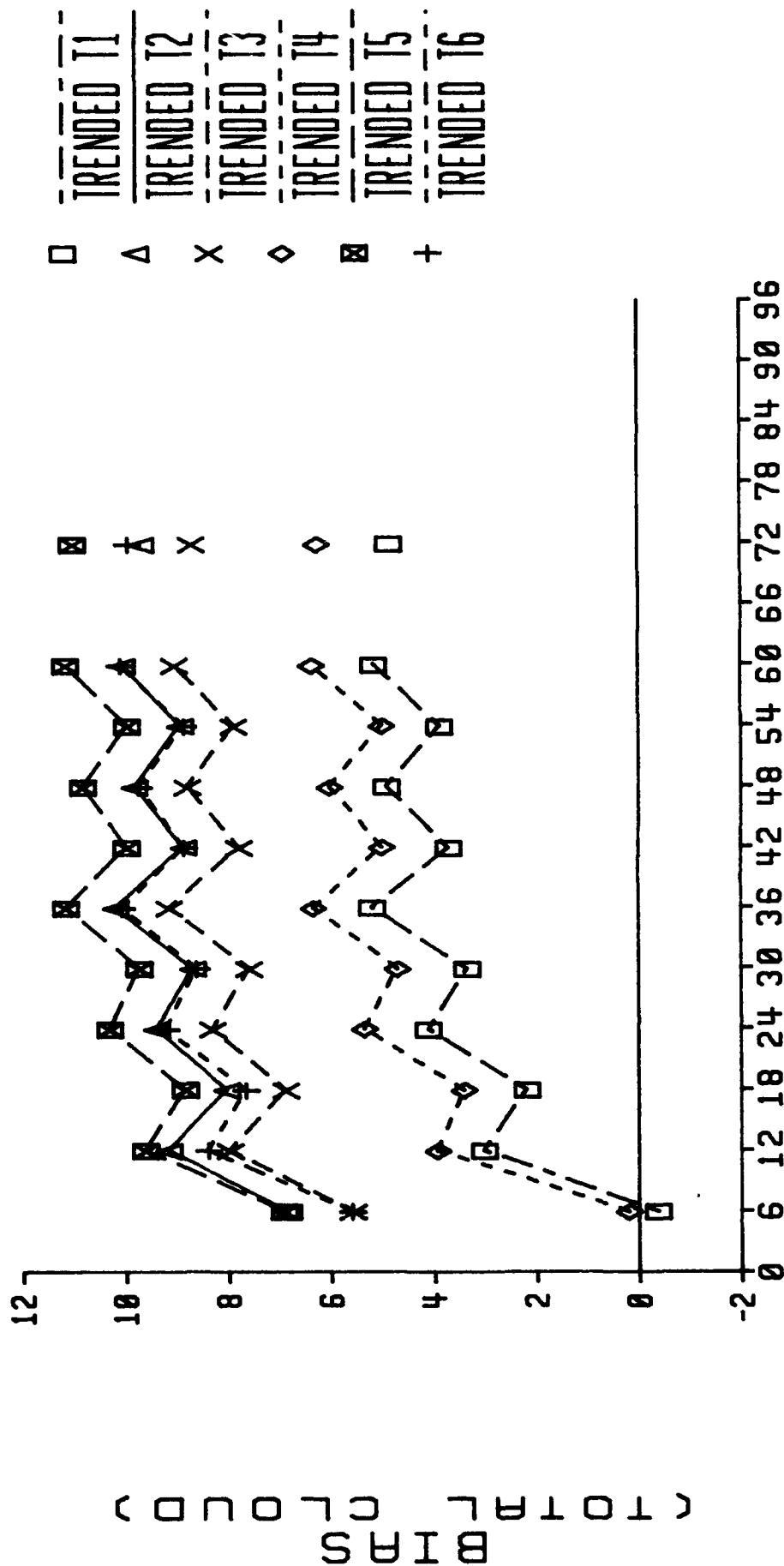


FORECAST LENGTH (HOURS)

Figure H-4

(TOTAL CLOUDS)

17 N H MID-LAT OCEAN 91 13 FEB 91



FORECAST LENGTH (HOURS)
Figure H-5

This page intentionally left blank

APPENDIX I:

**SHADED HEMISPHERIC DISPLAYS OF
RELATIVE HUMIDITY AND CLOUDS**

LIST OF FIGURES

- Figure I-1** Shaded Hemispheric Displays of 24 hour forecasts (24) of Northern Hemisphere (N) and Southern Hemisphere (S) Relative Humidity (RH) and Non-Trended (NT) Cloud Forecasts and the Verifying RTENPH Cloud Analysis (ANAL) for the Low Layer (L1 and L0) Valid at 06Z, 23 October 1990.
- Figure I-2** Shaded Hemispheric Displays of 24 hour forecasts (24) of Northern Hemisphere (N) and Southern Hemisphere (S) Derived Humidity (DH) and Trended (TR) Cloud Forecasts and the Verifying RTENPH Cloud Analysis (ANAL) for the Low Layer (L1 and L0) Valid at 06Z, 23 October 1990.
- Figure I-3** Shaded Hemispheric Displays of 24 hour forecasts (24) of Northern Hemisphere (N) and Southern Hemisphere (S) Relative Humidity (RH) and Non-Trended (NT) Cloud Forecasts and the Verifying RTENPH Cloud Analysis (ANAL) for the Middle Layer (MM and MI) Valid at 06Z, 23 October 1990.
- Figure I-4** Shaded Hemispheric Displays of 24 hour forecasts (24) of Northern Hemisphere (N) and Southern Hemisphere (S) Derived Humidity (DH) and Trended (TR) Cloud Forecasts and the Verifying RTENPH Cloud Analysis (ANAL) for the Middle Layer (MM and MI) Valid at 06Z, 23 October 1990.
- Figure I-5** Shaded Hemispheric Displays of 24 hour forecasts (24) of Northern Hemisphere (N) and Southern Hemisphere (S) Relative Humidity (RH) and Non-Trended (NT) Cloud Forecasts and the Verifying RTENPH Cloud Analysis (ANAL) for the High Layer (HH and HI) Valid at 06Z, 23 October 1990.
- Figure I-6** Shaded Hemispheric Displays of 24 hour forecasts (24) of Northern Hemisphere (N) and Southern Hemisphere (S) Derived Humidity (DH) and Trended (TR) Cloud Forecasts and the Verifying RTENPH Cloud Analysis (ANAL) for the High Layer (HH and HI) Valid at 06Z, 23 October 1990.

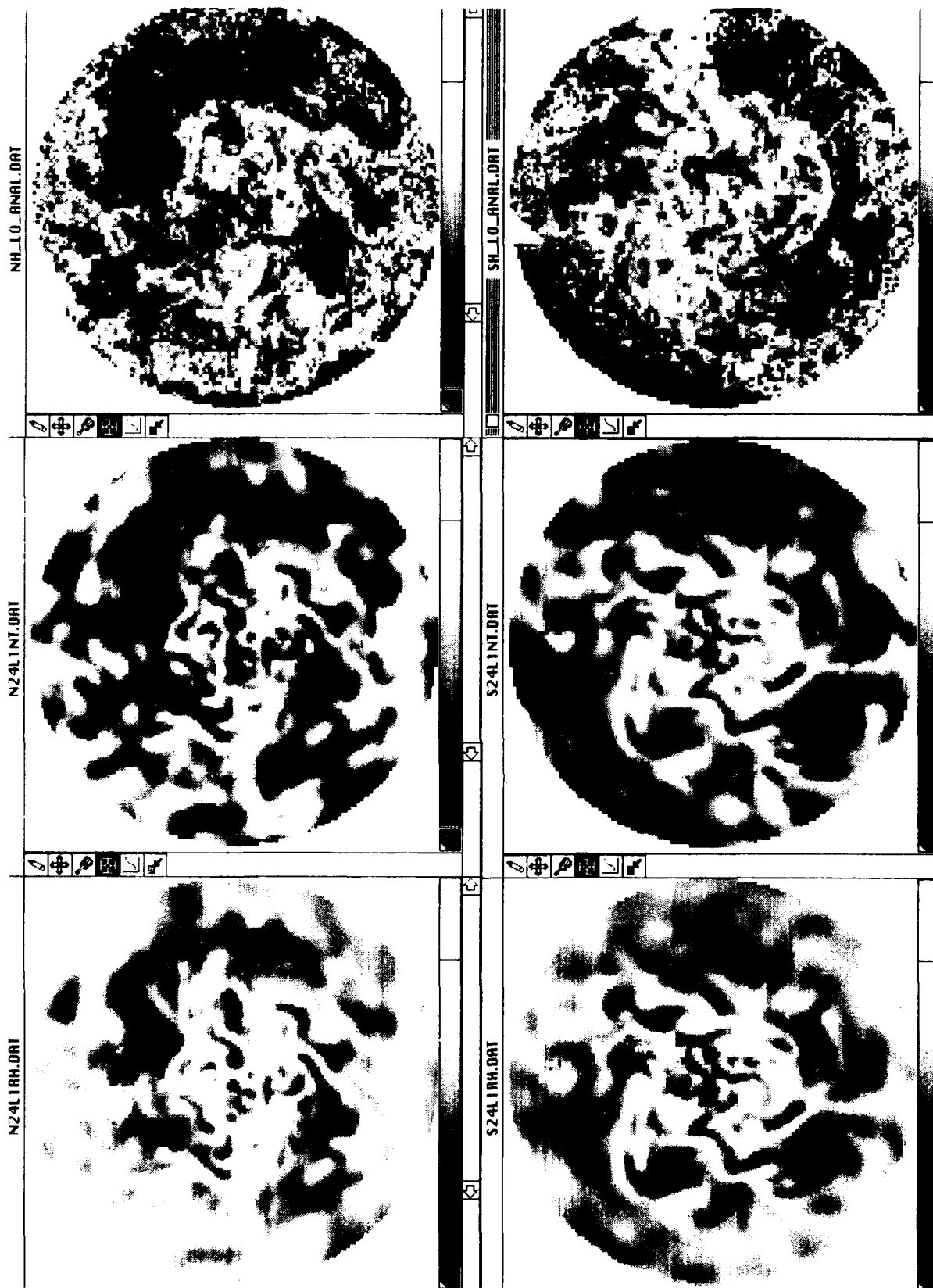


Figure I-1

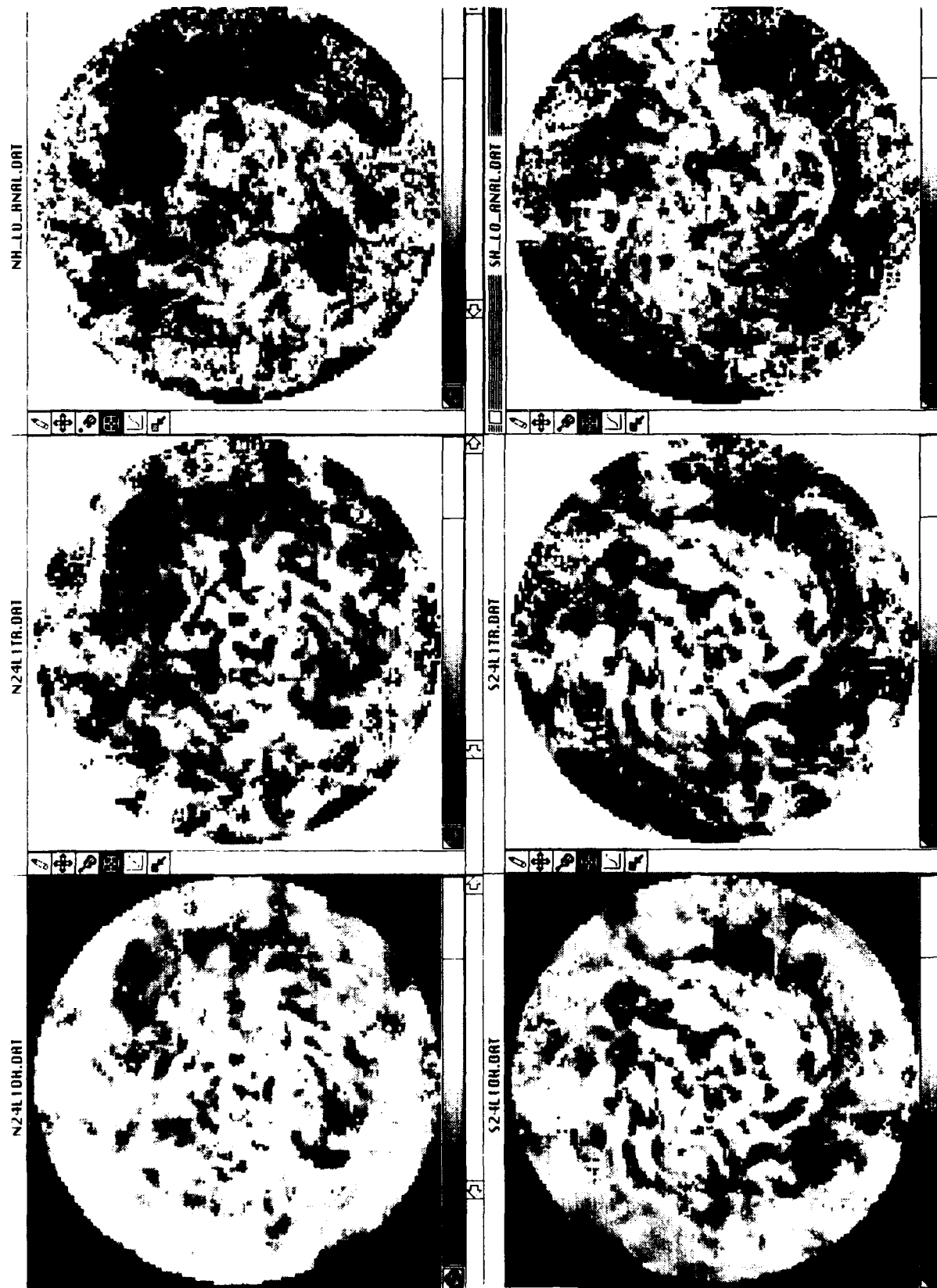


Figure I-2

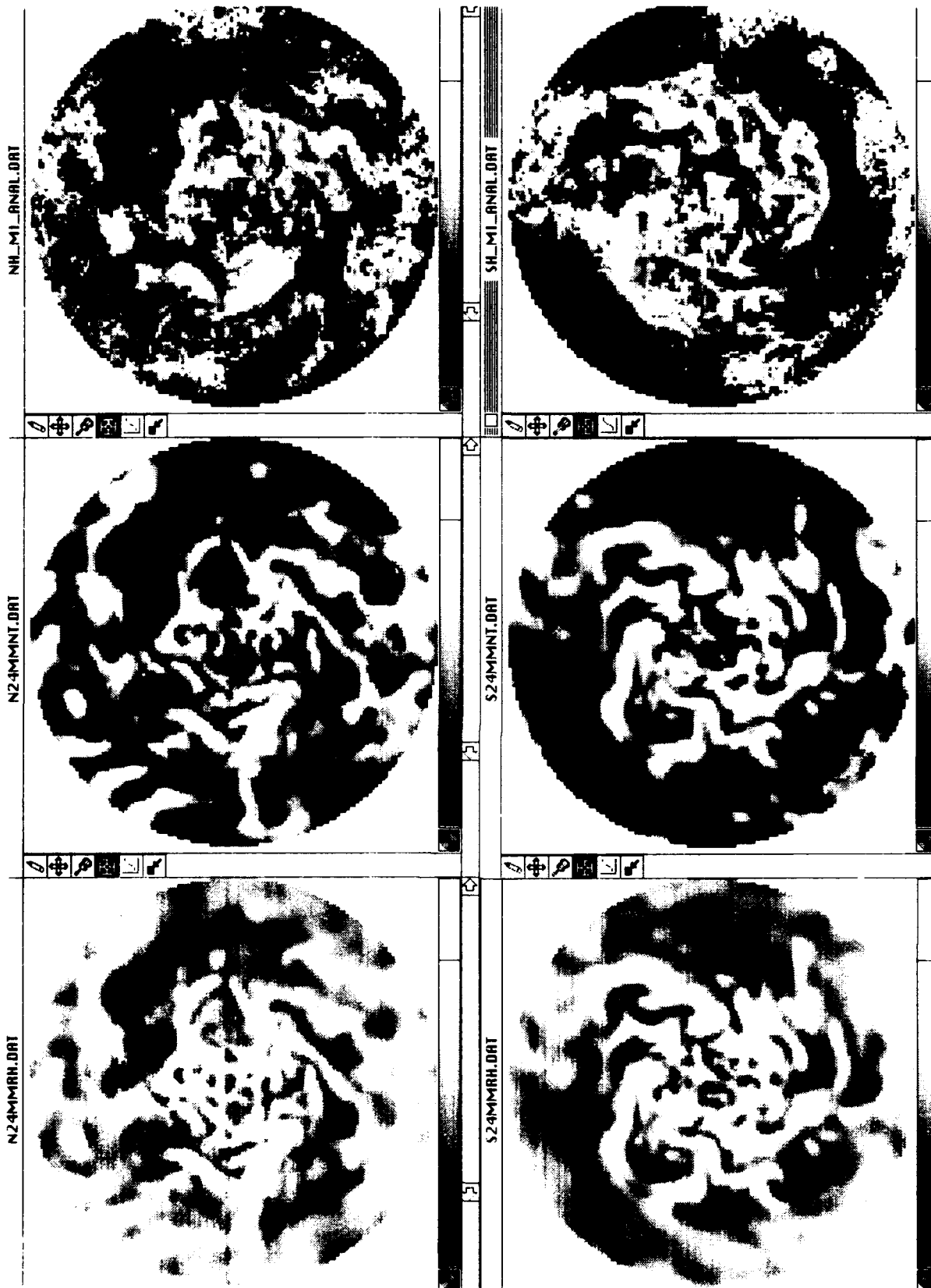


Figure I-3

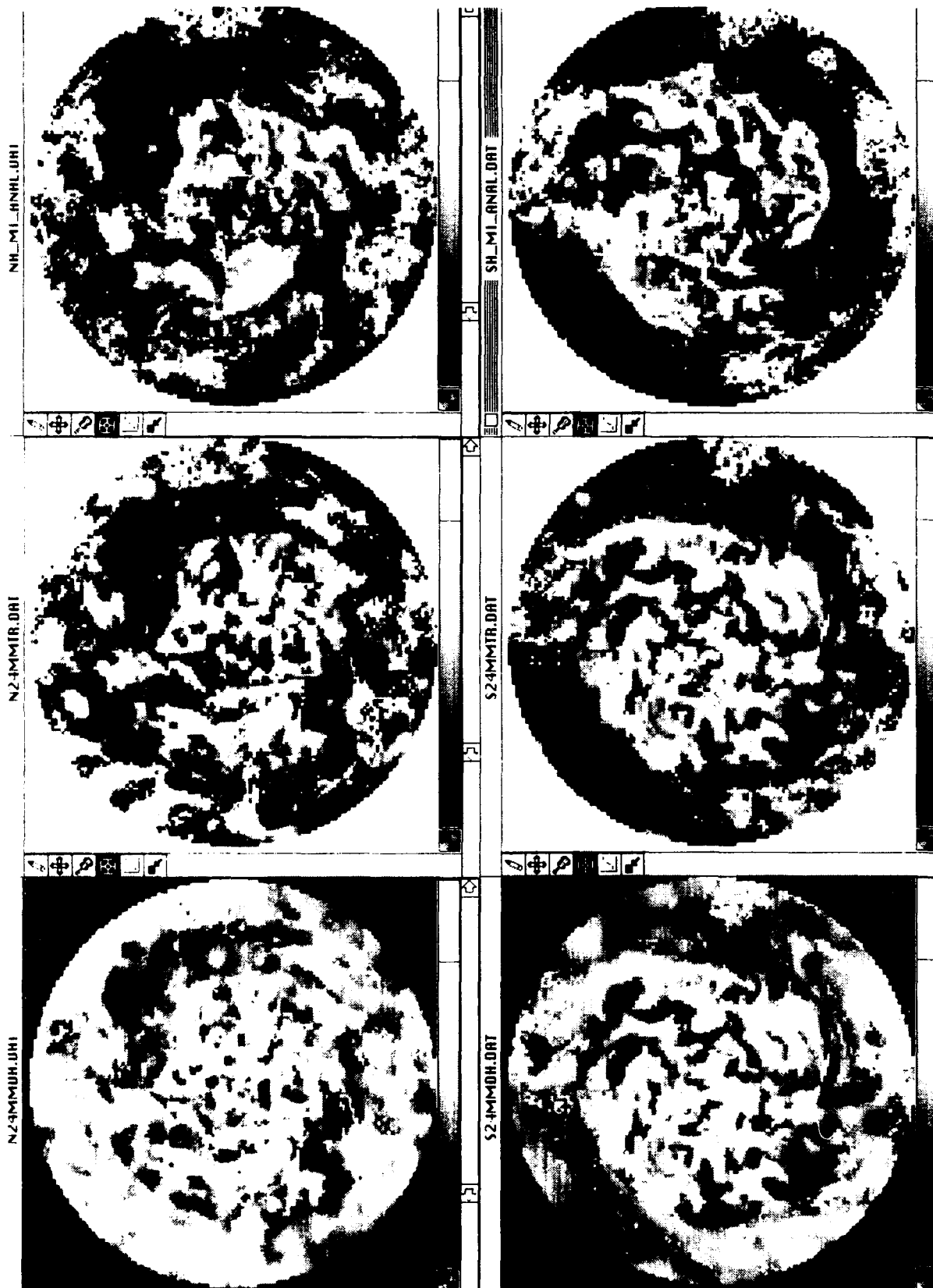


Figure I-4

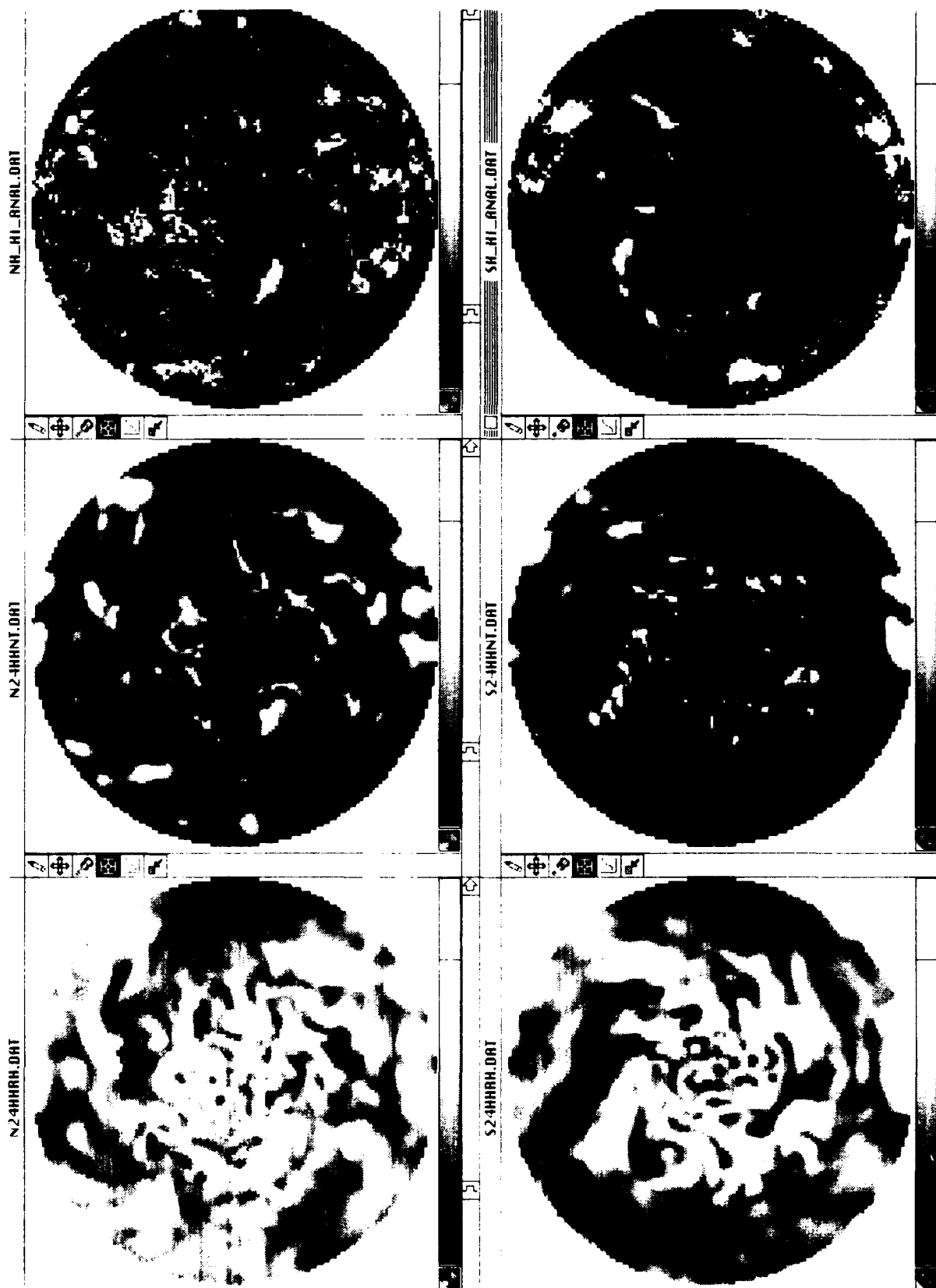


Figure I-5

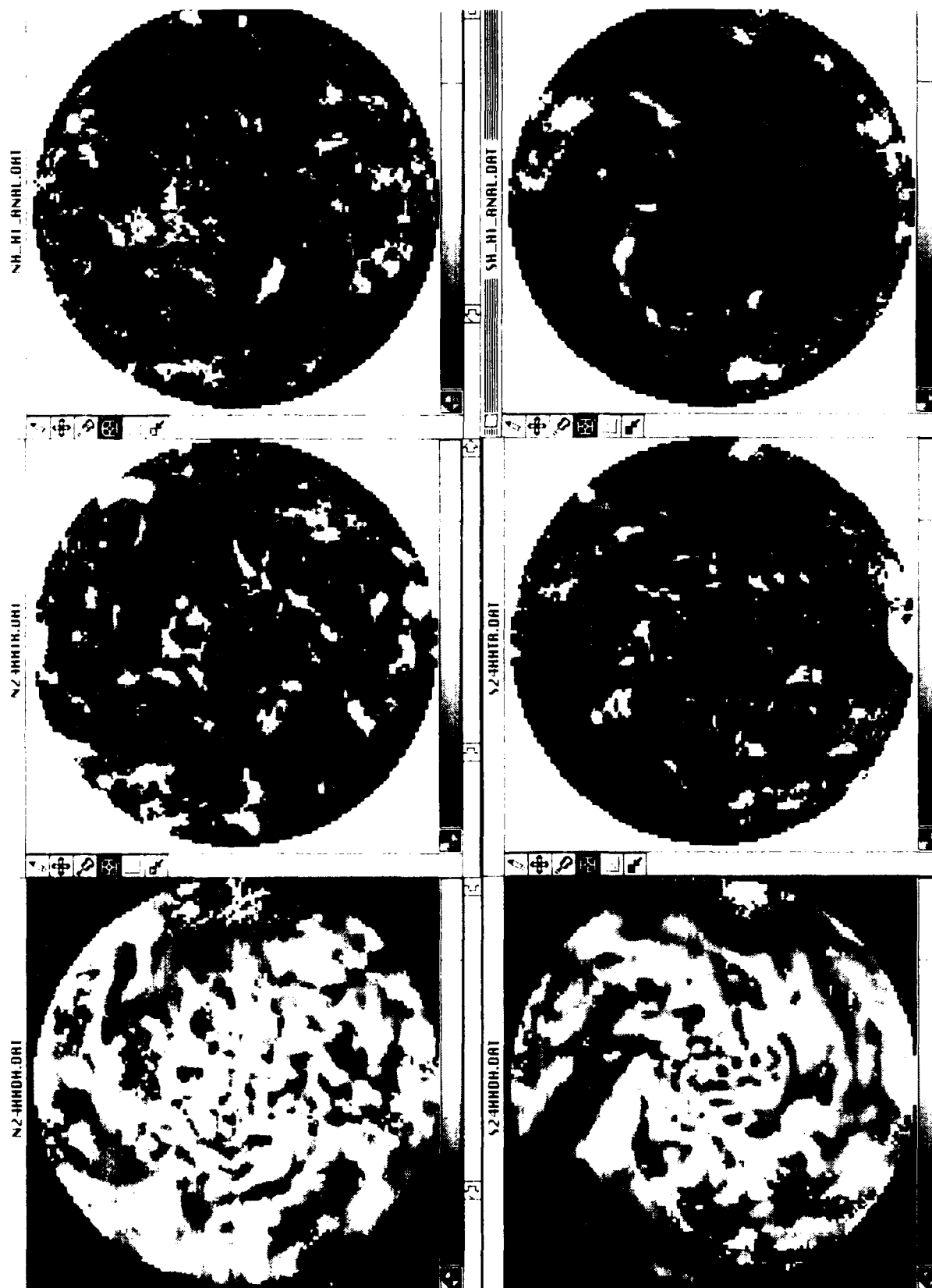


Figure I-6